



**DEVELOPMENT AND CHARACTERIZATION OF ZEOLITEY
FROM A NIGERIAN LOCAL RAW MATERIAL**

BY

BABALOLA Rasheed

(CUGP100344)

**A Thesis Submitted in the Department of Chemical Engineering to the
School of the Postgraduate studies**

**In partial fulfilment of the requirement for the award of
the degree of Doctor of Philosophy, (Ph.D)**

**In Chemical Engineering of Covenant University, Ota,
Ogun State, Nigeria**

February, 2015

DECLARATION

I, BABALOLA Rasheed, declare that the work in this thesis titled: “DEVELOPMENT AND CHARACTERIZATION OF ZEOLITE Y FROM NIGERIA LOCAL RAW MATERIAL” was carried out by me under the supervision of Professor J. A. Omoleye, Professor S. S. Adefila and Professor F. K. Hymore. No part of this work has been submitted elsewhere for award of similar degree in Chemical Engineering. All sources of information are formally acknowledged.

.....
R. Babalola

.....
Date

CERTIFICATION

This is to certify that this thesis titled “DEVELOPMENT AND CHARACTERIZATION OF ZEOLITE Y FROM LOCAL RAW MATERIAL” by BABALOLA Rasheed meets the regulations governing the award of the degree of Doctor of Philosophy [Chemical Engineering] of Covenant University , and is approved for its contribution to knowledge and literary presentation.

.....

Engr. R. Babalola

Dept of Chemical Engineering

.....

Pro. J. A. Omoleye

Supervisor

.....

Prof. J. A. Omoleye

Head of Chemical Engineering Department

.....

Prof. S. S. Adefila

Co Supervisor

DEDICATION

This Ph.D dissertation work is dedicated to Almighty Allah and to the memories of my late parents Mrs Sariyu Olalonpe Babalola and Chief Suleiman Opadokun Babalola and my late brother Mr. Abdul-Azeez Akanni Babalola for their love, encouragement, support, prayers and most importantly my brother for dreaming this for me since I was a baby. Any achievement in my life is a direct result of his sacrifices and a testimony to his excellent guidance. May their souls rest in perfect peace.

ACKNOWLEDGEMENTS

First and foremost, I would like to express my sincere thanks and appreciation to Almighty Allah for given me the strength, dedication, inspiration and for his guidance to achieve and complete this degree programme.

With deep sense of humility and appreciation, I thank God for the Chancellor of Covenant University, Dr David Oyedepo, for the vision behind the University's establishment. Today, I can attest that based on the privilege given to me on this platform, I have been imparted and empowered mentally and spiritually to positively affect my world Thank you sir.

With joy and gladness in my heart, I appreciate my boss and good friend Engr. Zakari Abubakar (popularly known as Mai Te-mako) and his amiable and kind wife Hajiya Aisha Abubakar for their commitment and doggedness, both financial and moral support, to ensure the successful completion of this Ph.D programme.

Special thanks to my phenomenal supervisor Professor James Abiodun Omoleye for his advice and guidance, continued support, tremendous help, encouragements, and insight and sharp criticism. Despite his busy schedule, he would always find the time to discuss anything on experimental results. His questions and mentorship inspired the series of experiments described in this dissertation. Sincerely I have learnt lots of things from his way of thinking and his research methodology. I can honestly say that this Ph.D. dissertation would not have been accomplished without his outstanding supervision, scientific knowledge and experience.

With respect, honour and appreciation I acknowledge the unparallel contributions of my amiable Co-supervisor, Professor S.S.Adefila. His in -loco -parentis and mentorship roles brought about the achievement and positive impact in the successful completion of my work. He engineered the research work, provided the platform, materials and in many cases financial support. The synthesis of Zeolite Y at Ahmadu Bello University was his good will and supervision. He was always on hand to answer my questions, make corrections and provide guidance on the appropriate path to go. The Almighty God shall richly bless you more and more.

I would like to acknowledge the former Head of Department and a Co-Supervisor, Professor Fredrick Kofi Hymore, who to me was a major motivation through his constant prodding, concern and encouragement which, gave me the much needed drive towards the successful completion of this work. Thank you sir.

Special thanks go to Dr. Olusegun Ayoola Ajayi of Ahmadu Bello University Zaria, My Zeolite Uncle. His mentorship roles brought about the achievement and positive impact in the successful completion of this Ph.D work. “*E seo*”.

I wish also, with deep sense of humility, to register my profound gratitude to the senior Faculty in the department Professor O. O. Omatete, Professor J.O. Odigure, Professor C. T. Ako for their immense contributions and moral support. Their words of encouragement and lectures were all the needed impetus that took me through this research work. I cannot fail to mention of the help I got from Dr. O. D. Orodu each time I needed to be guided during this thesis preparation.

I would like to thank Prof. A.S Ahmed the current PTDF Chair Ahmadu Bello University, Zaria for his permission for the use of their laboratory facilities and his staff Nurudeen Salaudeen, Suleiman Yunusa, Solomon G. Bawa, Mustapha Yusuf and Sani O. Nakakana for their cooperation.

I like to acknowledge Dr David Agbajelola for his total support for this programme especially during the setting up of reactor for performance testing in the Kaduna Refinery. Also acknowledged are Dr. Aloko Duncan, Dr. Martha Njewu my special editor. Dr. Aderemi B.O.

I would also like to express many thanks to the following people: Engr. Perry Awe, Engr. Bolanle Ayodele, Dr. Fred Njugwu of NNPC Kaduna refinery and the good people of the Quality Control Laboratory, both fuels and lubes, for giving me opportunity to use their facilities for testing the performance of the developed Zeolite Y. I say to all of you Thank you, sirs.

Furthermore, I wish to extend my warm thanks to all the good people of Nigerian Geosciences Survey Agency, Kaduna, National Steel Raw Materials Exploration Agency, Kaduna, Sheda Science and Technology Complex, Sheda, Abuja, DICON Kaduna, Department of Chemical Engineering, Covenant University Ota, National Research Institute for Chemical Technology, Zaria. Thanks for all the analysis.

My sincere thanks go to Engr.Mrs Modupe Esther Ojewumi, Engr.Adedeji Ayoola, Engr. Opeyemi Adeeyo, Dr. Omoniyi Augustine Ayeni, Engr. Uduhitinah Jacobs Smith for their moral support and co-operation. Many thanks go to Mr. Omodara Julius and Ahoda Jasper for their unquantifiable and invaluable assistance and co-operation all through the period.

I wish to acknowledge the support of our departmental secretary Mrs S.O. Ogunniyi for my Ph.D work, most time she has to spend her money to call me not to talk of staying late at odd hours to type my work. Thank you ma, and may God reward you.

I am deeply indebted to my dear wife, Love Mojisola Babalola and daughter, Maryam Omomayowa Babalola for their love, patience, care, and sacrifice during my study. Thank you so much for continuous assistance.

Finally and humbly, I would like to express my sincere thanks and appreciation to all members of NASFAT Kaduna Branch particularly; The Chairman Alh. Abdulwaheed Adepoju, Alh. Abdul-Azeez Olayanju and the Missioner for all their prayers. Also to all the Teachers of NASFAT Nursery and Primary School, words are inadequate to express my truthful and profound thanks

ABSTRACT

Zeolites are important chemical materials used in chemical processes. The manufacture of the materials usually involves the use of expensive chemicals. This study involves the use of Elefun Nigerian Kaolin (ENK) as precursor material for the development of zeolite Y. The synthesis of zeolite Y was successful following a sequence: collection of raw kaolin clay from Elefun area of Ogun state, Nigeria; subjecting it to, calcination, partial dealumination and final hydrothermal synthesis. The raw clay was refined using sedimentation technique to recover 98 percent kaolin. Both conventional and novel methods of metakaolinization technique were used to convert kaolin into the reactive metastable phase. Amorphous metakaolin was obtained at a temperature of 850°C at residence time of 6 hours. The percentage of the alumina in the metakaolin was reduced through reaction with sulphuric acid to give Silica/Alumina molar ratio of 4.7 after ageing for between seven and nine days. The unique procedure of gel formation and Crystallization to NaY zeolite was achieved after 24hours at 100°C. The NaY zeolite was modified by ion exchange process to give a more acidic zeolite HY with improved Bronsted active acid sites.

The synthesised Zeolite HY was characterized and confirmed through the XRD pattern and the silica/alumina ratio of about 3.62 using XRF, the results were corroborated with the analytical results from both SEM (Scanning Electron Microscope) and BET (Brunauer, Emmet and Teller). The activity of the synthesised zeolite Y was confirmed. It compared favourably to the market commercial brand through its very similar conversion in the cracking reactions of cyclohexane and Gas Oil to lighter products when tested in NNPC Kaduna Refinery Laboratory.

Keywords: Zeolite-Y, metakaolinization, dealumination, hydrothermal, metastable phase, Bronsted, microkinectic.

TABLE OF CONTENTS

TITLE PAGE	i
DECLARATION	ii
CERTIFICATION	iii
DEDICATION	iv
ACKNOWLEDGEMENTS	v
ABSTRACT	viii
TABLE OF CONTENTS	ix
LIST OF FIGURES	xv
LIST OF TABLES	xviii
LIST OF APPENDICES	xix
ABBREVIATION, DEFINITIONS, GLOSSARY AND SYMBOLS	xxv
CHAPTER ONE: INTRODUCTION	1
1.1 Statement of the Problem	4
1.2 Justification of the study	4
1.3 Aim / Objectives of the study	6
1.4 Scope of the Study	6

CHAPTER TWO:	LITERATURE REVIEW	7
2.1	Introduction to Zeolites	7
2.2	Structure and Nomenclature of Zeolites	10
2.3	Pore structure	13
2.4	Description of Zeolites Y	14
2.5	Properties of Zeolites	14
2.5.1	Ion-exchange	14
2.5.2	Catalysis	15
2.5.3	Adsorption	16
2.6	Application of Zeolites	17
2.7	Local raw material for zeolite synthesis	19
2.7.1	Rice husk	19
2.7.2	Clay and its classification	19
2.7.3	Kaolin clay	23
2.7.3.1	Structure of kaolinite	23
2.7.3.2	Formation of kaolinite clay	25
2.7.3.3	Nigeria kaolinite clay	26
2.7.3.4	Processing of kaolinite clay	27
2.7.3.5	Effect of heat on kaolinite clay (dehydroxylation)	28
2.7.4	Structure of metakaolin	32

2.7.4.1 Effect of acidification and alkalination on kaolin and metakaolin.	33
2.8 Synthesis of Zeolites	34
2.8.1 Zeolite crystals	37
2.8.2 Zeolite Y synthesis starting components	38
2.8.3 Crystallization of zeolite	40
2.8.3.1 Heating temperature	42
2.8.3.2 Ageingtime	43
2.8.3.3 Crystallization time	44
2.9 Catalytic cracking	44
2.9.1 Catalytic cracking processes	46
2.9.2 Cracking reaction	48
2.9.3 The mechanism of catalytic cracking	50
2.9.4 Catalytic cracking of alkyl aromatic hydrocarbon	51
2.9.4.1 Cracking of cyclohexane	52
2.10 Kinetics of the Cracking Reaction	54
2.10.1The kinetics of cracking reaction of developed and commercial zeolite	55
2.10.2 Adsorption	56
2.10.2.1Henry's Law and Adsorption Equilibrium	56
2.10.2.2 Estimation of the Adsorption Equilibrium Constant From Chromatographic Measurements	56
2.10.3 Mass Transfer Resistances	59
2.10.3.1 External Film Resistance	59
2.10.3.2 Macropore Resistance	61
2.10.4 Experimental measurement of diffusion	63
2.10.4.1 Uptake rate measurements	63
2.11 Chromatography	64
2.11.1 ZLC Method (Zero Length Column)	65
2.11.2 Zero length column theory	65
CHAPTER THREE: MATERIALS AND METHOD	69
3.1 Materials	69
3.1.1 Beneficiation equipment/material	69
3.1.2 Calcination equipment/material	69

3.1.3	Dealumination equipment/material	69
3.1.4	Gelation equipment/material	71
3.1.5	Chemicals used for performance test experiment	72
3.1.6	Equipment used for performance test experiment	72
3.2.1	Clay beneficiation	74
3.2.1.1	Procedure	74
3.2.2	Calcination	75
3.2.3	Dealumination of the calcined clay	76
3.2.4	Gel formation	78
3.2.5	Actual Synthesis of Zeolite Y from Elefun Clay	78
3.2.6	Determination of ion exchange Capacities	79
3.3	Performance Test for Zeolite Y developed from Elefun Kaolin	80
3.3.1	Experimental procedure	82
3.3.1.1	Preliminary preparation	82
3.3.1.2	Catalyst pre-treatment	82
3.3.2	Gas chromatograph	83
CHAPTER FOUR: RESULTS PRESENTATION AND DISCUSSION		85
4.1	Results of X-ray fluorescence (XRF) Analysis of Raw, Beneficiated and Calcined Elefun kaolin	85
4.1.2	XRD analysis	86
4.2	Clay Beneficiation	87
4.2.1	XRF Analysis	87
4.3	Metakaolinitization of Elefun kaolin	87
4.3.1	XRF Analysis of Calcined Elefun Kaolin	87
4.3.2	XRD Analysis	88
4.4 (a)	Dealumination of Metakaolin	89
4.4.1	Effect of dealumination time on kaolin composition	89

4.4.2	Novel approach to metakaolin dealumination	91
4.5	Gel formation and Zeolite Y synthesis	91
4.5.1	XRD Analysis	91
4.5.2	SEM result of the developed zeolite Y	99
4.5.3	Fourier Transform infrared Spectroscopy(FTIR) result of developed Zeolite Y	101
4.5.4	BET Surface area result of synthesized zeolite Y	102
4.6	Comparison of XRF results of Zeolite NaY , Zeolite NH ₄ Y and Zeolite HY	104
4.7	Results of Cracking Reaction of Developed and Standard zeolites Y	112
4.7.1	Cyclohexane cracking over locally synthesized zeolite Y and reference zeolite Y catalyst under helium atmosphere	116
4.7.2	Preliminary test of first order kinetics of cyclohexane cracking on synthesized zeolite Y Catalyst in Helium	118
4.7.3	Cracking of cyclohexane on developed zeolite Y	119
4.7.4	Cracking of cyclohexane on standard zeolite Y at 520 ⁰ C	121
4.7.4B	Comparism between the performance of synthesized and standard zeolite Y on cyclohexane	123
4.7.5	Cracking of gas oil on synthesized zeolite Y	127
4.7.6	Cracking of gas oil on commercial zeolite Y	133
4.7.7	Comparism between the performance of synthesized and standard zeolite Y a on gas oil	138
CHAPTER FIVE: RESEARCH CONCLUSION AND RECOMMENDATIONS		142
	Conclusions and Recommendation	142
5.1	Conclusion	143
5.2	Recommendations	143
5.3	Contributions to Knowledge	144
CHAPTER SIX: REFERENCES		145-156
APPENDICES		157
	Appendix A Calculation	157
	A ₁ Dealumination Calculation	157
	A ₂ Dilution Calculation	159
	A ₃ Gelation Calculation for DMK	159

APPENDIX B	166
B ₁ Results of Cyclohexane Cracking over Developed Zeolite Y and Commercial Zeolite Y Catalyst under Helium Atmosphere	166
B ₂ Cracking of Cyclohexane	168
B ₃ Cracking of Gas Oil	172
APPENDIX C	178
APPENDIX D	192
APPENDIX E	213

LIST OF FIGURES

Figure 1.0: World Energy Matrix in Percentage (IEA, 2008)	1
Figure 2.1 The primary building unit TO ₄ of zeolite-y (www.port.ac.uk/zeolite,2009)	11
Figure 2.2 Existing secondary Building Units (SBUs) in zeolite Framework (www.ch.ic.ac.uk , 2013).	12
Figure 2.3: 12- ring Pore structure of zeolite Y studied in this research [IZA, 2012]	13
Figure 2.4: Zeolite-Y structure type FAU (Ramirez, 2009)	14
Figure 2.5: Bronsted acid site in zeolites (http://copweb.com , 2012)	15
Figure 2.6: structure of kaolinite designed by Brindley Nakahra, viewed from the a-axis direction	24
Fig. 2.7: Crystallochemical Structure of Kaolinite	24
Figure 2.8: The change of the tetrahedral (light) and octahedral (dark) sheets	24
Figure 2.9: The Teflon-lined stainless steel autoclave used in this work	37
Figure 2.10: The Houdry fixed bed process (Shell international, 1998)	47
Figure 2.11: The fluid catalytic cracking process (NNPC, 2013)	47
Figure 2.12 Mass balance on a packed column	57
Figure 2.13: Sketch of breakthrough curve	59
Figure 2.14 Schematic diagram of composite adsorbent pellet showing the three principal resistances to mass transfer	60

Figure:3.0 Flow Diagram of zeolite Y Synthesis from Elefun clay	73
Figure 3.1: Modification of NaY to Zeolite HY	79
Fig.3.3 Experimental Set-up	81
Figure 3.4: Schematic diagram of typical GC set up	83
Figure 3.5 Gas Chromatograph system	84
Figure 4.1: XRD patterns for raw Elefun kaolin as-mined	86
Figure 4.2: XRD patterns for Calcined Elefun Kaolin at 850°C	88
Figure 4.3A: XRD pattern for synthesized zeolite Y from Elefun clay at 7 days ageing	93
Figure 4.3B: XRD pattern for synthesized zeolite Y from Elefun clay at 7 days ageing With peak indication	94
Figure 4.4: XRD pattern for synthesized zeolite Y from Elefun clay at 9 days ageing	96
Figure 4.5: XRD pattern of (A) Standard zeolite Y, (B) Synthesized Zeolite Y	97
Figure 4.6: SEM image of Zeolite Y synthesized from Elefun kaolin	100
Figure 4.7 SEM Images of (a) developed NaY zeolite (b) HY zeolite (c) Standard zeolite Y	100
Figure 4.8 Result of FTIR analysis for (a) Synthesized Zeolite Y (b) Standard Zeolite Y	101
Figure 4.9 : XRD Pattern of zeolite NH ₄ Y	105
Figure 4.10: SEM image of Zeolite NH ₄ Y synthesized from Elefun kaolin	106
Figure 4.11: XRD Pattern of zeolite HY	107
Figure 4.12: SEM image of Zeolite HY synthesized from Elefun kaolin	108
Figure 4.13: SEM image of Spent Zeolite HY synthesized from Elefun kaolin after Performance test	110
Figure 4.14: Variation of Conversion using Zeolite Y Matrix (25% HY: 75% metakaolin) at 520 ⁰ C with flowrate	116
Figure 4.15: Variation of Conversion using Zeolite Y matrix (25:75%) at 480 ⁰ C with flowrate C3 hydrocarbon is considered as Key Component for the test	117

Figure 4.16: Test of First Order Kinetic for cyclohexane cracking on synthesized zeolite Y Catalyst at 520 ⁰ C	119
Figure 4.17: Arrhenius Plot for cyclohexane cracking on synthesized zeolite Y at 440 – 520 ⁰ C	120
Figure 4.18: Test of First Order Kinetic for cyclohexane cracking on standard zeolite Y Catalyst at different temperature levels	121
Figure 4.19: Arrhenius plot for cyclohexane cracking on standard zeolite Y at 440-520 ⁰ C	122
Figure 4.20: Effect of catalyst type on propane yield of cyclohexane cracking at 520 ⁰ C	123
Figure 4.21: Effect of catalyst type on propane Yield of cyclohexane cracking 480 ⁰ C	124
Figure 4.2.2:Effect of catalyst type on propane yield of cyclohexane cracking at 460 ⁰ C	125
Figure 4.23:Effect of catalyst type on propane yield of cyclohexane cracking on at 440 ⁰ C	126
Figure 4.30: Test of First Order Kinetic for gas oil cracking on synthesized zeolite Y Catalyst at 520 ⁰ C	128
Figure 4.31: Test of First Order Kinetic for gas oil cracking on synthesized zeolite Y Catalyst at 480 ⁰ C	129
Figure 4.32: Test of First Order Kinetic for gas oil cracking on synthesized zeolite Y Catalyst at 460 ⁰ C	130
Figure 4.33: Test of First Order Kinetic for gas oil cracking on synthesized zeolite Y Catalyst at 440 ⁰ C	131
Figure 4.34: Arrhenius plot for cyclohexane cracking on Commercial zeolite Y	132
Figure 4.35: Test of First Order Kinetic for gas oil cracking on commercial zeolite Y Catalyst at 520 ⁰ C	133

Figure 4.36: Test of First Order Kinetic for gas oil cracking on commercial zeolite Y Catalyst at 480 ⁰ C	134
Figure 4.37: Test of First Order Kinetic for gas oil cracking on commercial zeolite Y Catalyst at 460 ⁰ C	135
Figure 4.38: Test of First Order Kinetic for gas oil cracking on commercial zeolite Y Catalyst at 440 ⁰ C	136
Figure 4.39: Arrhenius plot for gas oil cracking on commercial zeolite Y	137
Figure 4.40: Effect of temperature on propane yield of gas oil cracking on both catalysts at 520 ⁰ C	138
Figure 4.41: Effect of temperature on propane yield of gas oil cracking on both catalysts at 480 ⁰ C	139
Figure 4.42: Effect of temperature on propane yield of gas oil cracking on both catalysts at 460 ⁰ C	140
Figure 4.43: Effect of temperature on propane yield of gas oil cracking on both catalysts at 440 ⁰ C	141
Figure E1: Chromatograph of cyclohexane cracking over developed zeolite HY at 420 ⁰ C	213
Figure E2: Chromatograph of cyclohexane cracking over developed zeolite HY at 440 ⁰ C	214
Figure E3: Chromatograph of cyclohexane cracking over developed zeolite HY at 480 ⁰ C	215
Figure E4: Chromatograph of cyclohexane cracking over developed zeolite HY at 520 ⁰ C	216
Figure E5: Chromatograph of cyclohexane over commercial zeolite Y at 420 ⁰ C	217
Figure E6: Chromatograph of cyclohexane over commercial zeolite Y at 440 ⁰ C	218
Figure E7: Chromatograph of cyclohexane over commercial zeolite Y at 480 ⁰ C	219
Figure E8: Chromatograph of cyclohexane over commercial zeolite Y at 520 ⁰ C	220
Figure E9: Chromatograph of gas oil cracking over zeolite HY at 420 ⁰ C	221
Figure E10: Chromatograph of gas oil cracking over zeolite HY at 440 ⁰ C	222
Figure E11: Chromatograph of gas oil cracking over zeolite HY at 480 ⁰ C	223
Figure E12: Chromatograph of gas oil cracking over zeolite HY at 520 ⁰ C	224

Figure E13: Chromatograph of cyclohexane over Commercial zeolite at 420°C	225
Figure E14: Chromatograph of cyclohexane over Commercial zeolite at 440°C	226
Figure E15: Chromatograph of cyclohexane over Commercial zeolite at 480°C	227
Figure E16: Chromatograph of cyclohexane over Commercial zeolite at 520°C	228

LIST OF TABLES

Table 2.1: Some known natural zeolites with their codes and years of discovery (Breck and Flannigan 1968).	9
Table 2.2: Zeolite structure type used in commercial and emerging catalytic processes (Dyer, 1988, Weitkamp, 1999)	18
Table 2.3 summary of the principal characteristics of the clay mineral groups	22
Table 2.4: Location of Kaolin Deposit in Nigeria. (Onaji and Ahmed), 1995)	27
Table 2.5: Comparison of Catalytic and thermal cracking products. (Greenfelder, 1949)	49
Table 2.6: Products from Catalytic Cracking of Cyclohexane on Zeolite-Y.	53
Table 3.1: List of Materials/equipment used during Beneficiation	69
Table 3.2: List of Materials/Equipment used during Calcination	69
Table 3.3: List of Materials/equipment used during Dealumination	70
Table 3.4: List of Materials/equipment for Gel formation and actual synthesis of zeolite Y	71
Table 3.5: List of Chemicals used during performance test experiment	72
Table 3.6: List of Equipment used during Zeolite Y catalyst performance test	72
Table 4.1: XRF results of the Raw, Beneficiated and Calcined Elefun kaolin	85
Table 4.2: Effect of dealumination time on the Silica and Alumina content of dealumination Elefun metakaolin by 'novel' method	89
Table 4.3: Variation of dealumination time on Silica and Alumina composition of Elefun metakaolin by conventional method	90
Table 4.4: Variation of chemical constituents of various kaolin with dealumination time by 'novel' method	90
Table 4.5: Variation of chemical constituents of various kaolin with dealumination time by Conventional method	91
Table 4.6: Synthesized Zeolite Y Powder Pattern Identification Table	95
Table 4.7: Comparison of lattice spacing between the developed Zeolite Y and standards Zeolite Y	98

Table 4.8: BET Result analysis for synthesized zeolite Y	103
Table 4.9: XRF results of zeolite NaY, Zeolite NH ₄ Y and Zeolite HY	104
Table 4.10: BET Result for the synthesized zeolite HY	109
Table 4.11 BET Result for the Spent synthesized zeolite HY	111
Table 4.12 Cracking of cyclohexane on developed zeolite Y at 520 ⁰ C	114
Table 4.13 Cracking of cyclohexane on developed zeolite Y at 480 ⁰ C	114
Table 4.14 Cracking of cyclohexane on developed zeolite Y at 4600C	115
Table 4.15 Cracking of cyclohexane on developed zeolite Y at 440 ⁰ C	115
Table 4.16 Cracking coefficient (ka) for cracking cyclohexane	127
Table 4.17 Adsorption coefficient for cracking of gas oil	141
Table B1: Effect of flow rate F (mL/min) on cyclohexane Cracking in Helium Carrier Gas on synthesized zeolite Y catalyst at 520 ⁰ C (P=4.0KPa)	166
Table B2: Effect of flow rate F (mL/min) on cyclohexane Cracking in Helium Carrier Gas on synthesized zeolite Y catalyst at 480 ⁰ C (P=4.0KPa)	166
Table B3: Conversion Using Zeolite Y matrix (25% HY: 75% Metakaolin) at 520 ⁰ C	167
Table B4: Conversion Using Zeolite Y matrix (25% HY: 75% Metakaolin) at 480 ⁰ C	167
Table B5: Cracking of cyclohexane on developed zeolite Y at 520 ⁰ C	169
Table B6: Cracking of cyclohexane on developed zeolite Y at 480 ⁰ C	169
Table B7: Cracking of cyclohexane on developed zeolite Y at 460 ⁰ C	169
Table B8: Cracking of cyclohexane on developed zeolite Y at 440 ⁰ C	170
Table B9: Cracking of cyclohexane on commercial zeolite Y at 520 ⁰ C	170
Table B10: Cracking of cyclohexane on commercial zeolite Y at 480 ⁰ C	170
Table B11: Cracking of cyclohexane on commercial zeolite Y at 460 ⁰ C	171
Table B12: Cracking of cyclohexane on commercial zeolite Y at 440 ⁰ C	171
Table B13: Data for Arrhenius plot of cracking cyclohexane over developed zeolite Y	171
Table B14: Results of Cracking vacuum gas oil on developed zeolite HY at 520 ⁰ C	173
Table B15: Results of Cracking vacuum gas oil on developed zeolite HY at 480 ⁰ C	173
Table B16: Results of Cracking vacuum gas oil on developed zeolite HY at 460 ⁰ C	173
Table B17: Results of Cracking vacuum gas oil on developed zeolite HY at 440 ⁰ C	174
Table B18: Arrhenius plot for cracking gas oil over developed zeolite Y	174
Table B19: Results of Cracking vacuum gas oil on commercial zeolite Y at 520 ⁰ C	174
Table B20: Results of Cracking vacuum gas oil on commercial zeolite Y at 480 ⁰ C	175
Table B21: Results of Cracking vacuum gas oil on commercial zeolite Y at 460 ⁰ C	175
Table B22: Results of Cracking vacuum gas oil on commercial zeolite Y at 440 ⁰ C	175

Table B23: Arrhenius plot for cracking gas oil over commercial zeolite Y	176
Table B24: Results of adsorption coefficients for developed zeolite Y on cyclohexane	176
Table B25: Results of adsorption coefficients for commercial zeolite Y on cyclohexane	176
Table B26: Results of adsorption coefficients for developed zeolite Y on gas oil	177
Table B27: Results of adsorption coefficients for commercial zeolite Y on gas oil	177
Table B28: Effect of zeolite HY% in zeolite Y matrix on cyclohexane cracking at various temperature (P=4.0atm)	177
Table C1: BET isotherm data for zeolite NaY	178
Table C2: BET multi-point data for zeolite NaY	179
Table C3: BET single point surface area data for zeolite NaY	180
Table C4: BET Langmuir data for zeolite NaY	181
Table C5: BET Isotherm data for zeolite HY	182
Table C6: BET Multi-point data for zeolite HY	183
Table C6B: BET single point surface area data for zeolite HY	184
Table C7: BET Langmuir data for zeolite HY	185
Table C8: BET Area Volume data for zeolite HY	186
Table C9: BET Isotherm data for spent zeolite HY	187
Table C10: BET Multi-point data for spent zeolite HY	188
Table C11: BET Multipoint data for spent zeolite HY	189
Table C12: BET Multipoint data for spent zeolite HY	190
Table C13: BET Langmuir data for spent zeolite HY	191
Table D1: Result of cracking experiment using developed zeolite Y (HY) at 440 ⁰ C	192
Table D2: Result of cracking experiment using developed zeolite HY at 480 ⁰ C	192
Table D3: Result of cracking experiment using developed zeolite Y (HY) at 520 ⁰ C	193
Table D4: Result of cracking experiment using commercial zeolite at 440 ⁰ C	194
Table D5: Result of cracking experiment using commercial zeolite at 480 ⁰ C	194
Table D6: Result of cracking experiment using developed zeolite Y (NaY) at 440 ⁰ C	195
Table D7: Result of cracking experiment using developed zeolite Y (NaY) at 480 ⁰ C	195
Table D8: Result of cracking experiment using developed zeolite NH ₄ Y at 420 ⁰ C	196
Table D9: Result of cracking experiment using developed zeolite NH ₄ Y at 440 ⁰ C	196
Table D10: Result of cracking experiment using developed zeolite NH ₄ Y at 480 ⁰ C	197
Table D11: Result of cracking experiment using developed zeolite NH ₄ Y at 520 ⁰ C	197
Table D12: Reference experiment Cyclohexane without any catalyst	198
Table D13: Experiment feed: 40mL/s of gas oil il using HY catalyst at 480 ⁰ C	198

Table D14:	Experiment feed: 60mL/s of gas oil using HY catalyst at 480 ⁰ C	198
Table D15:	Experiment feed: 80mL/s of gas oil using HY catalyst at 480 ⁰ C	199
Table D16:	Experiment feed: 100mL/s of gas oil using HY catalyst at 480 ⁰ C	200
Table D17:	Cracking gas oil on HY at 420 ⁰ C	200
Table D18:	Result of cracking experiment using developed zeolite Y (HY) at 440 ⁰ C	200
Table D19:	Result of cracking experiment using developed zeolite Y (HY) at 480 ⁰ C	201
Table D20:	Result of cracking experiment using developed zeolite Y (HY) at 520 ⁰ C	201
Table D21:	Matrices of produced zeolite HY: Metakaolin (25%: 75%) feed: gas oil at 420 ⁰ C	202
Table D22:	Matrices of Produced zeolite HY: Metakaolin (25%:75%) feed: gas oil a 440 ⁰ C	202
Table D23:	Matrices of Produced zeolite HY: Metakaolin (25%:75%) feed: gas oil at 480 ⁰ C	203
Table D24:	Matrices of Produced zeolite HY: Metakaolin (25%:75%) feed: gas oil at 520 ⁰ C	203
Table D25:	Matrices of Produced zeolite HY: Metakaolin (50%:50%) at420 ⁰ C	204
Table D26:	Matrices of Produced zeolite HY: Metakaolin (50%:50%) at440 ⁰ C	205
Table D27:	Matrices of Produced zeolite HY: Metakaolin (50%:50%) at480 ⁰ C	205
Table D28:	Matrices of Produced zeolite HY: Metakaolin (50%:50%) at520 ⁰ C	206
Table D29:	Matrices of Produced zeolite HY: Metakaolin (75%:25%) at420 ⁰ C	206
Table D30:	Matrices of Produced zeolite HY: Metakaolin (75%:25%) at440 ⁰ C	207
Table D31:	Matrices of Produced zeolite HY: Metakaolin (75%:25%) at480 ⁰ C	207
Table D32:	Matrices of Produced zeolite HY: Metakaolin (75%:25%) at520 ⁰ C	208
Table D33:	Matrices of Produced zeolite HY: Metakaolin (90%:10%) at420 ⁰ C	208
Table D34:	Matrices of Produced zeolite HY: Metakaolin (90%:10%) at440 ⁰ C	209
Table D35:	Matrices of Produced zeolite HY: Metakaolin (90%:10%) at480 ⁰ C	209
Table D36:	Matrices of Produced zeolite HY: Metakaolin (90%:10%) at520 ⁰ C	210
Table D37:	Cracking of gas oil using commercial zeolite at420 ⁰ C	210
Table D38:	Cracking of gas oil using commercial zeolite at440 ⁰ C	211
Table D39:	Cracking of gas oil using commercial zeolite at480 ⁰ C	211
Table D40:	Cracking of gas oil using commercial zeolite at520 ⁰ C	212
Table D41	Cracking of gas oil using commercial Zeolite at 520 ⁰ C.	212
Appendix E		213

CHAPTER ONE

INTRODUCTION

At present, qualitative and quantitative improvement and effective application of hydrocarbon fuels are most keenly desired. Petroleum is the primary source of energy worldwide with global demand presently standing at about 12 million tonnes per day (84 million barrels oil equivalent a day) Pickett; (2010). Hydrocarbon fuels, which are estimated at about 35.3% of the total world's energy in 2010 (see Figure 1.0) have been a key factor in the growth of industry, transportation, the agricultural sector and many other areas serving basic human needs. Present projections suggest an increased demand of up to 16 million tonnes per day (116 million barrels a day) by 2030.

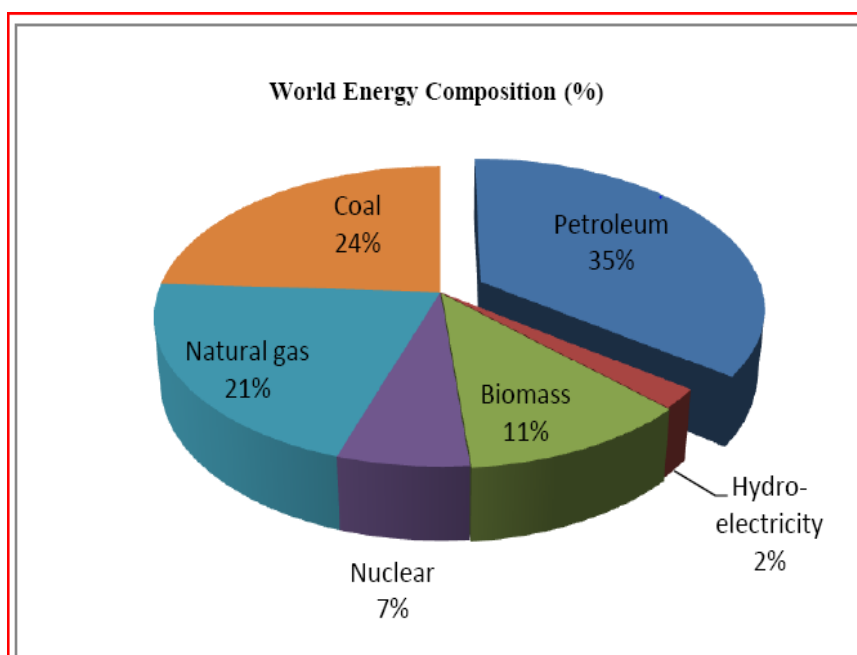


Figure 1.0: World Energy Matrix in Percentage (IEA, 2008)

The rising energy demand which calls for the processing of heavy petroleum feedstock has increased the importance of developing new catalyst systems. Heavier feeds have residue contents of about 40% and require further processing in order to find market. In many parts of the world, light oil production is declining and heavy oil conversion, therefore, becomes increasingly important, to maintain economic viability of these regions. Catalytic cracking is

a process used to break large hydrocarbon molecules into compounds that are used in the blending of gasoline. Further tightening of environmental regulations has extended the imposition on refiners to further reduce sulphur and aromatic levels of the finished products. Additional stringent requirements on the disposal of refinery residues such as coke encourage ‘‘minimum-waste’’ refinery strategies. Other promotional factors for the development of cracking catalysts, as advanced by Plank and Resinki, 1964, Venuto and Habib, 2007 are:

- High activity which allow economic throughput rates.
- High selectivity to gasoline versus coke and light gas compounds
- Attrition resistance
- Thermal and hydrothermal stability (resistance to the treatment in the regenerator)
- Resistance to poisons (metals, nitrogen, etc.)
- Acceptable low cost

According to these criteria zeolite Y seems to be the most attractive choice due to its superior activity, thermal and hydrothermal stability. Nigeria, with a huge amount of oil reserves estimated recently to be about 36.2 billion barrels and the 12th world producer of petroleum, with four refineries across the nation and a total processing capacity of over 450,000 barrel per day consumes approximately 1600 tonnes of zeolite catalysts per day. Over 500,000 tonnes of the catalysts are imported annually, at a cost of over five billion naira (Awe, 2012).

Zeolites are crystalline, microporous, aluminosilicate materials with a three dimensional fully crosslinked open framework structures that form uniformly sized pores of molecular dimensions. The materials have huge industrial, scientific and academic, interest in the areas of ion exchange (treatment of liquid waste, detergent industry, and radioactive waste storage), petroleum refining along with petrochemicals, coal and fine chemical industries (Breck, 1974; Chiang and Chao, 2001; Xu *et al.*, 2007) and separation (purification, drying, and environmental treatment). The ability of zeolite to act as multi-functional materials in many industrial applications is due to their inherent properties such as uniform pore size/shape, catalytic activity, mobile cation and hydrophilicity/hydrophobicity (Adefila and Olakunle, 2008). The pore size of a zeolite plays an important role for adsorbing molecules of different sizes, like a molecular sieve. Therefore, molecules of a certain size are adsorbed by a zeolite and others which are larger than the pore size are not adsorbed.

The discovery of natural zeolites dates back to 1756. Their discovery is attributable to A.F. Cronstedt (Barrer, 1982), who observed that the minerals (stilbites, in particular), when heated, releases vapour, and coined the term “zeolite” (from the Greek words zeo = to boil and litho = rock; that is, stones). As at present, there are about 34 species of natural zeolite minerals known (Table 2.1) and over 100 types of synthetic zeolites of which only very few have practical significance due to their loss of structure after dehydration. They are mainly used in the treatment of hard water, sewage and as a drying agent. Natural zeolites have problems of non uniform pore size, inadequate supply, impurities and low ion exchange capacities. As a result, synthetic zeolites have been developed into a type with better qualities and wider applications. As discussed in Chapter two the synthesis of zeolite involves mimicking the conditions of its natural formation but at lower temperature and much shorter time frame from a few hours to a few days.

Zeolite synthesis is conventionally performed by a hydrothermal crystallization process using commercial chemicals serving as sources of silica and alumina (Barrer, 1982). Such chemicals include sodium aluminate, sodium metasilicate, silica gel, tetraethylorthosilicate (TEOS) and aluminium hydroxide. The chemicals are generally expensive and their process of production is complicated leading to high costs for zeolite production which limits their commercialization (Yaping, *et. al.*, 2008), and uses in many industrial applications.

The use of cheap and readily available materials such as kaolin to serve as a combined source of silica and alumina is highly desirable. The preparation of kaolin into zeolite via a Metakaolinization process has been reported (Chandrasekhar, 1996; Chandrasekhar and, 1999; Bosch *et. al.*, 1983). However, this study is important because kaolin composition varies with location (Bergaya and Ligaly, 2006)]. The use of Elefun Nigerian kaolin (ENK) to prepare zeolites is of value to the industrial aspirations of Nigeria.

A cost comparison of obtaining a silica and alumina source from a chemical feedstock and kaolin/metakaolin has been carried out (Schweiker, 1978). It was shown that clay as a precursor to zeolite Y synthesis has a comparative cost advantage of about 25% over a commercial chemical. This indicates a current cost advantage for kaolin as source of zeolite synthesis over commercial chemicals such as aluminium hydroxide and sodium metasilicate. This experimental work was directed towards the development of zeolite Y from Nigeria Elefun kaolin as a way of understanding the fundamentals of kaolin zeolitization. Further investigations have been conducted to improve the catalytic properties of zeolite Y through generation of active sites otherwise called Bronsted sites through modification of NaY to HY zeolites.

The second area of research in this study is to characterize the developed zeolite Y by subjecting it to a catalytic cracking test in a laboratory scale fixed bed pulse reactor with cyclohexane as a feedstock.

1.1 Statement of the Problem

The Economic development of a nation requires harnessing all her available resources. Kaolin clay, the principal raw material for Zeolite Y production, is in abundance in part of Nigeria and at Elefun in Ogun state, although the country still imports Zeolite Y.

Zeolite Y is basically used as catalyst in the fluid catalytic cracking unit of a refinery for the conversion of higher molecular weight hydrocarbon into simpler, more desirable ones.

Nigeria, with a huge amount of oil reserve estimated recently to be about 36.2 billion barrels, four refineries across the nation with total installed capacity of over 450,000 barrels per day, consumes approximately 1600 tonnes of zeolite catalysts per day. The catalysts are imported annually to the tunes of over 500,000 tonnes, at a cost of over five billion Naira. (Awe; 2012). Furthermore, there is the political implication to national industrial development especially in times of international sanctions, either during war, or in the period of disaffection. Hence, there is an urgent need to develop an indigenous capability to manufacture zeolite Y catalyst.

1.2 Justification of the Study

In view of the above, the issue of local raw materials usage by Nigerian industries became a subject of special interest in the early 1980s, when the vulnerability of the Nigerian economy in general and the manufacturing sector in particular was brought into sharp focus by the worldwide recession that affected the importation of raw materials among other things, and thus gave birth to the idea of sourcing raw materials locally. Nigeria is blessed with abundant deposit of oil and gas as well as solid minerals like kaolin that could be harnessed for national development. Presently, the NNPC relies on the importation of Zeolite Y catalyst used for oil and gas processing in the fluid catalytic cracking unit of her refineries. By mid 2010 Zeolite Y was sold at US\$5/kg and just within seven months, inflation raised the price to US\$140/kg. (Awe; 2012). With four refineries across the nation and a total processing capacity of over 450,000 barrel per day, NNPC consumes approximately 1600 tonnes of zeolite catalysts per day thus spending over 5 billion naira annually for just about 500,000 tonnes of zeolite Y catalyst. Meanwhile, more refineries are expected from the on-going refinery and petrochemical projects in the country. These include :

- (a) Escravos Gas to Liquids (GTL) project jointly owned by the NNPC, Chevron Nigeria and SASOL of South Africa. Its initial capacity of 34,000 barrels per day would, within ten years, be expanded to 120,000 barrels per day and Zeolite Y is the preferred catalysts for GTL processes [Ahmed *et. Al.*, 2014].
- (b) NNPC-Chinese Refinery Agreement to establish three Greenfield refineries and petrochemical plant, in Nigeria, to commission the first one in Lagos with 350,000 barrel per day in 2016. Like any modern refinery the plant will utilize mainly Zeolite Y catalysts.
- (c) The Federal Government of Nigeria has signed a memorandum of Understanding with two US-based firms, to construct modular refineries with a combined capacity of 180,000 barrels of crude oil per day [Daily Trust, 25/9/2012]
- (d) Dangote, the Nigerian business mogul, announced plans in April 2013 to commission a 400,000 barrels per day refinery at Olokola Free Trade Zone on the gulf of Guinea near Lagos, in 2016. This also will require Zeolite Y. With these expected production increase there would be increase in the quantity of Zeolite Y catalyst consumption and hence, more money will be spent on its importation [Ahmed *et. al.*, 2014].

The Processing methods and conditions for zeolites Y synthesis from foreign clay are well known (Barrer, 1978; Zhdanov, 1962; Zhdanov, 1971; 1989; Aderemi, 2000) but there is little or no literature on Nigerian kaolin clays as raw material for zeolite development. It has been established that the nature (crystallinity, composition etc.) of the starting materials effects the type and properties of the final product (Breck, 1974, Aderemi, 2000 and Ajayi, 2012). It is therefore necessary to carry out a careful study of the behaviour of locally sourced kaolin clay, like Elefun kaolin in Ogun state of Nigeria as being done here for the accumulation of relevant information which could be used for the development and production of Zeolite Y Nigeria.

This project would also help to conserve foreign reserves and create employment for our teeming youth.

1.3 Aim and Objectives

The aim of this research is to develop zeolite Y from clay found in Elefun local government area of Ogun state, Nigeria, characterize it and subject it to performance test by using it to crack cyclohexane in a laboratory scale fixed bed reactor using a pulse technique.

This will be achieved through the following objectives:

1. Establishing optimal conditions for producing zeolite-Y from Elefun Nigerian kaolin.
2. Setting up equipment for the microcatalytic study of cyclohexane cracking .
3. Obtaining optimal conditions of cyclohexane cracking on the synthesized zeolite Y.

1.4 Scope of the Study

The scope of this study was limited to:

- (a) Development of Zeolite Y from Elefun clay
- (b) Conversion of the developed Zeolite Y to its Hydrogen form
- (c) Testing the performance of the developed catalyst on Cyclohexane and Gas oil using commercial Zeolite Y catalyst as reference
- (d) Characterize the materials using XRD, XRF, FTIR, SEM, BET surface area and Gas chromatograph

CHAPTER TWO

LITERATURE REVIEW

This chapter discusses some of the previous works done on:

Zeolites as a science, its history, structure and properties;

Local raw materials for developing zeolites;

The hydrothermal synthesis of Zeolite Y and its catalytic performance;

Application of zeolite Y as an important FCC catalyst in the refinery

2.1 Introduction to Zeolites

Zeolites belong to an important class of hydrated aluminosilicate minerals of Group I and Group II elements of the periodic table (Breck, 1974). A defining feature of zeolites is that their frameworks are made up of 4- interconnected networks of atoms. One way of thinking about this is in terms of tetrahedral, with silicon atom in the middle and oxygen atoms at the corners. The tetrahedral can be linked together by their corners to form a rich variety of beautiful structures. The framework structure may contain linked cages, cavities or channels, which are of the right size to allow small molecules to enter i.e. the limiting pore sizes are roughly between 3 and 10 Å in diameter.

Zeolites are highly crystalline and are based on fundamental building blocks of tetrahedral SiO₂ and Al₂O₃ giving rise to a three dimensional network. The structural formula is given as



where

M is the cation present in the zeolite,

n is the cation valency

w is the number of water molecules ,

q / p is the silica to alumina ratio,

(p+q) is the number of tetrahedra present in the unit cell.

The zeolite framework atoms are coordinated to four oxygen atoms bridging two framework atoms. Hence the aluminosilicate zeolite obtained from SiO₄ tetrahedra and AlO₄ tetrahedra possess residual negative charge and are compensated by extra-framework cation (e.g. K⁺ or NH₄⁺). Typical cation includes alkali metal ions, quaternary ammonium ions, etc, which are

usually introduced as templates during the zeolite synthesis to shape the geometry of the lattice during hydrothermal crystallization. The framework composition is represented by square bracket in equation 2.1 (Breck, 1974). The zeolite frameworks are generally open. Water and cations are located within the channel and cavities. The cation presence is needed in the zeolite framework to neutralise the negative charge created as a result of isomorphism substitution of Si^{4+} by Al^{3+} in the framework as explained earlier. The mobility of this cation among other behaviour is of the factors responsible for the unique properties of zeolites (Xu, *et al.*, 2007).

Zeolites were originally discovered as naturally- occurring minerals, about 200 years ago, but are now mostly prepared in the laboratory as will be explained in this research work. Zeolites were naturally found in cavities of basalt rock and later in sedimentary rock much closer to the earth crust. The formation was thought to have been due to several natural activities in the earth crust as enumerated below:

- Deposition resulting from low temperature alteration of marine sediment
- Crystal formation as a result of hydrothermal activity between solution and basaltic lava flows
- Volcanic deposition on alkaline soil
- Volcanic sediment deposition in closed alkaline and saline lake-system
- Formation due to activity of groundwater system on volcanic minerals
- Formation resulting from low grade burial metamorphism

Stilbite was the first natural zeolite discovered in 1756 and today, there are about 36 known natural zeolites (Table 2.1) with well defined structure and applications. They occur with low to medium silica to alumina ratio, hence their applications in industry are highly restricted when compared with their synthetic counterparts. Their best application is found in ion exchange mainly in radioactive treatment (clinoptilolite). They are also used in agricultural activities and as adsorbent (MOR) (Carrado and Garwood., 2003).

Table 2.1: Some known natural zeolites with their codes and years of discovery (Breck and Flannigan 1974).

NO	NAME	YEAR OF DISCOVERY	CODE USED BY IZA
1	Stilbite	1756	STI
2	Natrolite	1758	NAT
3	Chabazite	1772	CHA
4	Harmotome	1775	-
5	Analcime	1784	ANA
6	Laumontite	1785	LAU
7	Heulandite	1801	HEU
8	Scolecite	1801	-
9	Thomsonite	1801	THO
10	Gmelinite	1807	GME
11	Mesolite	1813	NAT
12	Gismondine	1816	GIS
13	Brewsterite	1822	BRE
14	Epistilbite	1823	EPI
15	Phillipsite	1824	PHI
16	Edingtonite	1825	EDI
17	Herschelite	1825	-
18	Levynite	1825	LEV
19	Faujasite	1842	FAU
20	Mordenite	1864	MOR
21	Clinoptilolite	1890	HEU
22	Erionite	1890	ERI
23	Offretite	1890	OFF
24	Kehoeite	1893	-
25	Gonnardite	1896	NAT
26	Dachiardite	1905	DAC
27	Stellerite	1909	STI
28	Ferrierite	1918	FER

29	Viseite	1942	-
30	Yugawaralite	1952	YUG
31	Wairakite	1955	ANA
32	Bikitaite	1957	BIK
33	Paulingite	1960	PAU
34	Garronite	1962	GIS
35	Mazzite	1972	MAZ
36	Merlinote	1974	MER
37	Barrerite	1974	STI

2.2 Structure and Nomenclature of Zeolites

Zeolites are a group of industrial chemical, primarily due to their unique structures. The area of application of zeolites such as ion exchange, catalysis, sorption e.t.c. are all attributed to their framework configurations and pore structure, hence understanding the structural characteristics is an important part of zeolite research. Both natural and synthetic zeolite have been demonstrated in the past to have catalytic properties, aside other usages, for various types of hydrocarbon conversions. They are mainly synthesized from soluble salts of aluminate and silicates, but other monomers are continuously being sort for material conversion and synthesis of advanced material-value addition to existing materials.

The structure of a zeolite is generally described as a three dimensional material with a framework atom connecting tetrahedral with four oxygen atoms (Dyer, 1988; Chandrasekhar, 1996). The framework atom is usually Silicon (Si) and Aluminium (Al. However other metals such as Gallium, Germanium, Boron and Titanium can take the place of Si and Al (Xu, *et. al.*, 2007). Certain zeolitic materials are ordered, porous crystalline aluminosilicates having definite crystalline structure within which there are a large number of smaller cavities which may be interconnected by a number of smaller channels. The cavities and channels are precisely uniform in size and since the dimensions of the pores are such that accept for absorption molecules of certain dimensions while rejecting those of larger dimensions, the materials have come to be known as “molecular sieves” and are utilized in a variety of ways to take advantage of their properties. Such molecular sieves, both natural and synthetic, include a variety of positive ion containing crystalline aluminium silicates. These aluminium silicates can be described as a rigid three-dimensional framework of SiO_4 and AlO_4 in which the tetrahedral are crosslinked by the starting of oxygen atoms whereby the ratio of the total aluminium and

silicon atoms to oxygen is 1:2. The electrovalence of the tetrahedral containing aluminium is balanced by the inclusion in the crystal of a cation, for example, an alkali metal or an alkaline earth metal cation.

The representation of a typical zeolite by its primary building unit is TO_4 where T is the framework atom as shown in Figure 2.1.

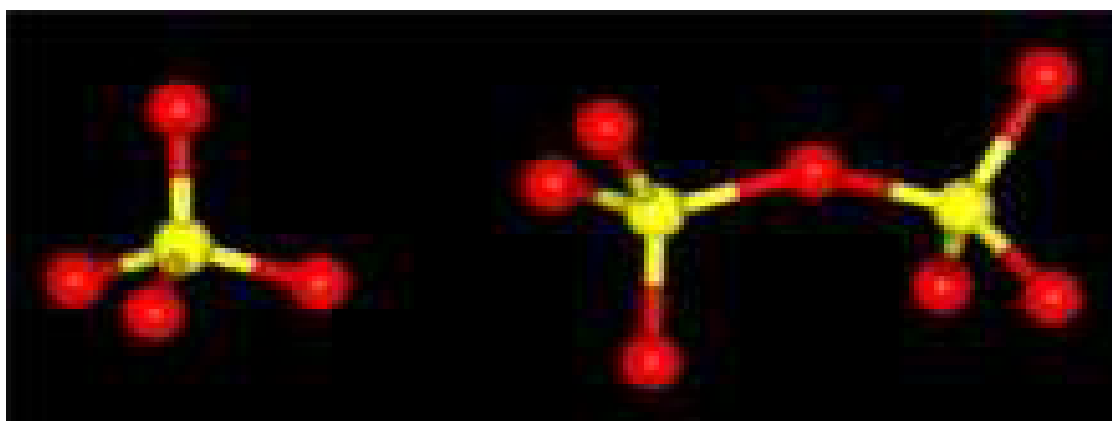


Figure 2.1 The primary building unit TO_4 of zeolite-Y (www.port.ac.uk/zeolite,2009).

The primary building block of zeolite is represented by (TO_4) tetrahedra. The primary building unit (PBU) creates an infinite lattice of identical building blocks of repeating unit called secondary building unit (SBU). The SBU is the main unit that describes the zeolite structure with the exception of the water and cation in the framework. There are twelve known SBUs that describe all the known zeolite frameworks as shown in Figure 2.2. Cations are located within the zeolite pores to compensate for the residual negative charge generated by the isomorphous substitution of Si^{4+} by Al^{3+} during the zeolite framework formation. Zeolite frameworks are created from the listed SBUs and in some cases combinations of SBUs are used to form zeolites. For example, zeolite A is generated using 4 ring or 6 ring and can also be formed from double 4 ring building unit. Zeolite Y can be obtained from sodalite framework which is made of 4-member ring or single 6 member ring. It can also be formed from double 6 ring building unit. A description of the structure of zeolite Y which is the nucleus of this work is given in Section 2.4. The molecules of water and cations present in zeolite framework are mobile with the water molecule capable of being removed reversibly at a temperature between 100-500°C when dehydrated. The zeolite structure is generally stable up to temperatures between 700 to 800°C. (Dyer, 1998).

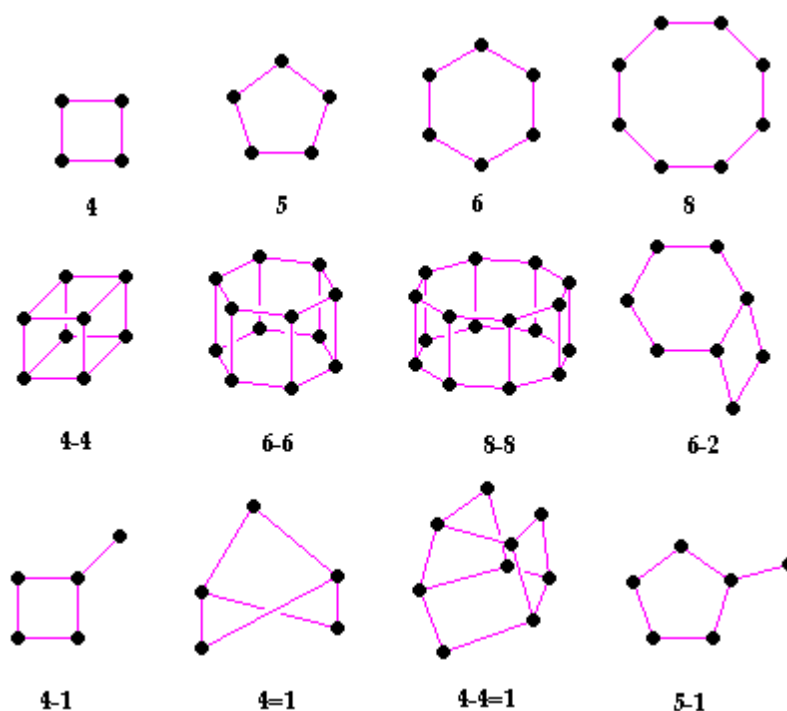


Figure 2.2 Existing secondary Building Units (SBUs) in zeolite Framework (www.ch.ic.ac.uk, 2013).

The nomenclature of zeolite framework has also changed over the years with the early zeolites synthesized by Breck and co-workers named using Arabic letters such as zeolite A, B, or Alphabets D, H, X, Y etc. This later progressed into the use of Greek letters to represent the zeolites produced by Mobil company researchers. Examples include zeolite Alpha, Beta, Omega etc. The naming of synthesized zeolite was later taken further by assigning the name of parent zeolite mineral when the synthesized zeolite has the same topology as the parent mineral. Examples include synthetic mordenite, chabasite and erionite.

The structural committee of International Zeolite Association (IZA) finally produced an atlas of zeolite structure in which each zeolite framework type is assigned a three-letter code to describe and define the network of corner sharing, tetrahedrally coordinated atoms irrespective of its composition (Xu, *et. al.*, 2007, Jiri, *et. al.*, 2007). The three letter codes are usually derived from the source material's name. There were about 200 different zeolite frameworks as at November 2012 and each with its individual code (IZA, 2012). For example zeolite X and Y are assigned code FAU meaning zeolite with faujasite. Zeolite A is assigned the code LTA meaning Linde type A framework and ZSM-5 and silicalite with illustrative

code as MFI. Today the name of zeolites follows the three major conventions and they are all accepted.

2.3 Pore Structure

The structure of zeolite cannot be completely explained without the understanding of its pore sizes. The adsorption properties of a zeolite in terms of its molecular sieving capacity and the selectivity are firmly rooted or dependent on the size and shape of the pores present in the zeolite framework. Zeolites can be classified based on the pore size which is defined by the number of T atoms present in the framework where T = Si or Al. The pore opening systems are known in zeolites especially for Catalytic and Adsorptive processes. They are: 8- member rings, also called small pore opening,(examples include zeolite A and erionite); 10- member rings, also called medium pore zeolite,(the prominent member of this group is ZSM-5 zeolite), 12 member ring opening also called large pore zeolite , for which zeolite X and Y are typical examples(an examples of the main pore systems in zeolite Y is shown in Figure 2.3).

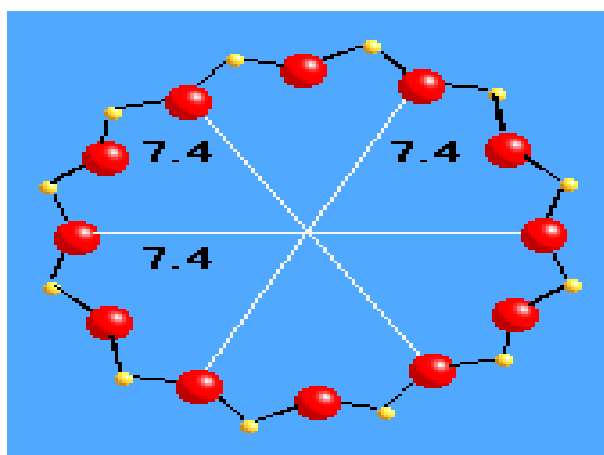


Figure 2.3: 12- ring Pore structure of zeolite Y studied in this research
[IZA, 2012]

To determine the nature of pore size in zeolites, a selection of molecular probes is used for adsorption process through the zeolite. For example, cyclohexane with size 6.5 to 7.4Å cannot be absorbed into 8-member ring pore system but can be readily absorbed into 12 member ring hence cyclohexane can be used as a probe for only large pore zeolite and not small pore zeolite. The classification of pore structure has also been based on the dimensionality of the pore system and the shape of the pore opening.

2.4 Description of Zeolite Y

Zeolite Y also known as faujasite has its sodalite cage linked with double 6-ring, resulting in a super cage with 12 ring pore opening (Figure 2.5). It has 3-dimensional channel system and can be imagined as stacking layers of sodalite cages similar to the arrangement of carbon atoms in diamond (Dyer, 1988). The X and Y type zeolites are known to have the same framework structures but only differ in their framework Si/Al ratio. Zeolite X has Si/Al ratio of 1 to 1.5 while zeolite Y has Si/Al greater than 1.5 but not more than 10 (Xu, 2007, Jen and Dutta, 1991). The large pore size and three dimensional channel systems in zeolite Y enable it to be thermally stable and it has become an important material in catalytic cracking operation. The thermal stability can be further increased by dealumination, by increasing the Si/Al ratio and producing ultra-stable zeolite (USY), a material currently used in the cracking of crude oil.

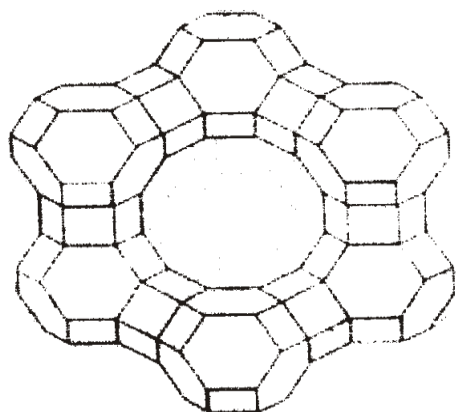


Figure 2.4: Zeolite-Y structure type FAU (Ramirez, 2009)

2.5 Properties of Zeolites

In this section, the properties of zeolites are discussed.

2.5.1 Ion- exchange

Ion exchange is an intrinsic characteristic of most zeolites and has become one of their most commercially important properties. It is the property that allows the replacement of cation held in the zeolite framework by an external ion present in a bulk solution or in a melt (Dyer, 2008). The ion exchange property is due to the isomorphous substitution of Si^{4+} by Al^{3+} in

the framework creating a net negative charge as explained in Section 2.1. Different types of cations can be used to compensate for the ionic imbalance in the zeolite framework and to maintain ionic neutrality. Zeolites are generally synthesised using Na^+ ion as the compensating cation in the framework and in an exchanging reaction. Other cations such as Mg^{2+} , Ca^{2+} , NH_4^+ and H^+ can replace Na^+ (Adefila Olakunle, 2008).

An example of exchanging of sodium ion in zeolite framework by Ca^{2+} is shown in equation 2.2



Where Z is the zeolite.

Similar reactions are used in the generation of the acid catalyst when the cations in the zeolite framework are exchanged with proton from mineral acid or ammonium hydroxide thereby producing a protonated zeolite used as catalyst. The properties of zeolites as ion exchange material is widely used and applied in detergents, waste water treatment and radionuclide separation (Jiri *et al*, 2007, Babalola, et al., 2014).

2.5.2 Catalysis

Zeolite has catalytic property which is responsible for its application in petroleum industries. About 99% of the world petrol from crude oil depends on zeolite as catalyst for its production. The catalytic characteristics of zeolites are due to the combination of the intrinsic properties of zeolite. The properties are responsible for the overall behaviour of zeolite as a catalyst. However, the generation of active sites otherwise called Bronsted sites (Figure 2.7) by ion exchange of ammonium hydroxide followed by calcination is the most important step in the production of zeolites as catalysts. Bronsted site is known as bridging hydroxyl and is generated at oxygen bridge site near the Si-O-Al cluster where the compensated cation is represented by protons (see Figure 2.7) being the main reason why zeolite is used as an industrial catalyst. This is because of the production of hydroxyl within the zeolite pore structure where there are high electrostatic field attracting organic reactant molecules and bond rearrangement can take place, especially for cracking reactions.

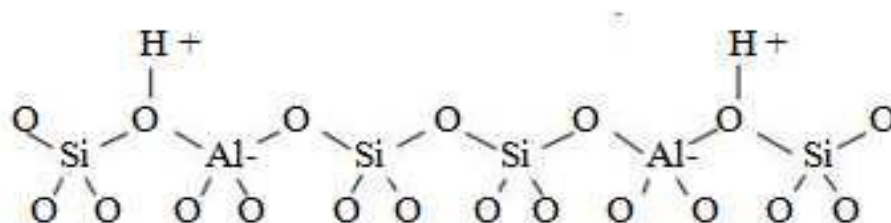


Figure 2.5: Bronsted acid site in zeolites (<http://copweb.com>, 2012)

2.5.3 Adsorption

Adsorption can be described as a process whereby molecules of a gas or liquid material adhere to the surface of solids. The process can be used to separate two mixtures of species depending on the affinity of the mixtures toward the solid surface. The solid surface is known as adsorbent while the adhering molecule is called adsorbate. The process of removing the adhered molecules is called desorption and this is achieved by changing the pressure-temperature equilibrium of the system which allows the reuse of the adsorbent. The adsorption mechanism in zeolites depends on several factors such as the pore size of the zeolite, the ion exchange, the physical and chemical composition of adsorbate. These mechanisms include:

- a. Equilibrium selective adsorption
- b. Rate selective adsorption
- c. Shape selective adsorption
- d. Ion exchange
- e. Reactive adsorption.

Adsorption is an important characteristic of all zeolite as it directly influences the use of the material as catalyst and separator. Adsorption in zeolite have both economic and environmental benefits because of its uses in oil refining and petrochemical over several years as catalysts just like its application in pollution abatement. Some of the important uses of the adsorption and molecular sieving properties of zeolite include drying agent (zeolite 4A is used as general purpose drying agent such as gas drying column in GC), gas separation (pollution control) and separation of bulk mixture such as i-paraffin/n-paraffin system. Other specific utilization of adsorption properties of zeolites include.

- Aromatic removal from linear paraffin in the C10-C15 range used in linear alkyl benzene production
- Nitrogenate removal
- Oxygenate removal
- Sulphur removal

2.6 Application of Zeolites

Both natural zeolites and synthetic zeolites have become an important and integral part of many process industries. The global market for zeolite production has continued to blossom to the extent that the world market for synthetic zeolite has been estimated to be around 1.8 million metric ton (t) while that of natural zeolite was projected to hit 5.5t in 2010 (Kulprathlpanja, 2010). Both types of zeolite have important uses while 90% of natural

zeolites are mainly applied in the construction industry with the remaining used in such processes as animal feeding, horticulture, waste water treatment, odour control and other miscellaneous applications. Synthetic zeolites are mainly applied in process industries. According to the data obtained in Bartholomew, 2001, 81% of synthetic zeolite is used in the detergent industry (zeolite A) while the rest are used in catalysis, adsorption and other applications. Zeolites utilize the ion exchanging characteristic to function as an additive in detergents. In detergency, zeolites typically zeolite A (LTA), act as water softener preventing carbonate precipitation through the exchange of calcium and magnesium ions with the highly mobile sodium ion present in the zeolite framework (Renzo and Fajula, 2005). The increased application of zeolites in the detergent industry can be attributed to environmental concern. The use of phosphate builder has been banned in most countries because it causes eutrophication and is difficult to degrade when placed in water bodies, hence zeolite A and zeolite X offer good replacement because of their high ion exchanging capacities. The application of zeolites has its largest economic impact in the FCC processes. Zeolites Y and ZSM-5 are two very important zeolites used in FCC to give increased yield over amorphous catalyst, to the tune of around 1 billion US dollar a year (Weitkamp and Puppe, 1999). In fact ZSM-5 zeolite is regarded as good octane booster. Other octane booster zeolites in fluid catalytic cracking operation include mordenite, silicalites, MCM-20 and zeolite beta. Another example of the use of zeolites in catalysis is in hydrocracking, which involves the conversion of higher paraffins over noble metal containing zeolite catalysts to yield distillate products. The description of the hydrocracking processes including all the mechanism is well documented (Ling, *et al.*, 2009) but the main point is the crucial role played by zeolite catalyst in the process replacing the old catalyst such as alumina. Examples of application of zeolites in different catalytic processes are presented in Table 2.2.

The physicochemical characteristics of zeolites have now been explored in novel and non traditional applications. Some of the most recent applications of zeolites in modern processes include:

- Optics and electronics (Zhang *et al.*, 2001)
- Bio-catalysis (Hartmann, 2005)
- Synthesis of nanostructure catalyst (Lei *et al.*, 2007) ,(Teo *et al.*, 2003)
- Drug release (Shan *et al.*, 2006), (Davis *et al.*, 1996)

Table 2.2: Zeolite structure type used in commercial and emerging catalytic processes (Dyer, 1988, Weikamp and Puppe, 199)

Zeolite type	Catalytic processes
FAU(Y)	Catalytic cracking, hydrocracking, aromatic alkylation,
MON(mordenite)	NOX reduction, acetylation
MFI(ZSM-5, TS-1 and silicalite)	Light alkane hydroisomerization, hydro cracking, dew axing, NOX reduction, Aromatic alkylation and
BEA (beta)	Dewaxing, methanol to gasoline, methanol to olefin and product, FCC additive, hydrocracking, olefin
LTL(KL)	Benzene alkylation, aliphatic alkylation, Acetylation
MWW(MCM-22)	Baeyer Villiger reaction, FCC additive, etherification
CHA(SAPO-34)	Alkane aromatization Benzene alkylation Methanol to olefin Long chain Alkane hydroisomerization,
AEL(SAPO-1) RHO (Rho)	Beck mann re- arrangement Amination
TON(ZSM-22)	Long chain alkene hydroisomerization

2.7 Local Raw Material for Zeolite Synthesis

The major raw materials for the development of zeolites are clay and rice husk.

2.7.1 Rice husk : Rice husks (also known as rice hulls) are the thin membranous coverings of rice grains and are agricultural wastes which are plentiful in rice producing nations like Nigeria. The world production of rice is at over 500 million tonnes per year.

Rice husks are used as raw materials for the synthesis of zeolites because of:

- (a) **High Silica Content;** rice husk is one of the most silica-rich raw materials with its ash (RHA) containing about 90-98% silica. With such large ash and silica content it is economical to manufacture sodium silicate which serve as precursor to zeolite synthesis.
- (b) **Solution to the Problem of Disposal;** rice husk is majorly used as boiler fuel and the ash recovered (*because of its low bulk density of about 200 kg/m³*) poses disposal problems. Rice husk causes environment problem because its a waste. It has no other uses than to be used as fuel. Meanwhile the production of sodium silicate utilizes both rice husk and its ash as a waste.
- (c) **High Quality of Sodium Silicate;** compared with other expensive methods and sources of silica such as the silica sand (or quartz) process, the rice husk process is less expensive and in addition solves disposal issues as opposed to using sand and quartz which have other competitive uses in construction. Thus, rice husk is an alternative to silica or quartz sand.

2.7.2 Clay and its classification

Clay may be regarded as fine-grain mixtures of several minerals which form a plastic mass with water. They may be classified according to the mineralogical composition or properties. (Guggenheim et al,1998). It is in abundance than rice husk. Therefore the main focus of this research is to develop zeolite Y from clay. It is very paramount here to have good understanding of the types, formation, structure and properties of clay. Ahmed and Onaji, (1995) classified clay according to its properties and uses as:

A. White- burning clays

I. Kaolins

(a) Residual (primary)

(b) Sedimentary (secondary)

II. Ball clays

B. Refractory clays (fusion point above 1600°C)

I. Kaolins (sedimentary)

II. Fireclays

III. High alumina clays

C. Heavy clay-products clays (low plasticity but containing fluxes).

D. Stoneware clays (plastic, containing fluxes)

E. Brickclays (plastic, containing iron oxide)

F. Slip clays (containing more iron oxide)

There are two types of kaolin- clay:

Residual clays are clays found side-by-side with the altered igneous rocks from which they are formed. They are usually extracted from the parent rock and obtained in comparatively pure state. An example of such clay is China clay in Cornwall, United Kingdom.

The sedimentary clay, are those which have been removed from their origin by natural agencies. As a result of this movement, many impurities (fine-grained in nature) are picked up in transit and are difficult or uneconomical to remove (Worrall, 1986). This is further divided into 4 groups:

- a. The kaolinite
- b. The Montmorillonite/smectite
- c. The Illite
- d. The Chlorite

Elefun kaolin in Ogun state, Nigeria is believed to belong to this class, i.e. sedimentary, resulting to its high level of impurities.

Clay minerals are part of a general but important group within the **phyllosilicates** (member of silicates family) that contain large percentages of water trapped between the silicate sheets. Most clays are chemically and structurally analogous to other phyllosilicates but contain various amounts of water and allow more substitution of their cations (Ahmed and Onaji 1995,). Many types of clays are found in nature, as shown in Table 2.2, with, kaolinite, montmorillonite, hydrous mica, vermiculite and allophone clay being the five most important. The first four are crystalline and can be regarded as small sheet-like particles.

Table 2.3 Summary of the principal characteristics of the clay mineral groups (Granizo et al., 2000)

	Kaolinite group	illites	smectites	vermiculites
Structure type:	1.1 tetrahedral and octahedral components Di-octahedral	2.1	2.1	2:1
Octahedral component:	Nil	Mostly di-octahedral	Di- or tri- octahedral	Mostly trioctahedral
Principal interlayer cations:	Nil	K	Ca,Na	Mg
Interlayer water:	Only in halloysite (one layer water mols) 7.1 Å (10 Å in hallosite)	Some in hydromuscovite	Ca, twolayers; Na, one layer water mols	Two layers
Basal spacing:	Taken up by hallosite only	10Å	Variable, most-15Åt(for Ca)	Variable:14.4 Å when fully hydrated
Glycol:	Al ₄ Si ₄ O ₁₀ (OH) ₅ little variation	No effect	Takes two layers glycol. 17Å	Takes one layer glycol,14 Å
Chemical formula:	Kaolinite scarcely soluble in dil.acids	K10-15 Al ₄ (Si ₄ A)O ₂₀ (OH) ₅	M ⁺ ₆ 4Y ³⁺ Y ³⁺ ₄ ⁻ 4(SiAl) ₄ O ₂₀ (OH) ₄ nH ₂ O	M ² _{0.44} (Y ²⁺ , Y ³⁺) ₆ (Si ₂ Al) ₄ O ₂₀ (OH) ₄ 8H ₂ O
Acids:	Halloysite collapse to approx 7.4Å. other unchanged	Readily attacked	Attacked	Readily attacked
Heating 200 ^o c	Kaolinite → Metakaolite (7Å)	No marked change	Collapse to approx.10Å	Exfoliation: Shrinkage Of layer spacing
650 ^o c	Dickite → Metadikite Strong (14Å)	10Å	9.6 10Å	Collapse to 9 Å
	1.55-1.56 1.56-1.57 -0.006 24.50°			
Optics z Y δ 2v _z	Alteration of acid rocks,feldspars etc Acidic condition	1.54-1.57 1.57-1.61 -0.03 <10	1.48-1.61 1.50-1.164 0.01-0.04 Variable	1.52 -1.57 1.53-1.58 0.02-0.03 < 18°
Paragement:		Alteration of micas, feldspars, etc. Alkaline conditions. High Al and K concentrations	Altration of basic rocks or Volcanic material. Alkaline conditions. Availability of Mg and Ca; Deficiency of K.	Alteration of biotite flakes or of volcanic material, chlorites, hornblende. etc.

2.7.3 Kaolin Clay

Kaolin is a chalk-like, lightweight, soft sedimentary rock that has an earthy odor and contains 85-95% of the mineral known as **kaolinite**. Beside kaolinite, kaolin usually contains mica, quartz and also, less frequently, anatase, montmorillonite, ilmenite, feldspar, haematite, bauxite, zircon, illite, rutile, kyanite, sillimanite, graphite, attapulgite, and halloysite. Rocks that are rich in kaolinite are known as **China clay** or simply **kaolin** (simplified Chinese: pinyin; Gǎolín tǔ), named after Gaolin (“High Hill”) in Jingdezhen, Jiangxi province, China and were traditionally used in the manufacture of porcelain. It was first described as a mineral species in 1867 when found in the Jari River basin of Brazil (www.mindat.org, 2005). Others claimed that, the name “kaolin” is derived from the word Kau-Ling, or high ridge, the name given to a hill near Jau-chau Fu, China, where kaolin was first mined (Sepulveda et al, 1983).

2.7.3.1 Structure of kaolinite

The theoretical formula for kaolinite is $\text{Si}_2\text{Al}_2\text{O}_5(\text{OH})_4$ (other formulae are $\text{Al}_2\text{O}_3 \cdot 2\text{H}_2\text{O}$ and $\text{Al}_2\text{O}_7\text{Si}_2 \cdot 2\text{H}_2\text{O}$), its molecular weight is 258071g/mol. Kaolinite is built up from pseudohexagonal triclinic crystals with diameter 0.2 – 10um, thickness 0.7nm and its density is 2.6 g/cm³ (www.chemicaland21.com,2007). Kaolinite has a 1:1 sheet structure composed of SiO_4 tetrahedra sheets and $\text{Al}(\text{OH})_6$ octahedral sheets (or, expressed in another way, $[\text{Si}_2\text{O}_5]$ sheet and $[\text{Al}_2(\text{OH})_4]$ sheet) with pseudo-hexagonal symmetry (Lee and Deventer, 2003). The sheets are created from planes, which are occupied as follows: $\text{O}_6 - \text{Si}_4 - \text{O}_4 - (\text{OH})_6$. The morphology of the kaolin crystals is plate-like. The c-axis of the kaolinite crystal is perpendicular to the basal plane. A crystal system of the kaolinite is triclinic, the space group is P1, and lattice parameters are $a = 0.515 \text{ nm}$, $b = 0.895 \text{ nm}$, $c = 0.740 \text{ nm}$, $\alpha = 91.68^\circ$, $\beta = 104.87^\circ$, $\gamma = 89.9^\circ$. An ideal cell of the kaolinite is electrically neutral. Its crystallochemical formula is $\text{Al}_4\text{Si}_4\text{O}_{10}(\text{OH})_8$ (Čičel *et. al.*, 1981).

Kaolinite, when mixed with water becomes plastic and easy to mold. However, it loses its water of crystallization between 390 and 450 degree Celsius. It is very soft with a hardness of 2.0-2.5 on the Mohs scales and has a specific gravity of 2.58-2.60. The first model of structure was designed by Bindley and Nakahira (1959), shown in figures 2.6, 2.7 and 2.8:

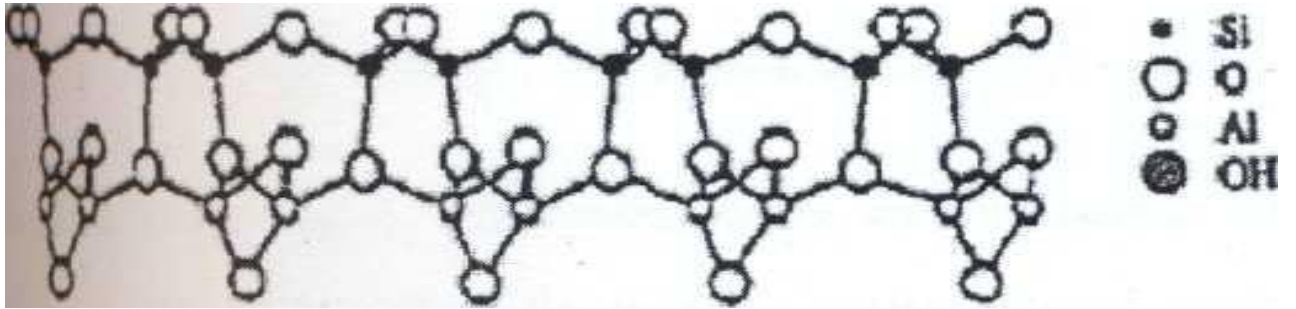


Figure 2.6: Structure of kaolinite designed by Brindley Nakahra, viewed from the a-axis direction

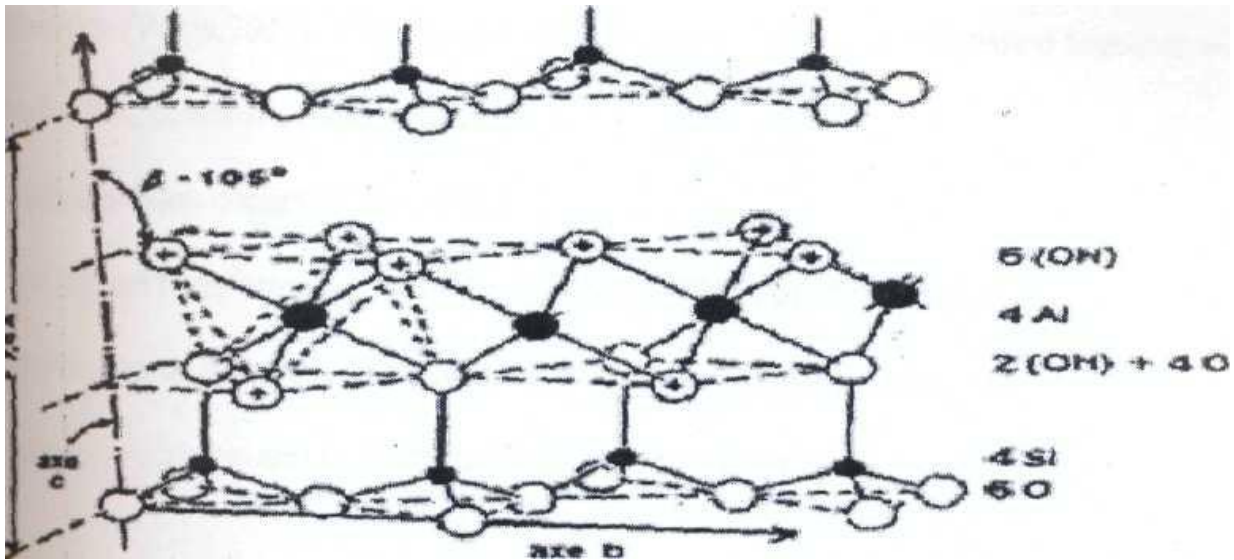


Figure. 2.7: Crystallochemical structure of kaolinite (Brindley and Nakahra.,1959)

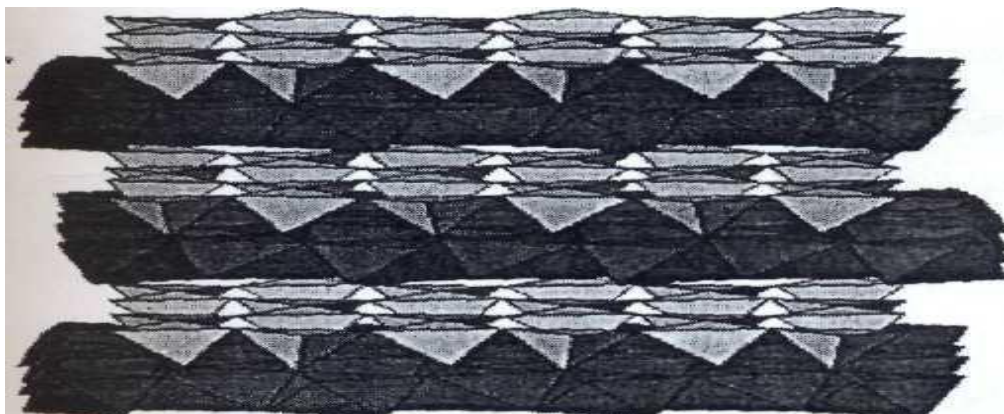


Figure 2.8: The change of the tetrahedral (light) and octahedral (dark) sheets (Brindley and Nakahra.,1959)

2.7.3.2 Formation of kaolinite clay

Kaolinite is formed by rock weathering and its colour varies from white to grayish-white, or slightly coloured. Kaolinite is thought to be formed mainly by decomposition of feldspars (potassium feldspars), granite, and aluminum silicates. The process of kaolin formation is called kaolinization (Varga, 2007). It is also not uncommon to find kaolin deposited together with other minerals (illite, bentonite, halloysite, etc).

Kaolinite formation occurs in three ways:

- Transformation of rocks due to hydrothermal effects (Cornwall type).
- Crumbling and transformation of rocks due to the effects of climate factors (Zettlitz type).
- Formation by climate and hydrothermal effects (mixed type)

Earlier workers' visualization of simple transformation from primary minerals such as feldspars to clay minerals like kaolinite has shown a nonconforming attitude, considering that the structures of the two minerals differ. For many situations it seems that the primary minerals undergo fairly complete decomposition to simple substances followed by the synthesis of the individual clay minerals. This involves principally the arrangement of the silicon-oxygen tetrahedral and the aluminium octahedral both of which become aligned to form sheet within the clay minerals (Varga, 2007). The nature of the weathering environment plays an important role in determining type(s) of mineral that can be formed and extent of purity.

Prolonged leaching of a soil in which montmorillonite has formed can lead to the development of high acidity and conditions favourable for breakdown of montmorillonite and the formation of kaolinite. Kaolinite is frequently formed directly from primary minerals in the soils of the humid tropics. Although kaolinite is very stable, it can weather to form gibbsite, $Al(OH)_3$. Kaolin can also be formed by the resilication of aluminum oxide if the weathering zone is invaded by silica-rich waters.

Ironically, noncrystalline or amorphous minerals exist where volcanoes throw ash and cinders into the air, and they solidify before the atoms become organized into crystalline lattices. In the humid tropics, amorphous mineral weather rapidly into crystalline allophone. The soil formed lack discrete mineral particles and are like a gel and feel like mucky soils when wet. Slowly, the allophane clays become more crystalline or organized (Varga, 2007).

2.7.3.3 Nigeria kaolinite clay

Ahmed and Onaji (1995) reported that there are about 46 known clay deposits at various locations in Nigeria, where kaolin type of clays suitable for local sourcing of industrial raw materials and for application in ceramic industries are found RMRDC (2000) and also published information on availability and suitability of kaolin clay in the country. Emofuriefu, (1992), in his work explains that Nigeria clay deposits are basically of two types- the basement derived (residual) clay and the decrial (sedimentary) clay. He concludes that Nigeria decrial clay deposits were probably laid down as sedimentary mud in the ancient marine and blackish water environment which is most likely the reason for the high content of inherent impurities, found in some Nigeria kaolinite clays. Kovo, (2010) carried out a study in United Kingdom on Ahoko Nigeria kaolin and concluded that the deposits is suitable for the development of faujasites zeolites and its membrane though was faced with the challenge of high quartz content. Similarly, Ajayi et al, (2010) developed zeolite with large pores from Kankara kaolin though faced with the challenge of low crystallinity which probably was due to effect of composition of deposit. This research is looking into the possibilities of developing a highly crystalline zeolite Y from Elefun kaolin of Ogun state, Nigeria to serve as a potential replacement for the imported ones.

Table 2.4: Locations of Kaolin Deposit in Nigeria. (Onaji and Ahmed,1995)

Clay	Location (State)	Al ₂ O ₃ %	Si ₂ O ₃ %	Fe ₂ O ₃ %	CaO+MgO %	LOI	Refractoriness (PCE)	
							Cone Equiv. No	T°C
Alkaleri	Bauchi	25.43	54.30	1.05	1.00	15.73	33.5	1740
Onibode	Abeokuta(Ogun)	39.30	42.30	Trace	1.05	14.20	>34	>1740
Elefun	Abeokuta (Ogun)	37.0	53.80	2.57	0.30	0.69	33	1730
Oshiele	Abeokuta (Ogun)	28.30	53.40	1.35	0.88	15.00	33	1730
Orun	”	34.55	50.55	2.05	1.10	15.50	33	1730
Ozubulu	Nnewi (Anambra)	19.31	58.30	1.55	1.25	14.16	32	1710
Enugu	Enugu(Enugu)	22.71	55.00	2.42	1.95	16.35	29	1650
Nsu	Okigwe(Imo)	30.22	50.60	1.90	1.08	10.54	32	1710
Okpekpe	Auchi (Edo)	24.30	53.20	1.45	1.30	16.86	29	1650
Kankara	Kankara(Kastina)	38.64	44.50	Nil	1.30	16.70	34	1760
Giro	Giro(Sokoto)	38.72	43.54	2.10	1.48	14.00	34	1760
Warram	Warram(Plateau)	37.13	43.54	1.15	0.58	14.20	34	1760
Sabon Gida	Jos(Plateau)	25.88	25.32	13.10	3.20	18.36	27	1610
Ukpor	Nnewi (Anambra)	33.20	48.00	1.20	0.73	12.12	33	1730
Ifon	Ifon (Ondo)	36.80	47.90	0.67	1.11	12.32	33	1730
Oza Nagoga	Oza Nagogo(Edo)	38.07	46.00	0.78	0.23	13.7	33	1730

2.7.3.4 Processing of kaolinite clay

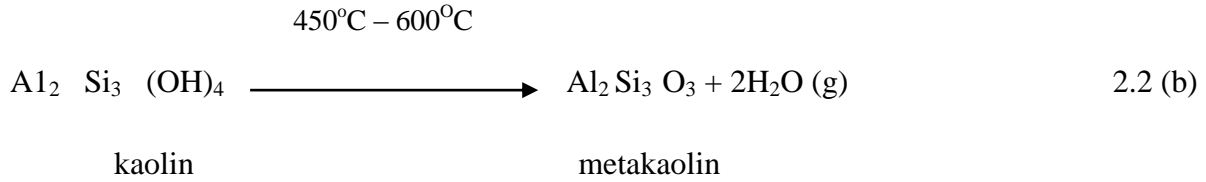
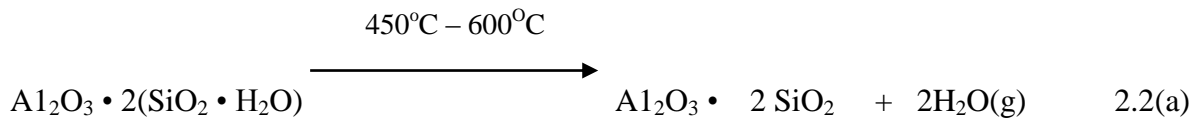
As earlier stated, it is difficult to obtain kaolin without impurities. The associated minerals here termed inherent impurities impair the primary characteristics of kaolin and affect its utility for various applications (Murat et al., 1992). Deposits of kaolin are usually associated with various impurities like quartz, anatase, rutile, pyrite, siderite, feldspar, etc, depending on the origin and depositional environment (Grimshaw, 1971). One of the most important effects of impurities is its fluxing ions like Na, K, Ca and Mg, derived from micas and other associated compounds. The ions, when present, lower the melting point of the system and, in particular, react with silica at a temperature as low as 100°C to form viscous liquid, which on cooling does not crystallize but solidifies to form glass, in which the fluxing ions occupy holes in the Si-O network. Sometimes, the impurities are finer than the clay mineral, which therefore, present difficulties in the separation processes (Asmatulu and Turk, 2002). In addition, improvement on the properties of kaolin by chemical methods is difficult, because

of the high passivity of the material (Belver et al, 2002). Despite the aforementioned, various processing methods for clay involving both physical and chemical methods have been developed and are in use today.

The processes of upgrading kaolin includes sieving, magnetic separation (Shoumkov, et al, 1987; Asmatulu, and Turk,2002), selective flocculation (Farhount, 1989), application of ultrasound (Komsakaja, et al, 1971), leaching with various chemicals like oxalic acid and other organic acids (Veglio and Toro, 1994; Ambikadevi Lalithambika, 2000) etc. The use of confirm organic acids in the presence of a fermented medium (de Mesquita et al, 1996), containing microbially, produced oxalic & hydrochloric acid (Groudev, 1999), carbohydrates (Veglio & Toro, 1994), EDTA (Borggaard, 1979), sodium dithionate-H₂SO₄ mixture (Conley & Lloyd, 1970), etc. This has been found suitable for removal of most impurities in the mined kaolin. Recently, due to the environmental protection issues, researchers are looking into use of microorganism in pretreating minerals especially kaolin. One of such organisms that has found application in this area is *aspergillus niger*, used to digest iron oxide and co-cultured enzymes for removal of combined oxides in kaolin (Hosseini *et. al.*, 2007; Lee, *et. al.*, 2002, and Pradhan *et. al.*, 2006). Most of the listed methods require pure grade chemicals and enzymes which are pretty expensive and most often not readily available in developing countries like Nigeria. Combination of various methods of beneficiation is applied for kaolin treatment, namely; wet method (i.e. soaking and sieving), deflocculating, thermal and acid treatment. Additionally, most by-products resulting from use of chemical method of purification, as highlighted before, might enchanter' challenges during separation procedure.

2.7.3.5 Effect of heat on kaolinite clay (dehydroxylation)

Resulting from the mechanical and electrical properties of kaolin, dehydroxylation begins at the temperature of about 450°C. A later finding shows that the beginning of dehydroxylation can be shifted to about 420°C. A chemical equation of dehydroxylation can be represented by several ways. The chemical equations describing this process are shown in Equations 2.2 a and b.



It can be considered that in a unit cell there are eight OH groups, which undergo the change, represented in Equations 2.3a and b.



Or



The water vapour (in Equation 2.3) carries away about 13.96% of the mass of the stoichiometric kaolinite during dehydroxylation, which occurs primarily on the phase boundary. A mechanism of dehydroxylation includes a transport of OH⁻ groups to the phase boundary, then the reaction of the groups on the boundary and, finally transport of the products (molecules H₂O) to the edge of the crystal (Horvath and Kranz, 1980). The rate of dehydroxylation is determined by the slowest step in the process. It was revealed that this process is diffusion of the water molecules between layers of the kaolinites structures (Kozik *et. al.*, 1992; Horvath 1976; Toussaint *et. al.*, 1963). Accordingly, the dehydroxylation is controlled by diffusion. Activation energy of dehydroxylation for the following degree of the conversion $0 < \alpha < 0.65$ is 140 – 190 kJ.mol H₂O depending on size and defects of the kaolinite crystals. The smaller the crystal size and the more the defects, the less activation energy is observed, which can decrease to 100 kJ/mol H₂O (Horvath and Kranz, 1980) the rate of dehydroxylation is also influenced by the partial pressure of the H₂O vapor (Garn & Anthony, 1969; Anthony and Garn, 1974).

From a different perspective, there are also experimental evidences for dehydroxylation as a reaction of the first order. Brindley and Nekahira (1957) came to this conclusion through isothermal TGA while Anthony and Garn, (1974) used gas chromatographic analysis. These researchers discovered that dehydroxylation may be related to a reaction of the first order if

H₂O molecules can escape without obstacles. The first order dehydroxylation kinetics is regarded also in a review (Mackenzie, 1970). Dehydroxylation rate is directly proportional to the surface area of the kaolinite crystals. The precise nature of the first product of dehydration however has been a matter of dispute. Formerly believed to be a mixture of amorphous alumina and silica, the residue has now been shown to possess some definite structural features, some of the original kaolinite structure persisting. Moreover, if the temperature is not been too high, the residue can be rehydrated to kaolinite.

Some authors (Mackenzie, 1978; Hanyky and Kutzendoerfer, 2000) assume that homogeneous and inhomogeneous mechanisms of dehydroxylation are possible. In the homogeneous process water is formed by reaction between adjacent OH group and migrates through the crystal. A consequence is the large disruption of the crystal lattice, which results in stability of the tetrahedral layer while the octahedral layer is destroyed with decreased distance between the layers. Every crystal cell loses one molecule of H₂O which is created by the jump of H⁺ between two neighbouring OH⁻ groups. In the inhomogeneous process, migration of H⁺, corresponding counter-migration of Al³⁺ and Si⁴⁺ between close microscopic regions are assumed. Water is lost from the first regions, which became micropores, and the structural continuity is preserved in the second regions, which became metakaolinite. The mechanism of the dehydroxylation was investigated in detail by Switch (1986) and it was determined that this mechanism was inhomogeneous for the temperature lower than 455°C. The inhomogeneous mechanism explains the creation of the micro porosity well. Liberation of the outer OH group appears at the temperature range 420-600°C and the liberation of the inner OH group appears at higher temperatures as high as 850-950°C (Freund et al., 1978).

In kaolinite, the hydroxyl ions are strongly bonded to the aluminosilicates framework structures and can only be eliminated at temperatures above 550°C. During the dehydroxylation process considerable atomic rearrangement occurs (Granizo et al., 2000; Madani *et. al.*, 1990 and Alkan *et. al.*, 2005). The result is a partly ordered structure that cannot rehydrate in the presence of water (or does so very slowly). Owing to its disordered nature (X-ray amorphous) it has huge reactive potentials in the presence of an alkali/alkaline earth containing solution and mineral acid.

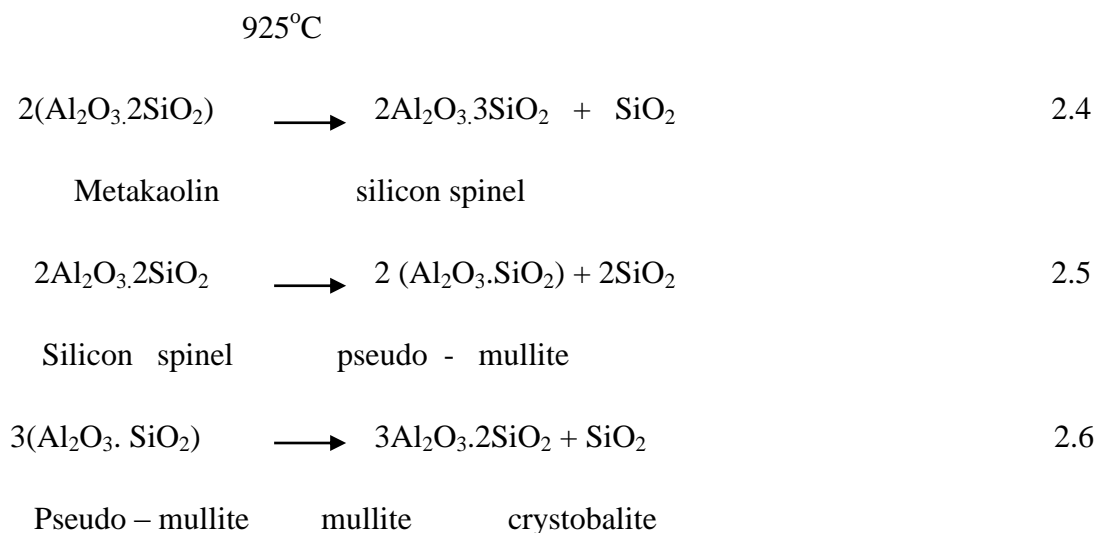
At still higher temperature (about 925°C) the metakaolin undergoes further reaction to form crystalline compounds, the end-product being free silica (cristoballite) and mullite,

$3\text{Al}_2\text{O}_3 \cdot 2\text{SiO}_2$ shown in Equations 2.4 to 2.6. Thus, it is clear that there occurs a separation into an alumina-rich compound and free silica but the precise manner in which this takes place is still a matter of controversy.

An earlier work, based primarily on X-ray diffraction, indicated that at 1000°C a spinel type compound was formed and thought to be Al_2O_3 at the temperature, (Brindley et al., 1959). Thermal analysis shows an exothermic peak, also thought to be associated with the recrystallisation of Al_2O_3 . Granizo, et al., 2000 however, attributed this exothermic peak to the formation of mullite; but this now seems unlikely, since recent X-ray diffraction work strongly suggests that mullite is not formed until much higher temperatures are attained. i.e. $1150\text{-}1300^\circ\text{C}$ (Fernandez, et al., 2006). It has been reported from experiments with silica alumina gels that sillimanite, $\text{Al}_2\text{O}_3 \cdot \text{SiO}_2$, a compound structurally similar to mullite can be formed at temperatures as low as 1000°C , (see equation 2.5), but this might be because the silica alumina gels are much more reactive than metakaolin and moreover may even retain a proportion of their combined water at higher temperature.

More recent accurate measurements of the unit cell dimensions of the spinel compound have shown that it is probably not Al_2O_3 but as silicon aluminum spinel of formula $2\text{Al}_2\text{O}_3 \cdot 3\text{SiO}_2$ (Fernandez, et al., 2006). The latter compound is then said to lose silica by a progressive diffusion of silica ions from the lattice, forming a mullite compound $\text{Al}_2\text{O}_3 \cdot \text{SiO}_2$ as an intermediate stage, and by further loss of silica true mullite, $3\text{Al}_2\text{O}_3 \cdot 2\text{SiO}_2$ is formed, as depicted in Equation 2.6.

The entire process may therefore be represented by the following chemical equations:



The liberated silica, it will be noted, forms cristobalite but the transformation is commonly believed not to occur below 1350°C. However, the mechanism in equation 2.4 to 2.6, first proposed by Brindley and Nakahira (1959) is the currently accepted one. There is some evidence that disordered kaolinite behaves in a slightly different manner to that described, because of its lower crystallinity and the presence of ions other than aluminium and silicon in the structure. The other kaolin minerals, halloysite, dickite and nacrite, have all been reported to develop spinel type phases when heated above 1000°C (Alkan *et. al.*, 2005), but the mechanism of the changes have not been as thoroughly investigated as that of kaolinite.

The conditions of kaolin calcinations strongly influence the reactivity of the solids obtained; the best conditions for obtaining very reactive metakaolins have been discussed by different authors who reported values between 600 and 800°C (Belver *et. al.*, 2002); only a small part of Al₂O₆ octahedral is maintained while the rest are transformed into much more reactive tetra and pentacoordinated units. This is the reason for the observed semi amorphous and semi crystalline phases noticed in the so called calcined kaolin.

Since the transformation temperature ranges from 600 to 900 °C, various authors have declared that the temperature of calcinations affects the rate of dealumination and phase of zeolite formed (Chandrasekhar, 1996; Chandrasekhar and Pramada, 2008). Another school of thought (Granizo *et al.*, 2000) claims that most of the inherent impurities in kaolin could be eliminated at very high temperature but the problem of having silica in its easily depolymerized form still remains.

The work done by Zhang *et. al.*, 2001 sheds more light on this challenge when the effect of calcinations temperature on the amount of active Al₂O₃ (expressed by solubility) and the amount of active SiO₂ (expressed by alkali solubility). Showing the relationship between calcinations temperatures and solubilities of active Al₂O₃ as presented in Figure 2.5

2.7.4 Structure of metakaolin

Dehydroxylation is a thermal decomposition of kaolinite crystals to a partially disordered structure. The result of dehydroxylation is a new phase called a metakaolinite. During the action as XRD showed, the higher order reflections lost their intensity and vanished in the XRD background. This result led to the opinion, that the metakaolinite can be amorphous. The loss of high order reflection indicates that dehydroxylation result in structural disturbances through the breaking of unstable bonds. As a result, the degree of ordering became lower than that in kaolinite as dehydroxylation progressed.

The metakaolinite does not collapse but, rather retains a layered structure. The first attempts to compile a crystallographic model of metakaolinite was made by Brindley and Nakahira, (1959), who proposed the ideal well ordered lattice presented in Figure 2.6

Metakaolinite maintains the kaolinite parameters, but some of its parameters disappears, leading to diffusion of the XRD patterns. Octahedral layer is likely to be changed more than the tetrahedral silica layer during dehydroxylation process. Presumably, the remnant oxygen and vacant anion sites rearrange as a way to lower lattice energy. The structure of metakaolinite allows the kaolinite to collapse to 0.63 nm, in agreement with the measured densities of kaolinite and metakaolinite. Proposed structure of the metakaolinite shows no OH groups. A recent work by Lee *et. al.*, (2003) assumes the rearrangement of the oxygen and vacant sites, which gives stability to the layered structure. This rearrangement builds modulations along the c-axis in metakaolinite with a period of 0.14 nm. If the metakaolinite has a structure shown in Figure 2.6 it means a regular one that should be displayed by XRD reflection. But as it was mentioned before, it is impossible to accurately determine the metakaolinite structure only by XRD analysis. Consequently, the structure of metakaolinite presented in Figure 2.6 must therefore be considered as almost idealized.

A revisited structural model of metakaolinite was proposed by Mackenzie (1970) using computer simulation and nuclear magnetic resonance studies. This structure accounts for the presence of 11-12% residual OH Group, which are incorporated in the Al-O layers. This structure is shown in Figure 2.7. Mackenzie assumed that homogeneous and inhomogeneous mechanisms of the dehydroxylation are possible. Water is lost from the first region which become micropores, and the structural continuity is preserved in the second regions, which became metakaolinite. From the model of Mackenzie, it could be concluded that the residual OH group would be liberated at higher temperature.

2.7.4.1 Effect of acidification and alkalination on kaolin and metakaolin.

The treatment of kaolin with acid and alkaline has been of great interest to clay researchers around the world in the past decades. However, the treatment on the properties of kaolin by chemical methods is difficult because of the high passivity of the materials. Thus, it is not significantly affected by the acid or alkaline treatments, even under strong conditions (concentrated solution and/or high temperatures). A pioneer in this area, Mackenzie (1978) while working with montmorillonite, found that acid removed alkali metals, alkaline earths, irons and aluminum from clay. The first effect of acids is to remove the exchangeable

cations, thereby producing H-clays and the alumina octahedral layer of a clay mineral is also attacked. and later the silica tetrahedral layer.

Alkalines first attack the tetrahedral layer and if the attack is prolonged and severe, the mineral structure is destroyed. The kaolinite structure on the other hand, resists prolonged treatment in concentrated sulfuric acid (Murray, 1951). Carrolo and Garwood (2003) reported that kaolin is attacked by acid following montmorillonite on the reactivity series with acid, while kaolin minerals are more strongly attacked by sodium hydroxide in comparison with other clay families investigated. This method involves leaching of clay particles with inorganic acids, releasing disaggregation of clay particles, elimination of mineral impurities and dissolution of the external layers, thus altering the chemical composition and the structure of clays. This produces an increase in the surface area, the porosity and the number of acid centers with respect to the clays, depending on the intensity of the treatment. The treated solids are composed of a mixture of non attacked clay layers and a hydrous, amorphous and partially protonated silica phase (Murray, 1951; Belver, *et. al.*, 2002).

In addition, the activation of metakaolins with acid has been dealt with also in articles (Caballero, *et. al.*, 2007; Aderemi 2000; Ajayi et al., 2010, Hulbert and Huff 1970). These reports showed that metakaolin is more reactive and is easily attacked by both acids and alkalis, causing partial destruction of the metakaolin structures. This is dependent on the concentration of the acid/alkali and time of reaction.

2.8 Synthesis of Zeolites

The formation of natural zeolite is a result of natural reactions taking place between water present in several environments (marine sediment, alkaline lake, saline soil, open hydrological system) with other solid materials present in such environment. The key materials which supply chemical species used in zeolite formation such as Si and Al include volcanic glass, crystalline clay, biogenic silica and quartz. The formation processes depend on several factors such as high temperature and high pressure. The reaction can take several thousands or more years to complete. Early developed zeolites such as clinoptilite and phillipsite are metastable and are soon transformed to more stable zeolite such as analcime and heulandite. As earlier explained million tonnes of natural zeolites are produced annually but laboratory synthesis has also improved (Barrer, 1983). Further interest in the synthesis

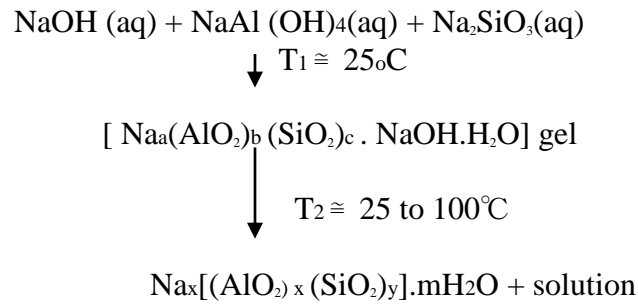
of zeolite can be attributed to its advantages over natural zeolite among which includes: high purity, uniform pore size, ion exchange capabilities etc (Xu et al, 2007).

Synthetic zeolite was first reported by Steclaire Deville in 1862 when he prepared Levynite by hydrothermal treatment of potassium silicate and sodium aluminate in a sealed glass tube. Even though there were no definitive characterization techniques, mineralogical and chemical analysis was used to identify the products (Breck, 1974). Barrer (1982) made the breakthrough in the 1940s when they successfully synthesised analcime, however the real success was achieved by Breck and his colleagues working at Union Carbide Corporation (UCC) utilizing mild hydrothermal conditions and temperatures at 100°C and self generated pressure to synthesis the first non–natural zeolites A, X and Y. One remarkable discovery from the work of Breck and co-workers was the revelation that zeolites can actually be prepared at low temperature rather than the high temperature and thousand of years used for the preparation of natural zeolites. Continuous research in zeolite synthesis led to another significant development when (Barrer and Denny, 1961) reported the synthesis of high silica zeolite using organic quaternary ammonium salt cation. This achievement led to the use of organic molecules as structural directing agent in zeolite synthesis by G. Kerr of Mobil oil Company, producing high Si/Al ratio zeolite such as ZSM-5 and silicalite-1 (Xu et al, 2007). Several other developments continued to take place on zeolite synthesis including the synthesis of aluminophosphate material by Flanigen et al (1971) and the introduction of elements other than Si and Al into the zeolite framework such as the synthesis of titanosilicate (TS-1) (Xu et al, 2007).

The synthesis of zeolite as a subject has been reviewed in several books and the literature (Breck, 1974; Xu et al., 2007; Ginter et al., 1992) but in general hydrothermal, solvothermal and recently ionothermal are the basis of most of the work on the preparation of synthetic zeolites (Xu et al, 2007). Solvothermal is one of the new techniques used in the preparation of microporous compounds such as aluminophosphate. The technique utilizes organic solvents such as alcohol and amine to act as reaction medium rather than water during the zeolite synthesis. It primarily plays the role of dissolution of the reactants forming the solvent-reactant complex and this influences the reaction product based on other conditions of the interaction. The organic molecule can sometimes act as a template directing the synthesis of a particular structure. This method was used by Bibby and Dale (1985) to prepare sodalite in ethylene glycol medium also by Okamoto et al., (2001) to prepared NaA and by Bowen et al., (2003) for ZSM-5. As in all synthesis process, solvothermal synthesis depends on the physical and chemical characteristics of the initial starting materials, the regularity of

synthetic reactions and conditions and the relationship between the structure of the solvent and the desired products. The conditions of the reactions such as the initial starting gel compositions, crystallization temperature and time along with the polarity of the solvent significantly affect the types of zeolite formed. Examples of solvent recently used to prepared zeolites include tetraethylene glycol and cyclopentylamine for the synthesis of aluminophosphates (Xu et al., 2007). Ionothermal synthesis is another novel technique used to prepare zeolites and other porous materials such as metal organic framework (MOF). It uses ionic liquid or eutectic liquid to act as a solvent and template during zeolite crystallization. Ionic liquid is described as organic solvent with high polarity and pre-organised structure. The properties of ionic liquid include high solvating characteristic, near absence of vapour pressure and high thermal stability. Eutectic liquids are composed of two or more compounds with lower melting point than their constituents. It shares similar properties with ionic liquid but are less expensive. The reactions which occur during ionothermal synthesis take place in ionic form. It is essentially different from hydrothermal synthesis and the mechanism is crystallized from solution. Because some ionic liquids used are hygroscopic in nature, water is not completely absent in the synthesis and are said to act as mineraliser, aiding dissolution. Fluoride is also sometimes added to perform the same function. As an example, new structure such as SIZ-I and SIZ-6 have been synthesised using ionic liquid called 1-ethyl-3-methylimidazolium bromide (Parnham and Morris, 2007). The use of solvents other than water to synthesise zeolite has continued to gain interest. However, the present work on the synthesis of zeolite Y from Elefun kaolin Ogun state, Nigeria is restricted to hydrothermal synthesis. Hydrothermal syntheses are broadly divided into sub-critical reactions in which the reaction temperature is mild within 100 to 240°C and super critical reactions whereby the reaction temperature can reach up to 1000°C. However most zeolite syntheses are performed at mild temperature and autogenous pressure (Xu et al., 2007). The hydrothermal synthesis of zeolite can be divided into two broad steps (Break, 1974; Byrappa and Yoshimura, 2001; Auerbach, 2003; Xu et al., 2007). The initial formation of aluminosilicate gel and its subsequent crystallization with ageing (curing).

A reaction scheme can also be presented for zeolite crystallization from the system of $\text{Na}_2\text{O}-\text{Al}_2\text{O}_3-\text{SiO}_2-\text{H}_2\text{O}$ showing the gel preparation and crystallization:



2.8.1 Zeolite crystals

The gel is formed from copolymerization or condensation-polymerization mechanism. The crystallization process of zeolite formation usually takes place in an autoclave as shown in Figure 2.9, for the type used in this work. Other type of autoclave and reactor are also used to prepare zeolites. A typical procedure for hydrothermal synthesis of zeolites includes (Barrer, 1978, Mintova et al., 2002), mixing of source materials usually in a strongly basic environment and stirring to form a homogenous gel. Ageing of the resulting gel under certain conditions is carried out before crystallization in a sealed autoclave at a specified temperature for a certain time. The recovery of the zeolite is usually done by washing and drying



Figure 2.9: The Teflon-lined stainless steel autoclave used in this work

2.8.2 Zeolite Y synthesis starting components

The basic reactants used in the synthesis include (Breck, 1974, Xu et al, 2007, Auerbach, 2003, Dyer, 1988 and Kovo, 2010):

- Silicon source
- Aluminium source
- Metal ion
- Base
- Mineraliser
- Water

The silica, along with alumina, function to provide the primary building unit(s) of the framework with the alumina further creating the framework residual charge. The alkali cation is the counter ion which neutralizes the residual charge in the framework and also acts as a guest molecule, generating the ion exchanging characteristic. The OH⁻ is the mineraliser and provides the necessary environment or media suitable for nucleation and crystal growth and finally water acts as a solvent and also guest molecule.

Other materials termed structural directing agent (SDA) or templates are used to enhance crystallization of specific or targeted zeolites. These are divided into two main groups namely:

- organic template
- inorganic template

Templating is defined as a process in zeolite synthesis during gelation or nucleation in which organic/inorganic molecules organise the oxide tetrahedra into a particular geometric topology around itself and provides the initial building block for a particular structure Lee and Dutta (2002). Template or SDA is an important component of zeolite crystallization that influences the type of structure formed at the end of the synthesis. Inorganic templates (cation) have always been part of zeolite crystallization process. However, the introduction of organic template has widened the number of zeolite structures that have been prepared. Templates are generally selected based on some important criteria such as:

- ❖ the solubility of the solution,
- ❖ stability under synthesis conditions,
- ❖ steric compatibility
- ❖ possible framework stabilization
- ❖ ease of removal of the templates without destroying the zeolite framework or impacting negatively on the environment.

The template, whether organic and inorganic, basically performs four functions according to Byrappa (2001); Kovo, (2010)

- Influence the gelation and/or nucleation process
- Lower the chemical potential of the lattice formed
- Improvement of the stability
- Control of the formation of a particular topology through its size and shape

Templates used in zeolite Y synthesis include cations such as Li^+ , Na^+ , K^+ , Ca^{2+} and Ba^{2+}

Organic templates like tetrapropyl ammonium and neopentyltrimethylammonium are also used to direct specific zeolite structure especially high silica zeolite such as zeolite ZSM-5, ZSM -11 etc.

The choices of specific crystallization conditions determine the exact nature of zeolite products formed (Xu et al., 2007). The sequence of events leading to zeolite synthesis can be described as a crystallization of gel mixture comprising silica and alumina source combined with water in the presence of high pH (Dyer, 1988) . The choice of parameters and other thermodynamic factors such as temperature, pressure; time etc have considerable influence on the nature of zeolitic product formed.

There are a number of materials which are used as silicon and aluminium sources including water glass ($\text{Na}_2\text{O} \cdot x\text{SiO}_2$), sodium silicate, Ludox AS-40, colloidal sol, sodium aluminate and aluminium hydroxide. However, clay usage as a combined source of silicon and aluminium offers a more cost effective means of zeolite synthesis and this is the central point of this research work. Some of the basic materials used in the preparation of Zeolite Y are presented below:

Cation

- Alkali metal hydroxide
- Alkaline earth hydroxide and oxides
- Other oxides and hydroxides
- Salts (fluorides, halides, carbonates, phosphates, sulphates etc)
- Organic bases and ammonium hydroxide especially quaternary bases
- Mixture of two or more of the above

Aluminium

- Metal aluminate

- $\text{Al}(\text{OH})_3$, Al_2O_3 , AlO.OH
- Al alkoxides
- Al salt
- Glasses
- Sediment
- Mineral especially clay mineral feldspathoids, feldspar, and other zeolite

Silicon

- Silicates and silicate hydrate
- Water glass
- Silica sol
- Silica gels
- Silica and other synthetic glasses
- Minerals, including clay minerals, feldspathoids, feldspars and other zeolite
- Basalts and mineral mixtures, sediments

2.8.3 Crystallization of zeolite

The crystallization process is a most important step in zeolite Y synthesis and it involves a condensation reaction taking place between silicate and aluminate in a strong basic solution. The process of zeolite Y crystallization can be divided into two major steps. These are nucleation and crystal growth.

Nucleation is the most important stage in zeolite Y crystallization. It involves the formation of unstable nuclei formed from the supersaturated solution, which is prepared from the initial precursor. These become large enough with time, to form stable nuclei, where crystal growth takes place. Nucleation can either be homogenous or heterogeneous in nature depending on whether it occurs spontaneously or induced by the presence of impurities.

Nucleation and crystal growth are promoted by several parameters such as incubation time and history of the system. Again the size of the crystal can be controlled based on the choice of conditions of the crystallization.

Understanding the mechanism of zeolite Y formation will help in the rational design of zeolite of specific structure and properties. The actual mechanism of zeolite Y formation throughout

the entire process of crystallization is still the subject of much speculation with three routes currently accepted for its formation. These are:

Solid hydrogel transformation: This suggests that zeolite Y synthesis takes place as a result of direct transformation of the solid gel phase used in zeolitization. In this mechanism it is understood that the liquid component of the aluminosilicate gel takes no part in the reaction toward zeolite formation. The mechanism was originally proposed by Breck and Flanigen, (1967) when they noticed that the resultant zeolite phase and the hydrogel always have the same composition during zeolite synthesis. It was later explained that zeolite Y crystallization takes place via structural rearrangement of the framework of the solid aluminosilicate hydrogel under hydrothermal conditions. The process has now been briefly described.

Following the mixing of the source materials, the aluminosilicate gel are formed by condensation reaction followed by depolymerization and structural arrangement under the action of OH⁻ acting as catalysts (Xu et al., 2007).

Solution mediated transport mechanism: This mechanism is almost a direct opposite of the solid hydrogel system because the concept of the mechanism is that nucleation and crystal growth take place in solution. The solution mediated system takes place via four major steps:

- Nucleation occurs in solution or at the interface
- Silicate and aluminate consumption occur in solution
- Crystal growth facilitated by the solution
- Continuous dissolution of gel throughout the crystallization process leading to increased zeolite Y growth. An equilibrium is formed between the components of the aluminosilicates gel following mixing of the source material. Increase in the temperature of the mixture leads to shift in equilibrium between the solid gel and the liquid phase causing an increase in the concentration of polysilicate and aluminate. This then forms zeolite Y nuclei followed by crystal growth. Continuous dissolution of the gel happens because of consumption of the polysilicate and aluminate ion in the liquid phase.

Dual-phase transition mechanism: This mechanism was proposed as a compromise between the two mechanisms earlier discussed. It was later believed, with more advance detection technique, that zeolite Y formation can proceed utilizing the two mechanisms. These strongly depend on the source of materials.

The absence of In-situ tools that can be used to monitor the crystallization route of zeolite synthesis especially the state of the polysilicate and aluminate ions in solution, the structure

of hydrogel, the nucleation process of zeolites and the role of SDAs is mainly responsible for divergent opinions on the exact mechanism that control zeolite synthesis.

The three mechanisms discussed have all their merits but, it is more likely that the solution mediated mechanism predominates during zeolite Y crystallization because nucleation is most likely to happen in solution than in solid phase, In addition, the composition of the liquid at the initiation of reaction usually changed at the end of the crystallization.

The conditions of reactions mixture during zeolite synthesis is a major factor that determines the type of zeolite formed eventually. There are already general conditions which have been highlighted as common to most synthesis. The composition of the starting material is the most important and they are usually given or known from experience and the nature of starting material (reactive or not) such as freshly co-precipitated gels, or amorphous solid. Other conditions include the presence of relatively high pH introduced in the form of an alkali metal hydroxide or other strong base and high degree of super-saturation of the component of the gel leading to the nucleation of a large number of crystals (Xu et al., 2007; Dyer , 1988; Breck and Flangen,1967).

Other factors influencing zeolite Y crystallization include:

- Aging conditions/time
- Crystallization temperature
- Crystallization time
- Reaction container
- Seeding
- Structural directing agent (SDA)

The effects each of these factors are covered in literature (Barrer, 1982; Weitkamp and Puppe, 1999). However, for the purpose of this research work, the effect of temperature, time and ageing of synthesis gel are studied.

2.8.3.1 Heating temperature

Temperature has a considerable effect on the synthesis of zeolite Y. It acts as generator of the pressure that promotes crystallization and structure of the zeolite. The change in temperature can affect the polymeric state of silicate, the dissolution, and the transformation of the gel (Xu et al., 2007). Increasing the temperature of crystallization beyond mild temperature of around 90-110°C normally used to synthesise most commercial zeolites leads to co-crystallization of different zeolite phases. For example, a study by Xu *et al.*, (2007) showed

that zeolite X and Y can be crystallized from synthetic system $\text{Na}_2\text{O-SiO}_2\text{-Al}_2\text{O}_3\text{-H}_2\text{O}$ when the crystallization temperature is within 100 to 150°C. However the increase in temperature to the range of 200 to 300°C will cause the co-crystallization of zeolite sodalite and mordenite.

Temperature is an important control parameter in zeolite crystallization processes. Sources of heating in zeolite synthesis presently come from two areas. These are conventional oven and microwave heating (Chandrasekhar and Pramada, 2008). While ovens have been used over a long time as a source of heating in zeolite Y preparation, the use of microwave heating was introduced to hasten or shorten the crystallization time. What is however important in the use of microwave as a source of heating is the quality of the starting aluminosilicate gel. The aluminosilicate gel is aged prior to microwave treatment thereby promoting strong nucleation, reduction of induction and short crystallization process when in the microwave. Several zeolites have been synthesised by microwave heating with the zeolite crystallization completed within minutes compared to conventional heating that can take several hours or days.

Increase in temperature influences basic properties of zeolites such as the phase, change in induction period and increase in the crystallization rate. The control of crystallization temperature during hydrothermal reaction is important because of the metastability of zeolite phase. Increase in temperature can generally lead to increased dissolution of both the silicates and aluminate species and this can cause a shift leading to the formation of the most stable phase of the targeted zeolite obeying the Ostwald's rule of successive transformation (Szostak, 1989).

2.8.3.2 Ageing time

Ageing is defined as the gap in time between the formation of aluminosilicate gel and crystallization (Xu, et al., 2007; Ginter, et al., 1992; Breck and Flannigan, 1967). Ageing increases the number of nuclei present in the synthesis mixture and can lead to growth of more crystals. During the ageing process, the aluminosilicate gel is expected to be chemically and structurally reorganised increasing the supersaturation level necessary for zeolite nucleation (Weitkamp, and Puppe, 1999). Conclusively showed in thier work that ageing of zeolite synthesis gel causes an increase in the degree of crystallization when the right conditions of experiment are chosen. According to their paper, ageing of aluminosilicate gel at room temperature causes an increase in the silica to alumina ratio as it promotes the incorporation of more silica into the framework even at low level of alkalinity. This assertion

was also confirmed by Ginter, (1992) who pointed out that prolonged ageing leads to insertion of additional silica into aluminosilicate solid and increase the number of smaller nuclei reacting to give better and higher yield of zeolite NaY.

2.8.3.3 Crystallization time

Crystallization time is also an important parameter that controls the type of final zeolite product obtained. The key objective during the synthesis of zeolite is to use the minimum time to prepare the desired zeolite material. Therefore optimization of crystallization time depends absolutely on the choice of other parameters such as crystallization temperature, concentration of mineraliser and seeding. In most cases, increase in such parameters ultimately reduces the induction time and indeed the crystallization time. Dyer, (1988) stated the two roles time plays in the formation of zeolite Y from reacting species or gels to be:

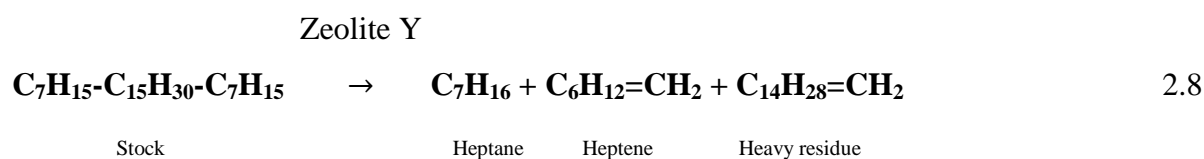
- An induction period during which the reaction mixture is held near ambient temperature prior to raising the crystallization temperature often optimizes the yield of zeolite Y
- Different zeolites crystallize from one reaction mixture at different times. The second time element is because zeolites are metastable species, whereby the initial zeolite formed is an open structure which, with time are transformed into more dense or closed structure following Ostwald's law of successive transformation. An example is the conversion of Philipsite (an open structure) to clinoptilolite (a less open structure) and finally to dense and most stable analcime. Similarly, mordenite can also transform to analcime.

It is however difficult to isolate single factors to study. Therefore to study the synergic effect of the factors, several experiments are required. The choice of factors used in this research is based on experience and the economic production of the final material.

2.9 Catalytic Cracking

Catalytic cracking in petroleum refining is a process of converting or breaking large hydrocarbon molecules into smaller molecules by the action of catalyst. Higher-compression gasoline engines required higher-octane gasoline with better antiknock characteristics. The introduction of catalytic cracking processes in the mid-to late 1930's met the demand by providing improved gasoline yields and higher octane numbers, (Plank and Rosinki, 1964; Venuto and Habib, 2007; Ezekiel, 2014). Catalytic cracking is conducted at relatively less

severe conditions. Temperatures in all catalytic cracking operations lie in the range of 440-520°C while pressure although specified for each type of reactor, does not exceed two atmospheres in fluidized bed reactors. In addition to these operating variables, catalyst- to- oil ratio is a set factor for a particular kind of operation. The feed material used for catalytic cracking is usually obtained by vacuum distillation of atmospheric residue (vacuum distillates), or blends of thermally cracked oils or gas oil are used directly and the most economically viable catalyst is zeolite Y. An example of the process is as shown in Equation 2.8.



During cracking, hydrocarbon molecules, $\text{C}_n\text{H}_{2n+2}$ with n (i.e number of carbon atoms greater than 25 split into two, almost at the middle, given a saturated molecule and another unsaturated molecule. All cracking reactions ultimately give rise to coke (but less in catalytic cracking) and hydrogen.

According to the criteria for successful commercial catalyst as listed in the introductory part of this thesis, zeolite Y seems to be the most attractive choice due to its superior activity-thermal and hydrothermal. Feed to a catalytic cracking reaction contains a wide variety of high boiling-point hydrocarbons.

In general, zeolite Y is a very effective catalyst for cracking but when the feed consists of paraffinic compounds, the fraction remains essentially unconverted in the process. Especially in the presence of aromatics, paraffinic feeds which yield gasoline product that has a relatively low octane number and an unconverted fraction that is unsuitable for use as a gasoline blending component. Also, the recycle to the cracking unit is not appropriate because of the refractory nature of the material which is not suitable for paraffinic materials. Therefore, hydro-dewaxing processes have been developed using catalysts which have an intermediate pore size in order to selectively crack paraffinic compounds; ZSM-5 is such a catalyst. It is considered to be a highly effective dewaxing catalyst. However, it is unsuitable for use as a cracking catalyst because it does not allow the bulky molecules such as polycyclic aromatics into the internal pores where cracking takes place. The problem of processing these feeds (Van der puij, 1958) has persisted even when small pore zeolites have been combined with conventional cracking catalyst.

Zeolite Y, a large pore size zeolite, has been found to be extremely effective in cracking highly paraffinic feeds (Van der puil, 1958). Using a waxy feed, zeolite produces more gasoline with a higher octane number than other commercial catalysts. It is not only a good dewaxing catalyst but may also promote the reaction of a wide range of high-boiling point hydrocarbons. Highly siliceous forms of zeolite are more resistant to hydrothermal degradation.

2.9.1 Catalytic cracking processes

Catalytic cracking was developed when thermal cracking was no longer capable of meeting the demands for more and better gasoline. Higher concentrations of isoparaffins and aromatics are required for a higher octane number. Catalytic cracking enables this improvement with lower concentrations of unsaturates (olefins, especially diolefins) which improves the stability of the gasoline by reducing the tendency towards gum formation.

There are three steps in catalytic cracking operations. The reaction step where the cracking of hydrocarbons takes place, the stripping step to eliminate adsorbed hydrocarbons and the regeneration step in which the carbonaceous deposit or coke is burned off the catalyst. The temperature prevailing during cracking ranges from approximately 400 to 540 °C and in the regeneration step it is approximately 540 to 590 °C.

The main types of catalytic cracking processes are fixed bed (Fig 2.10) and moving bed process

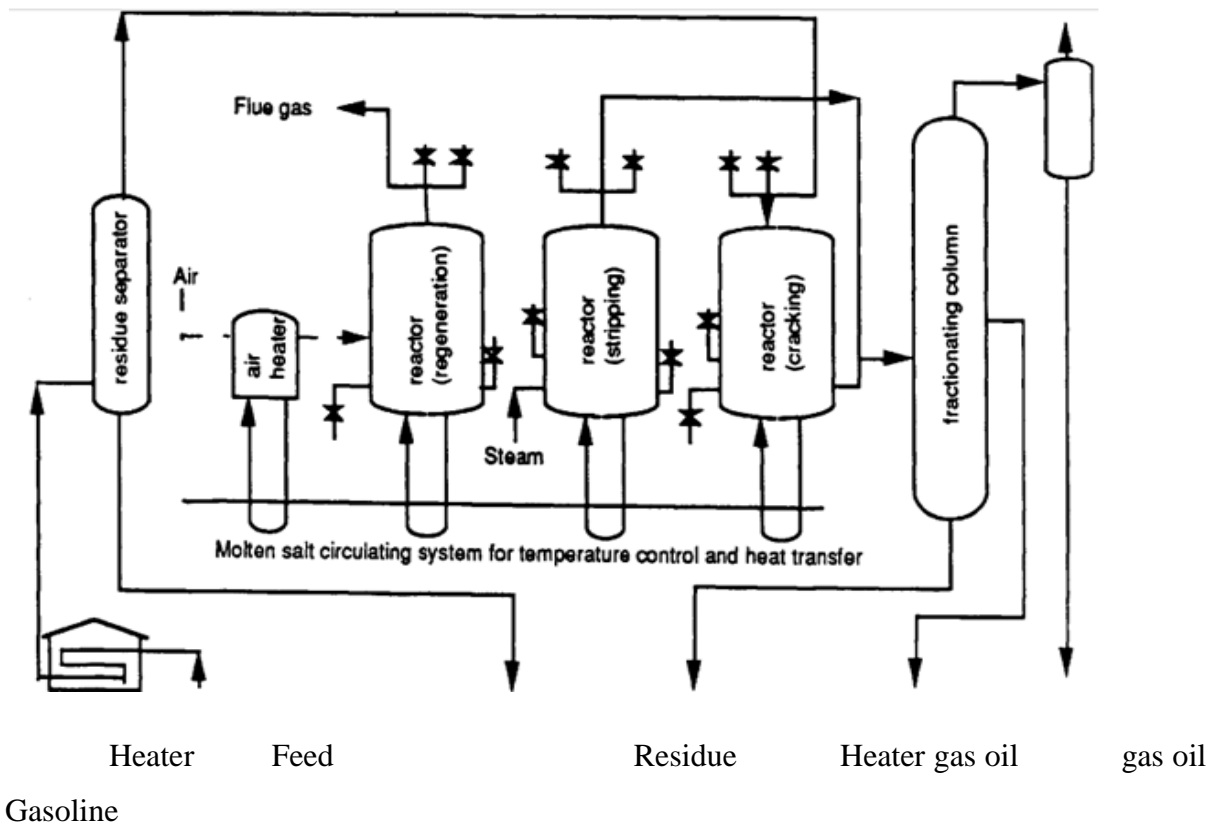


Figure 2.10: The Houdry fixed bed process (Shell international, 1998)

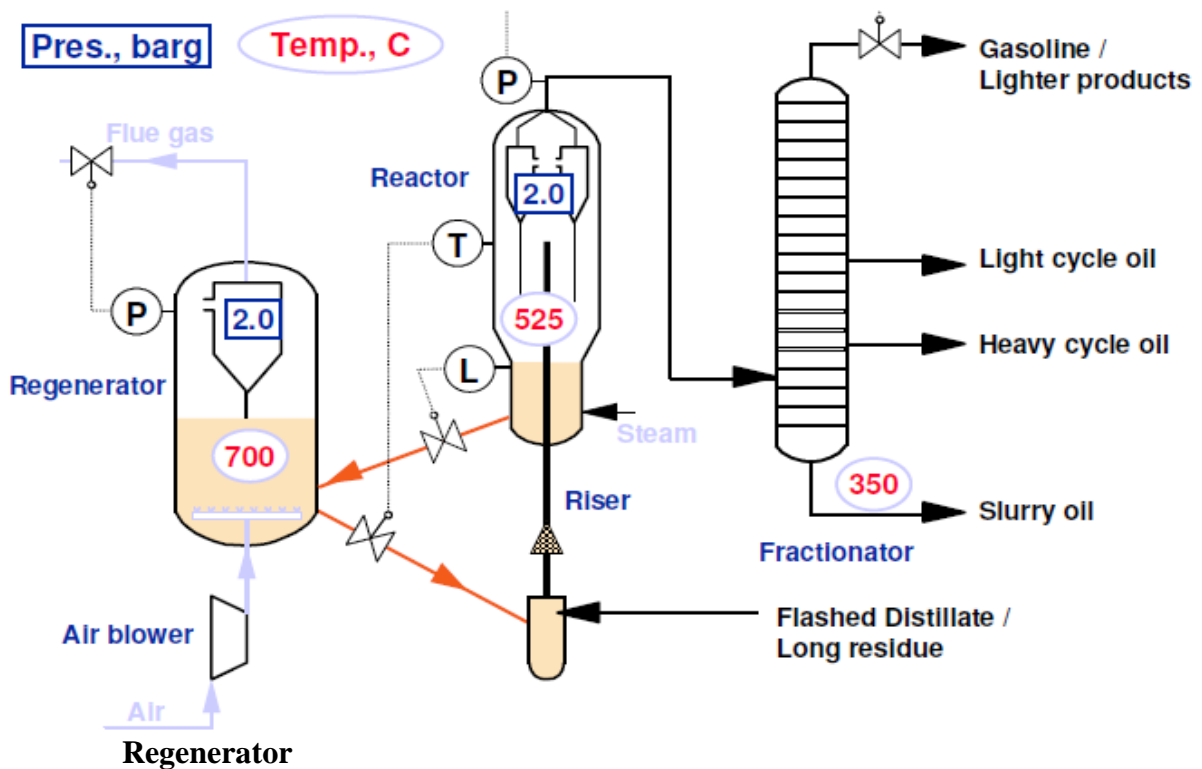


Figure 2.11: The fluid catalytic cracking process (NNPC, 2013)

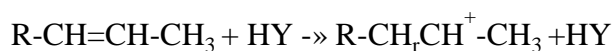
Regeneration is needed to burn the coke off and so the cracking reaction is stopped resulting in non-continuous operation (Omoleye, 1986). To maintain continuous operations, the moving bed processes were developed to replace it. The thermofor catalytic cracking process (T.C.C.) eliminated the problem of interrupted operation but was mechanically complicated and allowed only a limited ratio of the catalyst circulation rate to oil feed rate (1:11). Both are now obsolete or in only very limited operation.

Nowadays fluid catalytic cracking (FCC) shown in Fig. 2.11 is the most widely used process due to its higher efficiency: the yield of gasoline is increased (though by less than an equivalent amount of fresh feed). It is called "fluid" because the fine powder catalyst used behaves very much like a liquid when gas is passed through it.

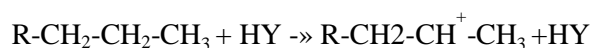
2.9.2 Cracking reaction

Experimental studies have revealed that the reactions occurring in catalytic cracking differed markedly from those in thermal cracking processes. Catalytic cracking produces C₃ and C₄ gases predominantly while the high yields of C₂ and higher gases are obtained from thermal cracking. (Greenfelder, 1949 Ako, Awe, 2012) position that catalytic cracking reactions take place through the formation of carbonium ions and thermal cracking reactions involve a free-radical mechanism (Omoleye, 1986). In this study attention is paid only on catalytic cracking: the details of which follow. Catalytic cracking occurs via carbonium ions as intermediates that are formed on the surface of the catalyst by the following three ways:

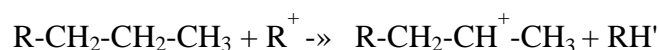
- (1) The addition of a cation to an unsaturated molecule by the interaction with an acid HY- the unsaturated molecule is combined with an available proton from the catalyst (Bronstel acid site)



- (2) Hydride ion abstraction: The stable molecule such as paraffin reacts with a Lewis acid (L), the reaction proceeds by the extraction of a hydride ion from that molecule and leaves a carbonium ion.



- 3) The removal of an electron from an electrically neutral species. A carbonium ion (R⁺) reacts chain wise with a fresh paraffin molecule to give a new paraffin and a new carbonium ion by way of a hydride ion (H⁻) exchange.



Thomas in (1949) investigated the rate determining step of saturated compounds and concluded that the cracking rate of paraffinic hydrocarbons is relatively slow. This implies that the most important way to form the carbonium ion is the first reaction. There is no question that thermal cracking occurs to some extent in catalytic cracking and a low concentration of olefins which undoubtedly form by thermal cracking is required to start the carbonium-ion reaction.

Table 2.5 Comparison of Catalytic and Thermal Cracking Products. (Greenfelder, 1949)

Hydrocarbon	Thermal cracking	Catalytic cracking
n-Hexadecane (Cetane)	Major product is C ₂ with large amount of C ₁ and C ₃ and C ₄ to C ₁₅ n- α -olefins. Few branch ali-phatics.	Major product is C ₃ to C ₆ . few n-a-olefins above C ₄ . Aliphatics mostly branched.
Aliphatics	Small amounts of aromatics formed at 500 ⁰ C.	Large amounts of aromatics formed at 500 ⁰ C.
Alkylaromatics	Crack within side chain.	Crack next to ring.
n-Olefins	Double bond shifts slowly. Little skeletal isomerization.	Double bond shifts rapidly. Extensive skeletal isomerization.
Olefins	Hydrogen transfer is a minor reaction and is nonselective for tertiary olefin. Cracking is about same rate as corresponding paraffins.	Hydrogen transfer is an important reaction and is selective for tertiary olefin. Crack at much higher rate than corresponding paraffins.
Naphthenes	Crack at lower rate than paraffins.	Crack at about same rate as parafins with equivalent structural groups.

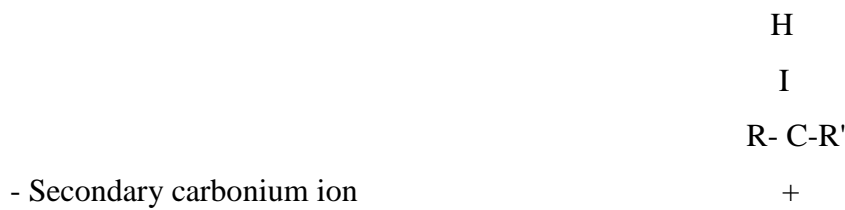
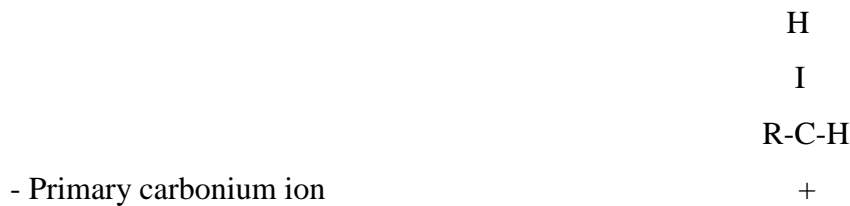
2.9.3 The mechanism of catalytic cracking

Catalytic cracking mechanism comprises of the following steps:

Step 1. Formation of a carbonium ion. The hydrocarbon attaches itself to an active site on the catalyst surface. Then the carbonium ion is formed as described before. This carbonium ion still remains adsorbed on the surface.

Step 2. Hydrogen and carbon shift towards a more stable structure.

There are three types of carbonium ions:



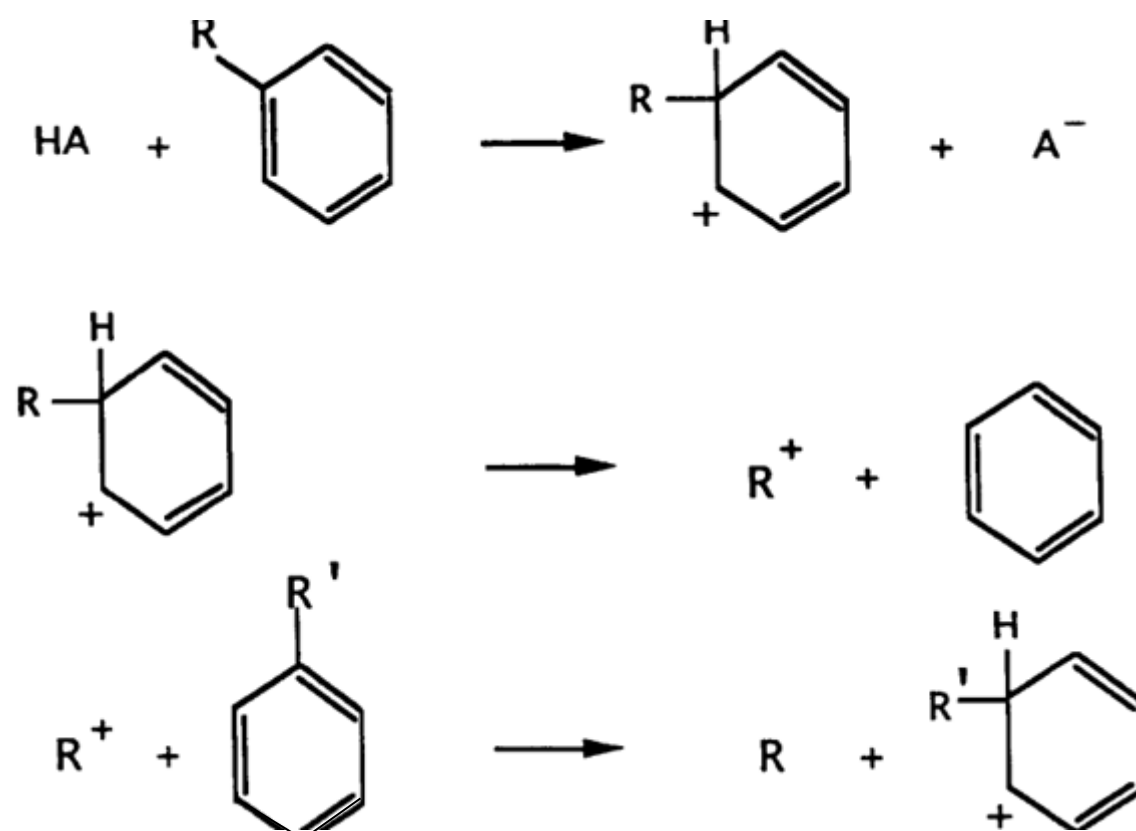
Primary carbonium ions are less stable than secondary ions, which in turn are less stable than the tertiary ions.

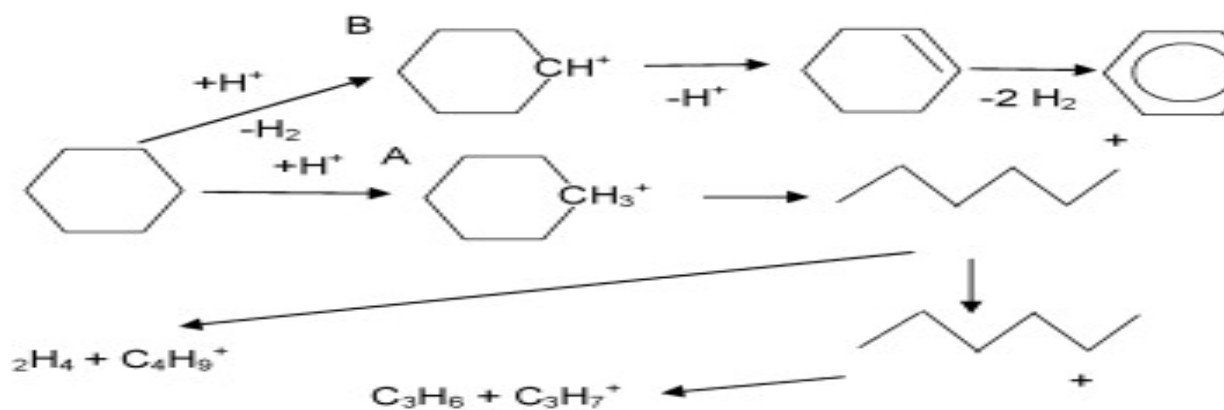
Step 3. The formed carbonium ion reacts according to the beta rule (Hayne and Sarma, 1973) (carbon-carbon bond scission takes place at the bond located beta to the carbon atom bearing the positive charge)

The new carbonium ion may react with a fresh hydrocarbon molecule to form another small carbonium ion and the pattern of cracking is continued. The smallest olefin that can split off from a secondary carbonium ion would be C₃ (propylene) and from a tertiary carbonium ion, C₄ (isobutylene). This explains the preponderance of C₃ and C₄ in the gases from catalytic cracking processes. Ethylene is not formed by this mechanism according to the beta scission rule.

2.9.4 Catalytic cracking of alkylaromatic hydrocarbon

The main features of catalytic cracking reactions of aromatic compounds are the great stability of the benzene ring and the high selectivity of the cleavage of alkyl groups from substituted benzenes. As the size of the alkyl group increases the ease of cracking becomes greater; the selectivity of the cleavage, as evidenced by the yield of benzene, remains high. Two mechanisms have been proposed for the carbonium ion as intermediates. The first, according to Thomas (1949) is the mechanism of the direct addition of an acidic proton on the catalyst to one of the double bonds of the benzene ring, thus forming the carbonium ion and then decomposition occurs at the HY position on the carbonium-ion carbon atom.





Different routes to benzene cracking products (Best and Wojciechowski, 1977). This mechanism suggests that the major products of cyclohexane cracking are benzene and propylene. Best and Wojciechowski (1977) have reported a comprehensive study of the product distribution for the catalytic cracking of cyclohexane using a La-exchanged Y zeolite and zeolite Beta respectively. Products that were observed in the liquid phase (at concentrations greater than 0.01%) were benzene, toluene, ethylbenzene, while gaseous products identified were methane, ethylene, propylene, and n-butane. The remaining reaction products present were in lower concentrations and are summarized in Table 2.6. The results show that the cracking of cyclohexane is not a simple, clean reaction, and consequently its use as a test reaction is not straightforward. However, the major products, benzene and propylene, may be obtained by appropriate selection of temperature and feed rate.

Table 2.6: Products from Catalytic Cracking of Cyclohexane on Zeolite-Y. (Best and Wojciechowski, 1977)

Methane
 Ethylene
 Propene
 2- Butene
 Iso-butane
 n- Butane
 1, 3- butane
 Cyclohexene
 n-Hexane
 Toluene
 Xylene
 E.T.C

2.10 Kinetics of the Cracking Reaction

A kinetic reaction scheme which involves the adsorption of one hydrocarbon molecule A on one active site of the catalyst is followed by the cracking of the adsorbed molecule to give product B and C.



If the reaction is a first order with respect to A, the reaction rate is

$$-r_A = -\frac{dC_A}{dt} = kC_A = kC_{A0}(1-X_A) \quad 2.10.1$$

Where

C_A is the adsorbed phase concentration (mol/gm).

C_{A0} is the initial adsorbed phase concentration (mol/gm).

X_A is the fraction of A converted to products,

k is the reaction rate constant.

$-r_A$ is rate of reaction based on unit mass of catalyst (mol/gm. sec).

For a steady state plug flow system:

$$F_{A0} dX_A = -r_A dW \quad 2.10.2$$

where

F_{A0} is the molar flow rate of A entering (mol/sec).

W is the mass of the catalyst (gm).

Rearrangement gives:

$$\int_0^W \frac{dW}{F_{A0}} = \int_0^{X_A} \frac{dX_A}{-r_A}$$

Since the molar flow rate of A entering is constant, F_{A0} can be taken out of the integration and from the reaction rate $-r_A$ (which is then a function of X), we may write:

$$\frac{1}{F_{A0}} \int_0^W dW = \int_0^{X_A} \frac{dX_A}{kC_{A0}(1-X_A)}$$

OR

$$\frac{WC_{A0}}{F_{A0}} = -\frac{\ln(1-X_A)}{k} \quad 2.10.3$$

The above equation is used to find the reaction rate constant at different temperatures and from the Arrhenius' Law:

$$k = k_0 \exp\left(\frac{-E}{RT}\right) \quad 2.10.4$$

or

$$\ln k = \ln k_0 - \frac{E}{RT} \quad 2.10.5$$

Where k_0 is the frequency factor.
 E is the activation energy of the reaction.
 R is the gas law constant.
 T is the absolute temperature.

A plot of $\ln k$ versus $1/T$ will give the value of the activation energy of the cracking reaction.

2.10.1 The kinetics of cracking reaction of developed and commercial zeolites

Experimental devices for studying the cracking activities of synthesized zeolite Y catalyst fall into two categories: those which use a batch of solids, and those which use a through flow of solids (Levenspiel, 1999). Because of ease of experimentation batch-solids devices are much preferred.

The type of batch-solids flowing-fluid reactor that we find convenient to use depends on whether the cracking rate expression da/dt is concentration independent or not. When it is independent of concentration, any type of batch-solids system may be used and can be analyzed simply, but when it is dependent on concentration, then unless one particular type of reactor is used (that in which C_A is forced to stay unchanged with time) the analysis of the experimental results becomes awkward and difficult.

A kinetic reaction scheme which involves the adsorption of one hydrocarbon molecule A on one active site of the catalyst is followed by the cracking of the adsorbed molecule to give product B and C. [Olson and Hang, (1984); Levenspiel, (1999); Bartholmew, (2001)]

2.10.2 Adsorption

2.10.2.1 Henry's law and adsorption equilibrium

In the Henry's Law region the reactants at sufficiently low concentration are adsorbed on a uniform surface such that all molecules are isolated from their nearest neighbours. The adsorbed phase concentration may be obtained from the linear expression:

$$q = KC \quad \text{or} \quad q = K'P \quad 2.10.6$$

\acute{K}

Where q and C are molecules or moles per unit volume in the adsorbed and fluid phase, P is partial pressure and K , K' are the Henry constants expressed in terms of concentration and pressure.

The Van't Hoff equation:

$$\frac{d \ln K}{dT} = \frac{\Delta U_0}{RT^2} \quad 2.10.7$$

$$\frac{d \ln K^l}{dT} = \frac{\Delta H_0}{RT^2} \quad 2.10.8$$

Expresses that the Henry constant is a function of temperature in which ΔU_0 is the internal energy of adsorption and ΔH_0 represents the enthalpy between adsorbed and gaseous states. Integration of the above equations yield:

$$K = k_o \exp\left(\frac{-\Delta U_0}{RT}\right), \quad \acute{K} = \acute{K}_0 \exp\left(\frac{-\Delta H_0}{RT}\right) \quad 2.10.9$$

Plots of $\ln K$ versus $1/T$ are used to find ΔU_0 and ΔH_0 which are called the heats of adsorption.

2.10.2.2 Estimation of the adsorption equilibrium constant from chromatographic measurements

Chromatography is very useful in the determination of equilibrium constants of a sorbate-sorbent system. The measurement is made from the response curve of an input to the adsorption column. The input can be either a step change in sorbate concentration or the injection of a small pulse of sorbate at the column inlet. The response to a step input is called

the breakthrough curve while the chromatographic response refers to a response curve from the pulse input.

Consider the mass transfer of a packed bed in Figure. 2.12 The differential mass balance equation for an element of the adsorption column is:

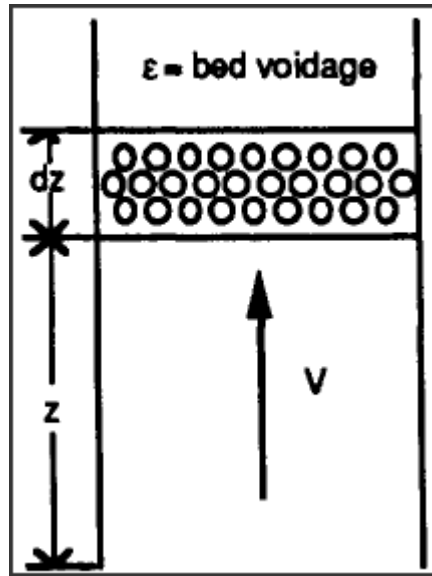


Figure 2.12 Mass balance on a packed column

$$-D_L \frac{\partial^2 C}{\partial Z^2} + \frac{\partial(vC)}{\partial z} + \frac{\partial C}{\partial t} + \left(\frac{1-\epsilon}{\epsilon} \right) \frac{\partial q}{\partial t} = 0 \quad 2.10.10$$

Where

D_L is the axial dispersion coefficient

V is the interstitial velocity of gas; free volume of zeolite cage

C is the sorbate concentration in gas phase

q is the sorbate concentration on the adsorbed phase

Z is the distance measured from column inlet

t is time

and the adsorption rate is

$$\frac{dq}{dt} = f(q, C). \quad 2.10.11$$

The solution obtained from the Laplace transform by applying van der Laan's theorem Van (1958) is:

$$\mu \equiv t \equiv \frac{\int_0^{\infty} Ct dt}{\int_0^{\infty} C dt} \quad 2.10.12$$

The first moment is therefore:

$$\mu = \frac{L}{v} \left[1 + \left(\frac{1-\epsilon}{\epsilon} \right) K_p \right] \quad 2.10.13$$

Where C^* is sorbate concentration in equilibrium with

μ is the first moment.

t is mean retention time.

L is length of the column,

ϵ is bed voidage.

K_p is the equilibrium constant based on
Sorbate concentration in a pellet

When the tracer is injected into the adsorption column, the elements of the fluid will take some time to pass through the column. In the case of a step input the response curve (breakthrough curve) which is a time record of the tracer leaving the column can be represented in Figure. 2.14 (Levenspiel, 1972). The break time (t') is the time at which the effluent concentration reaches its maximum permissible level and t is the average residence time of the effluent to flow through the adsorption column.

The mean retention time is obtained from the breakthrough curve. If L , v and ϵ are known, K_p can be found. The temperature dependence according to Thevant Hoff equation and the heat of adsorption may then be obtained.

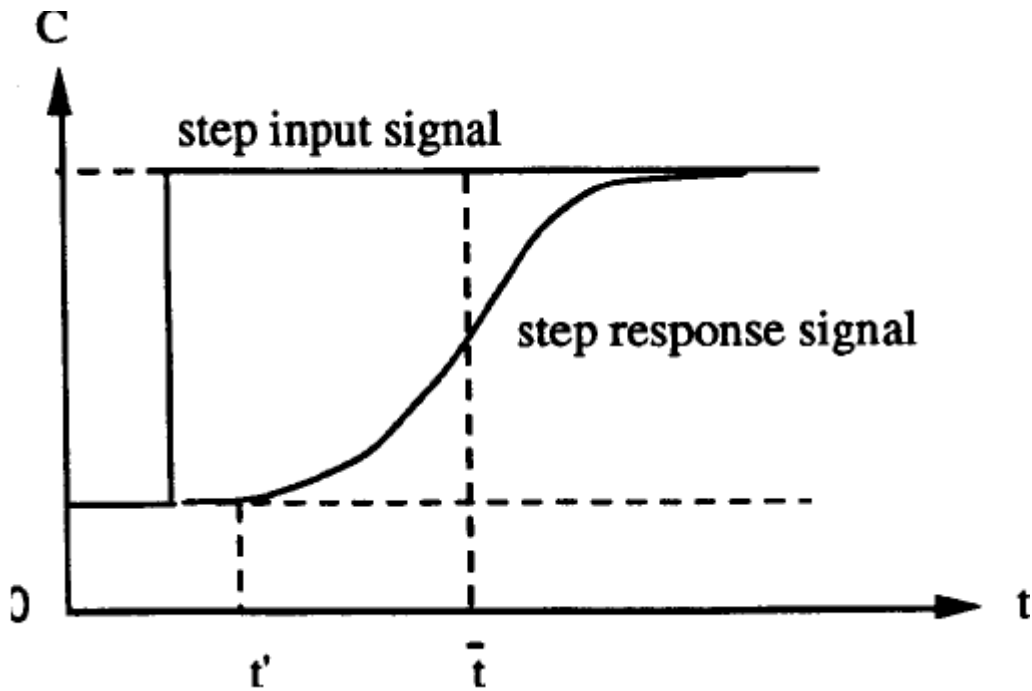


Figure 2.13: Sketch of breakthrough curve

2.10.3 Mass transfer resistances

In a bed packed with porous particles, there are many distinct resistances to mass and heat transfer present in the system and the overall rate of adsorption is usually controlled by these resistances. Three diffusional resistances involved in the transfer of mass are the external film resistance, the macropore resistance of the pellets and the micropore resistance of the adsorbent crystals. Figure.2.14 schematically shows these resistances.

2.10.3.1 External film resistance

When reactants diffuse from the main body of the fluid to the exterior surface of the zeolite Y catalyst and the reaction is controlled by the diffusion through the film surrounding the solid particle, the transfer of mass occurs by molecular diffusion. The external film resistance is expressed by a linear driving force equation:

$$\frac{\partial q}{\partial t} = K_f(C - C^*) \quad 2.10.14$$

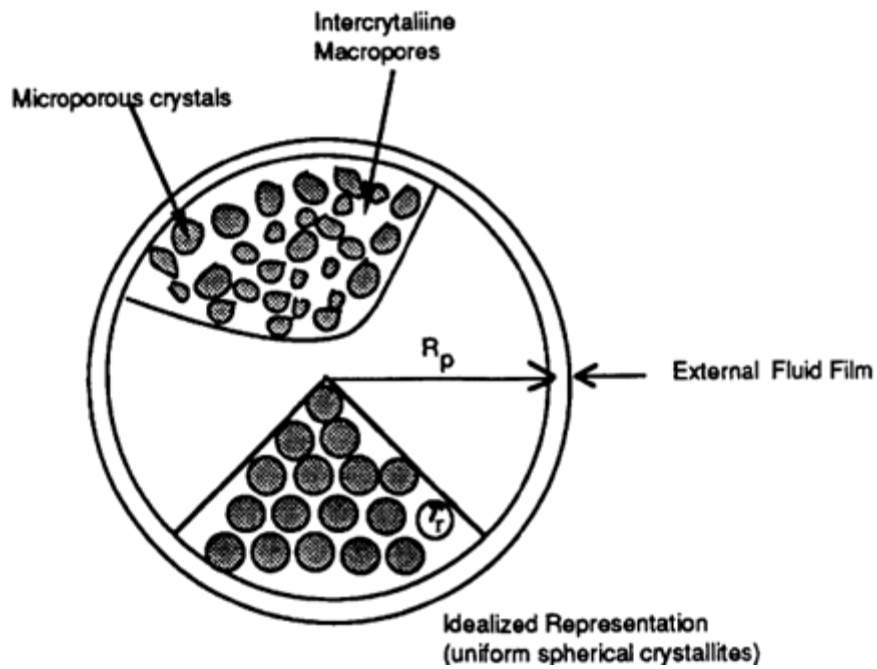


Figure 2.14 Schematic diagram of composite adsorbent pellet showing the three principal resistances to mass transfer

Where

q is the adsorbed phase concentration average over a particle.
 t is time.

K_f is an effective mass transfer coefficient.

A is the external surface area per unit particle volume.

C is sorbate concentration in the fluid phase.

C^* is sorbate concentration in equilibrium with q

Correlations of the Sherwood number are used to estimate the value of k_f .

$$Sh = \frac{2k_f R_p}{D_m} = 2.0 + 0.6 Sc^{1/3} Re^{1/2} \quad 2.10.15$$

R_p = catalyst diameter.

D_m = the molecular diffusivity.

Sc = Schmidt number = μ/pD_m

Re = Reynolds number = $\rho v (2R_p)/\mu$,

μ = the viscosity of the gas phase

ρ = the density of the gas phase

2.10.3.2 Macropore resistance

Macropore (intercrystalline) resistance may also be present in a catalyst which is formed from a composite of crystals into a macroporous pellet. The size of the macropore may range from 50 to 20000 Å. This resistance can be divided into 4 different types depending on the details of the pore structure:

- ✓ Molecular Diffusion
- ✓ Knudsen Diffusion
- ✓ Surface Diffusion
- ✓ Poiseuille Diffusion

Molecular Diffusion: dominant in large macropores in which the mean free path of the gas (average distance travelled between molecular collisions) is small relative to the pore diameter. At high pressure the rate of collision between diffusing molecules in the bulk fluid is higher than that between molecules and the pore wall. The molecular diffusivity for gas systems can be estimated from the Chapman-Enskog equation:

$$D_m = \frac{0.00185T^{3/2} \left(\frac{1}{M_1} + \frac{1}{M_2} \right)^{1/2}}{P \sigma_{12} \Omega \frac{\epsilon}{kT}} \quad 2.10.16$$

Where

D_m is the molecular diffusivity (cm²/sec)

T = absolute temperature (K).

M_1 & M_2 = molecular weight of the collided molecules.

P = total pressure (atm).

σ_{12} = collision diameter (Å) from the Lennard-Jones

Potential = $1/2(\sigma_1 + \sigma_2)$.

Ω = function of ϵ/kT .

Where $\epsilon = \sqrt{\epsilon_1 \epsilon_2}$:the Lennard-Jones force constant

K: = Boltzmann constant

If molecular diffusion is the only rate controlling process, the pore diffusivity, D_p , is given

$$\text{by: } D_p = \frac{D_m}{\tau} \quad 2.10.17$$

Where τ = tortuosity factor

Knudsen Diffusion: occurs in small-pore adsorbents at low pressures due to the collisions between the molecules and the wall of the pores which are more frequent than the collisions between the molecules themselves. This is because the mean free path of the gas is longer than the pore diameter.

The Knudsen diffusivity, D_K , can be estimated from the Kinetic Theory of gases:

$$D_K = 9700 r \left(\frac{T}{M} \right)^{1/2} \quad 2.10.$$

Where

r = mean pore radius (cm).

T = absolute temperature (K).

M = molecular weight of the diffusing species.

Equation 2.10.18 shows that Knudsen diffusivity depends on the pore size, temperature and the molecular weight of the colliding molecules and not the concentration of the gas.

In the case where both Knudsen and molecular diffusion control the rate of adsorption, the pore diffusivity is estimated from the expression:

$$\frac{1}{D_p} = \tau \left[\frac{1}{D_K} + \frac{1}{D_m} \right] \quad 2.10.19$$

Surface Diffusion: involves the transport of molecules within the adsorbed layer along the pore wall. These layers obstruct the mobility of new molecules to be adsorbed. The thickness is significant at low temperatures and pressures and is difficult to measure because other processes such as molecular or Knudsen diffusion always exists. It is usually obtained from the difference between the measured flux and the flux due to either molecular or Knudsen diffusion.

Poiseuille Flow: occurs when there is a high pressure drop across the particle, since there will then be a contribution to the adsorption flux from the forced laminar flow through the macropores. This effect can be neglected if the pressure drop is very small and it becomes dominant in the pores of radius $10^{-5} - 10^{-4}$ cm. The diffusivity from Poiseuille's equation is given by:

$$D = \frac{P r^2}{8\mu} \quad 2.10.20$$

Where

P = absolute pressure (dynes/cm²).

μ = viscosity (poise).

r = pore radius (cm).

This equation implies that at low pressure and small pore radii Poiseuille flow resistance becomes dominant.

2.10.3.3 Micropore Resistance

The diffusion through the micropore (for pore sizes less than 20 Å), the transfer of reactants to the active sites in the crystals may be retarded by the size of the pore. The micropore or intracrystalline diffusivity, D_c , is usually expressed in terms of the diffusional time constant (D/r_c^2) and may be determined from the appropriate expression of the uptake experiment

$$\frac{q - q_0}{q_0 - q_0} = \frac{m_t}{m_\infty} \quad 2.10.21$$

Where

q = initial adsorbed phase concentration.

q_0 = final adsorbed phase concentration.

$-q$ = average concentration through the particle,

t = time.

m_t, m is the mass adsorbed at time t and at infinite time.

2.10.4 Experimental measurement of diffusion

Many experimental techniques have been developed to measure diffusivity in zeolites. The following is a brief description of the techniques used in the measuring of diffusivity.

2.10.4.1 Uptake rate measurements

This measurement determines the transport diffusivity which can then be related to the self diffusivity. The principle of this method is quite straightforward and uses the measurement of the adsorption and desorption rate obtained from the transient uptake

curve generated by a step change in ambient sorbate concentration. The diffusivity is obtained by matching the experimental curve to the relevant solution of the diffusion equation. Gravimetric, volumetric or piezometric methods may be used to observe the transient uptake curve. The limitations arise mainly from the difficulty of eliminating the intrusion of extraneous heat and mass transfer resistances. Ruthven (1984) commented on some of the obvious precautions which should be accounted for experimentally determining the intracrystalline diffusivity:

- To minimize external mass transfer and heat transfer resistances, a very small amount of adsorbent and very thin bed should be used. The uptake rate should be independent of the configuration of the sample for intracrystalline control since the external heat or mass transfer resistance is sensitive to the sample configuration.
- Since the time constant (D/r_c^2) should vary with the square of the crystal radius, experiments with different crystal sizes can be used to confirm the dominance of intracrystalline diffusion control.

For a linear (constant diffusivity) system the uptake curve should remain the same when the step size of sorbate is changed. Therefore the linearity of the system can be confirmed by varying the concentration step.

2.11 Chromatography

In chromatographic method, the diffusivity is determined by measuring the dynamic response from an injection of the sorbate to a packed column as either a pulse or step input. The mass balance for the adsorbed species leads to an expression for the mean retention time as a function of the adsorption equilibrium constant while the second moment shows the combined effect of dispersion and mass transfer resistances Haynes (1973).

1st moment:

$$\mu = \frac{\int_0^\infty Ct dt}{\int_0^\infty C dt} = \frac{L}{v} \left[1 + \left(\frac{1-\varepsilon}{\varepsilon} \right) K \right] \quad 2.11.1$$

2nd moment:

$$\frac{\sigma^2}{2\mu^2} \equiv \frac{\int_0^\infty C(t-\mu)^2 dt}{\int_0^\infty C dt} \quad 2.11.2$$

$$\frac{D_L}{vL} + \left(\frac{v}{L}\right) \left(\frac{\varepsilon}{1-\varepsilon}\right) \left\{ \frac{R}{3k_f} + \frac{R^2}{15\varepsilon_p D_p} \frac{r_c^2}{15KD} \right\} \left\{ 1 + \frac{\varepsilon}{(1-\varepsilon)K} \right\}^{-2} \quad 2.11.3$$

In principle macropore and micropore time constants may be determined in this way but the method is limited when both resistances are significant and the response peak is due to the combined mass transfer resistances. To separate one resistance from the other requires additional experiments.

2.11.1 ZLC Method (Zero Length Column)

Although the chromatographic method has the advantage of improved heat transfer resistance compared to the classical uptake rate experimental technique, the retention times are inconveniently long for strongly adsorbed species such as C₉ aromatics. A modified technique, ZLC by Ruthven (1984), retains those basic advantages while results may be obtained within a short period of time.

2.11.2 Zero Length Columns: Theory

The principle of this method is to observe the desorption curve obtained from purging a very small sample of adsorbent previously equilibrated at a low sorbate concentration with an inert carrier gas. In order to minimize external heat and mass transfer resistances and also to keep the concentration level at the surface as low as possible, essentially zero, a very high purge flow rate is used during the desorption.

The diffusion equation for a spherical crystal with evaporation at the surface is:

$$\frac{\partial q}{\partial t} = D \left(\frac{\partial^2 q}{\partial r^2} + \frac{2}{r} \frac{\partial q}{\partial r} \right) \quad 2.11.4$$

With the initial and boundary conditions:

$$t \leq 0, q = q_0 = K C_0 \quad \text{for all } r. \quad 2.11.5$$

$$t > 0, r = 0, \delta q / \delta r = 0 \quad 2.11.6$$

$$t > 0, 0 < r < r_c, q = K_C \quad 2.11.7$$

$$R < r_{c,-D} \left(\frac{\partial q}{\partial r} \right)_{r_c} = \frac{\varepsilon v r_c}{3(1-\varepsilon)z} \frac{q}{K} \quad 2.11.8$$

It is assumed that many significant inter crystalline resistances are negligible so that the sorbate concentration at the crystal surface is zero - this can be verified experimentally in three ways. One method is to use different purge gases such as He and Ar which have different molecular diffusivities. The other two are varying the purge flow rate and crystal size. The solution of the diffusion equation (from the analysis of diffusion in a sphere with surface evaporation) is given by Ruthven (1988), in terms of concentration us:

$$\frac{C}{C_0} = 2L \sum_{n=1}^{\infty} \frac{\exp(-\beta_n^2 Dt/r_c^2)}{[\beta_n^2 + L(L-1)]} \quad 2.11.9$$

where β_n is the root of equation:

$$\beta_n \cot \beta_n + L - 1 = 0 \quad 2.11.10$$

And

$$L = \frac{1r_c^{2*} \text{purge flow rate}}{3KD \text{ crystal volume}} \quad 2.11.11$$

$$= \frac{1r_c^2 * \varepsilon v}{3D (1-\varepsilon)Kz} ; z = \text{bed length}$$

In the long time limit only the first term is significant, the other terms can be neglected. Determination of the higher order terms in Equation 2.11.10 shows that the error of the estimation of the diffusional time constant does not exceed 8%. Therefore, the expression for the uptake curve reduces to:

$$\frac{C}{C_0} \approx 2L \frac{\exp(-\beta_1^2 Dt/r_c^2)}{\beta_1^2 + L(L-1)} \quad 2.11.12$$

$$\ln \frac{C}{C_0} \approx \ln \frac{2L}{\beta_1^2 + L(L-1)} - \beta_1^2 \frac{Dt}{r_c^2} \quad 2.11.13$$

A plot of $\ln(C/C_0)$ vs t should be linear with the slope of

$$S = -\frac{\beta_1^2 D}{r_c^2} \quad 2.11.14$$

and the intercept of

$$I = \ln \frac{2L}{\{\beta^2 + L(L-1)\}} \quad 2.11.15$$

and this is the region in which $C/C_0 \ll 1$ is varied. The value of β can be obtained from equation 2.11.11 and 2.11.15. By substituting this into equation 2.11.14 the diffusional time constant and diffusivity can be determined.

For very low purge flow rates the desorption rate is controlled by the rate of removal of sorbate in the purge gas since the diffusion through the particle is fast and the concentration through the crystal is always maintained at equilibrium. With these conditions the desorption

curve is given by:

$$\ln \left(\frac{C}{C_0} \right) = - \frac{\varepsilon v t}{(1-\varepsilon)Kz} \quad 2.11.16$$

A plot of $\ln(C/C_0)$ vs. t gives a straight line with the slope of $-\varepsilon v / (1-\varepsilon)Kz$; the uptake depends only on the purge rate and the equilibrium constant, not on D/r_c^2 .

If the limiting slope obtained under gas velocity v_1 is designated as S_1 , then at a much higher gas velocity V_2 the corresponding value of L is:

$$L \frac{D}{r_c^2} = \frac{1}{3} \left(\frac{v_2}{v_1} \right) S_1 \quad 2.11.17$$

Therefore, another way to obtain the diffusional time constant is to measure two response curves: one at a low purge rate (V_1) which is valid in the region of Equation (2.11.16) and another at higher purge rate (V_2). The slope obtained from Equation (2.11.16) at the low purge flow region is used to find LD/r_c^2 in Equation (2.11.17). The slope and intercept of the high flow rate should obey Equation (2.11.14) and (2.11.15), hence giving three equations and three unknowns, D/r_c^2 , p and L can be determined.

CHAPTER THREE

MATERIALS AND METHODOLOGY

In this chapter, the experiments conducted are reported. The focus of this research is to develop a chemically, thermally stable and most probably commercially viable Zeolite Y catalyst for cracking of higher hydrocarbon molecules e.g vacuum gas oil into a lower one of more economic value e.g gasoline. The first step to achieving this goal was to identify different materials suitable for the synthesis from literature as explained in Section 2.5 of this work and clay was found to be suitable, particularly the one from Elefun Local Government Area of Ogun State.

The sequence of work adopted includes all the experiments starting from collection of raw Elefun clay to the refinement of the raw samples, metakaolinization, up to the actual synthesis of Zeolite Y and its characterization. Subsequently, the developed NaY was subjected to modification by ion exchange process to create active acid sites (Bronsted sites) needed for cracking and stability improvement and was followed by performance test in a fixed bed pulse reactor.

Elefun clay was procured and subjected to refinement by beneficiation and calcinations before application in zeolite sample formulations. The formulated samples were strictly monitored at stages involved by carrying out analysis using analytical equipment such as x-ray fluorescence, x-ray diffractometry, scanning electronic microscope. Other allied characterization methods were employed to identify crystallite type and the determination of other utility properties. These procedures are detailed in the appropriate section.

3.1 Materials

- (a) Kaolin source from Elefun Local Government Area of Ogun State.
- (b) Reagents

In carrying out this experiment, the listed materials and equipment were used.

3.1.1 Beneficiation equipment/material

Table 3.1: List of Materials/equipment used during Beneficiation

Equipment /Material	source	Quantity/model
Raw Elefun kaolin	Elefun ,Ogun state	4kg
Plastic bucket		20 litres (4 nos)
Sieve	.	75 μ m mesh
No. 64 Michem instrument		-

3.1.2 Calcination equipment/materials

The equipment/materials used for calcination of Elefun kaolin are presented in Table 3.2

Table 3.2: List of Materials/Equipment used during Calcination

Equipment /Material	Source	Quantity/model
Locally fabricated crucible		0.5litre (5nos)
Electric furnace	-	No:LH120/14m/temp 1400, 400v, 50/60Hz, 26.0A,18.0kw
Desicator with silica gel		Nr/No 182487

3.1.3 Dealumination material/equipment

The equipment/materials used in carrying out dealumination of metakaolin are presented in Table 3.3.

Table 3.3: List of Materials/equipment used during Dealumination

Equipment /Material	Source/manufacurer	Quantity/model
Metakaolin	Babalola/Omoleye/Adefila/Hymore	2kg
Electronic weighing machine		PW 184, M:180g - accuracy 10-4g
Heating mantle with voltage	Addis chemical,Zari	500ml capacity
Sulfuric acid (H ₂ SO ₄)		250ml,1ml for each
Three neck-round bottom flask,thermometer and reflux condenser	Edward England	96% w/w 1 set
Vacuum pump		
pH meter		No:ES00 1

3.1.4 Gelation material/equipment

Table 3.4: List of Materials/equipment for Gel formation and actual synthesis of zeolite Y

Equipment /Material	Supply by	Quantity/model
Dealuminated metakaolin with Silica/Alumina ratio of 4.49	Babalola/Omoleye/Adefila/Hymore	2kg
Electronic weighing machine		PW 184, M:180g accuracy 10-4g
Sodium hydroxide (NaOH)	Addis Chemical, Zaria.	500ml capacity
Deionized water	ABU, Mkt	200g
1 litre Plastic cup for aging	ABU Zaria	96% w/w
Electrically driven magnetic stirrer		20Lit 2 nos
Vacuum pump	ABU Zaria	
pH meter		No:ES00 -
Laboratory oven	ABU Zaria	1 -
	Model No:MD6C-64, Michem Instrument	1
Teflon/polyethylene		6nos
Standard zeolite Y	KRPC	1kg

3.1.5 Chemicals used for performance test experiment

The chemicals used for this study are listed in Table 3.5.

Table 3.5: List of Chemicals used during performance test experiment

Material	Manufacturer	Comment
Locally developed zeolite Y	Babalola, Omoleye, Adefila ,Hymore	Si/Al ratio of 4.79
Commercial zeolite Y Catalyst	Grace Gmbh USA	Si/Al ratio 5.70
Cyclo-Hexane	Johan Hattermann,	99.99% purity
Vacuum Gas Oil	NNPC/KRPC,Kaduna	Supplied by KRPC
Nitrogen Gas	NNPC/KRPC	Supplied by KRPC.
Silica Gel	BDH Chem. Poole England	6-20 mesh
Copper Oxide	Hopkin & Williams	Assay 90.0% min.

3.1.6 Equipment used for performance test experiment

The equipment used in the research work is presented in Table 3.6.

Table 3.6: List of Equipment used during Zeolite Y catalyst performance test

Equipment	Make	Comment
Gas Chromatograph and accessories		Spec. No. ,KRPC
Electronic Weighing Balance	OHAUS, U.S.A.	Supplied by KRPC
Electronic Stop Watch	Not Available	Supplied by KRPC
Gas Cylinder and Regulators	Unknown	Supplied by KRPC
Temperature Reading Meter	Shinohara Ltd	Purchased from Power-link
	Not Available	Electrical, Kaduna
Rheostat	-	Purchased at Kaduna.
Split Valve	Not Available	Benue road,Kaduna,Nigeria
Control Valves	Valco instrument	Benue road, Kaduna,Nigeria
Tubular Oven + Thermocouple	Co. Inc.	Purchased at , Kaduna
Flow Meter	-	Not yet available
Stainless Tube (6mm int. diameter)	Not available	Owode-Onirin,Lagos,Nig.
Glass Wool	Not Available	Not yet provided
Teflon Tape	Not Available	Purchased at Iyana,Otta

Methodology of Zeolite Y synthesis from Elefun clay and its performance test

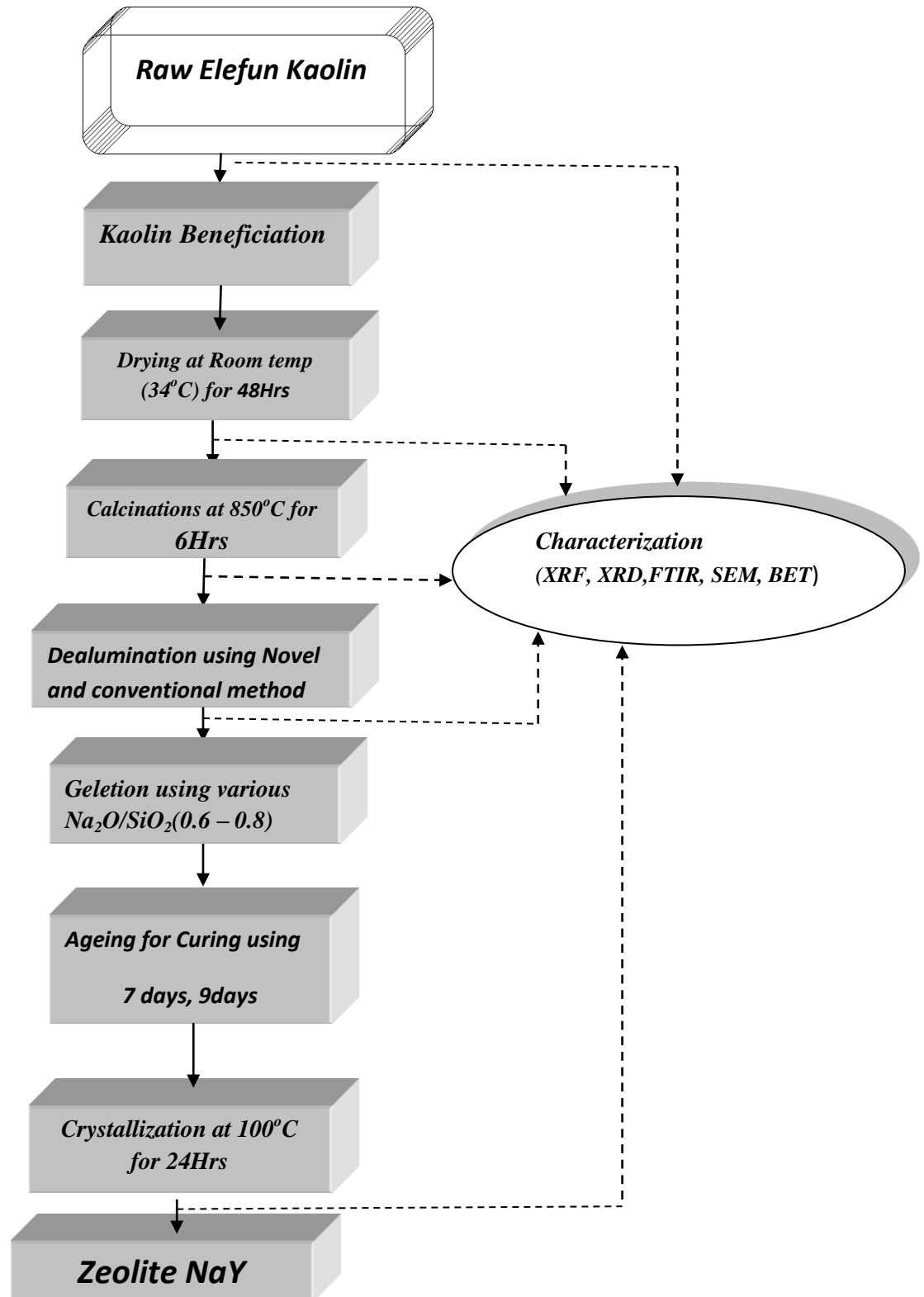


Figure 3.1: Flow Diagram of Zeolite Y Synthesis from Elefun Clay

3.2.1 Clay beneficiation

Beneficiation is the process of improving both the physical and chemical properties of crude kaolin. It includes:

- Chemical and mechanical dispersion of raw ore
- Screening and sieving to remove physical impurities e.g sand, mica etc.
- Selective flocculation and flotation to remove discolouring impurities
- Centrifugation using solid bowl and/or disc nozzle centrifuges to control particle size distribution.
- Chemical flocculation and leaching processes to solubilize iron and prepare kaolin slurries for subsequent dewatering.
- Dry size reduction equipment including cage mills, roller mills and high speed pulverizers
- Dewatering processes including the use of hydro separators, rotary vacuum filters rotary and vertical calciners.

3.2.1.1 Procedure

Exactly 4 kg of the kaolin procured from Elefun Local Government Area of Ogun State was soaked in 20 litre plastic container, with raw tap water filled up to three quarter (3/4) height, for a period of seven days. At every six (6hrs) the kaolin was masticated and agitated by continuous stirring using an automatic fast rotating three - blade stirrer. When the kaolin was completely settled, the floating dirt was decanted, alongside with the accompanying supernatant. The process of thorough mastication of kaolin resulted in the removal of stony particles achieved via handpicking or slurry decantation. Thereafter, fresh water was introduced, into the muddy kaolin, to effect frothing through mixing followed by layered settling. This was followed by repeated pulping processes through mastication, grinding, crushing, agitation and decantation until there was virtually no noticeable solid layers at the bottom of the plastic container. The topmost layer of the resulting slurry was removed and separated into a different container, washed with water and sieved using a 75 micron mesh sieve twice. The sieved material was dewatered dried atmospherically for 48hrs and further dried at 45°C in an electric oven (model No:MD6C-64, Michem instrument) for 4hrs. The

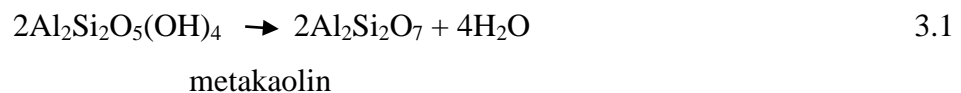
resulting dried cake was milled to very fine particle size with ball mill and the sample subsequently packaged for analysis.

3.2.2 Calcinations

This is the process used to put the beneficiated clay to a more reactive phase - metakaolin (semi-armorphous) as kaolin in its natural state is less reactive and forms hydrosodalite when reacted with sodium hydroxide (Chandrasekhar and Pramada,1999). Various authors reported calcinations temperature to range between 600-900°C and time range of 1 to 8 hrs (Yaping *et. al.*, 2008, Liu, and Pinnavaia, 2004)

The process of metakaolinization involves the loss of hydroxyl group and is followed by rearrangement of the octahedral layer to tetrahedral orientation in the calcined kaolin (Murat, et al., 1992 Klinowski and Joao, 1990] Kaolin is an aluminosilicate and the Al³⁺ ion can be in the form of IV and VI coordination state and it is essential in zeolite formation that Al³⁺ is in IV coordination, hence metakaolin with IV Al coordination and amorphous in nature is a necessary path toward zeolite synthesis from kaolin (Chandrasekhar, 1996, Patrylak et al., 2001).

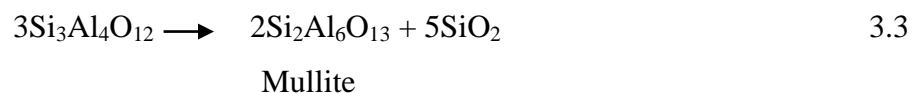
The changes that occur when kaolin is heated in a furnace has been well reported (Breck, 1974; Madani et al., 1990) and found to have a number of technological uses. This reaction series includes the formation of highly disordered metakaolin formed at around 550-900°C when kaolin is calcined as shown in Equation 3.1



On further heating, a new phase is obtained at around 925°C called spinel, a defected Alumina-silica structure



While mullite and cristobalite are formed at a temperature of 1050°C



This research is limited to formation of metakaolin from Elefun kaolinite clay using a new rapid but very reactive, and energy saving technique of dehydroxylation as presented .

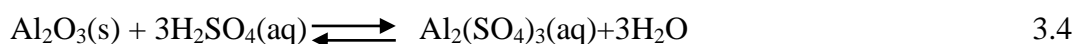
The thermal conductivity, specific heat capacity and thermal diffusivity of clay indicated that only small amounts of kaolin should be calcined at a time or alternatively the use of rotary furnace.

The optimal temperature used in this work was arrived at after investigating the effect of calcinations temperature and time on amorphousity and rate of solubility and digestion in acid/alkali, for all the kaolinite components, on one hand. On the other hand, investigation was conducted to study the best metakaolinization temperature required to convert both alumina and silica into more reactive, highly digestible forms for zeolite synthesis.

The result of the aforementioned preliminary investigation, informed the choice of calcining the beneficiated kaolin at 850°C. In the process, the clay was heated in a programmable electric furnace (Model no; LH 120/14), from room temperature (T) (34°C) to the calcinations temperature (T_{Cal}) at heating rate of 10°C/min. The sample was held at T_{cal} (850°C) for 6hrs (Babalola et al., 2014). Calcination was achieved by evenly placing about 500 grammes of beneficiated kaolin into a large, rectangular, locally fabricated crucible to allow for a relative good heat distribution, since, the specific heat capacity and latent heat of kaolin is poor. The metakaolin obtained was then cooled in a desiccator, prior to characterization and usage.

3.2.3 Dealumination of the Calcined Clay

To increase the SiO₂:Al₂O₃ ratio of the starting material, dealumination is an alternative route to addition of silica from other sources. Therefore, to determine the optimum concentration of acid required to effect the extraction (leaching) of alumina from the Clay, preliminary runs were made by treating 50 grammes of beneficiated clay each with 149.6864cm³ of 60% concentrations of H₂SO₄ solutions. The dealumination reaction is given as:



Dealumination

The silica-alumina ratio of the resulting metakaolin was determined from the compositional analysis, using XRF. The inherent Si/Al ratio for metakaolin was not good enough for the synthesis of faujasite type zeolite.

Accordingly, to meet the compositional requirement for the synthesis, removal of alumina (dealumination) and other impurities from metakaolin was carried out. This was achieved by making the calcined kaolin react with sulfuric acid. Dealumination by using sulfuric acid reaction was carried out by using a non heating method known as Novel approach. The extent of dealumination was determined by varying the reaction times.

(a) Conventional method of heating.

This method often requires the input of an external source of thermal energy to facilitate the needed kinetic energy for effective collision and successful reaction between the metakaolin and sulfuric acid. In all cases, dealumination was done by using three fold of the stoichiometric amount of 60wt% sulfuric acid required. This was done to enhance mass transfer and to reduce cake formation tendencies (Aderemi, 2000).

About 50g of metakaolin was mixed with 83.86cm³ of deionized water and 149.6864cm³ acid with vigorous stirring in a three necked round bottom flask. The neck at the center, of the flask which was placed on the heating mantle, was fitted with a reflux condenser; a thermometer was placed in the second neck while the third neck was closed with a rubber cork. The reaction time was varied for 3, 6, 8 and 10 minutes in order to establish the reaction time required to give the targeted silica-alumina ratio of between 3 and 10. The reaction time of 3 minutes gave the required silica-alumina ratio and was eventually used for bulk production.

The dealuminated samples were washed thoroughly, with hot deionized water to ensure almost complete removal of excess unreacted acid and other soluble salts resulting from the leaching process. These were subsequently dewatered, using suction pump and dried in an oven at 110°C for 3hrs. The dried dealuminated samples was packaged for various analysis

(b) Non-heating method of dealumination

This method of dealumination reaction does not require an external source of thermal energy to facilitate the dealumination of the metakaolin, but instead it employed the heat released when sulphuric acid was mixed with water. Although Similar approach as presented in section 3.3(a) above was employed.

The reaction time was varied between 3 and 11 minutes, at intervals of 2 minutes in order to establish the reaction time required to give the targeted silica-alumina ratio of 5 .For further

investigation on the relationship between reaction time and silica alumina ratio, reaction time of 17 and 21 minutes was used. At the end of the reaction period, the samples were quenched with water.

The dealuminated samples were washed thoroughly, with deionized water to ensure almost complete removal of unreacted acid and other soluble salts resulting from the leaching process. These were subsequently dewatered, using suction pump and dried in dust free natural air for 24hrs. The dried dealuminated samples were packaged for various analysis.

3.2.4 Gel formation

At this stage gellation was achieved with a desired molar composition as shown in Equation 3.5 and 3.6

$$\frac{\text{SiO}_2}{\text{Al}_2\text{O}_3} = 4.695; \quad \frac{\text{Na}_2\text{O}}{\text{SiO}_2} = 0.6; \quad \frac{\text{H}_2\text{O}}{\text{Na}_2\text{O}} = 30 \quad 3.5$$



The Silica/Alumin ($\text{SiO}_2/\text{Al}_2\text{O}_3$) ratio used in this work is obtained from the compositional analysis of the dealuminated samples as shown in Table 4.3 while the ratio of Sodium oxide to Silica ($\text{Na}_2\text{O}/\text{SiO}_2$) and that of water to Sodium oxide ($\text{H}_2\text{O}/\text{Na}_2\text{O}$) were kept constant. The mass of NaOH and volume of water required for gellating 50gm of dealuminated metakaolin was obtained as 20.3g and 136.4 cm³ respectively. Detailed calculations are shown in Appendix B. 50 g of the dealuminated metakaolin that was mixed with 136.404cm³ deionised water, firstly by pouring the first half (68.2cm³) into a 1 litre plastic cup and mixing in it the measured dealuminated metakaolin completely. 20.3g of sodium hydroxide pellets (96%w/w) supplied was added to the precursor and stirred vigorously until the pellets dissolved. The second half of the deionised water was subsequently introduced similar to method used by Ajayi, 2012, and mixed to form aluminosilicate gel using an electrically driven stirrer for a period of 4 minutes. The resulting gel was introduced into a polypropylene autoclave for aging purpose.

3.2.5 Actual Synthesis of Zeolite Y from Elefun Clay

Finally, Zeolite Y actual synthesis was carried out and the aging time, crystallization time and temperature were studied. The gel developed was aged at temperature of 34°C for 7 and 9

days respectively. This was followed by crystallization for 24 hours in the oven at a temperature of 100°C. At the end of the hydrothermal treatment, the autoclave was removed from the oven and the sample taken out, filtered and washed with deionised water until the pH of between 7 and 8 was obtained. The washed sample was completely dried and packaged for various analyses.

The products obtained were characterized with X-ray diffraction (XRD), Scanning Electronic Microscope (SEM), Fourier Transform Infrared Spectroscopy (FTIR) and BET surface area.

3.2.6 Determination of Ion Exchange Capacities

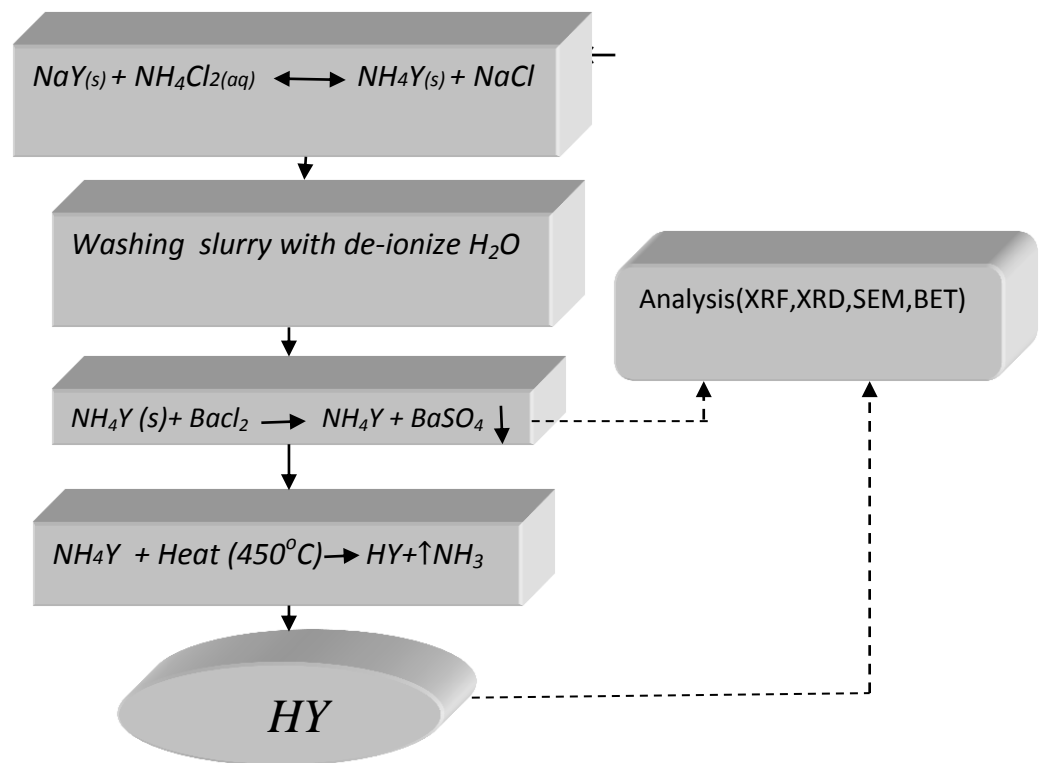


Figure 3.2: Modification of Zeolite NaY to Zeolite HY

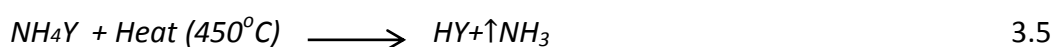
The product obtained from Section 3.4 is termed zeolite NaY and needs to be modified to its hydrogen form known as zeolite HY. The modification was achieved by measuring 10 grammes of the NaY to 100mL of 0.1M Ammonium Chloride solution in a 1litre plastic cup and stirred vigorously using magnetic stirrer for 10minutes and at room temperature. This operation was carried out twice.



The sample was then filtered from the slurry and washed with deionized water until the solid was free of chloride. Then 50mL of barium sulphate was added to the washed sample to confirm the absence of any trace of chloride which was confirmed by barium chloride precipitate at the bottom of the container.



The obtained solid (NH₄Y) was dried at room temperature for 24 hours and was subsequently transferred into the crucible and charged into the furnace at 450°C for residence time of 4 hours. The NH₄Y upon being heated drove away the ammonia leaving the zeolite Y in its hydrogen form



The solid zeolite HY was allowed to cool and was packaged for analysis.

3.3 Performance Test for Zeolite Y developed from Elefun kaolin

The Performance test for the zeolite Y synthesised from Elefun clay was carried out in a fixed bed reactor using a pulse microcatalytic technique, to crack cyclohexane.

The reactor was designed and constructed, using the guiding principles presented in Sections 2.10 and 2.11. Commercial zeolite Y catalyst sourced from NNPC was used as a reference test. The main apparatus consisted of a microcatalytic reactor, a gas chromatograph and an electric heater. The microcatalytic reactor, basically is a stainless steel tubing, 0.05m long and 0.006m internal diameter and was heated in a drum-shaped tubular oven. The flow diagram is as shown in Figure 3.3.

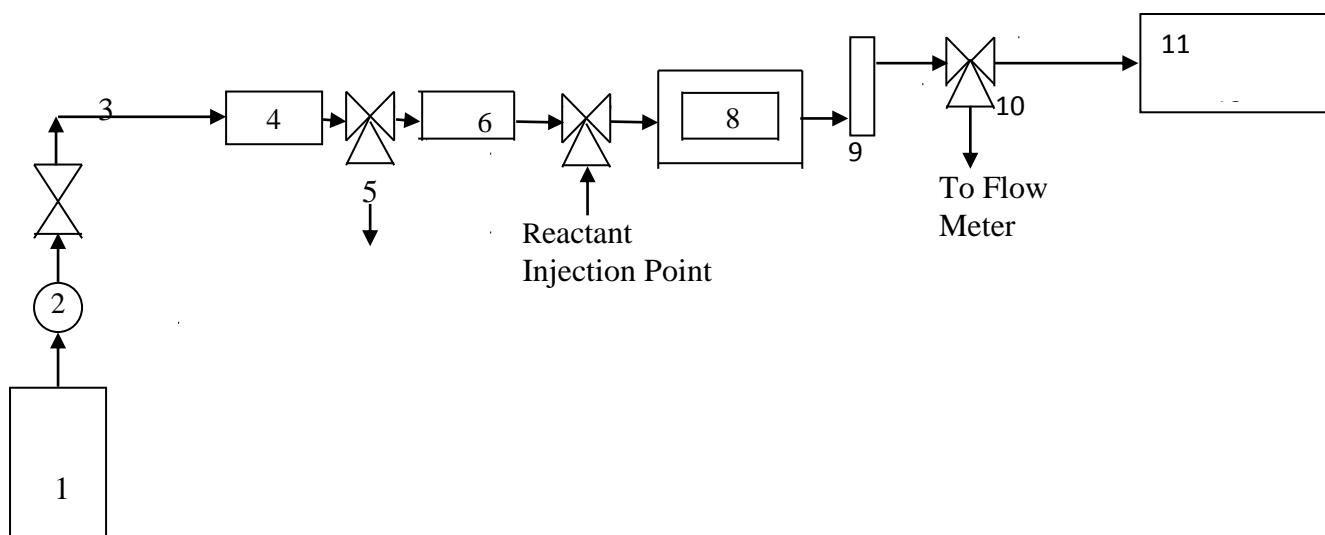


Fig.3.3 Experimental Set-up

Legend

1. High purity gas cylinders containing carrier gas .Helium
2. Cylinder regulator head for pressure regulation.
3. One-way control valves for the controlling of the carrier gas flow rate.
4. Silica gel bed for removal of traces of water.
5. Double way valve through which the removed water from (5) is flushed out.
6. Copper oxide bed for removal of oxygen.
7. Reactants injection point. The reactant is injected with the aid of a microsyringe and needle.
8. Micro catalytic reactor, which is a combination of a stainless steel tube 0.05m long and 0.006m internal diameter in a horizontal furnace equipped with temperature control devices.
9. Condenser for cooling the product mixture.
10. Three way valve, through which bubble-soap flow meter is connected.
11. Analytical Systems Gas Chromatography (Hitachi type fixed with FID, TCD).

The cracking rig was positioned in a tube furnace and the temperature measured with thermocouple. Each run of cyclohexane feed was injected into the reactor using a microsyringe.

The stainless pipe reactor was packed with fixed weights of the catalysts (0.15g). Various helium gas (carrier gas) flowrate between (40 to 100 mL/min at interval of 20mL/min) was passed through the reactor. The temperature of the furnace was also varied between 400°C and 520°C. The packed catalyst was left at the operating temperature for at least an hour for homogenization in each run before the cyclohexane vapour was injected. The exit compositions were determined by gas chromatographic method. The GC (Hitachi model:) was fixed with flame ionization detector (FID) capable of detecting the various components except hydrogen and other dry gases. This was done by varying both the carrier gas flowrate and the reaction temperature, while the catalyst was inside the reactor. The reaction time was 60 seconds and the cracked components were analyzed in the online gas chromatogram as shown in Appendix E.

3.3.1 Experimental procedure

The experimental procedure involves equipment set-up, catalyst preliminary preparation, catalyst pretreatment and undertaking cracking reaction on the pretreated catalyst, analyzing reaction product using Gas Chromatograph.

3.3.1.1 Preliminary preparation

Before the equipment was set up, the 6 mm internal diameter stainless tube was purged with industrial gas (purified air) under pressure. This was done to flush out dust particles and other impurities that may be contained in the pipe. The set-up was tested for air-tightness with the flow of helium at the pressure of 6.0atm/pa. This was done to avoid wastage of the carrier gas, and to avoid the danger of explosion .

3.3.1.2 Catalyst pretreatment

Zeolite Y catalyst was pulverized and sieved into 53-75 micrometer size. The choice of size was based on considerations of pressure drop and diffusion limitations. For each series of experiments, 0.15g of catalyst was loaded into the micro catalytic reactor. For effective loading of the catalyst into the 6mm diameter stainless tube reactor, cellophane funnel was used. The reactor was then plugged at both ends with glass wool to prevent the sweeping

away of the catalyst from the reactor. The catalyst was pretreated by drying it for 1 hour in 40ml/min nitrogen flow and at the temperature of 110⁰C in an oven. .

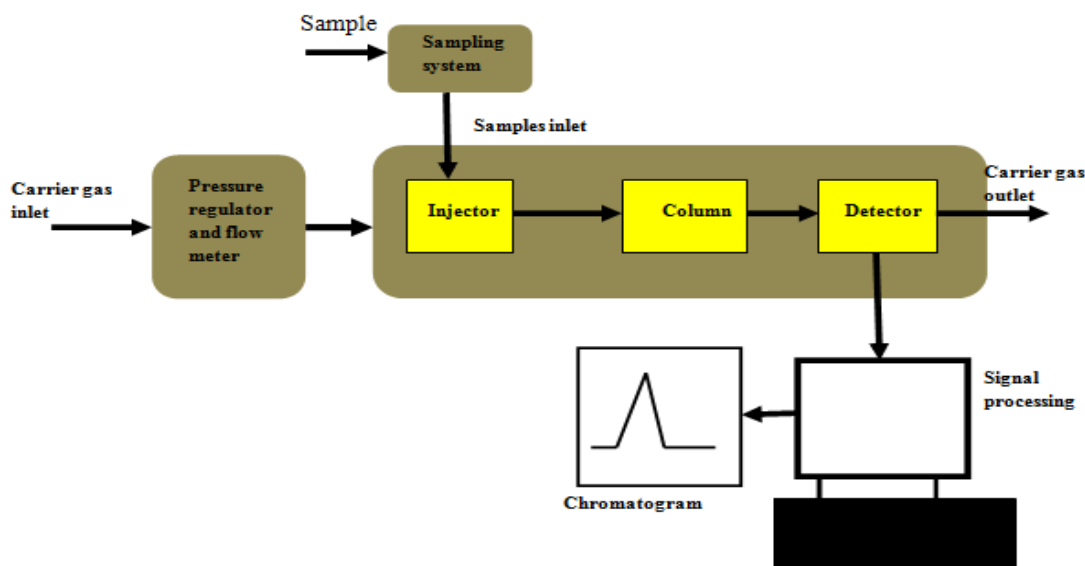


Figure 3.4: Schematic diagram of typical GC set up (Francis and Annick, 2000)

3.3.2 Gas chromatograph

The cracked cyclohexane sample was introduced into the gas chromatograph, heated, and carried by the gas phase through a column containing the stationary phase. The sample partition took place based on the difference in the solubility of the analyte at the given temperature. The general principle of GC is based on the affinity between the analyte and the stationary phase i.e. the more the analyte is retained in the column, the longer it takes to be detected or eluted.

GC operation was based on the introduction of the sample as a vapour onto the chromatography column. While in the column, the component solubility in the gas phase was dependent on its vapour pressure, column temperature and the affinity between the compound and the stationary phase. There is a partition of the molecules in between the gas phase and the stationary phase as a result of the different vapour pressure. The process of the partition continued until the molecules were pushed towards the detector by the gas phase. As a result of the difference in the vapour pressure, different compounds in the sample arrived at different times. The result of the cracked product was then displayed by the integrator in the form of peaks. A schematic diagram of GC is shown in Figures 3.4 and 3.5.

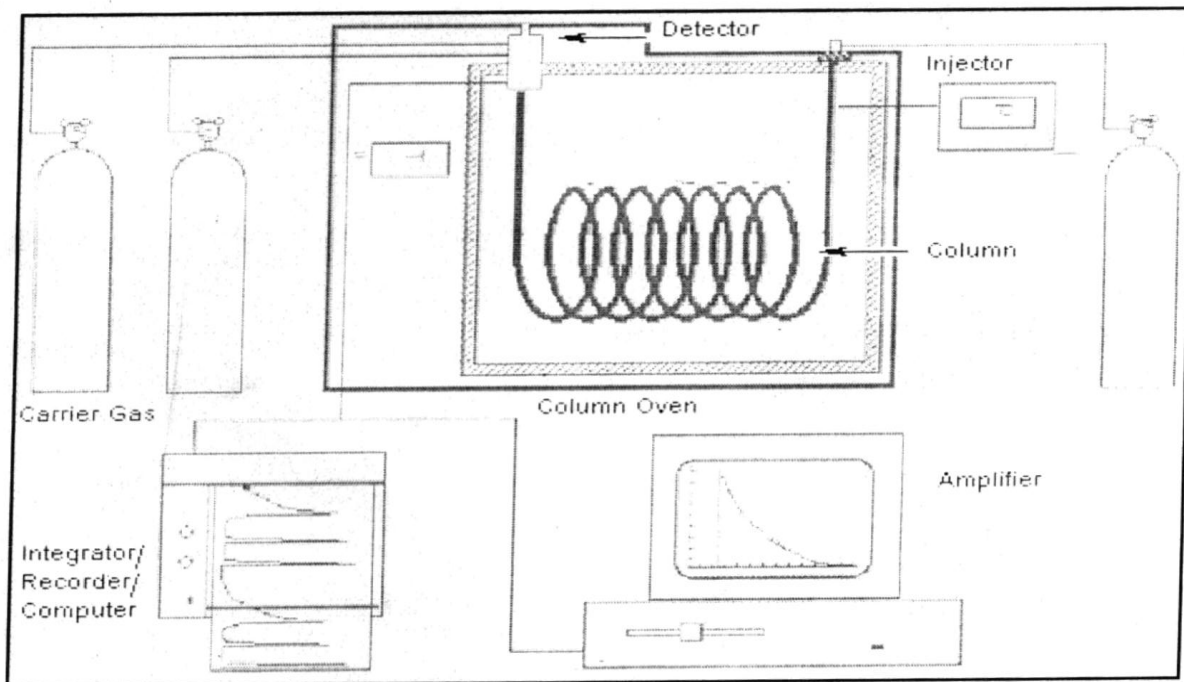


Figure 3.5: Gas Chromatograph system

CHAPTER FOUR

RESULTS AND DISCUSSION

INTRODUCTION

In this chapter all the results of this study are presented.

4.1 Results of X-ray fluorescence (XRF) Analysis of Raw, Beneficiated and Calcined Elefun Kaolin

Table 4.1: XRF results of the Raw, Beneficiated and Calcined Elefun kaolin

Chemical constituent	Raw kaolin	Mole%	Beneficiated kaolin	Mole%	Calcined kaolin	Mole%
	Weight %		Weight %		Weight %	
SiO ₂	53.80	35.86	51.60	35.86	51.5	35.86
Al ₂ O ₃	37.01	14.34	35.00	14.34	36.900	14.34
K ₂ O	0.63	0.40	0.54	0.40	0.615	0.40
TiO ₂	4.76	2.39	5.10	2.39	4.520	2.39
V ₂ O ₅	0.21	45.82	0.22	45.82	0.510	45.82
Fe ₂ O ₃	2.57	0.40	2.79	0.80	1.480	0.80
CaO	0.30	0.80	0.35	0.40	0.035	0.40
L.O.I *	0.69		0.78		4.41	
Total	99.97		96.38		95.49	
Silica/Alumina	1.45		1.47		2.373	

*Loss on Ignition

The compositional analysis conducted on the raw and beneficiated Elefun kaolins using X-Ray Fluorescence (XRF) are as shown in Table 4.1. The results show that Elefun kaolin contains contaminations of oxides of potassium, iron, titanium, and magnesium. It also indicates the effect of beneficiation on the treated raw kaolin as value of SiO₂ reduced from 53.80% to 51.60% due to removal of free silica (quartz) from raw kaolin. Table 4.1 also indicates that Elefun kaolin is ferric in nature due to its high content of iron oxide as compared with that of potassium. Similarly, the white colour of the raw and beneficiated Elefun Kaolin can be attributed to the significant content of TiO₂. It is also worth mentioning that the word ‘Elefun’ literarily means whitish in Yoruba Language.

Pure raw kaolinite clay is expected to have silica/alumina ratio of between 1 to 2 (Ajayi *et. al.*, 2010). Table 4.1 shows that the SiO₂/AlO₂ ratio of 1.45 and 1.47 for the raw and beneficiated kaolin respectively are within theoretical value.

4.1.2 XRD analysis

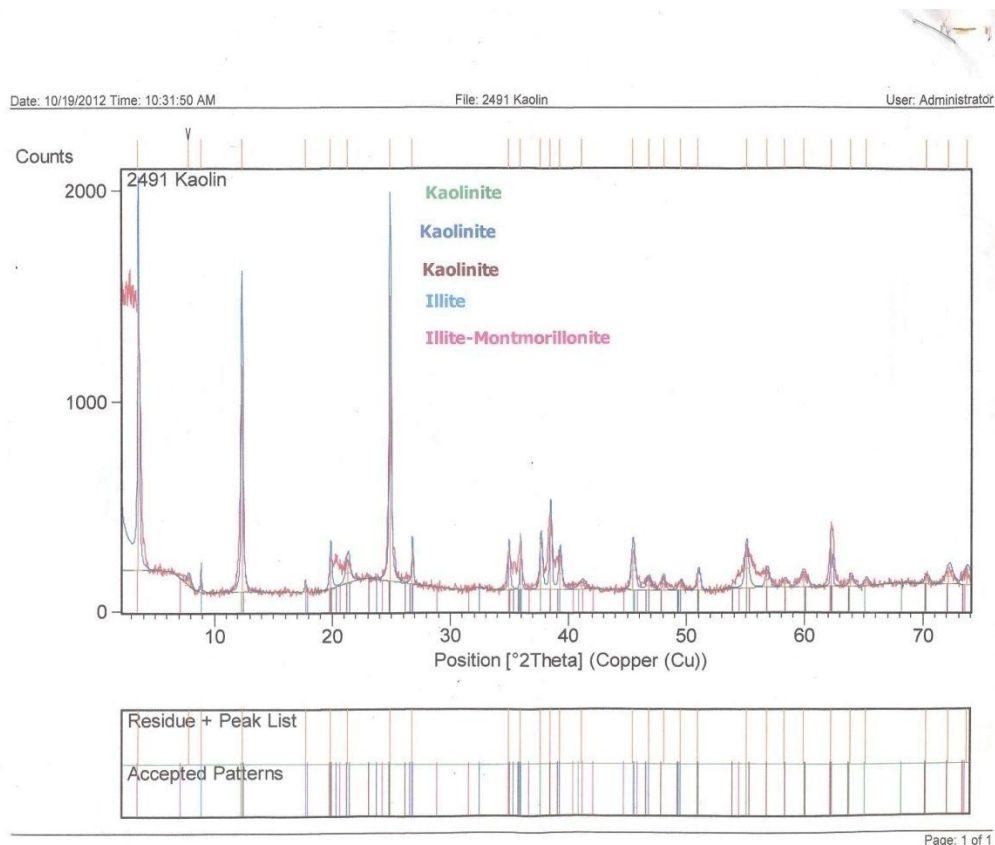


Figure 4.1: XRD patterns for raw Elefun kaolin as-mined

Figure 4.1 above is the result of X-ray diffraction (XRD) pattern for as-mined Elefun kaolin. It indicated several peaks due to the minerals present in the material. An analysis of the peaks shows a sharp peak with low intensity at $2\Theta = 12.34^\circ$ ($d =$). This is the main peak used in identification of kaolinite clay (Ramirez, 2007). Also, the peak obtained at position corresponding to $2\Theta = 25.90^\circ$ indicated the presence of large quantities of quartz. Kaolinite and quartz are predominant characteristics of natural kaolin (Tracy and Higgins, 2001, Evamako *et. al.*, 2001). Therefore the high level of quartz in Elefun kaolin is not surprising. Illite-montmorillonite, muscovite, hydrated mica and non-crystalline hydroxide iron are other types of impurities found with Elefun kaolin as-mined. However, the quartz content of Elefun kaolin needs to be reduced to minimum before its usage for industrial purpose especially in zeolites development. There were also peaks with features of smectite, muscovite, illite-Montmorillonite, halloysite and quartz. The XRF analysis (Table 4.1) corroborates with the results obtained with the XRD analysis.

4.2 Clay Beneficiation

4.2.1 XRF Analysis

As evident in Table 4.1, the compositional analysis of the beneficiated kaolin indicates a reduction in the composition of its free silica, alumina, potassium and other impurities, while there is an increase in iron content. These were due to proportionate reduction in silica content. It is expected that purification/beneficiation of raw kaolin will shift up its silica/alumina ($\text{SiO}_2/\text{Al}_2\text{O}_3$) ratio.

4.3 Metakaolinization of Elefun kaolin

4.3.1 XRF Analysis of Calcined Elefun Kaolin

The XRF analysis of metakaolin presented in Table 4.1 shows that there was little or no difference in the chemical composition of both the refined and calcined Elefun kaolin. The noticeable difference is in the values of the Loss On Ignition (LOI) increased from 0.78% to

3.63% for refined and calcined respectively this was due to the burning off of impurities such as Illite, dickite, brookite e.t.c during calcination.

4.3.2 XRD Analysis

The XRD patterns of Elefun metakaolin confirms that the clay is amorphous as all the kaolinite was converted to metakaolin as shown in Figure 4.2. The peaks at $2\theta = 12.34^\circ$ (kaolinite peak) disappeared but the peak at $2\theta = 25.49^\circ$ and 27.10° were not affected by the thermal treatment, attributed to the presence of quartz and haematite (Fe_2O_3), respectively. The same observations were made and reported by Ajayi et al., (2010) and Elimbi *et. al.*, (2011). Other inherent impurities such as microcline, illite, dickite and brookite were reduced by calcination.

Disorder within the metakaoline structure was due to calcinations at high temperature Bosch et al., (1983).

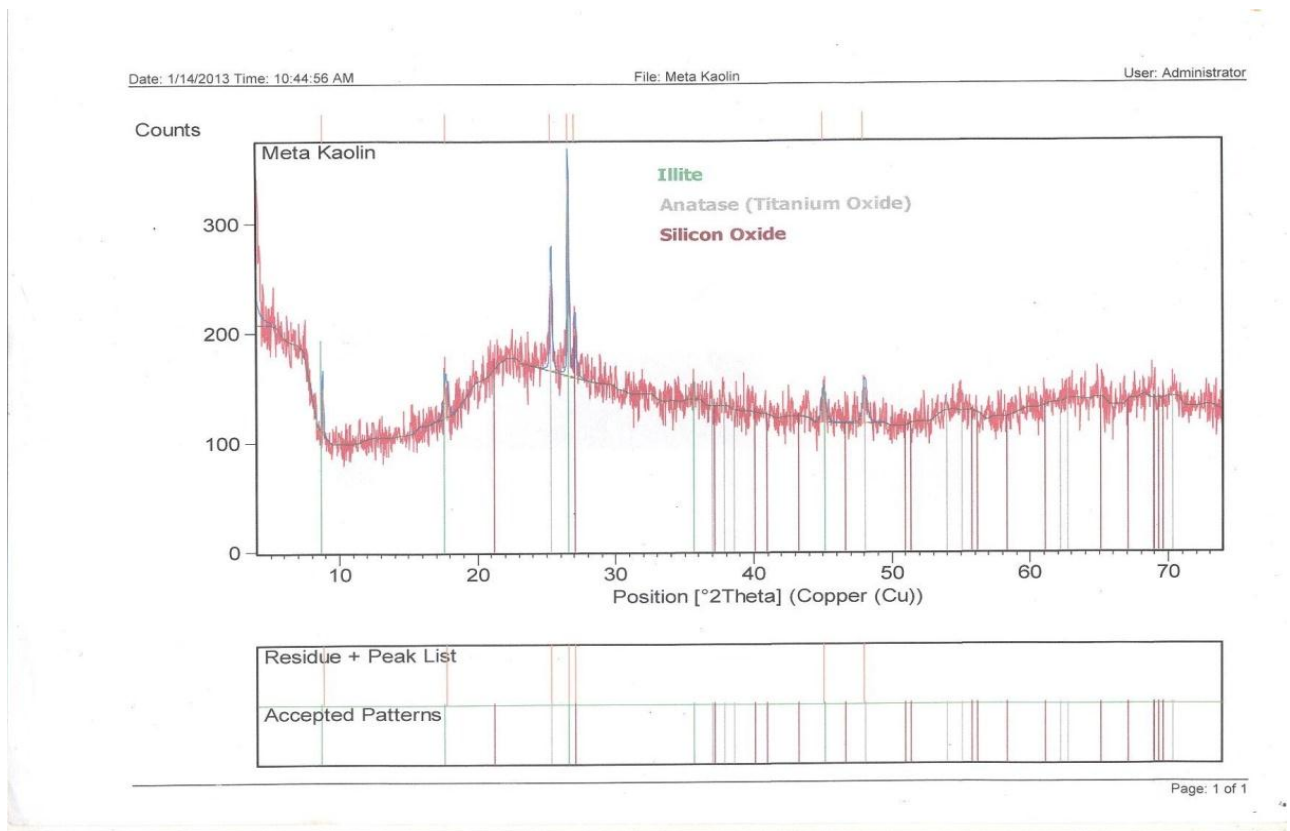


Figure 4.2: XRD patterns for Calcined Elefun Kaolin at 850°C

4.4 Dealumination of Metakaolin

4.4.1 Effect of dealumination time on kaolin composition

As explained in Section 3.3, the purpose of dealumination of Elefun kaolin is to create a kaolin that has the required Silica/Alumina ratio for the key materials in the starting gel of high silica zeolite Y synthesis. The acid treatment of metakaolin results in selective leaching of alumina, magnesium, and iron contents from the octahedral sheet, thus lowering the alumina content of Elefun metakaolin. The XRF results presented in Tables 4.4 and 4.5 show that the composition of the Elefun clay changed considerably during dealumination by both the novel and conventional method. The Fe_2O_3 content was reduced from 2.57 to 1.92, Alumina reduced from 37 to 18.50, MnO reduced from 0.21 to 0.024 with the exception of TiO_2 that increased from 4.70 to 5.73. This result was also confirmed by Belver, et al., (2002). Also, Table 4.2, 4.3 and 4.4 show that $\text{SiO}_2/\text{Al}_2\text{O}_3$ ratio increased with increase in the time of reaction e.g in Table 4.2 at 3 minutes the silica –alumina ratio was 2.59 whereas at 17 minutes it was 2.79 with a corresponding decrease in alumina content. However, the leaching of the alumina contents of Elefun metakaolin ultimately alters the chemical composition and thus changes the structure of the parent starting material.

Table 4.2: Effect of dealumination time on the Silica and Alumina content of dealuminated Elefun Metakaolin by novel method.

Time (min)	Alumina (wt)	Silica (wt)	Silica/Alumina ratio
3	34.20	52.00	2.59
5	33.00	51.90	2.76
7	32.70	52.10	2.70
9	32.30	52.00	2.74
11	31.90	52.50	2.77
17	31.80	52.10	2.79
21	31.90	52.20	2.78

Table 4.3: Variation of dealumination time on Silica and Alumina composition of Elefun Metakaolin by Conventional method

Time (min)	Alumina (wt%)	Silica (wt%)	Silica/Alumina ratio
3	18.50	51.15	4.70
6	11.40	81.57	12.14
8	-	90.75	-
10	-	90.17	-

Table 4.4: Variation of chemical constituents of various kaolin with dealumination time by novel method

Chemical constituent (wt%)	REK	BEK	CEK(850°C)	DEK(3min)	DEK(5min)	DEK(7min)	DEK(9min)	DEK(11min)	DEK(17min)	DEK(21min)
Al ₂ O ₃ (%)	37.010	35.000	36.900	34.200	33.000	32.700	32.300	31.900	31.800	31.900
CaO (%)	0.299	0.346	0.035	0.313	0.370	0.342	0.354	0.374	0.381	0.299
Fe ₂ O ₃ (%)	2.570	2.790	1.480	1.610	1.640	1.890	1.880	1.730	1.820	1.850
K ₂ O (%)	0.630	0.535	0.615	0.719	0.825	0.754	0.848	0.847	1.000	1.050
MgO (%)	0.210	-	0.810	0.960	1.040	1.060	1.080	1.090	1.080	1.090
MnO (%)	0.023	0.010	0.023	0.026	0.033	0.009	0.032	0.028	0.024	0.027
Na ₂ O (%)	0.080	-	0.900	1.050	1.160	1.230	1.240	1.250	1.240	1.260
TiO ₂ (%)	4.760	5.100	4.520	5.060	5.580	5.590	5.570	5.510	5.780	5.730
SiO ₂ (%)	53.800	51.600	51.5	52.000	51.900	52.000	52.100	52.000	52.100	52.200
P ₂ O ₅ (%)	-	-	0.510	0.630	0.640	0.860	0.780	0.790	0.730	0.830
MoO ₃ (%)	-	-	-	1.290	1.500	1.450	1.630	1.680	1.670	1.690
SO ₃ (%)	-	0.270	-	0.600	0.500	0.910	0.960	1.200	1.300	1.300
LOI (%)										
Si/Al(mol%)	2.472	2.506	2.373	2.585	2.674	2.698	2.743	2.772	2.785	2.780

Table 4.5: Variation of chemical constituents of various kaolin with dealumination time by Conventional method

Sample ID	DMK 3min	DMK 6 min	DMK 8 min	DMK 10 min
Al ₂ O ₃ (%)	18.5000	11.4000	-	-
CaO (%)	0.4310	0.1110	0.1360	0.132
Fe ₂ O ₃ (%)	1.9200	0.6270	0.7310	0.704
K ₂ O (%)	0.5220	0.6860	0.6570	0.602
V ₂ O ₅ (%)	0.2100	0.1060	0.1330	0.128
MnO (%)	0.0240	0.0130	0.0160	0.0150
Re ₂₀₇ (%)	0.2900	0.0620	0.0710	0.051
TiO ₂ (%)	5.9900	3.6500	4.8300	4.564
SiO ₂ (%)	51.1000	81.5700	90.7500	90.1700
Ag ₂ O (%)	4.6700	-	1.5300	1.5500
MoO ₃ (%)	7.0000	1.5000	1.1100	1.5000
SO ₃ (%)	5.1000	0.1900	-	0.2700
LOI (%)				
Si/Al(mol%)	4.700	12.160	-	-

Legend

REK	Raw Elefun Kaolin
BEK	Beneficiated Elefun Kaolin
CEK	Calcined Elefun Kaolin
DEK	Dealuminated Elefun Kaolin
DEK (x min)	Dealuminated Elefun Kaolin for x minutes

4.4.2 'Novel' approach to metakaolin dealumination

The motive behind the use of this method was to reduce the dependency of zeolite synthesis process on electrical power supply. This method used the heat of sulphonation resulting from mixing the acid and water. This resulted to an intense mixing of reaction mixture. The buoyancy obtained assisted in agitation, increased level of collision and subsequently in overall ability of acid-water mixture to do the work required for the realization of chemical reaction Ajayi et al., (2010).

4.5 Gel formation and Zeolite Y synthesis

4.5.1 XRD Analysis

The reaction of NaOH and calculated water with dealuminated metakaolin released heat and gradually increased in thickness with the introduction of more NaOH. There is increase in Na₂O content due to reduction in SiO₂ content during ageing (curing) period as a result of

partial depolymerization of silica or the solubility of the occluded silica grain in the heterogeneous skeleton in a process referred to as equilibrium. This consequently leads to increase in silicate anion in solution. The X-ray diffraction patterns of the developed Zeolite Y from Elefun kaolin at different ageing times at room temperature are shown in Figure 4.3 and 4.4. This pattern compared well with the pattern of standard zeolite Y (currently used by NNPC, Nigeria) as shown in Figure 4.5. However the crystallinity of zeolite increased with increasing aging time showing that the ageing of the zeolite mixture has considerable influence on zeolite synthesis from metakaolin even if it does not initiate the reaction (Takhtahysheva and Konovai,1990). Conclusively, it can be seen from the coordinated state of phases seen in the XRD spectra, in Figure 4.4 and 4.6 that the peak of 7 days ageing shows high level of crystallinity by giving a prominent peak for zeolite NaY as shown in Figure 4.3A. This showed that 7days was exactly adequate for NaOH to depolymerize the ingredient in Elefun clay as compared to that of 9 days ageing whose intensity was observed to decrease slightly (Babalola et al., 2014), resulting from the appearance of silica rich mineral phase known as quartz which have began to suppress the crystallinity. Ajayi et al., (2010), observed that a high degree of crystallinity could be obtained with increasing ageing time. However, from this work, when the ageing time exceed 7days, the relative crystallinity changed considerably. This is attributed to the occurrence of zeolite nucleation at the gel solution interface forming loose crystallites which grow by drawing nutrients from the gel and later from the clear solution (Takhtamysheva and Konoval'chikov,1990). This went contrary to the assertion of Ginter et al., (1992) who pointed out that prolong ageing give better and higher yield NaY. Similar work on synthesis of zeolite X from dealuminated kaolin was reported by Renzo and Fajla, (2005).

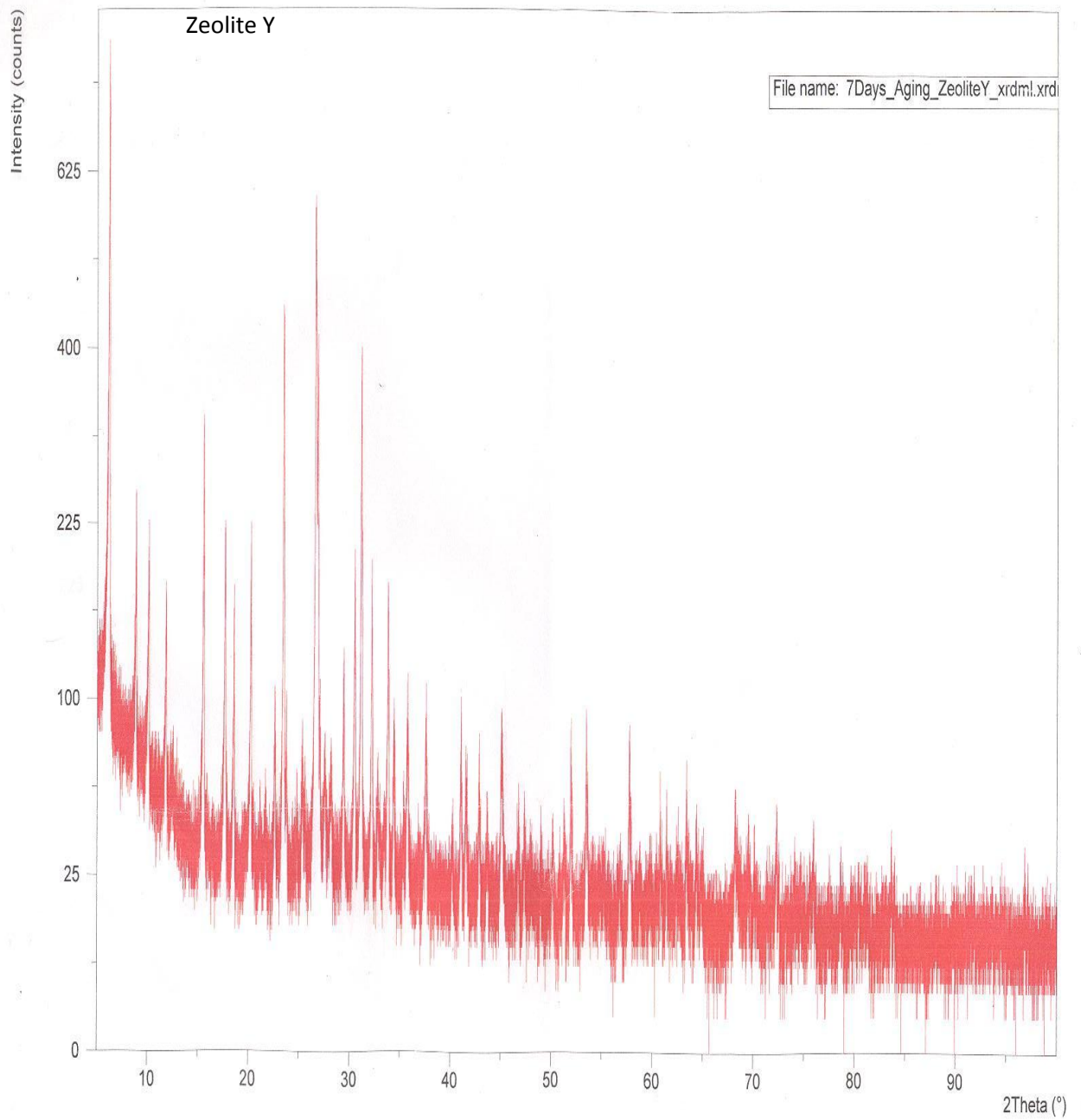


Figure 4.3 A: XRD pattern for synthesized zeolite Y from Elefun clay at 7 days ageing

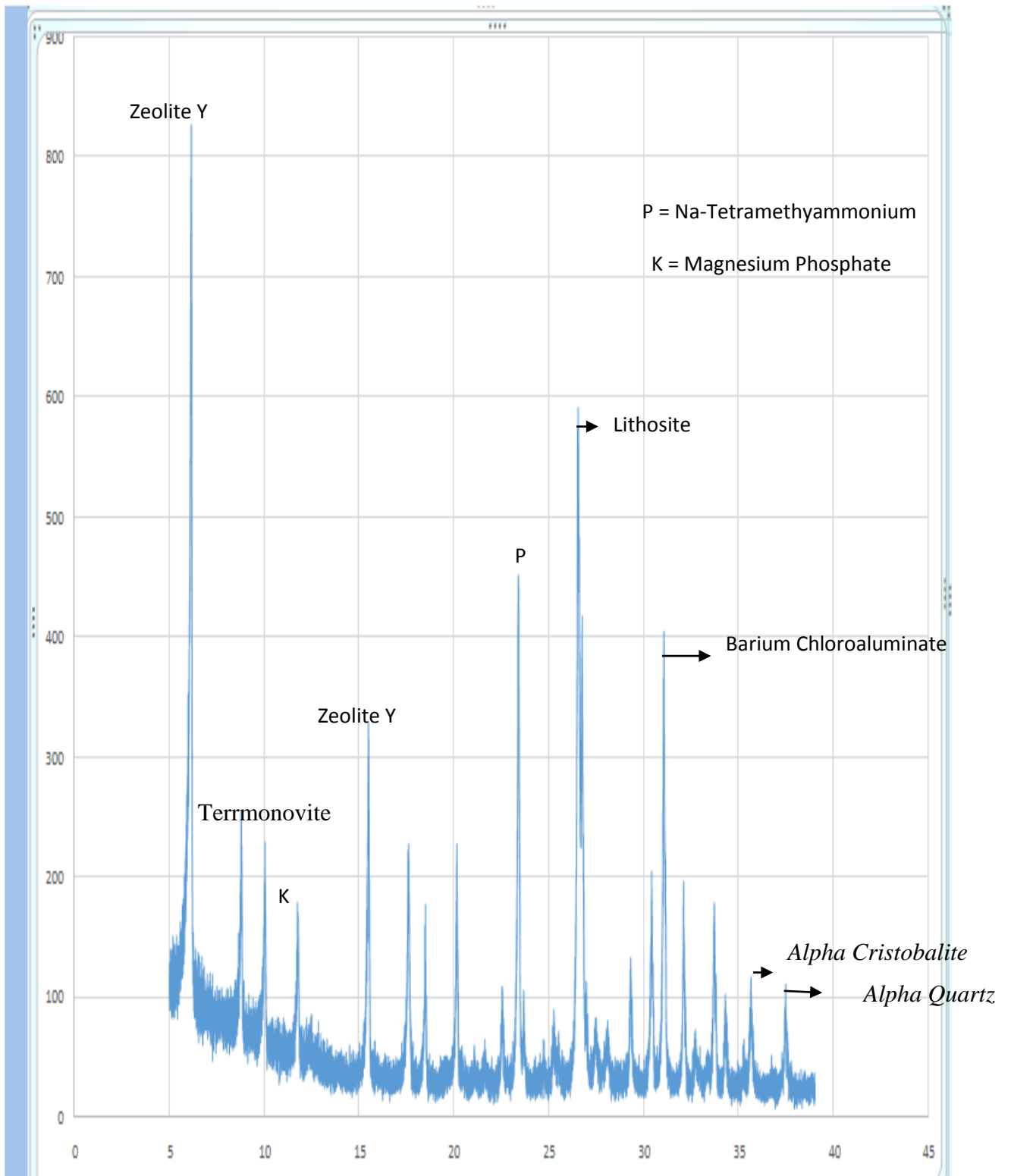


Figure 4.3 B : XRD pattern for synthesized zeolite Y from Elefun clay at 7 days ageing with peaks indicated

Table 4.6: Synthesized Zeolite Y Powder Pattern Identification Table

2θ⁰	Material
6.19	Faujasite-Zeolite Y
8.611	Terrmonovite
10.278	MCM-61
11.984	Magneium Phosphate
15.555	Faujasite-Zeolite Y
17.778	Lovadarite
18.611	Losod
20.278	XPO.SiO ₂
21.389	Bikitaite
21.667	Na-PF
23.056	Boggsite
23.611	Na-Tetramethyl ammonium E
23.889	Marinellite
25.278	Marinellite
26.944	Liottite
27.222	Lithosite
27.500	Tetramethyl ammonium
28.222	Carronite
29.169	Li ABW
30.556	Analcine
31.589	Alpha Cristobalite
32.222	Barium Chloroaluminate
34.445	Mg BCTT
35.556	Tiptopite
36.111	Alpha Cristobalite
38.333	

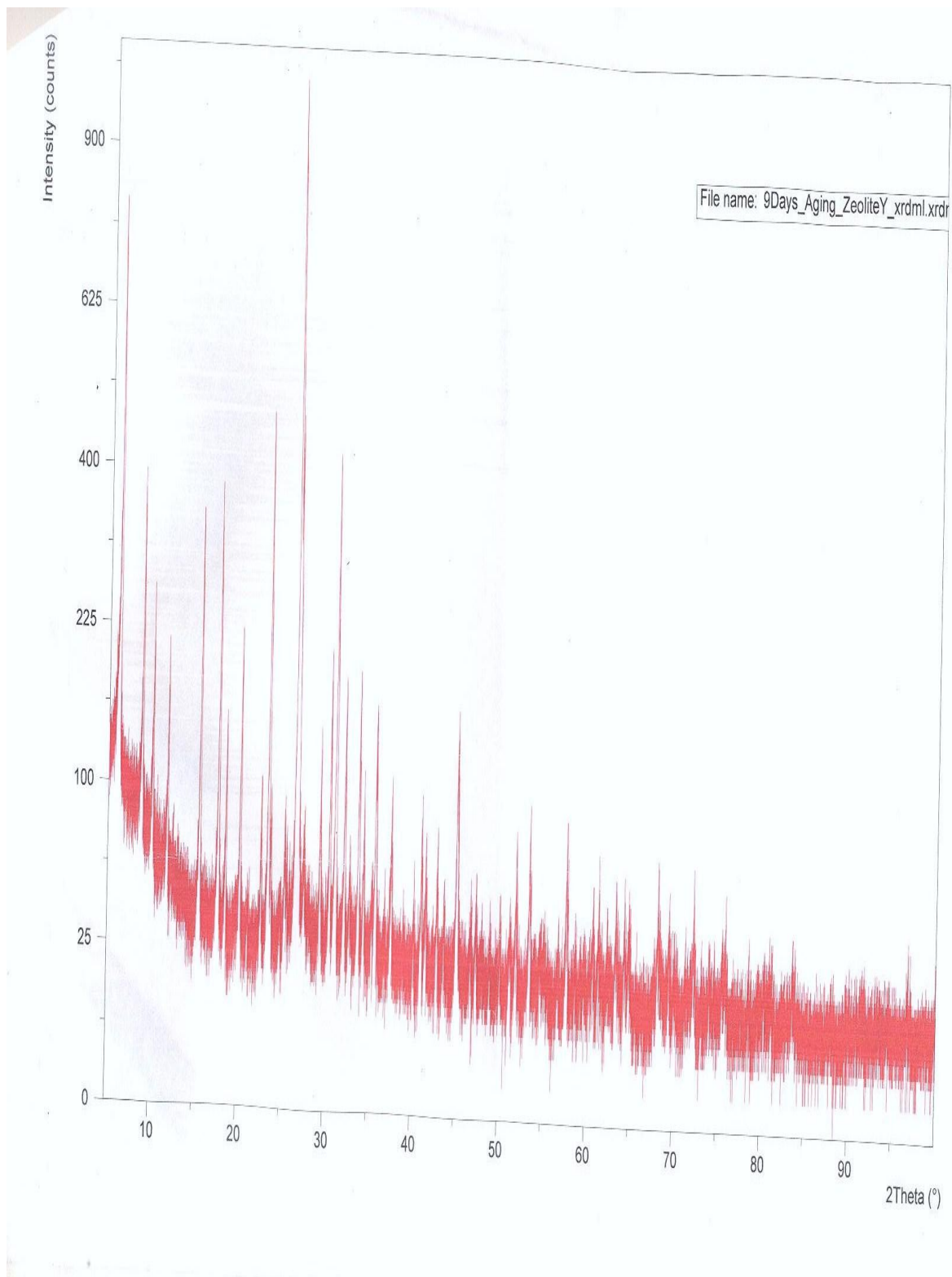


Figure 4.4: XRD pattern for synthesized zeolite Y from Elefun clay at 9 days ageing

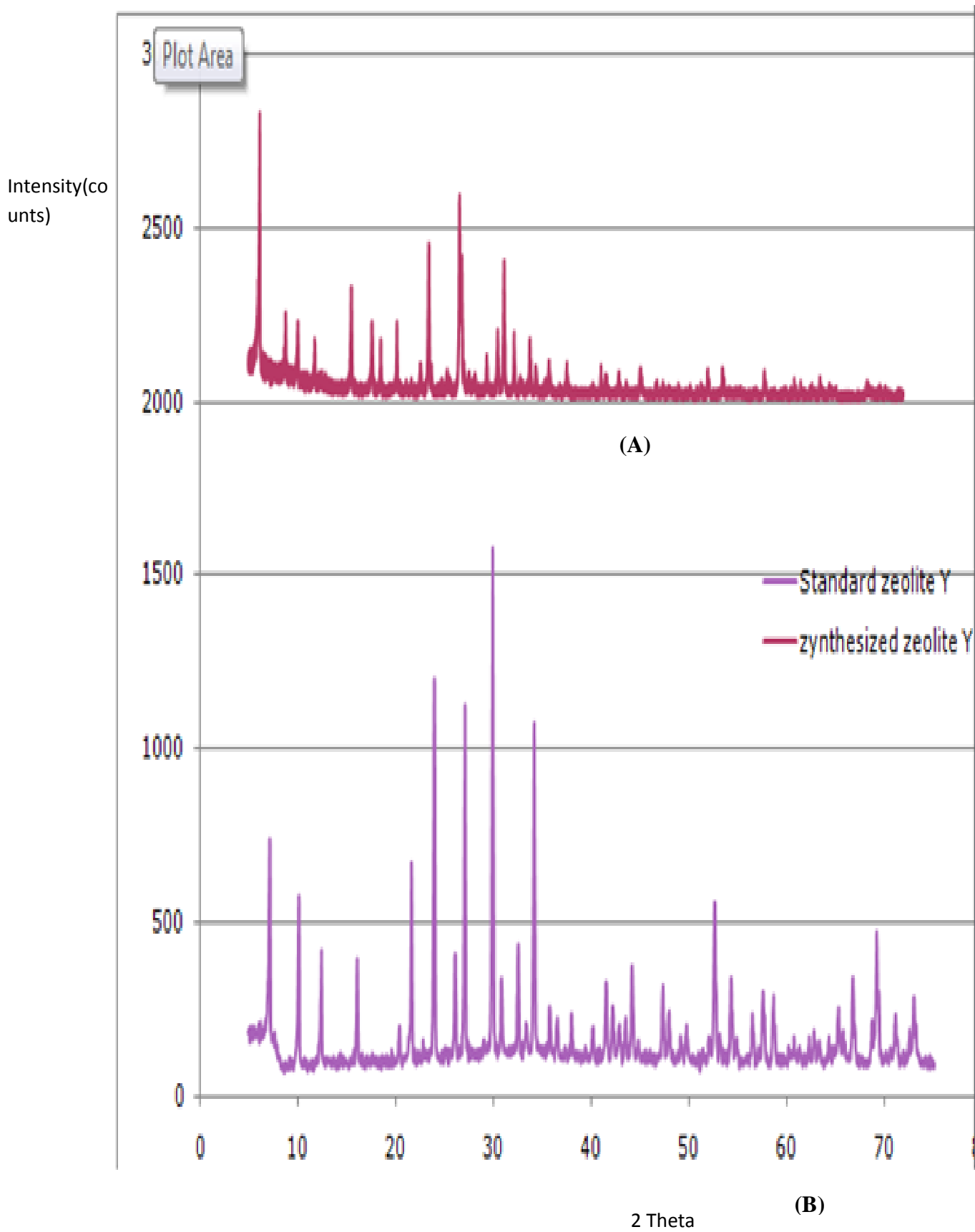


Figure 4.5: XRD pattern for (A) Standard Zeolite Y (B) synthesized zeolite Y

Table4.7: Comparison of lattice spacing, between the developed Zeolite Y and standard Zeolite Y

Zeolite Y catalyst prepared from Elefun kaolin		Standard Zeolite Y catalyst	
Angle (2Theta) deg.	d,spacing (Å)	Angle(2Theta)deg.	d,spacing (Å)
12.48	7.09	12.47	7.09
20.18	4.40	19.80	4.48
21.11	4.21	21.76	4.08
26.77	3.33	26.74	3.33
28.11	3.12	28.21	3.16
29.36	3.04	29.55	3.02
31.10	2.87	30.94	2.88
32.13	2.78	32.26	2.77
33.40	2.65	33.49	2.67
35.69	2.51	35.95	2.49
38.52	2.39	38.16	2.35
40.97	2.20	39.27	2.29

4.5.2 SEM result of the developed zeolite Y

Figure 4.6 is the SEM image of the developed zeolite Y. It reveals clear zeolite Y morphology with a hexagonal shape labeled “a”. The image also shows low concentration of impurities (quartz) in the sample labeled “b” which corroborated the XRD findings that few impurities are present in the dealuminated kaolin which transforms to zeolite. This compared well with similar images of zeolite Y in the literature (Chankim, *et. al.*, 2008). The hexagonal ordering of SEM images of the zeolite NaY, zeolite HY and standard zeolite Y as shown in Figure 4.7 (a), 4.7 (b) and 4.7 (c) respectively signifies a typical zeolite Y.

This illustrated that zeolite HY crystal has the same shape and size as the zeolite NaY. However, the zeolite coverage was different depending on the ratio of Na₂O and Al₂O₃. The SEM images of the synthesized NaY and HY demonstrated that by increasing the Na₂O and Al₂O₃ ratio, the Si/Al ratio decreases from 4.70 to 3.40 whilst the change in the water ratio had no effect on Si/Al ratio (Omisanya et al., 2012)

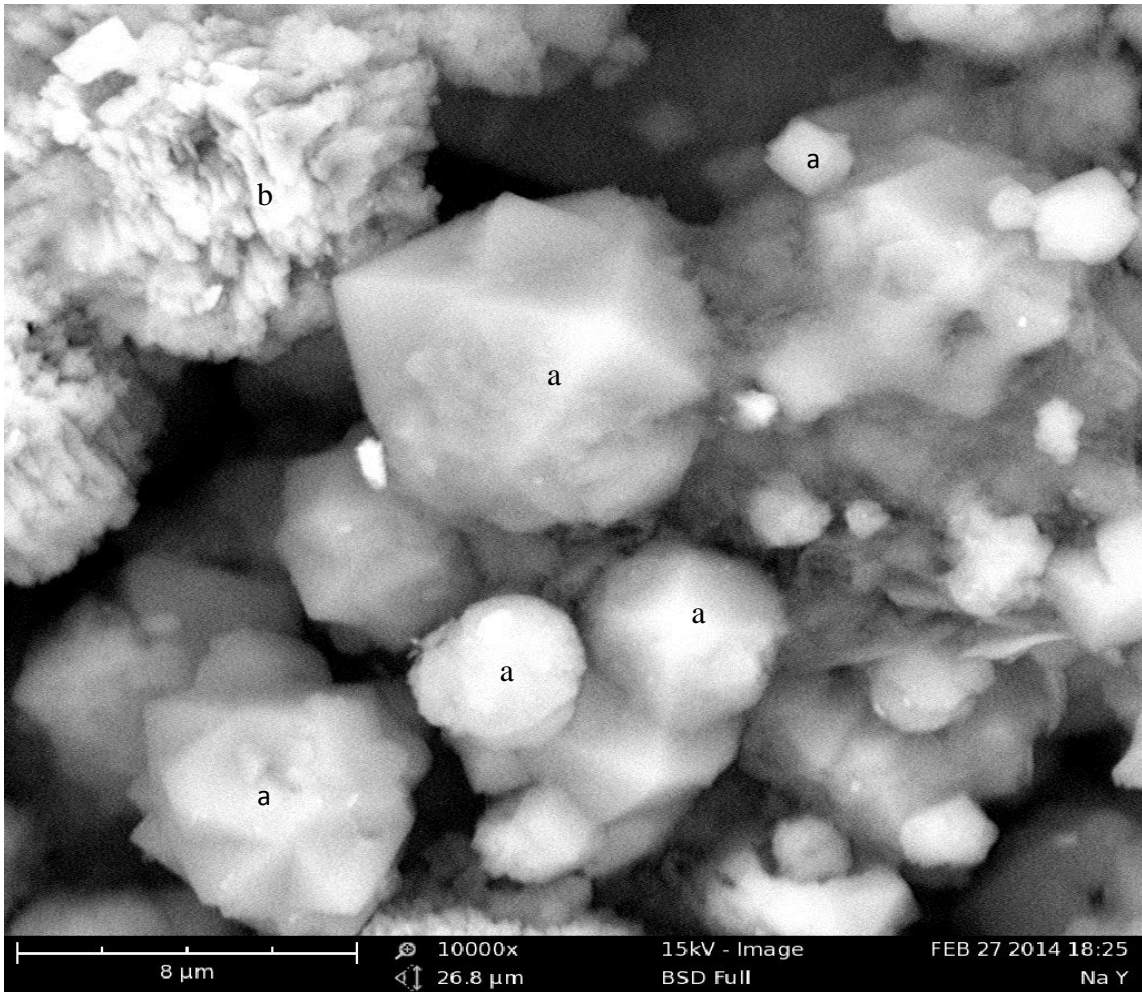


Figure 4.6: SEM image of Zeolite Y synthesized from Elefun kaolin

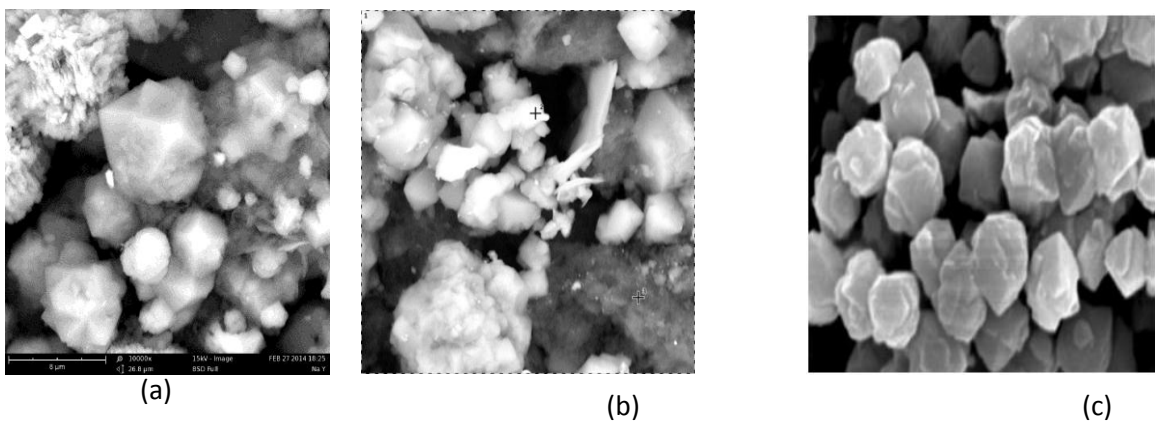


Figure 4.7: SEM Images of (a) developed NaY zeolite (b) HY zeolite (c) Standard zeolite Y

4.5.3 Fourier Transform infrared Spectroscopy (FTIR) result of developed Zeolite Y

The FT-IR spectroscopy for zeolite type Y catalyst prepared from Elefun kaolin and that for standard zeolite Y catalyst are shown in Figure 4.8(a) and 4.8(b) respectively. The spectrum demonstrate a very strong, intense and broad peak at 1041 cm^{-1} which corresponds to the Si-O-Si asymmetric vibration and due to the greater ionic character of the Si-O group, this band is much more intense than the corresponding C-O band. This spectrum also exhibits bands at 622 cm^{-1} which is identical to tridymite (crystalline phase) that shows the presence of the cristobalite phase.

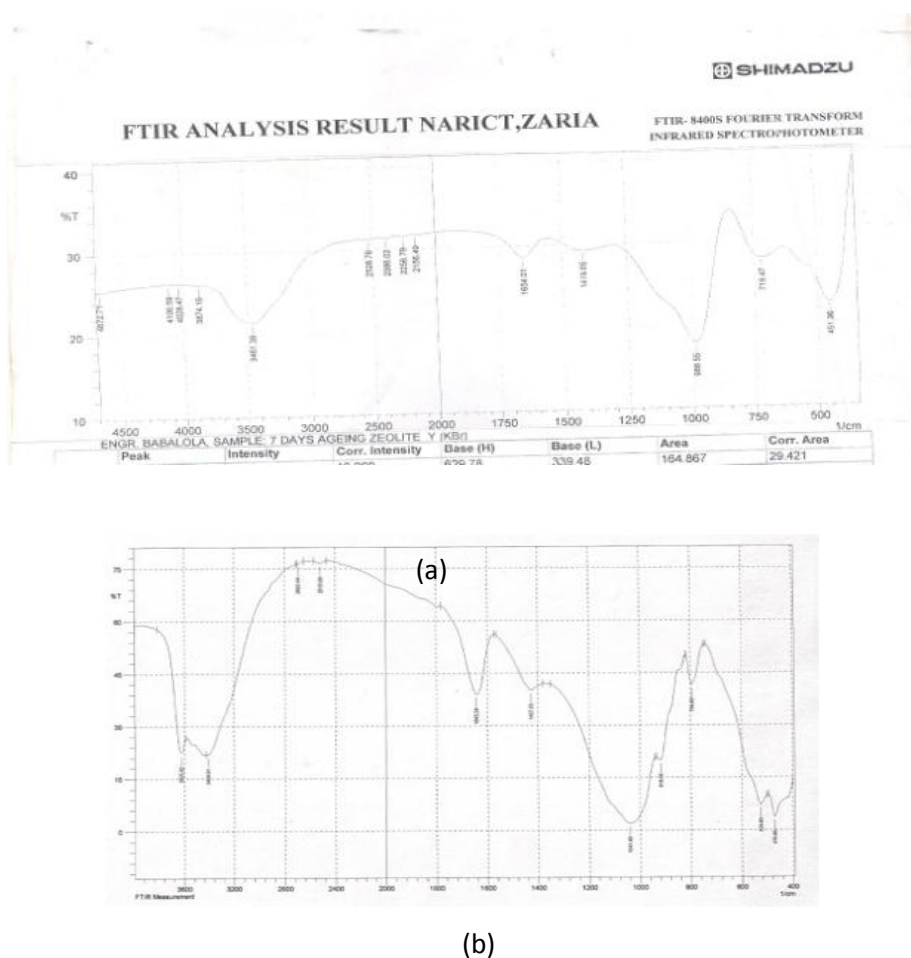


Figure 4.8B: Result of Infra Red analysis for (a) Synthesized Zeolite Y (b) Standard Zeolite Y

4.5.4 BET Surface area result of synthesized zeolite Y

The surface area of the synthesized zeolite NaY is $462\text{m}^2/\text{g}$ while that of the modified zeolite to HY has surface area of $242\text{ m}^2/\text{g}$. This shows a reduction of about 95% which signifies that treatment of zeolite Y material with ammonium hydroxide and further calcining at 450°C reduced the surface area. Also the surface area of spent Zeolite HY was $124\text{m}^2/\text{g}$ a reduction by about 90%. This reduction can be attributed to the deposits in the pores of catalyst of carbon resulting from the high temperature cracking of hydrocarbon. Table 4.8, 4.10 and 4.11 showed BET surface area results while the “Langmuir data”, “Isotherm data”, Multi- point BET plot”, “Single point surface area” and “Area volume” are shown in Appendix C1 – C13.

Table 4.8 BET Result analysis for synthesized zeolite Y

Quantachrome NovaWin - Data Acquisition and Reduction
for NOVA instruments
©1994-2013, Quantachrome Instruments
version 11.03



Analysis		Report	
Operator:	quantachrome	Date:	2014/03/29
Sample ID:	1	Operator:	quantachrome
Sample Desc:		Filename:	Zeolite NAY.qps
Sample weight:	0.28 g	Comment:	
Outgas Time:	0.0 hrs	Sample Volume:	1 cc
Analysis gas:	Nitrogen	OutgasTemp:	0.0 C
Press. Tolerance:	0.100/0.100 (ads/des)	Bath Temp:	273.0 K
Analysis Time:	36.9 min	Equil time:	60/60 sec (ads/des)
Cell ID:	1	End of run:	2014/03/29 7:27:12
		Equil timeout:	240/240 sec (ads/des)
		Instrument:	Nova Station A

Area-Volume Summary

Data Reduction Parameters Data

	Thermal Transpiration: on	Eff. mol. diameter (D): 3.54 Å	Eff. cell stem diam. (d): 4.0000 mm
	Po override: 760.00 Torr		
<u>t-Method</u>	Calc. method: de Boer		
<u>DR method</u>	Affinity coefficient (β): 0.3300		
<u>HK method</u>	Tabulated data interval: 1		
<u>SF method</u>	Tabulated data interval: 1		
<u>Adsorbate</u>	Nitrogen	Temperature	77.350K
	Molec. Wt.: 28.013	Cross Section:	16.200 Å²
	Critical Temp.: 126.200 K	Critical Press.:	33.500 atm
<u>Adsorbent</u>	Carbon	Liquid Density:	0.808 g/cc
	DR. Exp (n): 2.000	SuperCritic. K.:	1.000

Surface Area Data

SinglePoint BET.....	-1.148e+00 m²/g
t-method external surface area.....	-5.455e+00 m²/g
t-method micropore surface area.....	5.455e+00 m²/g
DR method micropore area.....	6.755e-08 m²/g

Pore Volume Data

t-method micropore volume.....	2.181e-03 cc/g
DR method micropore volume.....	2.401e-11 cc/g
SF method micropore volume.....	3.228e-02 cc/g

Pore Size Data

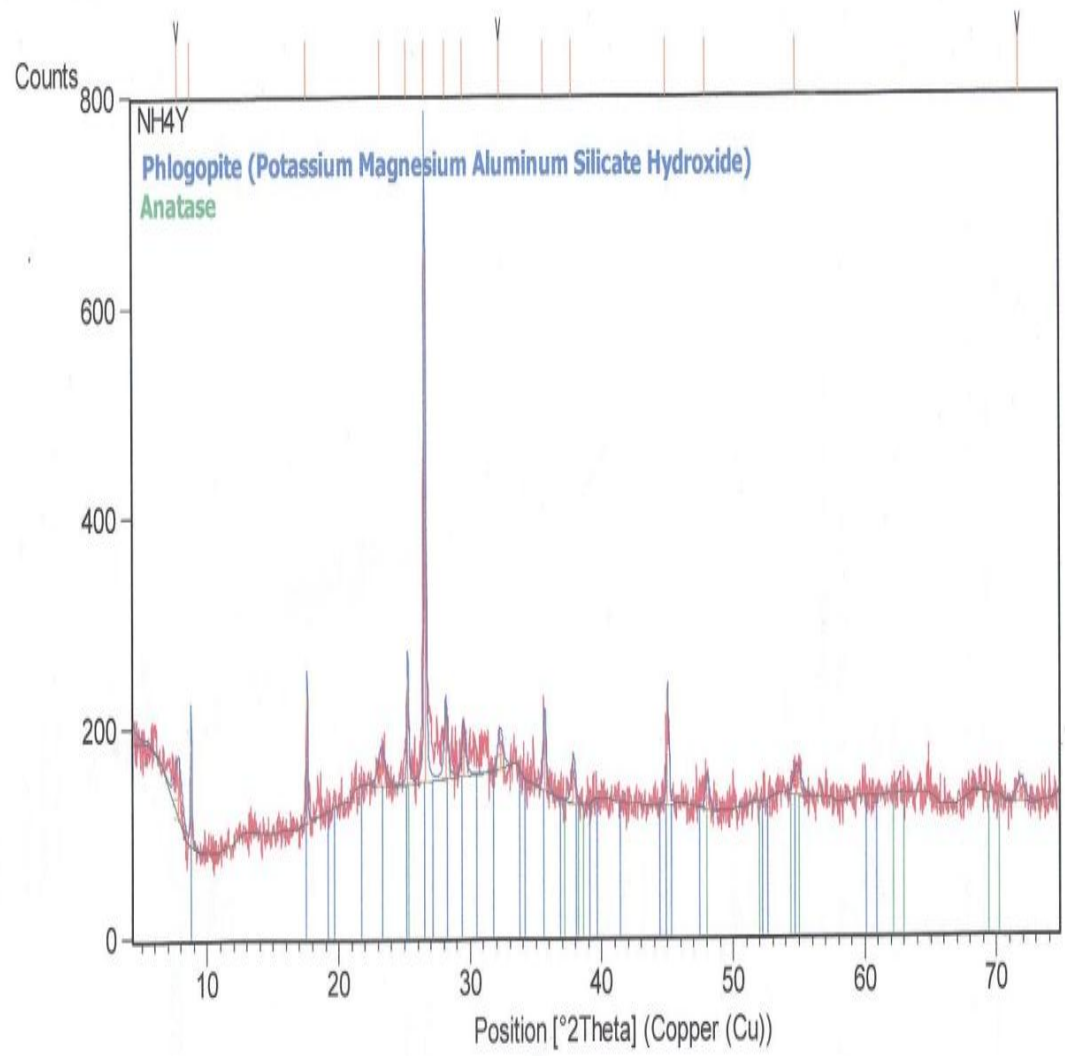
DR method micropore Half pore width.....	9.598e+01 Å
DA method pore Radius (Mode).....	1.550e+01 Å
HK method pore Radius (Mode).....	1.562e+00 Å
SF method pore Radius (Mode).....	1.754e+00 Å

4.6 Comparison of XRF results of Zeolite NaY, Zeolite NH₄Y and Zeolite HY

Table 4.9: XRF results of Zeolite NaY , Zeolite NH₄Y and Zeolite HY

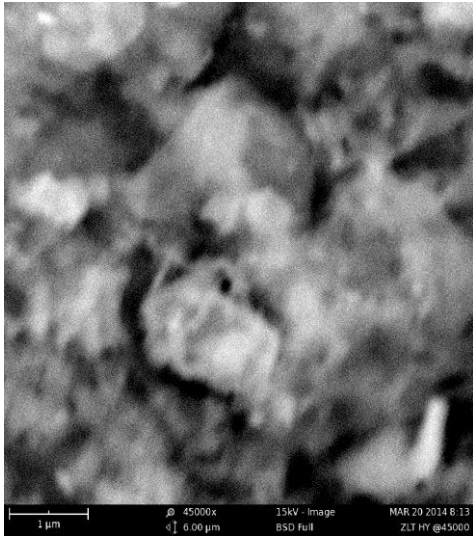
Zeolite type	Zeolite NaY	Zeolite NH ₄ Y	Zeolite HY
Chemical constituent	Weight %	Weight %	Weight %
SiO ₂	51.10	59.7	58.5
Al ₂ O ₃	18.50	29.60	31.30
K ₂ O	0.52	0.69	0.98
TiO ₂	5.99	4.88	5.04
SO ₃	5.100	0.51	0.55
Fe ₂ O ₃	1.92	1.33	1.42
CaO	0.43	0.21	0.17
V ₂ O ₅	0.21	0.14	0.14
MnO	0.03	0.02	0.02
CuO	-	0.01	0.01
L.O.I *	-	3.63	3.63
Total			
Silica/ Alumina	4.70	3.43	3.18

* Loss on Ignition

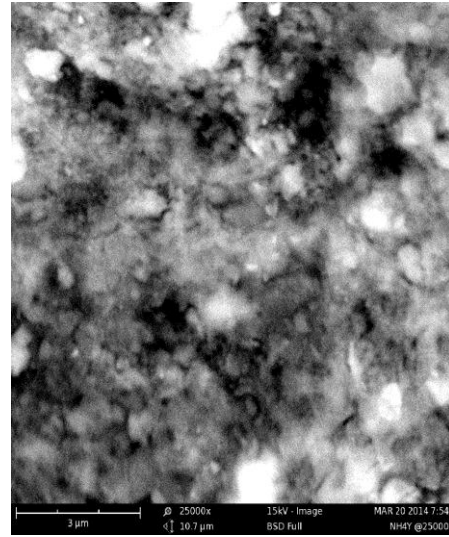


Residue + Peak List
Accepted Patterns

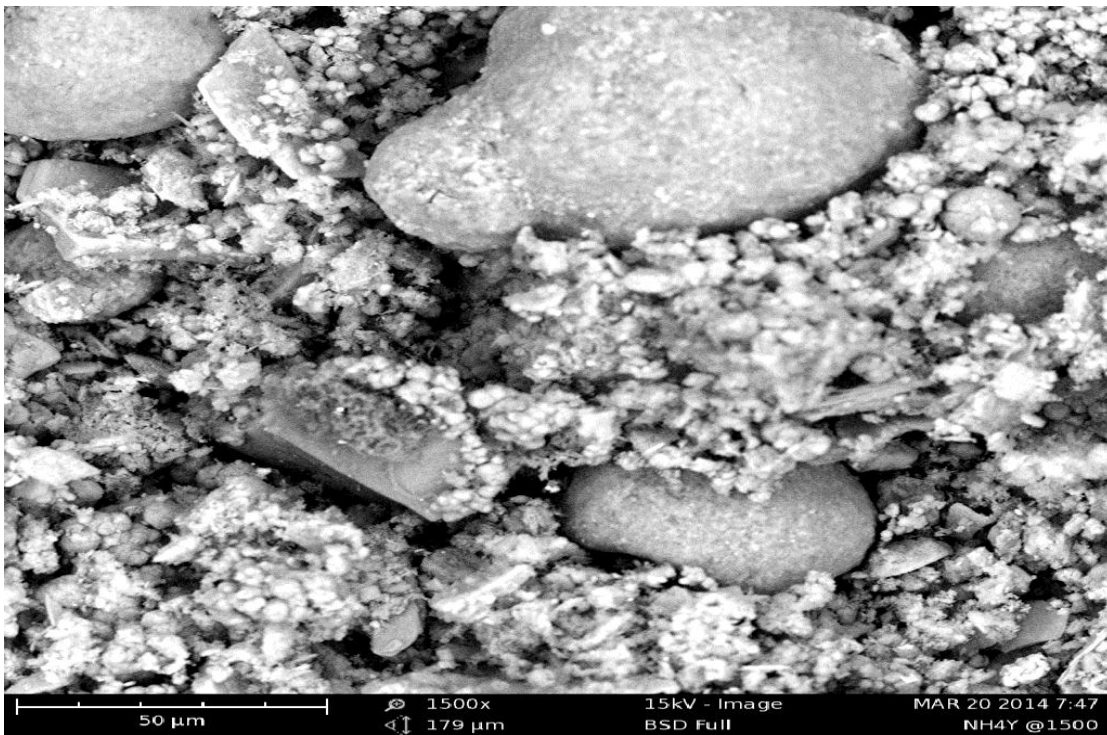
Figure 4.9: XRD Pattern of zeolite NH₄Y



6μm



10.7μm



179μm

Figure 4.10: SEM image of Zeolite NH₄Y synthesized from Elefun kaolin

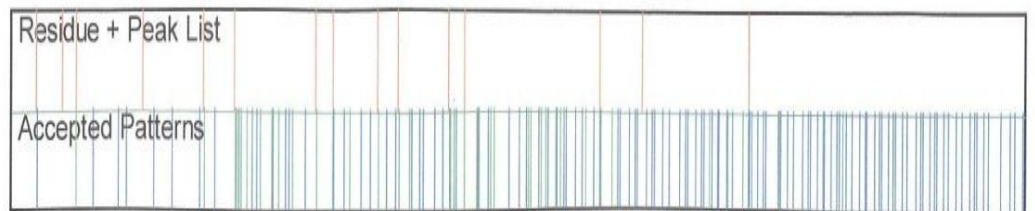
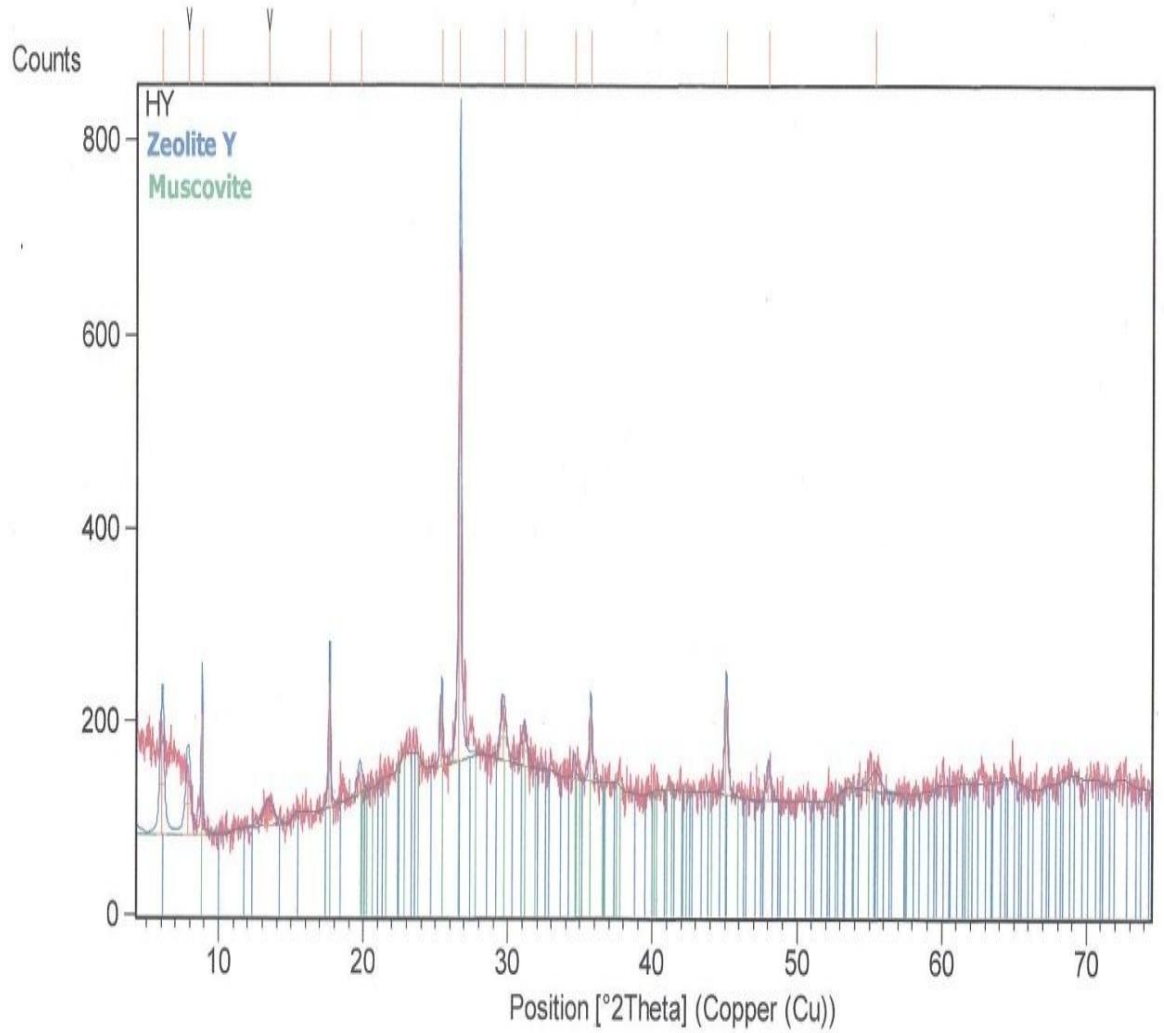
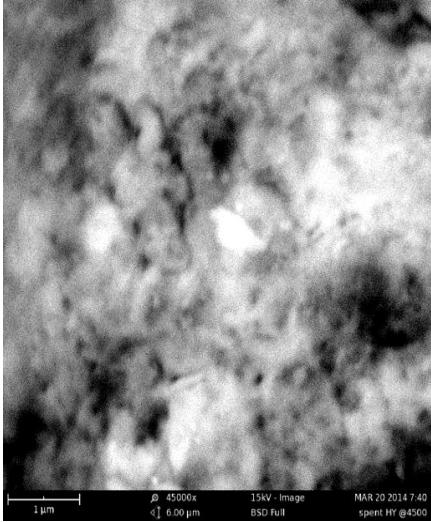
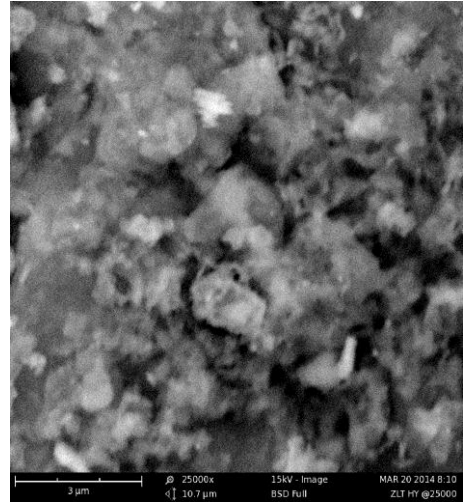


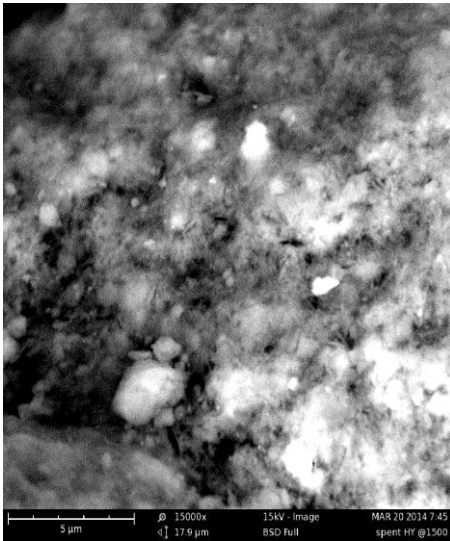
Figure 4.11: XRD Pattern of zeolite HY



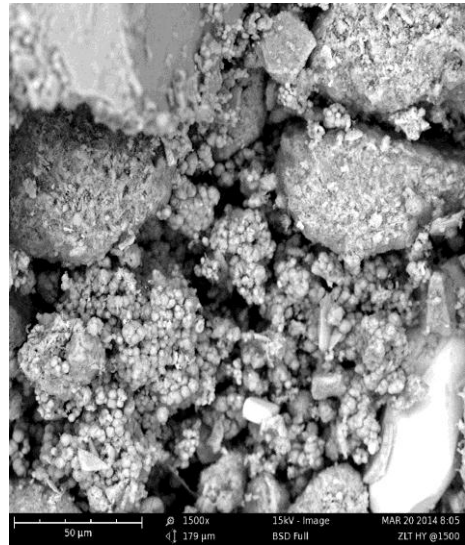
6μm



10.7μm



17.9μm



179μm

Figure 4.12: SEM image of Zeolite HY synthesized from Elefun kaolin

Table 4.10 BET Result for the synthesized zeolite HY

Quantachrome NovaWin - Data Acquisition and Reduction
for NOVA instruments
©1994-2013, Quantachrome Instruments
version 11.03



Analysis		Report	
Operator:	quantachrome	Date:	2014/03/30
Sample ID:	1	Operator:	quantachrome
Sample Desc:		Filename:	Zeolite HY.qps
Sample weight:	0.17 g	Comment:	
Outgas Time:	0.0 hrs	Sample Volume:	1 cc
Analysis gas:	Nitrogen	OutgasTemp:	0.0 C
Press. Tolerance:	0.100/0.100 (ads/des)	Bath Temp:	273.0 K
Analysis Time:	33.0 min	Equil time:	60/60 sec (ads/des)
Cell ID:	1	End of run:	2014/03/30 19:11:18
		Equil timeout:	240/240 sec (ads/des)
		Instrument:	Nova Station A

Langmuir

Data Reduction Parameters Data

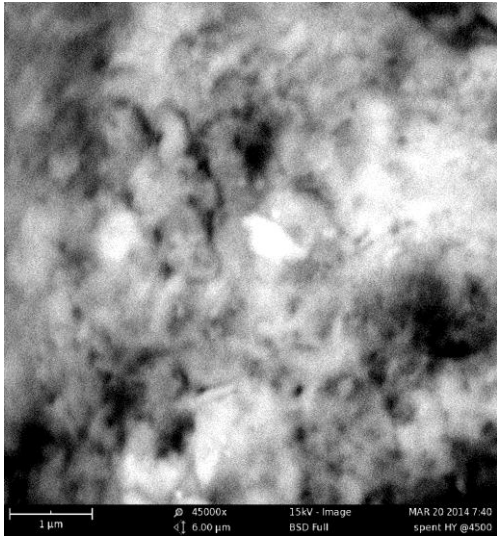
Adsorbate	Po override: 760.00 Torr	Temperature	77.350K	Liquid Density:	0.808 g/cc
	Nitrogen	Cross Section:	16.200 Å²		
	Molec. Wt.: 28.013				

Langmuir Data

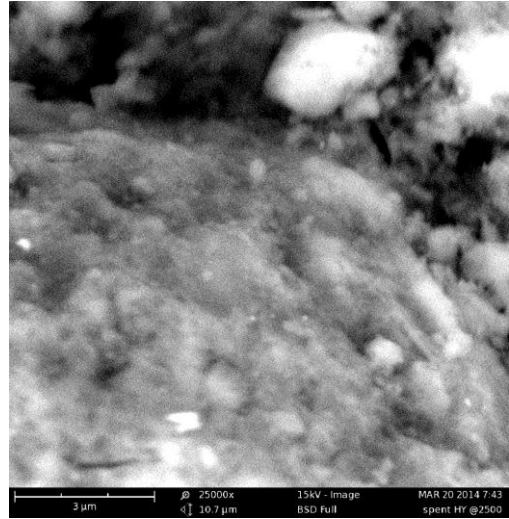
P/Po	P/Po/W [(g/g)]	P/Po	P/Po/W [(g/g)]
1.00166e-01	-1.3769e+01	2.95883e-01	-1.0245e+01
1.72646e-01	-1.1666e+01	3.53660e-01	-1.0038e+01
2.35550e-01	-1.0679e+01		

Langmuir summary

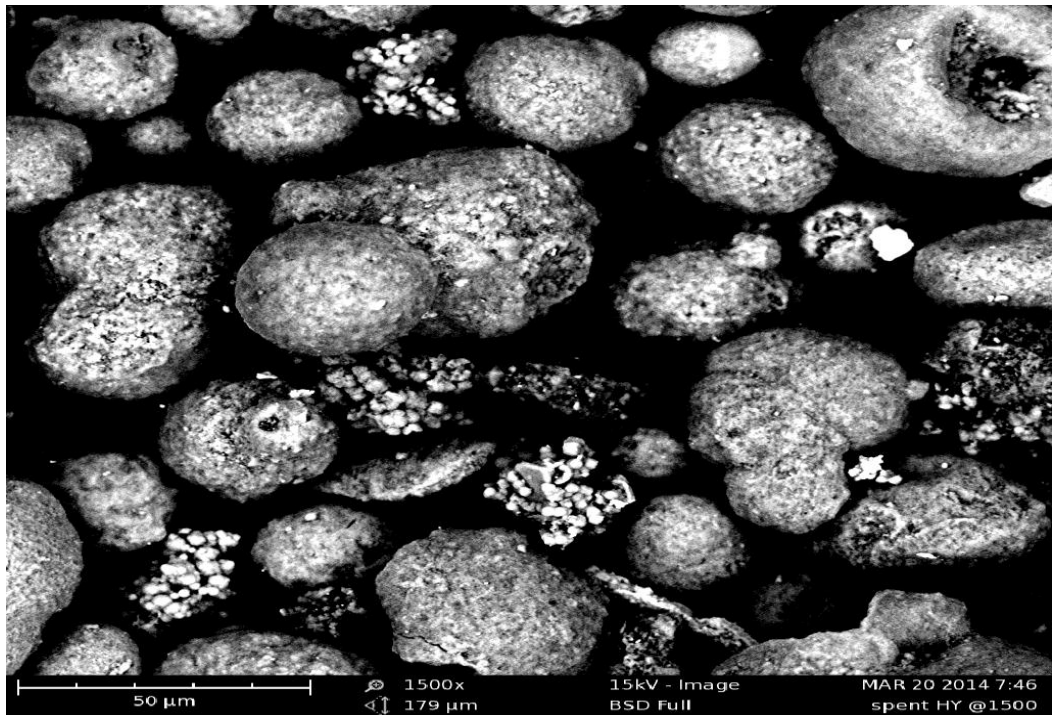
Slope = 14.33618
Intercept = -14.59940
Correlation coefficient, r = 0.937
Surface Area = 242.918 m²/g



6.0 μm



10.7 μm



179 μm

Figure 4.13: SEM image of Spent Zeolite HY synthesized from Elefun kaolin after performance test

Table 4.11 BET Result for the Spent synthesized zeolite HY

Quantachrome NovaWin - Data Acquisition and Reduction
for NOVA instruments
©1994-2013, Quantachrome Instruments
version 11.03



Analysis		Report	
Operator:	quantachrome	Date:	2014/03/30
Sample ID:	1	Operator:	quantachrome
Sample Desc:		Filename:	Zeolite HY.qps
Sample weight:	0.17 g	Comment:	
Outgas Time:	0.0 hrs	Sample Volume:	1 cc
Analysis gas:	Nitrogen	OutgasTemp:	0.0 C
Press. Tolerance:	0.100/0.100 (ads/des)	Bath Temp:	273.0 K
Analysis Time:	33.0 min	Equil time:	60/60 sec (ads/des)
Cell ID:	1	End of run:	2014/03/30 19:11:18
		Equil timeout:	240/240 sec (ads/des)
		Instrument:	Nova Station A

Area-Volume Summary

Data Reduction Parameters Data

	Thermal Transpiration: on	Eff. mol. diameter (D): 3.54 Å	Eff. cell stem diam. (d): 4.0000 mm
	Po override: 760.00 Torr		
<u>t-Method</u>	Calc. method: de Boer		
<u>DR method</u>	Affinity coefficient (β): 0.3300		
<u>HK method</u>	Tabulated data interval: 1		
<u>SF method</u>	Tabulated data interval: 1		
<u>Adsorbate</u>	Nitrogen	Temperature	77.350K
	Molec. Wt.: 28.013	Cross Section:	16.200 Å²
	Critical Temp.: 126.200 K	Critical Press.:	33.500 atm
<u>Adsorbent</u>	Carbon	Liquid Density:	0.808 g/cc
	DR. Exp (n): 2.000	SuperCritical. K.:	1.000

Surface Area Data

SinglePoint BET.....	-7.931e+01 m²/g
Langmuir surface area.....	2.429e+02 m²/g
t-method external surface area.....	2.072e+02 m²/g
t-method micropore surface area.....	2.072e+02 m²/g
DR method micropore area.....	2.049e-06 m²/g

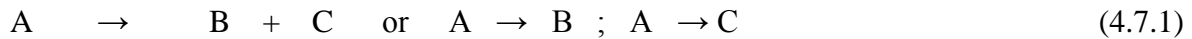
Pore Volume Data

t-method micropore volume.....	6.778e-02 cc/g
DR method micropore volume.....	7.280e-10 cc/g
SF method micropore volume.....	1.808e+00 cc/g

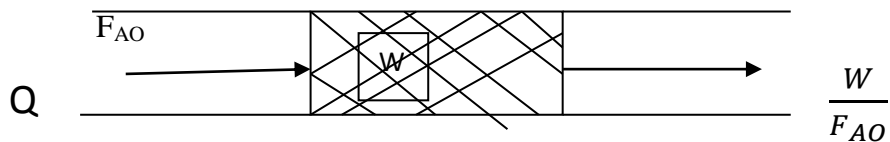
Pore Size Data

DR method micropore Half pore width.....	2.065e-06 Å
HK method pore Radius (Mode).....	1.562e+00 Å
SF method pore Radius (Mode).....	2.261e+00 Å

4.7. Results of Cracking Reaction for Developed and Standard Zeolite Y



For packed bed pulse reaction system



$$\frac{W}{F_{AO}} = \int_0^{X_A} \frac{dX_A}{-r_A} \quad (4.7.2)$$

If the reaction is a first order with respect to A, then let the reaction be represented by Langmuir-Hinshelwood rate equation

$$-r_A = \frac{KC_A}{1+K_A C_A} \quad (4.7.3)$$

where

C_A is the adsorbed phase concentration (mol/gm).

C_{A0} is the initial adsorbed phase concentration (mol/gm) when $x = 0$.

X_A is the fraction of A converted to products,

k is the reaction rate constant.

K_A is adsorption coefficient

$-r_A$ is rate of reaction based on unit mass of catalyst (gmol/g cat. sec).

F_{AO} is the molar feed rate of A entering (mol/sec).

W is the mass of the catalyst in the reactor (gm).

The equation arrived at based on Sica's equation for the first order reaction in a pulse reactor (Omoleye, 1986) is:

$$\ln \left[\frac{1}{1-x_0} \right] = k \frac{W}{F_{AO}} + \frac{K_A}{K} \quad 4.7.4$$

A plot of $\ln \left[\frac{1}{1-x_0} \right]$ versus $\frac{W}{F_{AO}}$ will have,

k is the slope and $\frac{K_A}{K}$ is the intercept with K_A as adsorption coefficient.

$$\text{To determine } \frac{F_{AO}}{C_{AO}} \equiv \frac{\text{mole/s}}{\text{moles/m}^3} \equiv \frac{\text{m}^3}{\text{s}} \equiv Q$$

F_{AO} = moles of A injected /time.

$$\text{But } dt = \frac{V_{bed}}{Q}$$

Therefore

$$F_{AO} = \frac{nQ}{V_{bed}}$$

n = number of mole

V = Volume of catalyst bed

$$\text{But } Q = \frac{F_{AO}}{C_{AO}}$$

$$\text{And } C_{AO} = F_{AO}/Q$$

$$= \frac{n}{V_c}$$

$$\text{Therefore } F_{AO} = C_{AO} \times Q \quad 4.7.5$$

$$\text{Mole/s} = \text{mole/m}^3 \cdot \text{m}^3/\text{s}$$

$$= \text{mole/s}$$

The catalytic activity of zeolite Y developed from Elefun kaolin was determined in the temperature interval of 440 – 520°C using a flow of cyclohexane and helium in a range extending from 40mL/min to 100 mL/min and having different concentrations of cyclohexane in the fluid phase. The results is as presented in Table 4.12 - 4.15 below and Table B1 – B25 of the appendix.

Table 4.12: Cracking of cyclohexane on developed zeoliteY at 520°C

W(gm)	Flowrate (mL/s)	F _{AO} (mol/sec)	X _A	W/F _A x 10 ⁻³ (mph)	ln (1/ 1-X _A)
0.15	40	57.144	0.9965	2.625	5.675
0.15	60	86.716	0.9850	1.750	4.264
0.15	80	114.288	0.9801	1.312	3.997
0.15	100	142.86	0.9727	1.050	3.709

Table 4.13: Cracking of cyclohexane on developed zeoliteY at 480°C

W(gm)	Flowrate(mL/s)	F _{AO} (mol/sec)	X _A	W/F _A x 10 ⁻³ (mph)	ln (1/ 1-X _A)
0.15	40	57.144	0.9857	2.635	4.309
0.15	60	86.716	0.9735	1.750	3.729
0.15	80	114.288	0.9580	1.312	3.309
0.15	100	142.86	0.9681	1.050	3.559

Table 4.14: Cracking of cyclohexane on developed zeoliteY at 460°C

W(gm)	Flowrate (mL/s)	F _{AO} (mol/sec)	X _A	W/F _A x 10 ⁻³ (mph)	ln (1/ 1-X _A)
0.15	40	57.144	0.9931	2.625	5.011
0.15	60	86.716	0.9870	1.750	4.400
0.15	80	114.288	0.9799	1.312	3.987
0.15	100	142.86	0.9790	1.050	3.946

Table 4.15: Cracking of cyclohexane on developed zeoliteY at 440°C

W(gm)	Flowrate (mL/s)	F _{AO} (mol/sec)	X _A	W/F _A x 10 ⁻³ (mph)	ln (1/ 1-X _A)
0.15	40	57.144	0.998	2.625	6.502
0.15	60	86.716	0.988	1.750	4.492
0.15	80	114.288	0.982	1.312	4.012
0.15	100	142.86	0.636	1.050	1.011

4.7.1 Cyclohexane cracking over locally synthesized zeolite Y and reference zeolite Y catalyst under helium atmosphere are shown below:

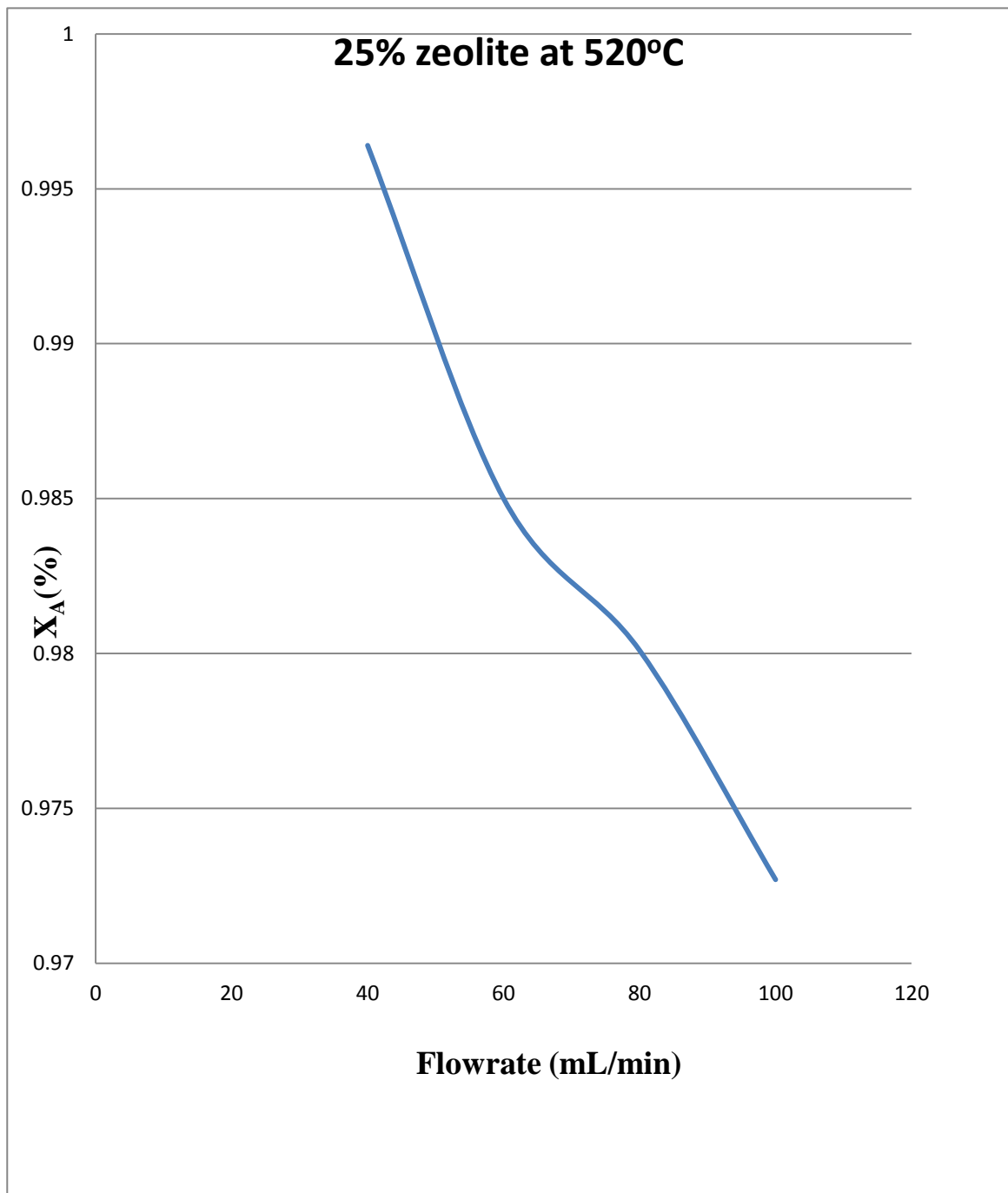


Figure 4.14 : Variation of Conversion with Flowrate using Zeolite Y matrix (25% HY:75% metakaolin) at 520°C

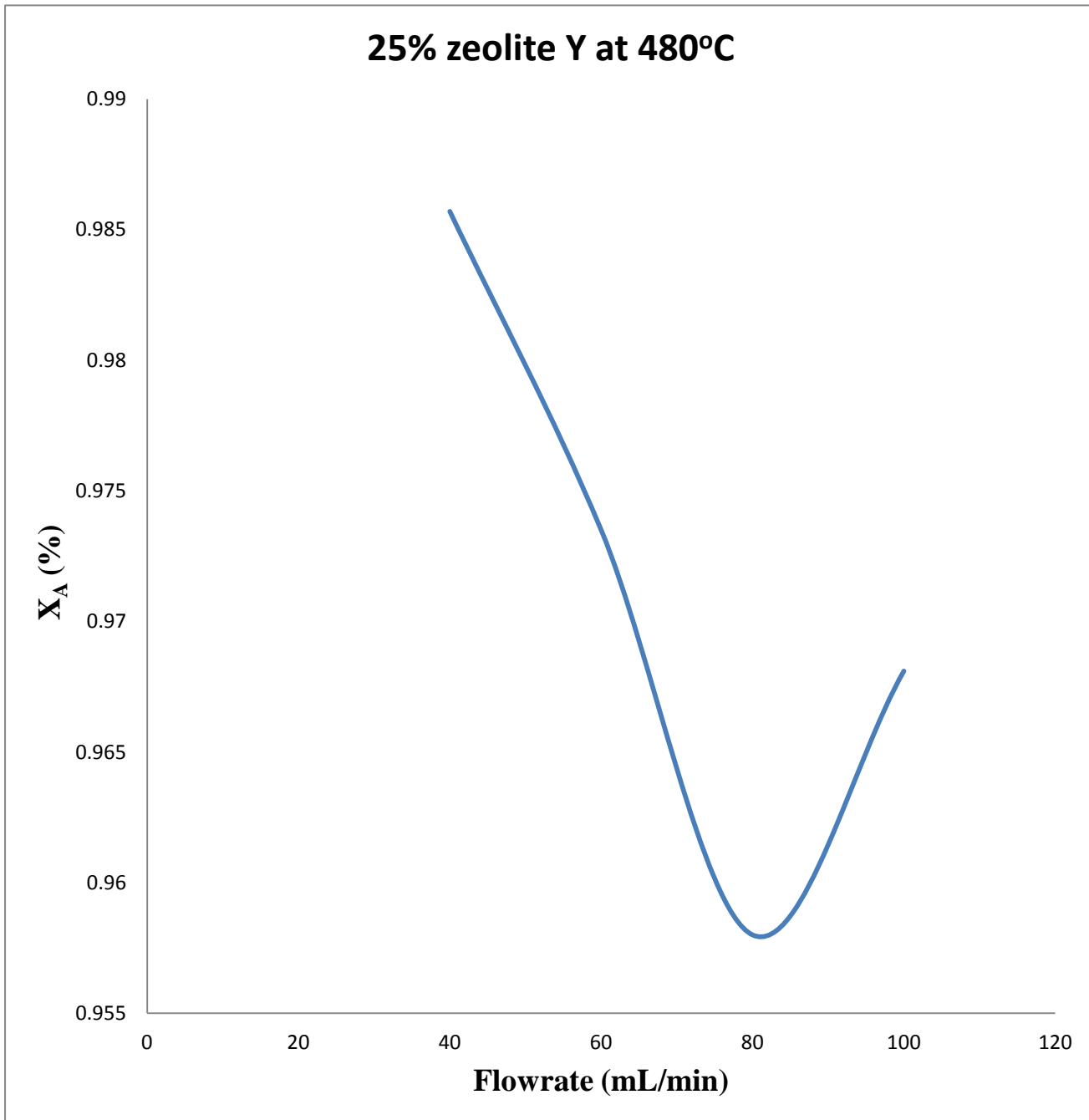


Figure 4.15: Variation of Conversion with Flowrate using Zeolite Y matrix (25% HY:75% Metakaolin) at 480°C

4.7.2 Preliminary Test of First Order Kinetics of Cyclohexane Cracking on synthesized zeolite Y Catalyst in Helium

The equation arrived at based on Sica's equation for the first order reaction in a pulse reactor is:

$$\ln \left[\frac{1}{1-x_A} \right] = k \frac{W}{F_{AO}} + \frac{K_A}{K} \quad (4)$$

If the graphical method of data analysis is to be employed it means that a plot of $\ln \left[\frac{1}{1-x_A} \right]$ versus $\frac{W}{F_{AO}}$ will be a straight line if the reaction is truly a first order reaction.

Figures 4.16 - 4.19 show the plot for preliminary test of first order kinetics of Cyclohexane cracking on 25% of synthesized zeolite Y_{matrix} in Helium, while Figures 4.21 – 4.24 show the plot for commercial Zeolite Y catalyst in Helium respectively.

The slopes obtained from the plot of $\ln \left[\frac{1}{1-x_A} \right]$ versus $\frac{W}{F_{AO}}$ at different temperatures represent k . Therefore, from the Arrhenius equation $k = k_0 e^{-E/RT}$ which when rewritten in the logarithm form is $\ln k = \ln k_0 - \frac{E}{RT}$. A plot of $\ln k$ versus $\frac{1}{T}$ will give a slope of $-\frac{E}{R}$, from where the activation energy E can be calculated.

The Arrhenius plot for Cyclohexane and gas oil cracking over 25% synthesized zeolite Y_{matrix} in Helium is shown in Figures 4.20 and 4.25 respectively, while the data are presented in Tables B13 and B18 respectively

$$= \ln k_0 - \frac{E}{RT} \quad (5)$$

4.7.3 Cracking of cyclohexane on developed zeolite Y

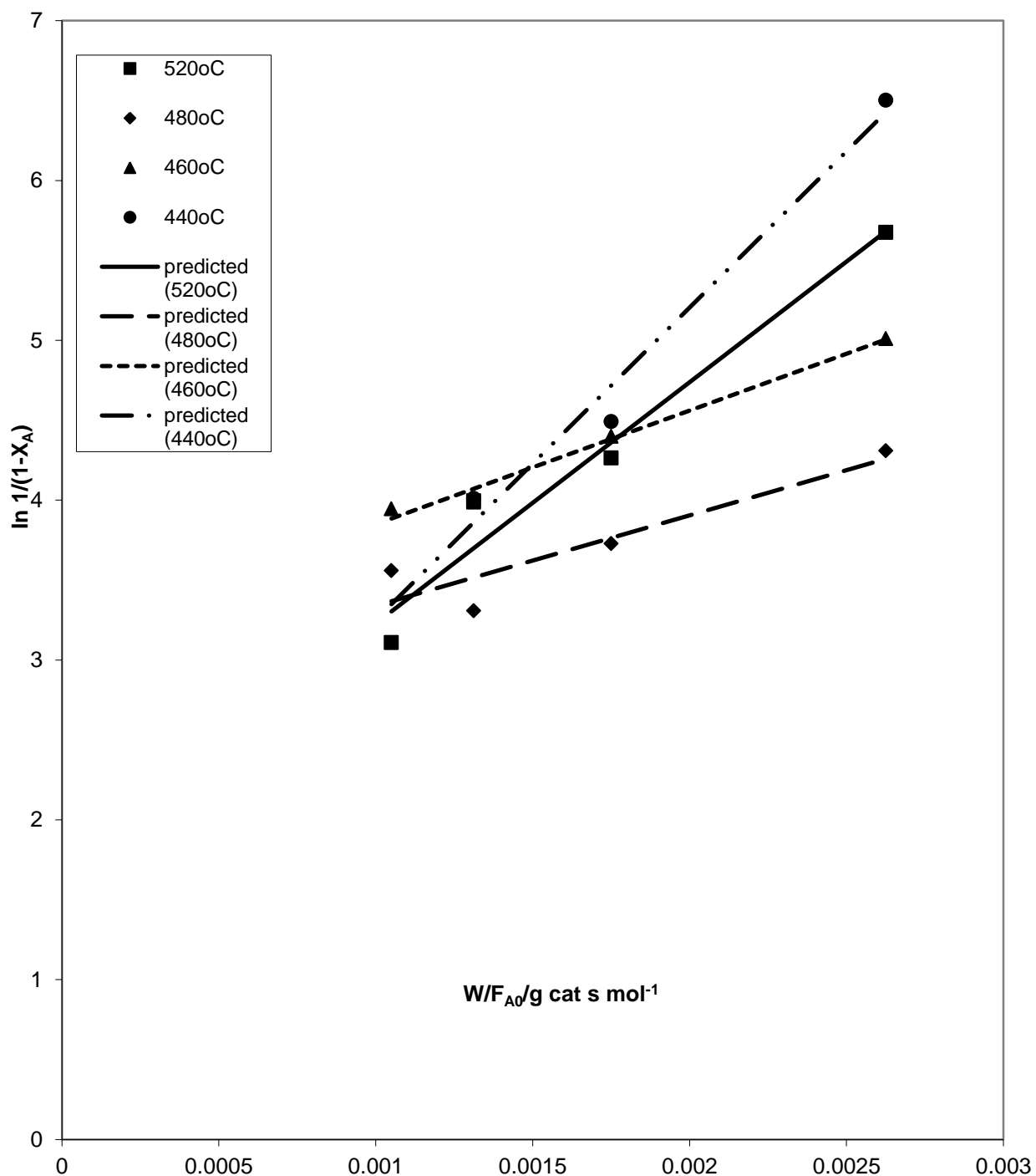


FIGURE 4.16: Test of First Order Kinetic for cyclohexane cracking on synthesized zeolite Y Catalyst at different temperature levels

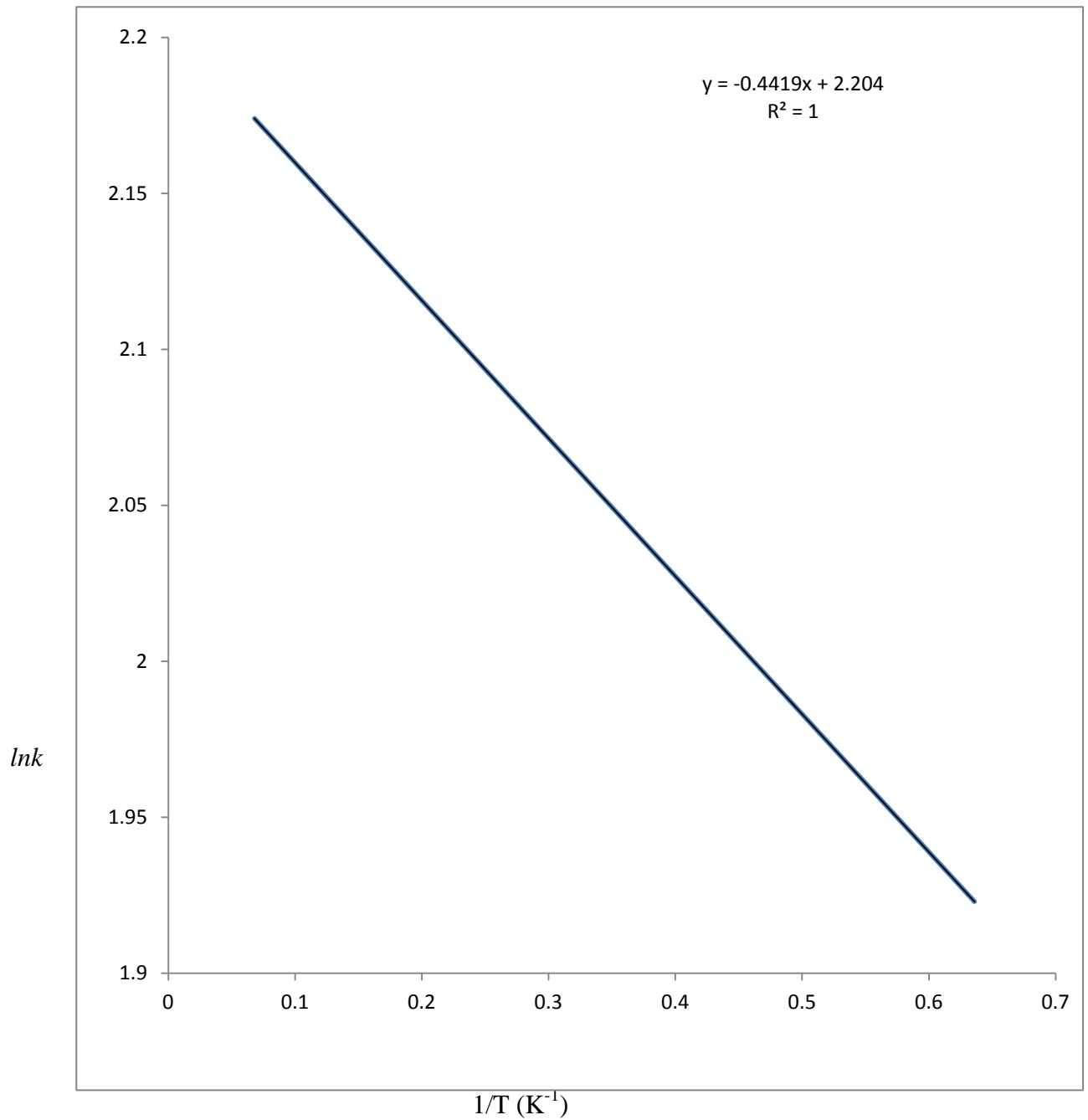


Figure 4.17: Arrhenius plot for cyclohexane cracking on synthesized zeolite Y at 440°C-520°C

$$\text{Slope} = \frac{-E}{R} = -0.441$$

$$E = R \times 0.441$$

$$E = 8.314 \times 0.441$$

$$= 3.666 \text{ kcal/mole}$$

4.7.4 Cracking of cyclohexane on standard zeolite Y

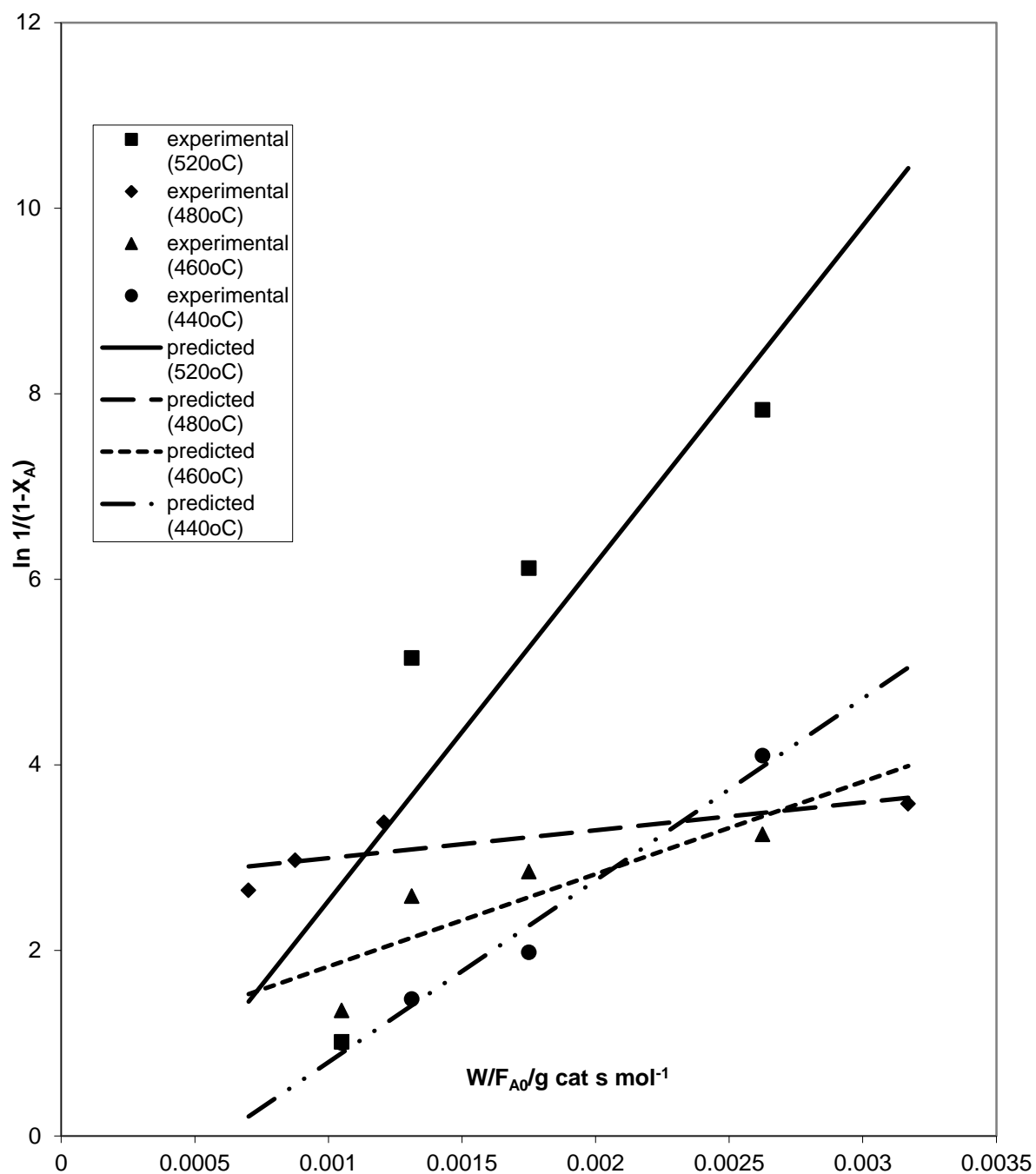


FIGURE 4.18: Test of first order kinetics for cyclohexane cracking on standard zeolite Y Catalyst at Temperature levels

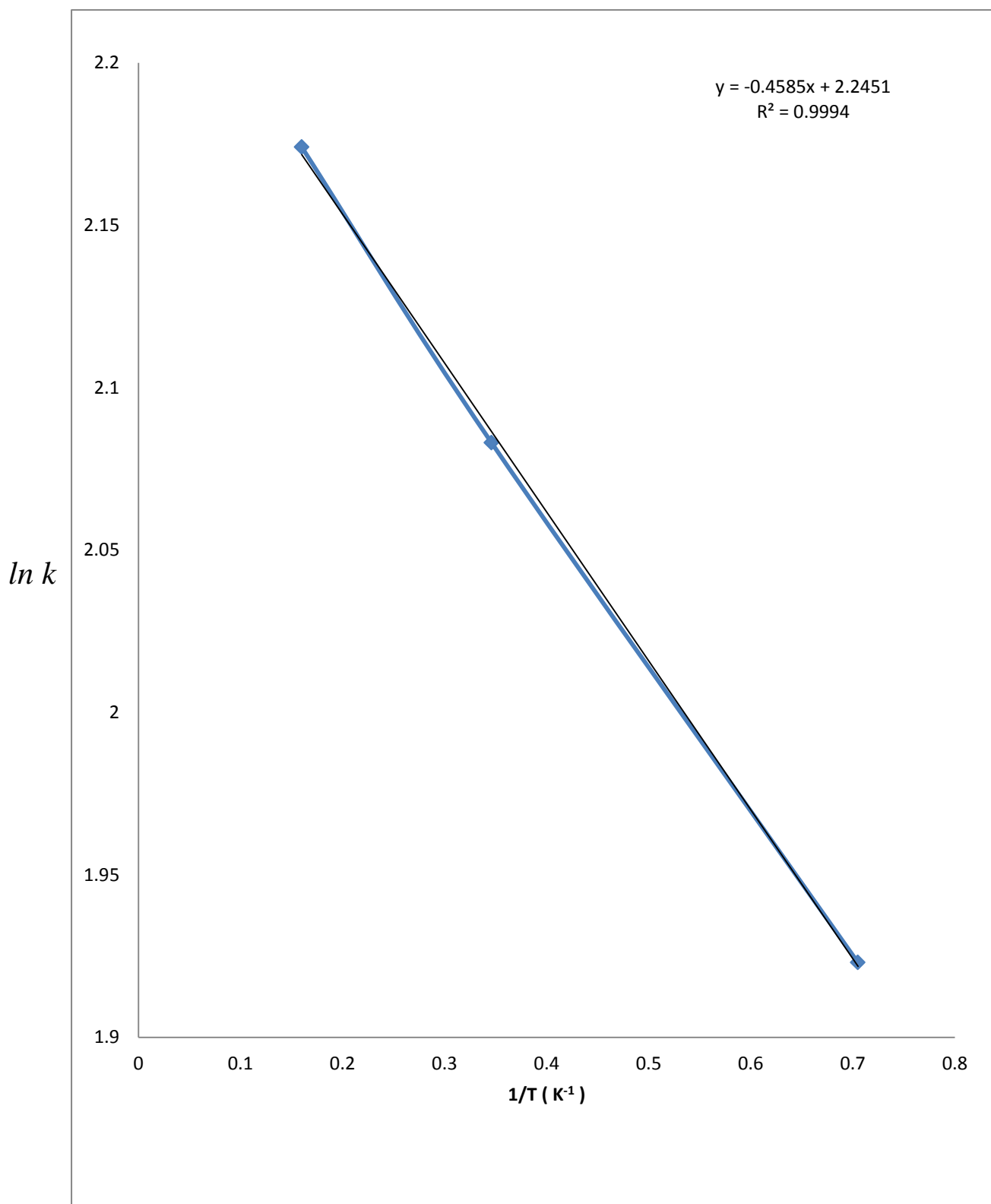


FIGURE 4.19: Arrhenius plot for cyclohexane cracking on standard zeolite Y at 520°C -440°C

4.7.5: Comparison between the performance of synthesized zeolite Y and commercial zeolite Y on cyclohexane

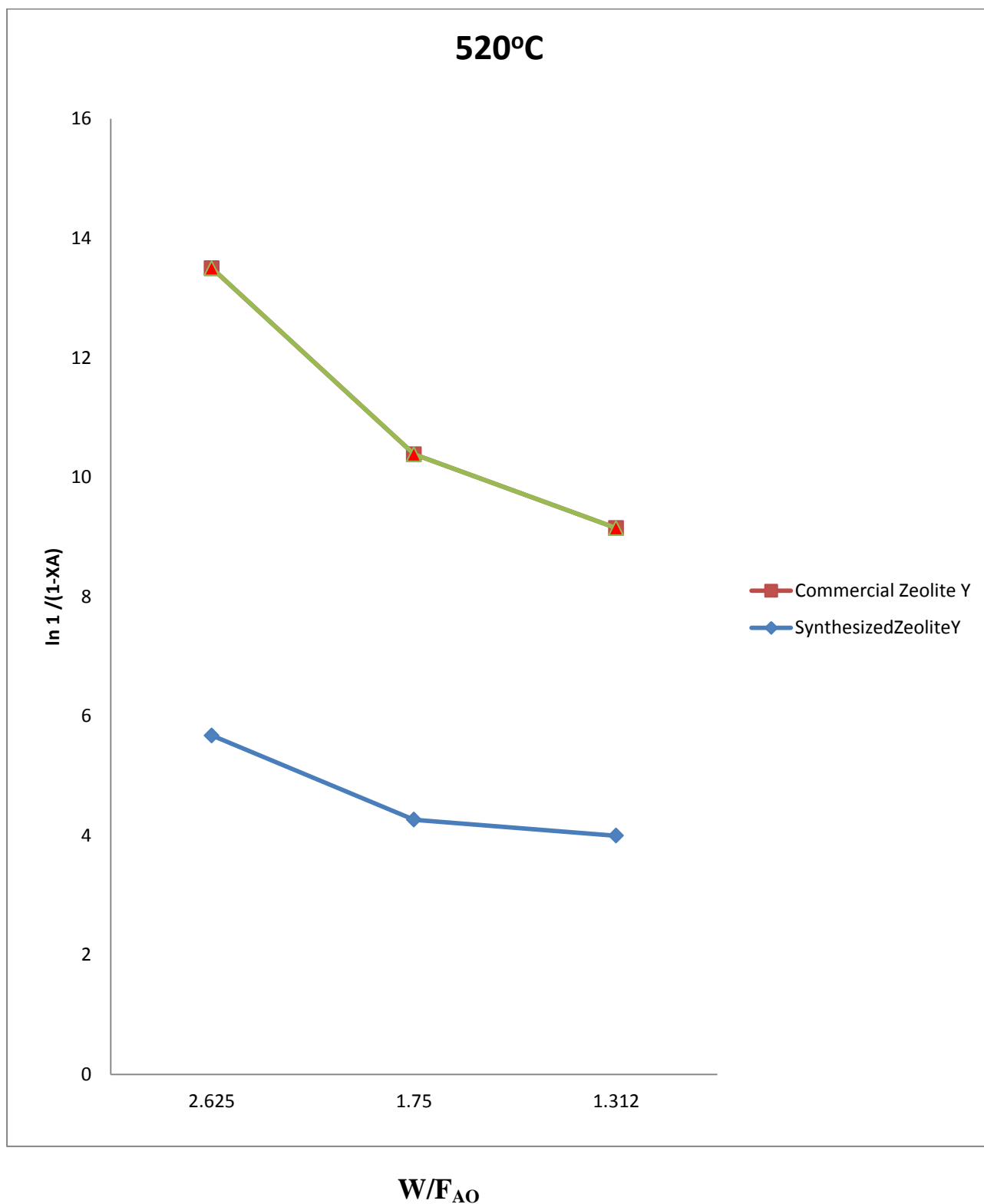
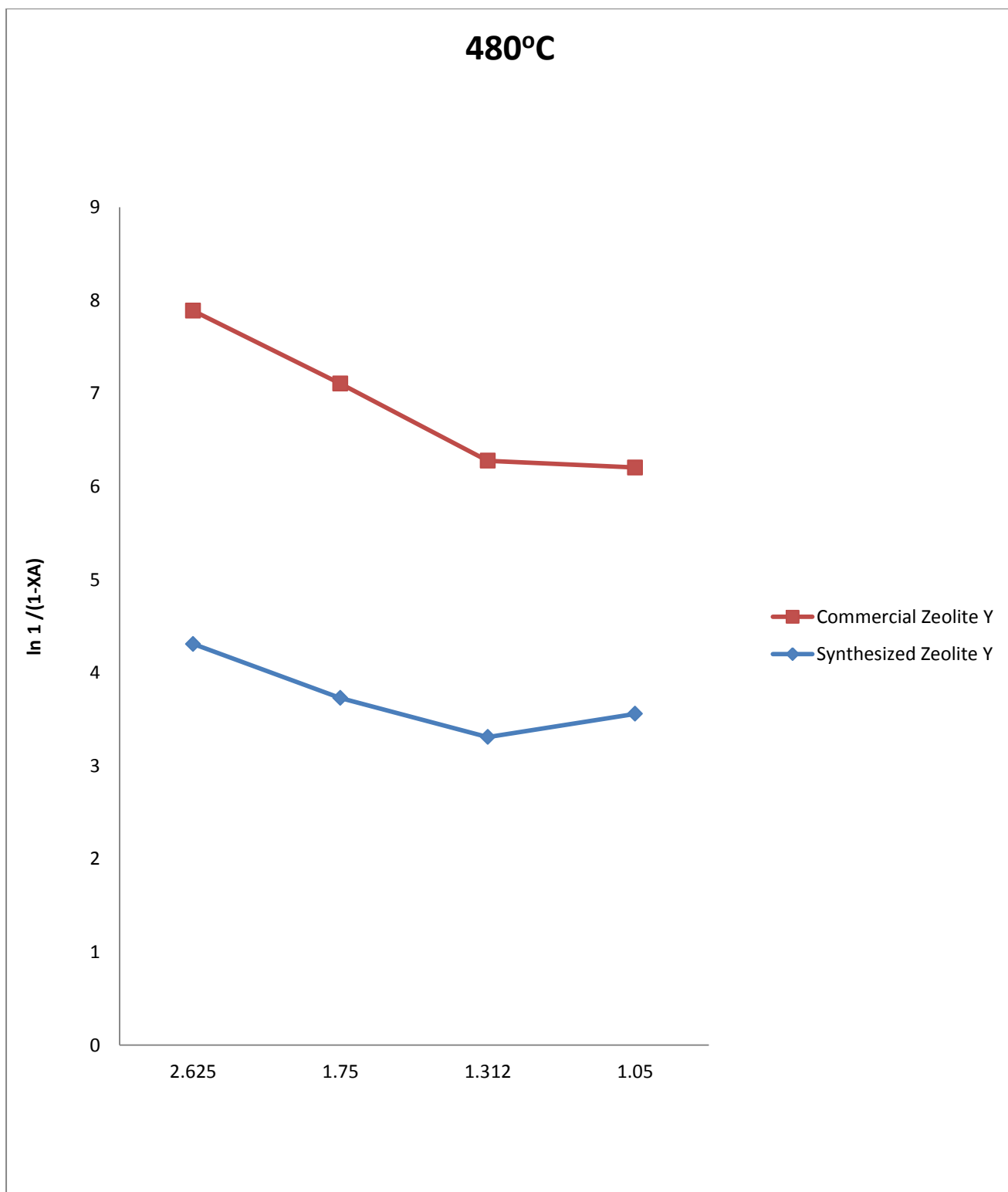


FIGURE 4.20; Effect of Catalyst type on Propane Yield of Cyclohexane Cracking at 520°C



**W/F_{AO} FIGURE 4.21; Effect of catalyst type on Propane Yield of Cyclohexane
Cracking at 480°C**

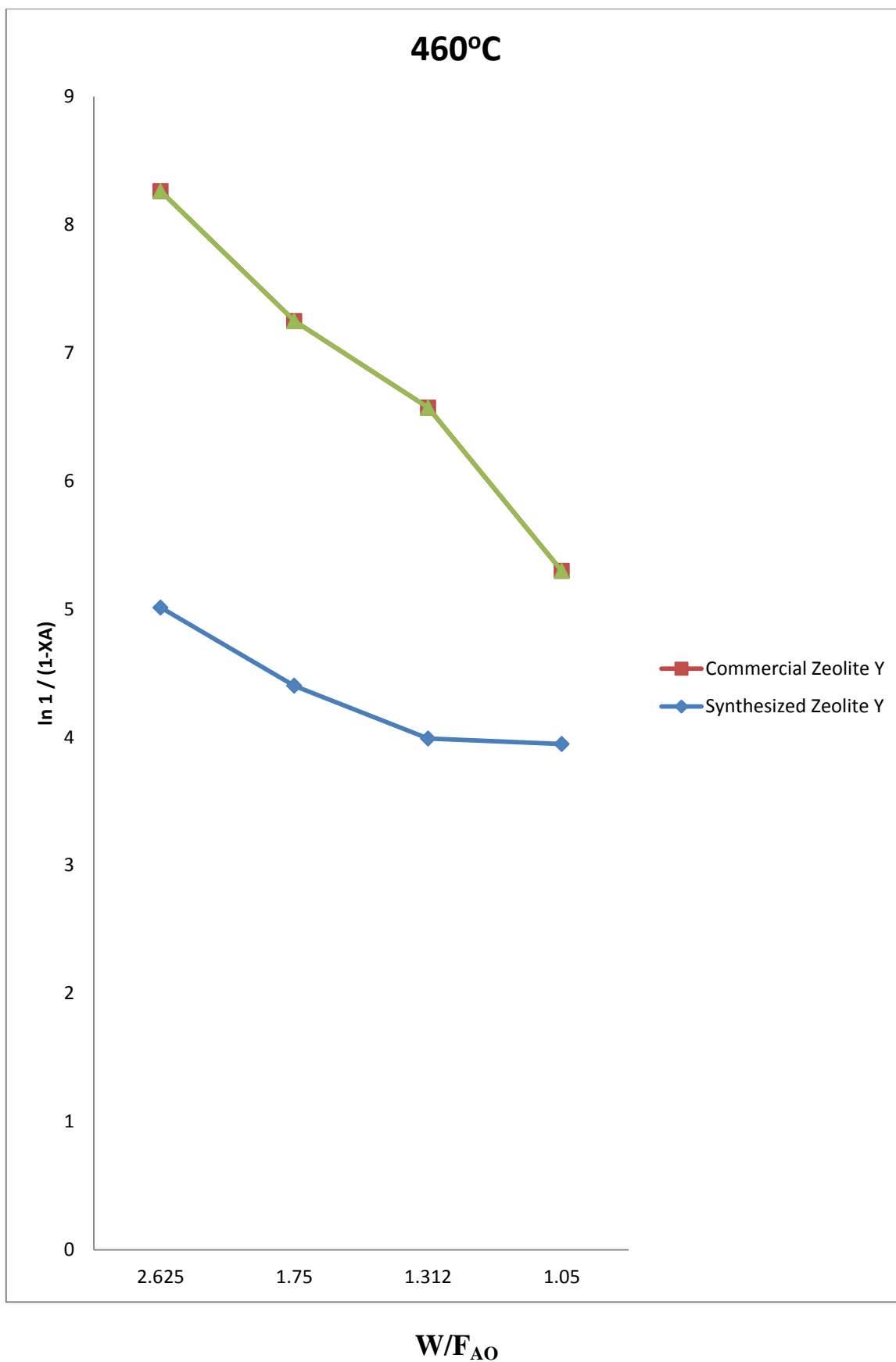


FIGURE 4.22: Effect of catalyst type on Propane yield of Cyclohexane Cracking at 460°C

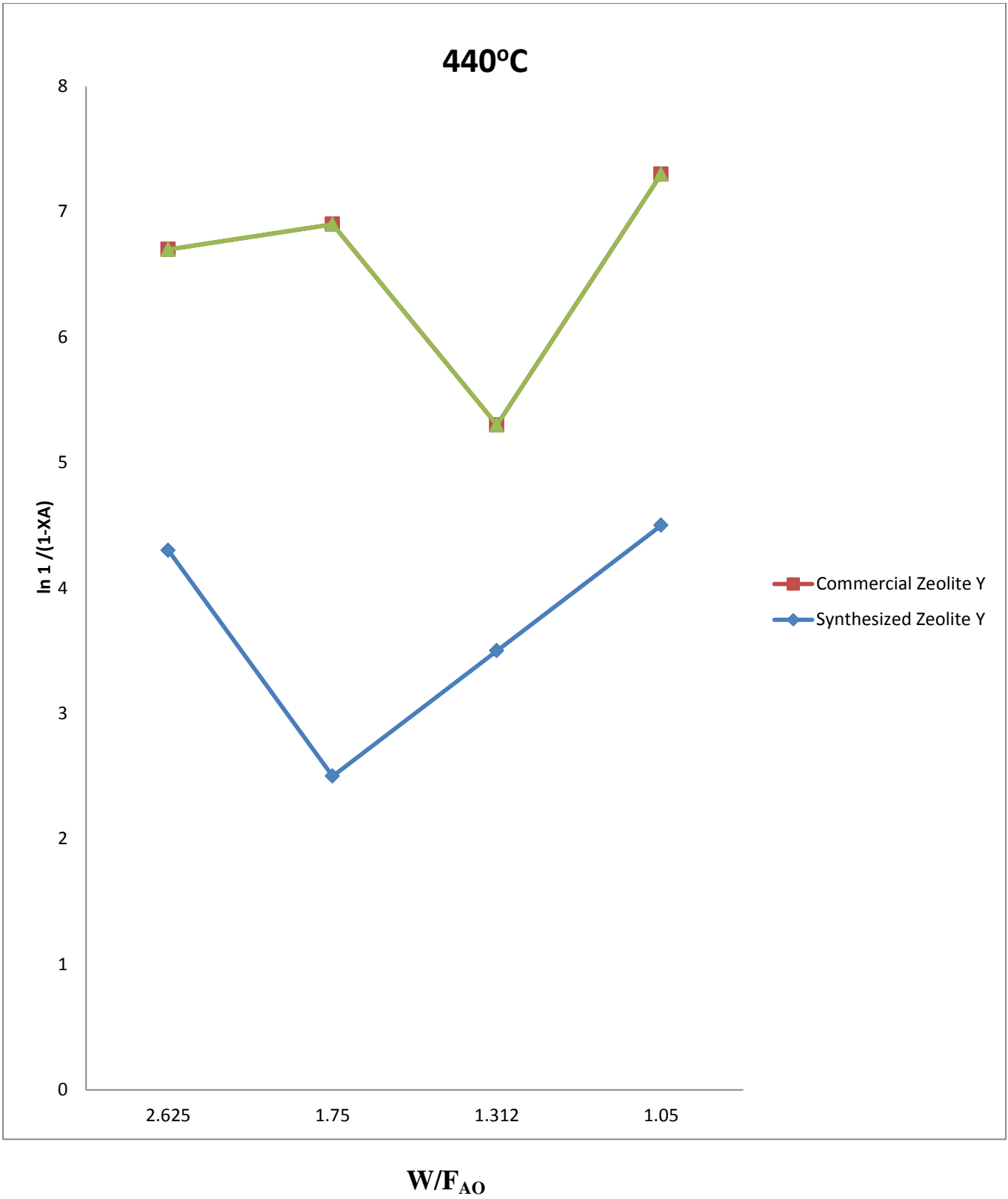


FIGURE 4.23; Effect of Catalyst type on Propane Yield of Cyclohexane Cracking at 440°C

Table 4.16: Adsorption coefficient (k_a) for cracking cyclohexane

Temp °C	Synthesised Zeolite Y	Commercial Zeolite Y
520	2.978	5.115
480	5.115	2.378
460	2.185	0.420
440	-7.610	-2.169

4.7.5 Cracking of gas oil on synthesized zeolite Y

Weight of catalyst $w = \text{constant} = 0.15\text{g}$

Length of packing = 0.05m

Moles Gas Oil injected = 2mL = $2 \times 10^{-6}\text{m}$

Molecular mass of Gas Oil = 285g

Carrier gas flowrate = $Q = 40, 60, 80, 100\text{mL/s}$

Detail calculation are shown in appendix B

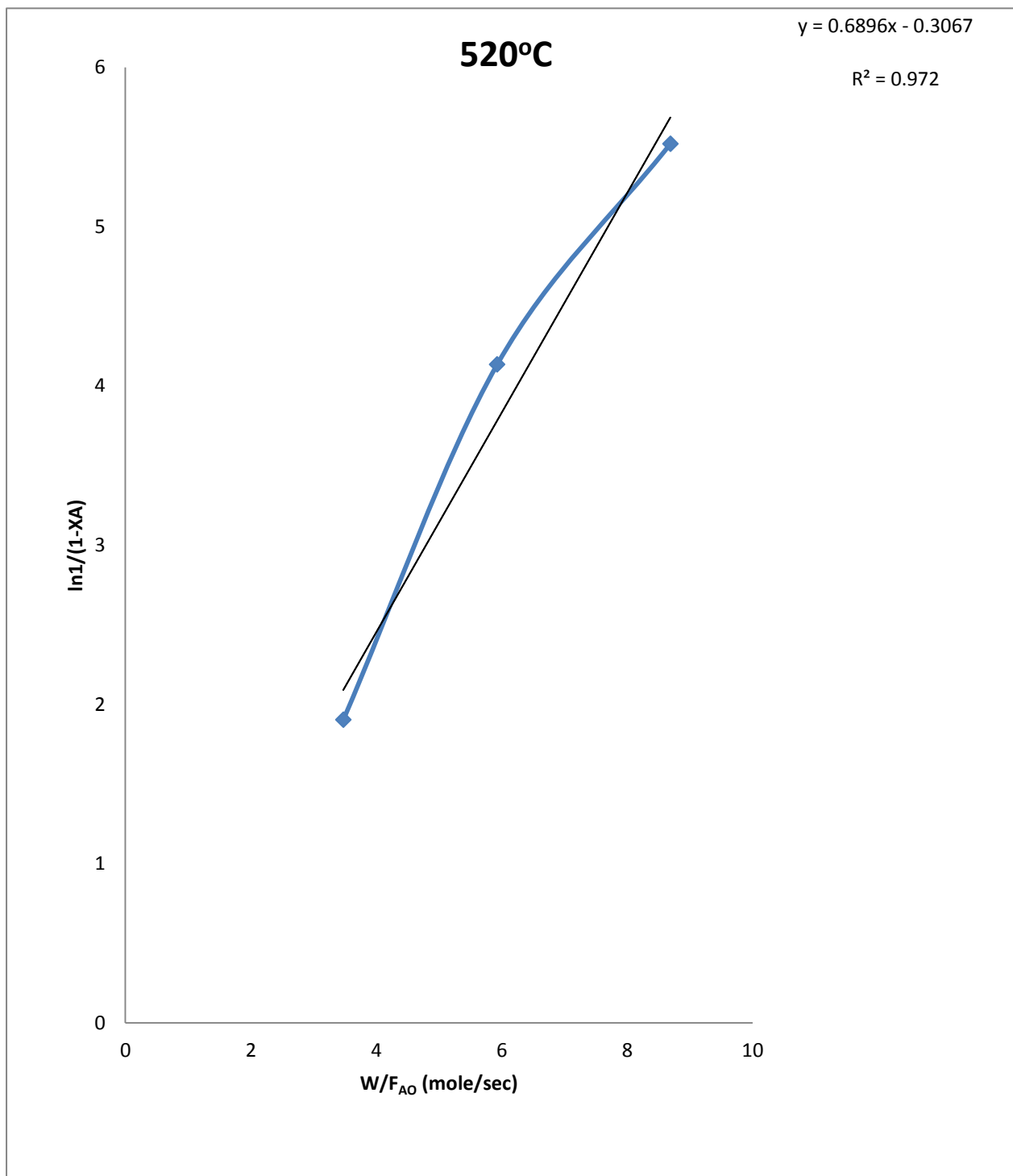


FIGURE 4.30: Test of first order kinetic for gas oil cracking on synthesized zeolite Y catalyst at 520°C

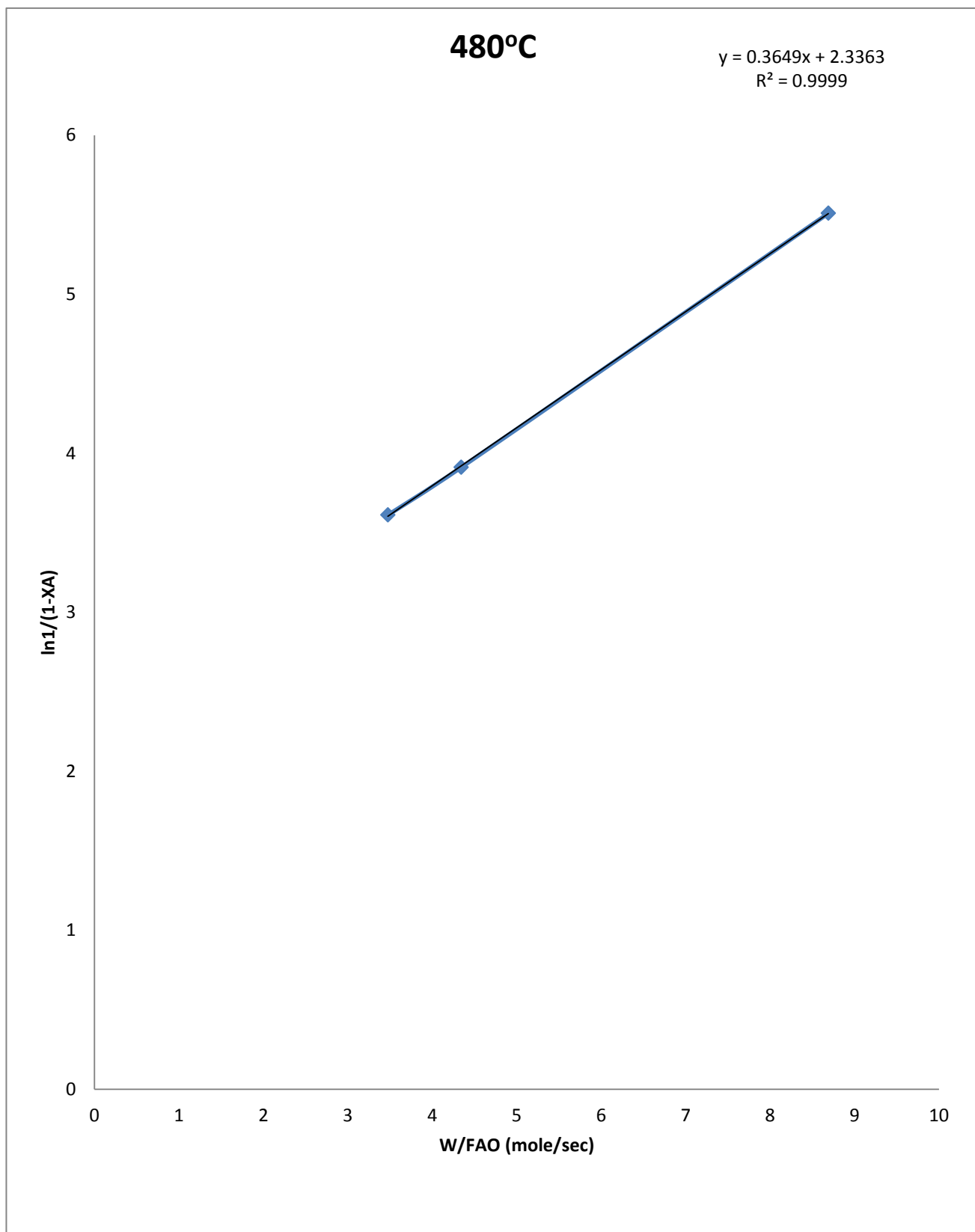


FIGURE 4.31: Test of first order kinetic for gas oil cracking on synthesized zeoliteY catalyst at 480°C

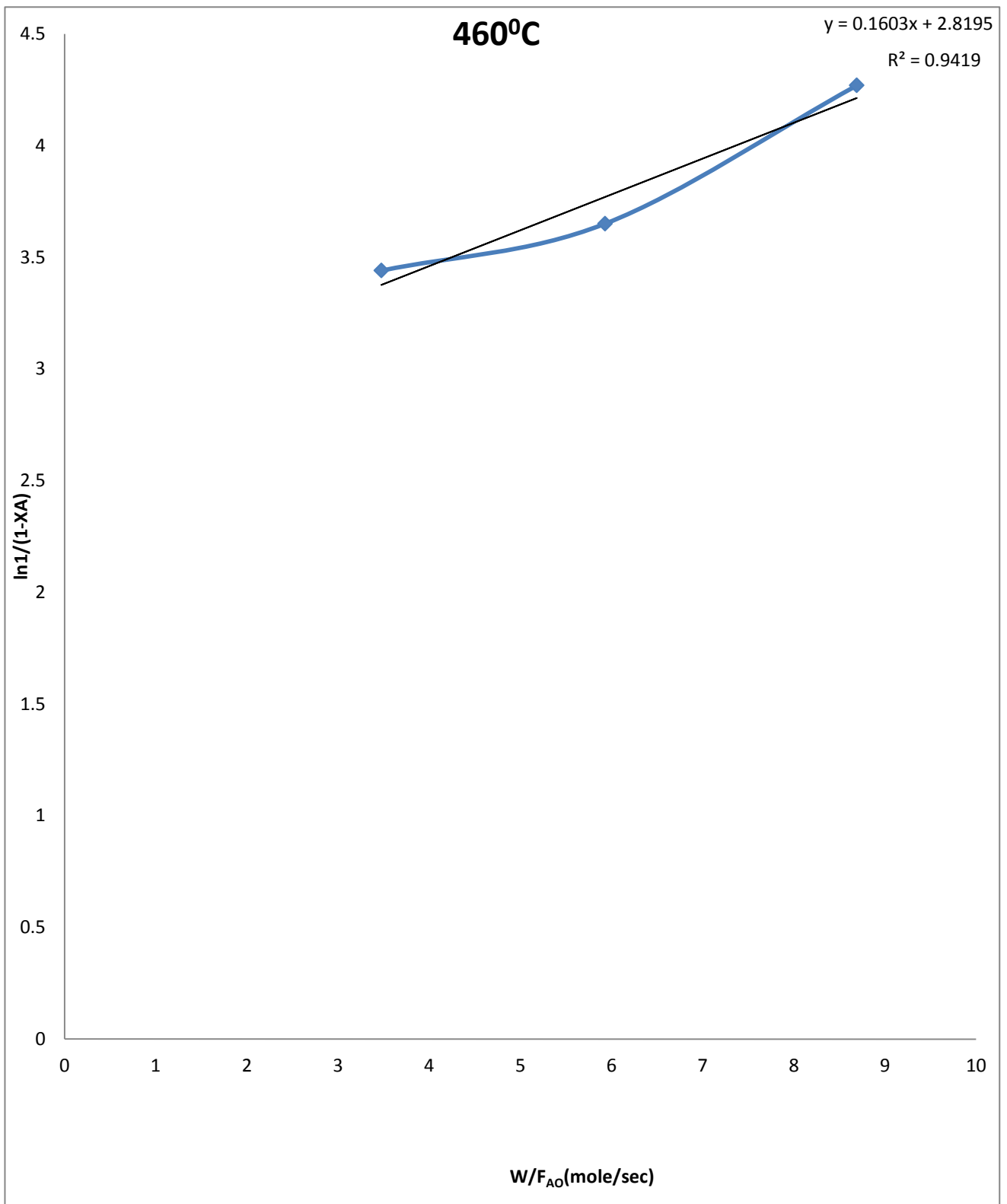


FIGURE 4.32: Test of first order kinetic for gas oil cracking on synthesized zeolite Y catalyst at 460°C

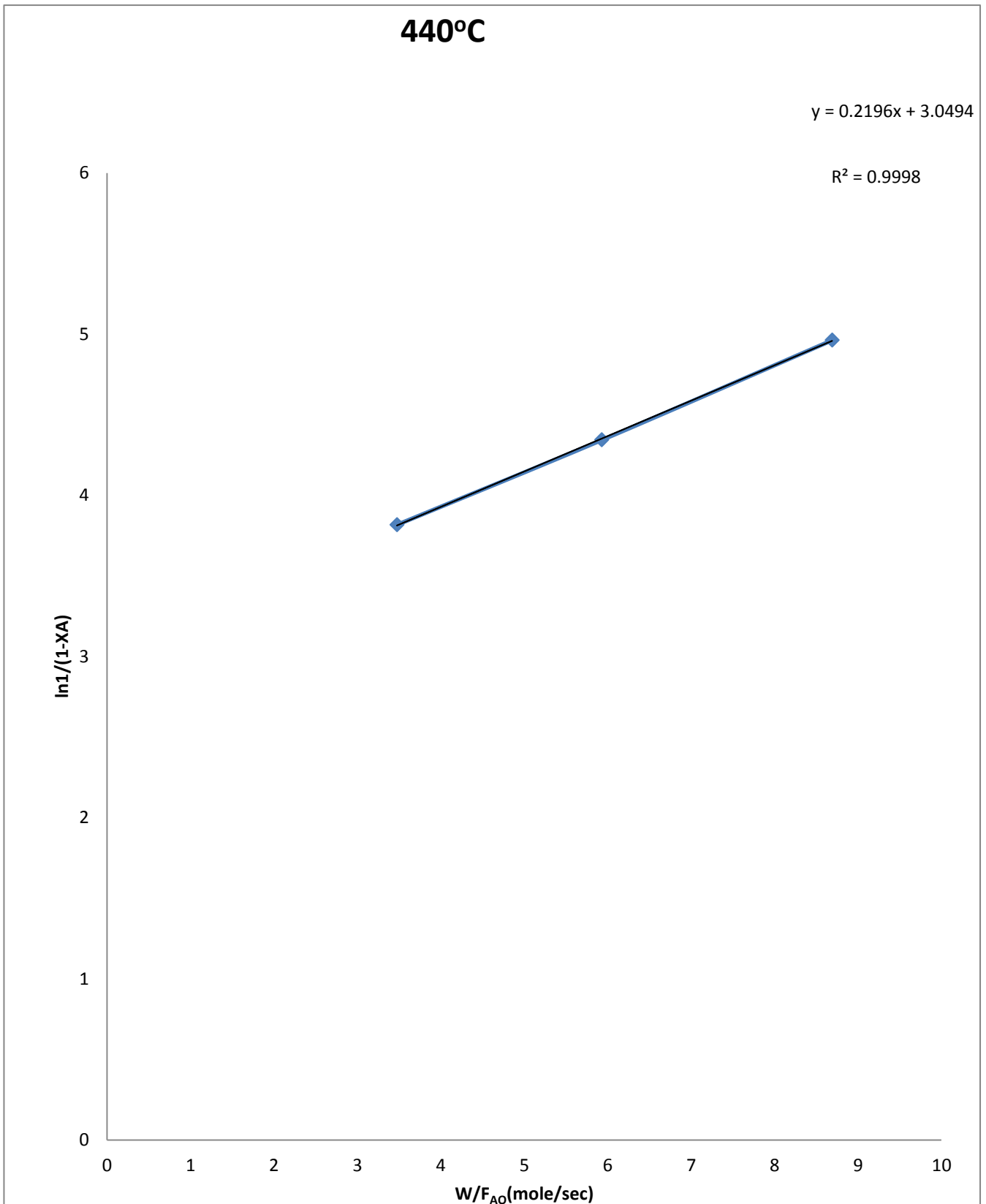


FIGURE 4.33: Test of first order kinetics for gas oil cracking on synthesized zeolite Y catalyst at 440°C

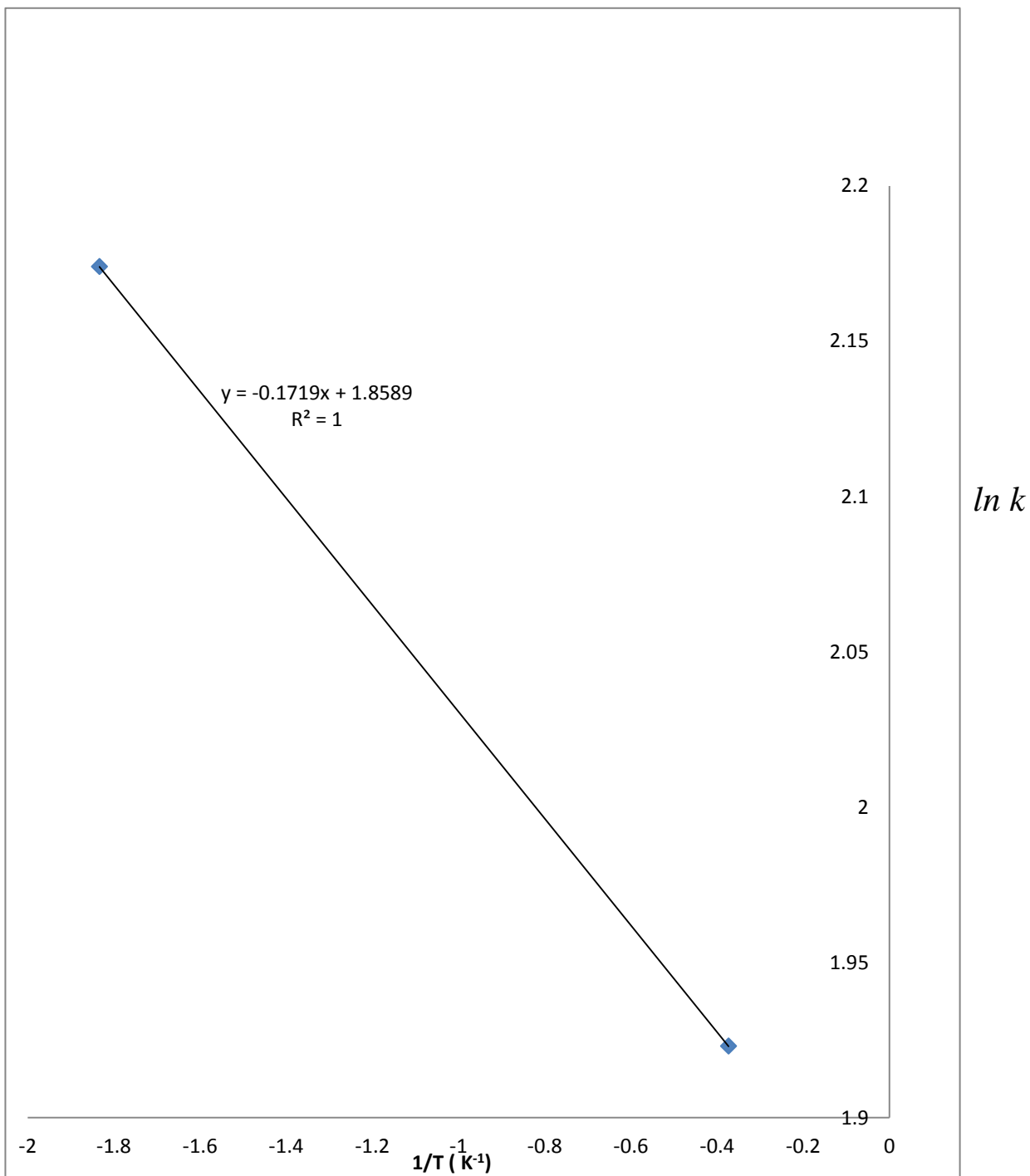


FIGURE 4.34: Arrhenius plot for cyclohexane cracking on commercial zeolite Y

$$\text{Slope} = \frac{-E}{R} = -0.458$$

$$E = R \times 0.458$$

$$E = 8.314 \times 0.458 = 3.808 \text{ kcal/mole}$$

4.7.6: Cracking of gas oil on standard zeolite Y

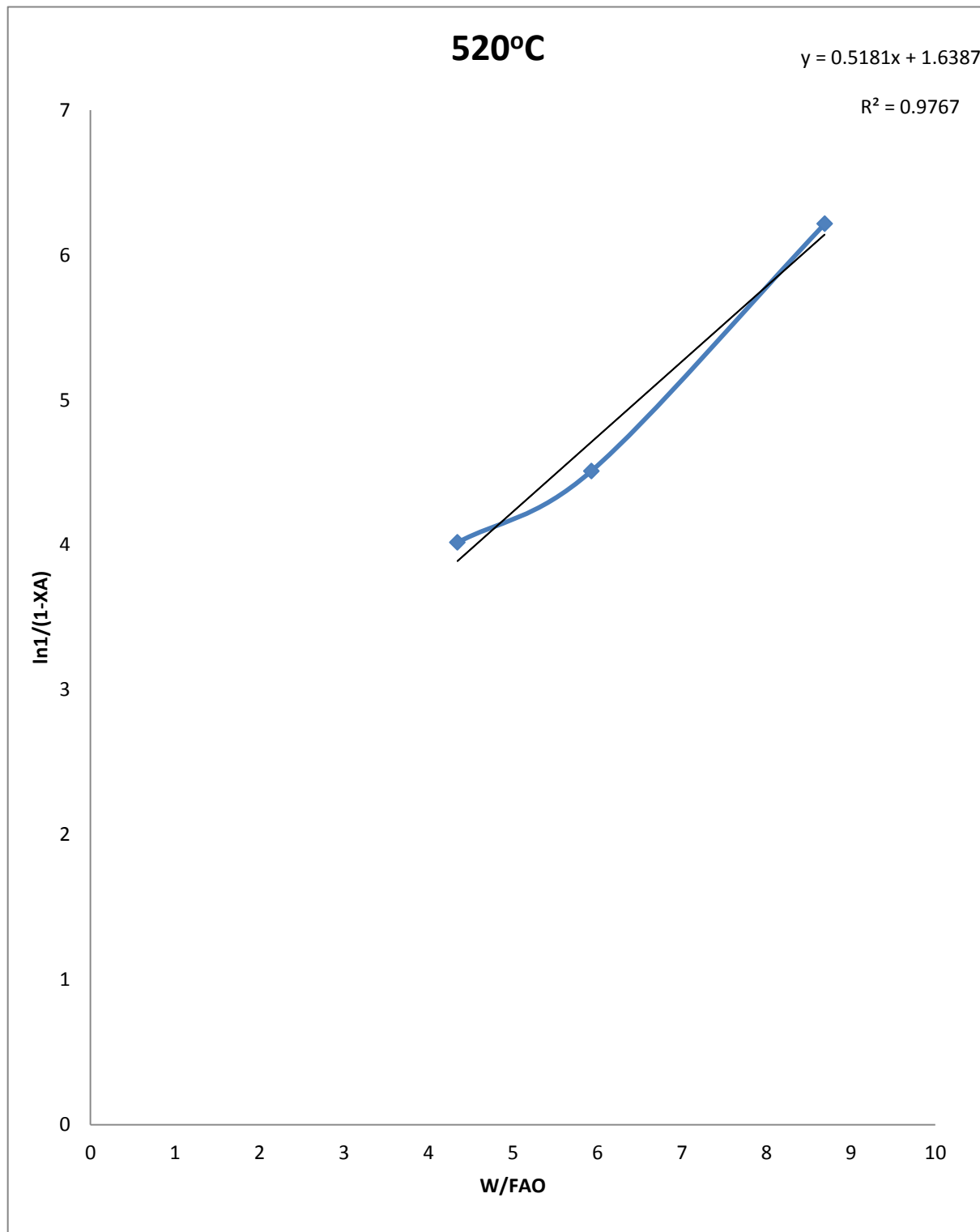


FIGURE 4.35: Test of First Order Kinetics for gas oil cracking on commercial zeolite Y catalyst at 520°C

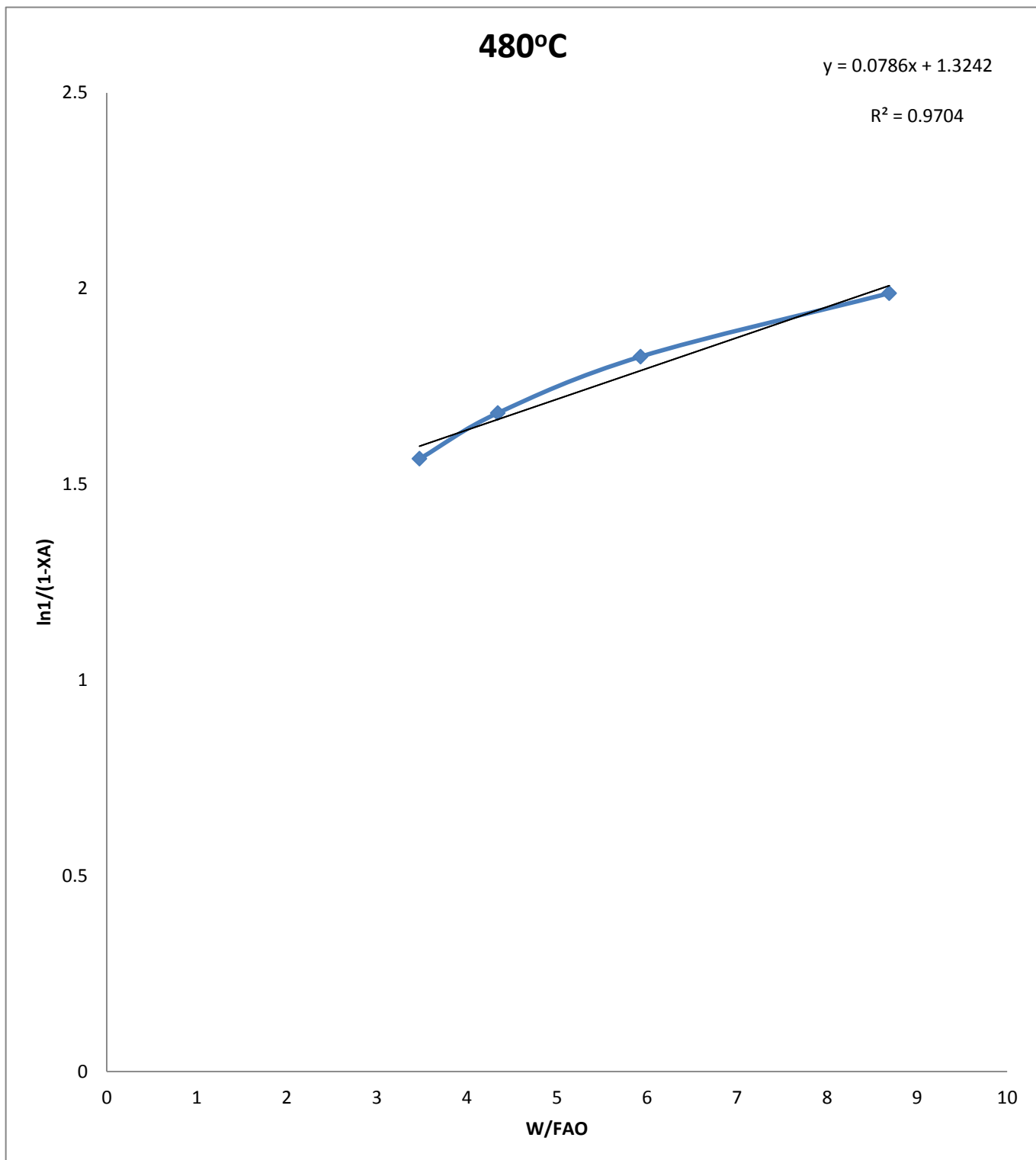


FIGURE 4.36: Test of First Order Kinetic for gas oil cracking on commercial zeoliteY catalyst at 480°C

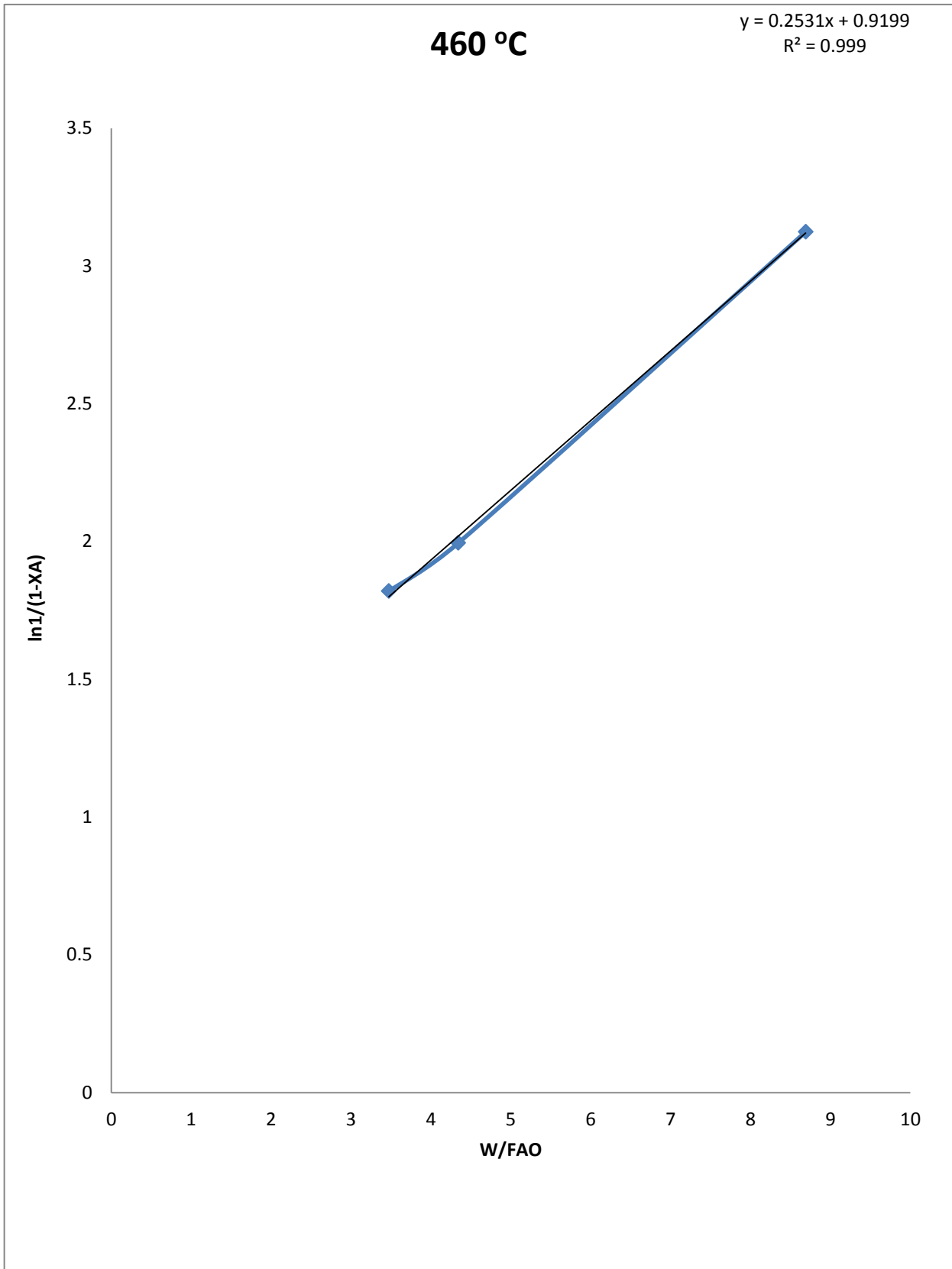


FIGURE 4.37: Test of First Order Kinetic for gas oil cracking on commercial zeolite Y catalyst at 460°C

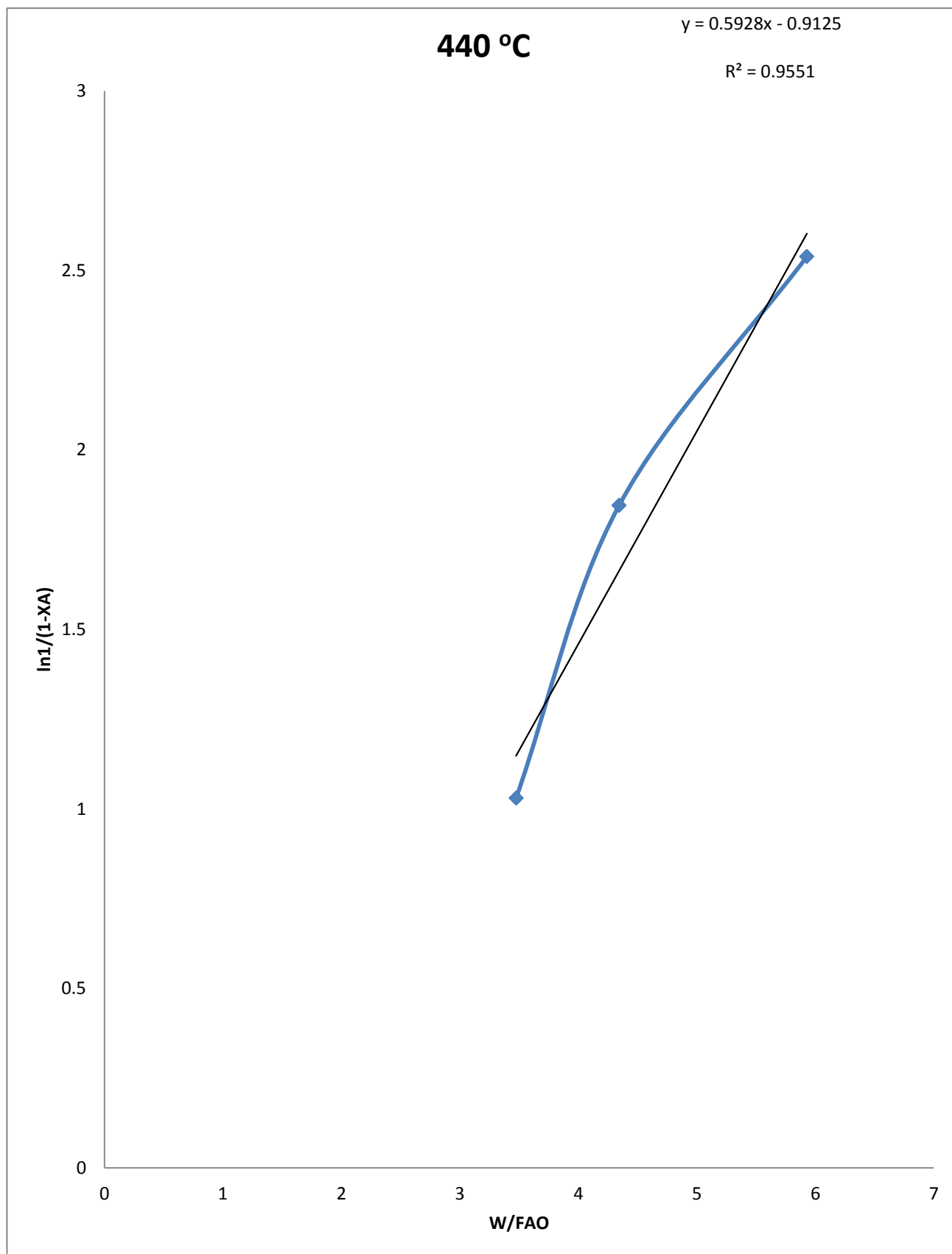


FIGURE 4.38: Test of first order kinetic for gas oil cracking on commercial zeolite Y catalyst at 440°

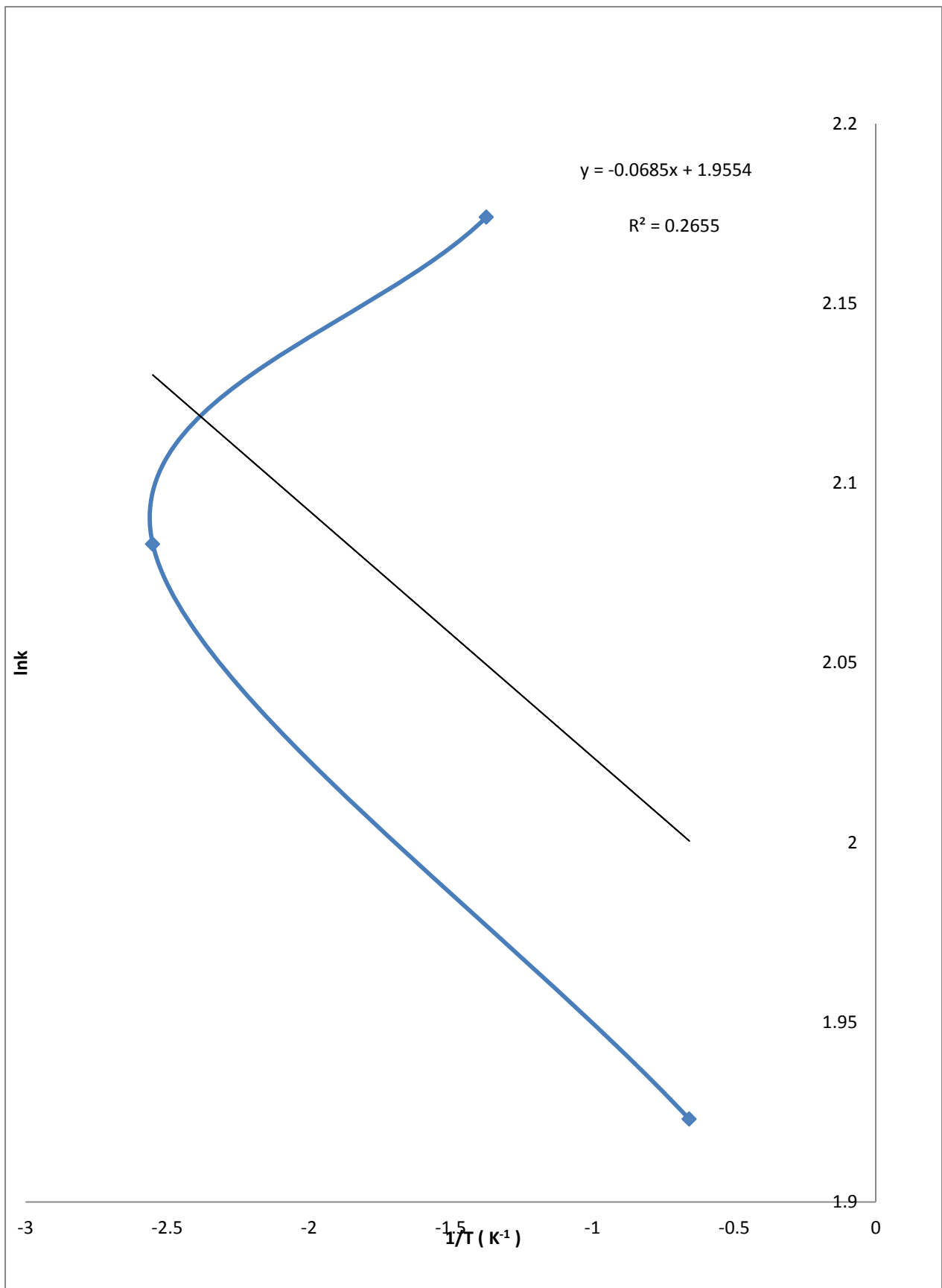


FIGURE 4.39: Arrhenius plot for gas oil cracking on commercial zeolite Y

4.7.7: Comparison between the performance of synthesized zeolite Y and commercial zeolite Y on gas oil

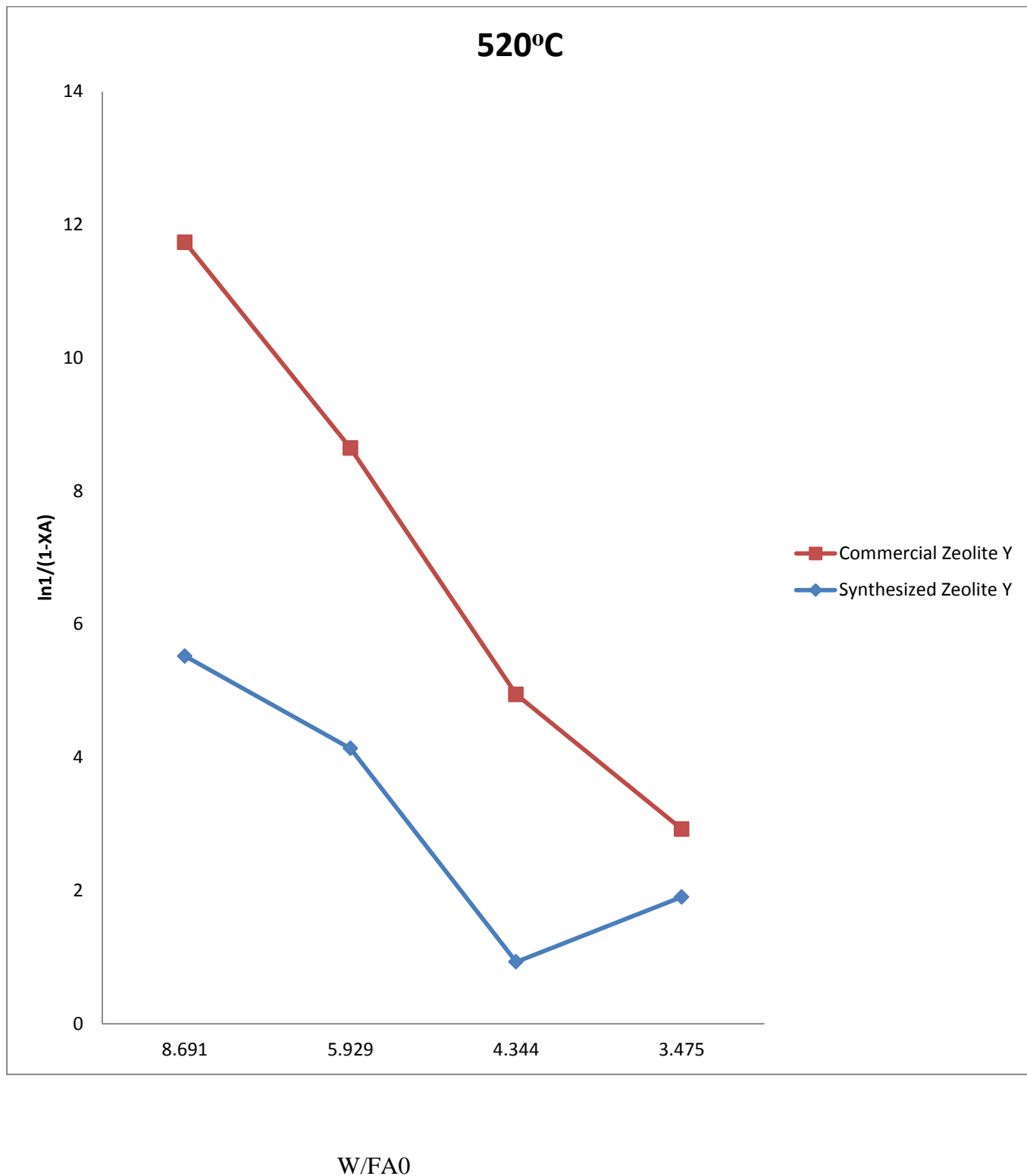


FIGURE 4.40; Effect of catalyst type on propane yield of gas oil cracking on 520°C

480°C

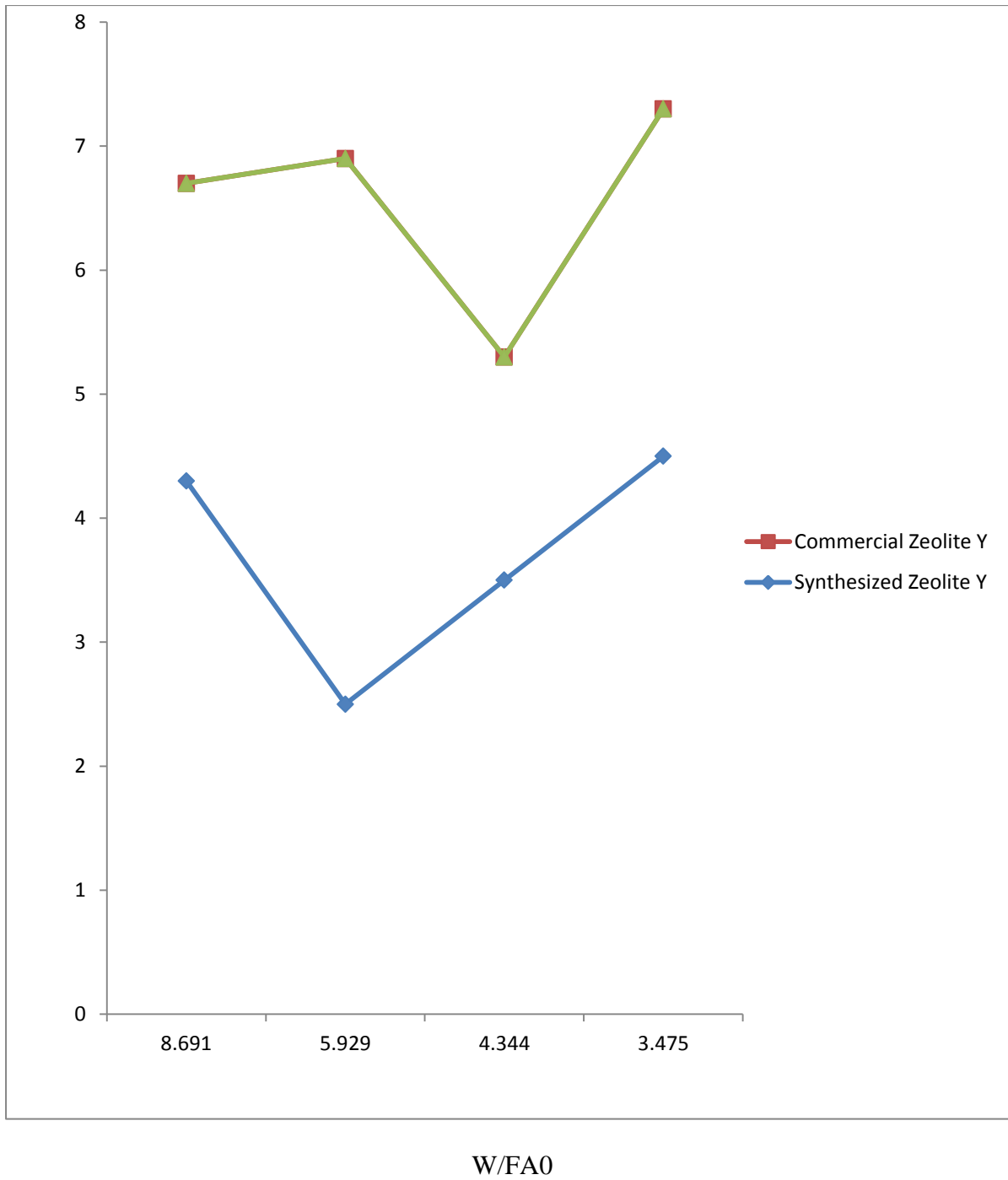


FIGURE 4.41; Effect of catalyst type on propane yield of gas oil cracking at 480°

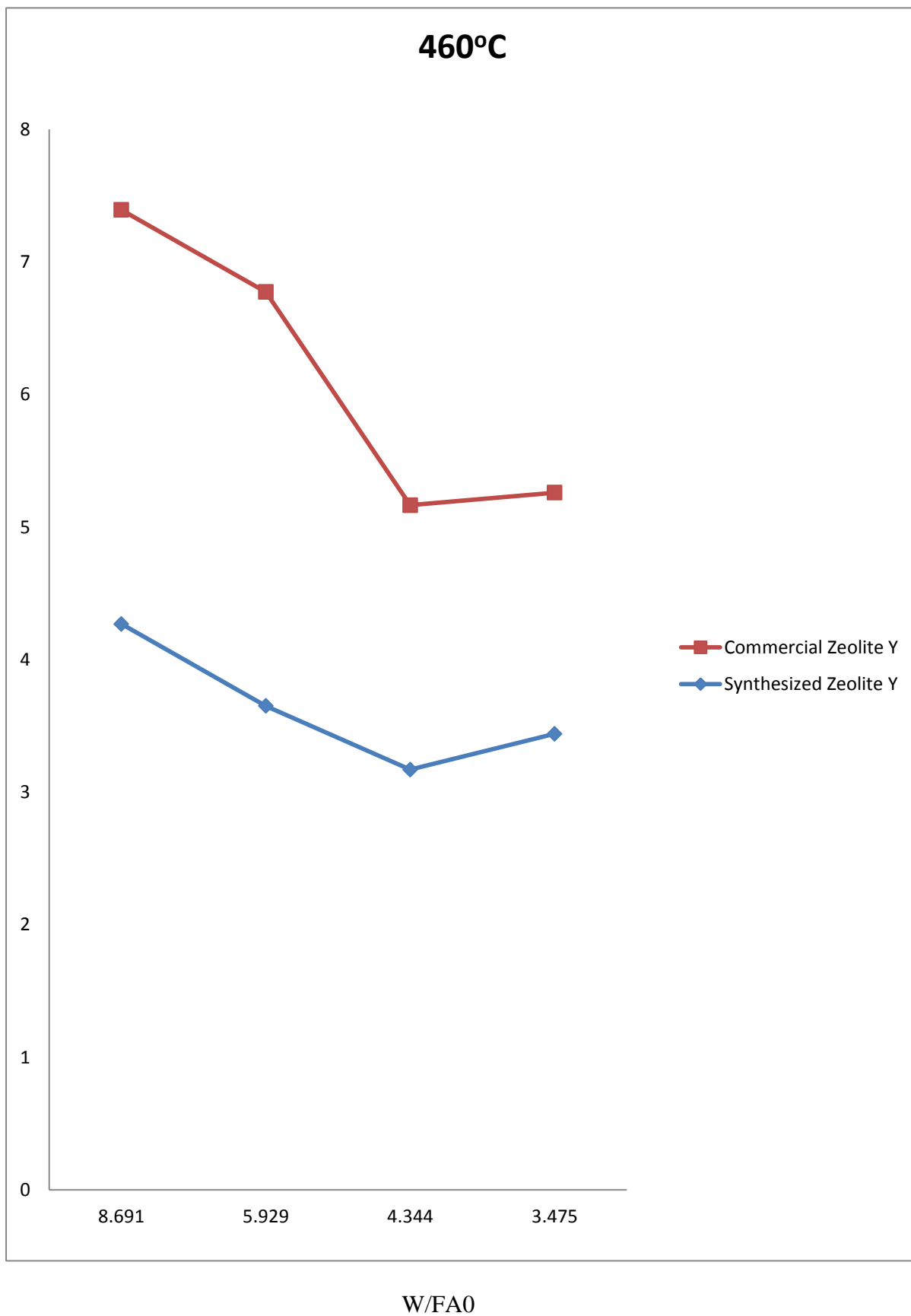


FIGURE 4.42; Effect of catalyst type on propane yield of gas oil cracking at 460°

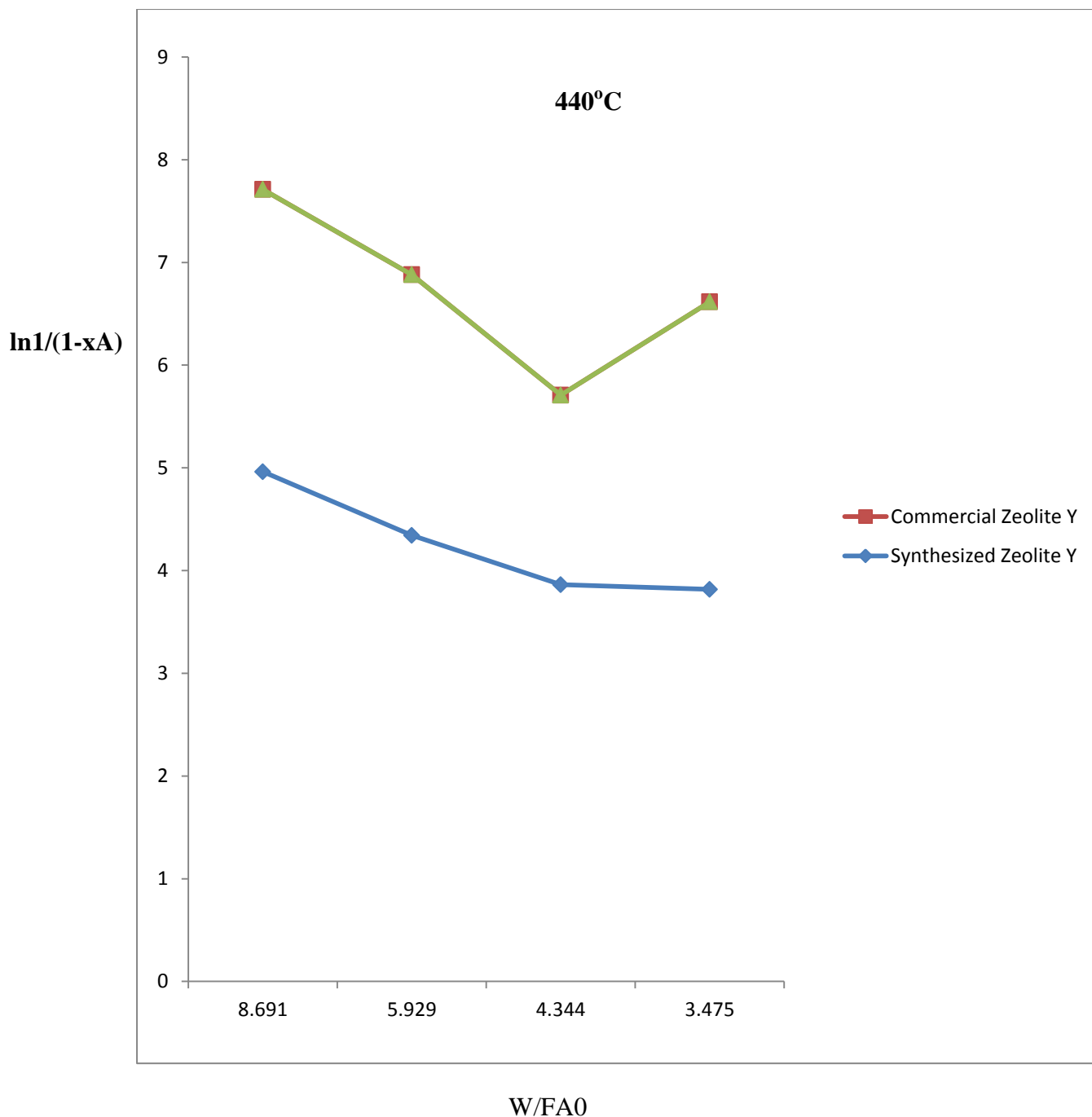


FIGURE 4.43; Effect of catalyst type on propane yield of gas oil cracking at 440°C

Table4.17: Adsorption coefficient for cracking of gas oil

Temp °C	Synthesised zeolite Y	Commercial zeolite Y
520	-0.211	0.848
480	0.850	0.103
460	0.451	0.233
440	0.668	-0.540

4.8: Summary of Research Work

The objectives of this research have been largely met. The sequence of the synthesis involved the collection of raw kaolin from Elefun, subjecting it to calcinations, partial dealumination and final hydrothermal synthesis. The raw clay was refined using sedimentation technique to recover about 98 percent kaolin. Both conventional and novel methods of metakaolinization technique were used to convert the refined kaolin to a reactive metastable phase. The amorphous metakaolin was obtained at a temperature of about 850°C and a residence time of about 6 hours. The percentage of the alumina in the metakaolin was reduced through reaction with sulphuric acid to give silica/alumina molar ratio of about 4.7 after aging for between seven and nine days. Our unique procedure of gel formation and Crystallization to NaY Zeolite was achieved after 24 hours at 100°C. The NaY Zeolite was modified by ion exchange process to give a more acidic Zeolite HY with improved Brosted acid active sites.

The synthesised Zeolite HY was characterized and confirmed through the XRD pattern and the silica/alumina ratio of about 3.62 was obtained using XRF these results were corroborated with the analytical result from both SEM and BET.

The evidence of the industrial grade of our synthesised catalyst is confirmed through its efficient cracking of Cyclohexane and Vacuum Gas Oil when tested in NNPC Kaduna Refinery laboratory Nigeria using the cracking rig set up shown in Figure 3.3.

The activity of the synthesised Zeolite Y was confirmed favourably compared to the market commercial brand through its very close conversion in the cracking reactions of Cyclohexane and vacuum Gas Oil to lighter products when tested in NNPC Kaduna Refinery Laboratory.

In conclusion, it can be said that Nigerian clay sourced from Elefun can serve as a good raw material for developing highly crystalline Zeolite Y.

CHAPTER FIVE

Conclusions and Recommendations

5.1 Conclusion

This chapter present the conclusion and recommendations based on the obtained results.

5.1 From the results of this study, the following conclusions can be drawn:

- I. Zeolite Y have been produced from kaolin deposits from Elefun in Ogun state
- II. The production of Zeolite Y involved beneficiation, calcinations at 850°C, dealumination, ageing, crystallization, drying and ion exchange
- III. The produced zeolite Y has successfully cracked cyclohexane and gas oil into lighter products when tested in NNPC Kaduna Refinery Laboratory.

5.2 Recommendations

The following suggestions and recommendations are hereby made in order to advance and improve on what is reported here in

- 1 Better method of kaolin purification targeted at potassium removal should be investigated.
- 2 Further study should be carried out on Novel approach for economic reasons.
- 3 Studies should be carried out on synthesis of Zeolite ZSM-5 to enable perfect use of our zeolite Y as it tend to overcrack the cyclohexane and even the gas oil
- 4 Set up of pilot plants to produce at least 10kg per batch of zeolite Y should be developed by the School for eventual commercialization.
- 5 Analytical equipment like XRF, XRD, and SEM etc should be made available.
- 6 Sedimentation method of refining Elefun kaolin can only achieve 98% purification as can be seen in this work. Hence other method like selective flocculation, magnetic separation or flotation method can be applied for complete removal of quartz which is a major obstacle toward the application of locally developed zeoltes in chemical processes

7 Further study should be carried out on means of preserving synthesized zeolite Y, to avoid further depolymerization.

5.3 Contribution to Knowledge

1. Identification and confirmation of Elefun Clay as a good deposit for the production of Zeolite-Y.
2. Identification of specific conditions, temperature and Time, required for the development of Zeolite-Y from Elefun Clay
3. Production, with reproducibility, for the first time of good crystalline industrial grade Zeolite-Y from Nigerian Clay
4. Successful evaluation, for the first time, of the reactivity of Zeolite-Y produced from Nigerian Clay as compared to imported industrial grade sample

REFERENCES

Adefila, S.S., B.O. Aderemi, O.A. Ajayi and D.A Baderin (2003), “Comparative surface area determination using water adsorption method”, *Nigerian Journal of Engineering*, vol.11, Pages: 89-97..

Adefila S. S. Olakunle M.S, (2008) “Thermodynamics of Zeolite formation”, First *PTDF Workshop on Zeolite Development in Nigeria*, pages: 47-76.

Aderemi, B. O. (2000), “development of zeolite cracking catalyst from local raw materials” *Ph.D Thesis*, Ahmadu Bello University, Zaria.

Ahmed, A. S and P.B. Onaji. (1995).”The effect of beneficiation on the properties of some Nigerian Clay”. *Journal of Nigerian Society of Chemical Engineering* 6(2): 119-129.

Ahmed, A. S.; Nuradeen, S.; Suleiman, Y. (2014) “Indegenous process technology development for the production of zeolite catalysts from kaolin” *Annual lecture of the PTDF Professorial chair in chemical engineering*.

Alkan, P., H, C., Yilmaz, Z., Guler, H (2005). “The effect of alkali concentration and solid/liquid ratio on the hydrothermal synthesis of zeolite NaA from natural kaolinite microporous mesoporous materials”, 86, 176-184.

Ajayi, O. A, Adefila S. S. Aderemi B. O, (2010), “Novel method of metakaolin dealumination-preliminary investigation”. *Journal of Applied Science Research*, 6(10), 1539-1546.

Ajayi, O. A. and Aderemi, B. O. (2008),”Zeolite synthesis from kaolin”*Science and Engineering in Zeolite Development, PTDF workshop on zeolite development in Nigeria, ABU, Zaria.18-41.*

Ajayi, O. A, Adefila, S. S., Aderemi, B. O, Ahmed, A. S, Ityokumbul, M. T. (2012), “Development of large pore zeolite from kaolinite”.*Ph.D Thesis*. Ahmadu Bello University, Zaria

Ambikadevi, V. R. and Lalithambika, M. (2000). “Effect of organic acids on ferric iron removal from iron- stained kaolinite”. *Applied Clay Sciences* 16, 133-145.

Anthony, G.D and Garn, P. D (974). Kinetic of kaolinite dehydroxylation. Journal American Ceramic Society, 57, N3, 132-135.

Asmatulu, R. and Turk. J (2002). “Removal of discoloring contaminants of east Georgia kaolin clay and its dewatering”.. *Engineering environmental science.* 26, 447-453.

Auerbach, S., K.A. Carrado, and P.K. Dutta, (2003), *Handbook of zeolite science and technology*, New York Marcel Decker Inc 1170

Awe P.J. (2012), “NNPC Refining processes and current challenges” –*SOTP 049*

Babalola, R., Omoleye, J.A. and Hymore, F. K, (2014), “Development of Industrial Grade Zeolite Y from Nigeria clay” *Proceedings of the 1st Nigeria International conference on Zeolite (2014), 24 – 28.*

Barrer, R. M. and Denny, P., (1961). Hydrothermal Chemistry of the Silicates, Part IX Nitrogenous Aluminosilicates,, *Journal of Chemical Society*, 971 - 1000

Barrer, R. M (1982), “Hydrothermal chemistry of zeolites”.: Academic Press, New York, 360.

Barrer, R.M., (1978), “Zeolites and Clay Minerals as Sorbent and Molecular Sieves”, Academic Press. London, 497.

Barrer R. M., “Zeolite synthesis”, *Proceedings of the sixth inters zeolite conference* (1983), 17-30.

Bartholomew, C.H. (2001). Mechanism of Catalyst Deactivation. *Applied Catalysis A: General* 212, 17-60.

Belver, C., M.A.B Muinoz and M.A. Vicente (2002). “Chemical activation of a kaolinite under acid and alkaline conditions”. *Chemical materials* 14: 2033-2043.

Berendsen, W.R., P. Radmer, and M. Reuss (2006), “Pervaporative separation of ethanol

from an alcohol-ester quaternary mixture”. *Journal of membrane science*, 280(1-2): p. 684-692.

Bergaya, F., and G. Lagaly, (2006), *Handbook of Clay science* ed. F.Bergaya, B.K.G. Theng, and G.Largaly.

Bibby, D. M and M. P. Dale (1985). “Synthesis of silica sodalite from non aqueous systems” *Nature* (London), 317, 157 – 158.

.Borggard, O.K (1979). “Selective extraction of amorphous iron oxides by EDTA from a Danish sandy loam”. *Journal of soil sciences* 30, 727-734.

Bosch, P., L. Ortiz, and I. Schifter (1983), “Synthesis of faujasite type zeolites from calcined kaolins”. *Industrial & Engineering Chemistry, Product Research and Development*, 22(3): p. 401-406

Bowen, T.C.,H. Kalipcilar, J.L. Falconer, and R.D. Noble(2003) “Pervaporation of organic/water mixtures through B-ZSM-5 zeolite membranes on monolith supports”. *Journal of Membrane Science*, 215(1-2): p. 235-247

Breck, W.D. and Flannigan, E. M. (1967), “Synthesis and properties of Union Carbide Zeolites L, X and Y”. *Molecular sieves conference*, London, 47-61.

Breck, D.W. (1974), “Zeolite molecular sieves: Structure, Chemistry and Use” *Journal of porous materials* p. 771, volume 18.

Brindley, G.W. Nakahira, M. (1959), “The kaolinite mullite reaction series, II, Metakaolin”. *Journal of American Ceramic Society*, 42, N7, 314-318

Byrappa, K. and M. Yoshimura, 2001, *Handbook of hydrothermal technology*, New Jersey: William Andrew Publishing, LLC

Caballero, I.; Colina, F. G.; Costa, J. (2007). “Synthesis of X-type zeolite from dealuminated kaolin by reaction with sulfuric acid at high temperature”, *Industrial and Engineering Chemistry Research* 46, 1029-1038.

Carrado, K. A. ; Garwood, W. E. (2003), “Reactivity of clay minerals with acids and alkalies Clays and Clay Minerals”, *Handbook of zeolite science and technology*, New York Marcel Decker Inc 1170 C (1971). Vol. 19, 321-333.

Chandrasekhar, S. (1996), “Influence of metakaolinization temperature on the formation of Zeolite 4A from kaolin clay Minerals”, . 31: p. 253-261.

Chandrasekhar, S. and P.N. Pramada, (2008), “Investigation on the synthesis of zeolite NaX from kerala kaolin”. *Journal of porous materials*,. 6(4): p. 283-297

Chiang, A. S.T. and Chao, K. J., (2001), “Membranes and films of zeolite and zeolite-like Materials” *Journal of physics and chemistry of solids*, (62): p. 1899-1910.

Clementi loop (2007), “Porous Materials: Synthesis and Structure”, John Wiley, Singapore, 679

Cicel, B. Novak, I. Horvath, I. (1981). “Mineralogy and crystallochemistry of clays”. SAV, Bratislava.

Daily Trust, Newspaper, (25, Sept., 2012).

Davis, M. E., Katz, A. and Ahmad, W. R. (1996) “Rational catalyst design via imprinted nanostructured materials”. *Chemistry of materials*., 8(8): p.1820-1839.

Dyer, A. (1988), “Zeolite Molecular Sieves”, Chichester John Wiley. 149.

Greensfelder, B.S. (1949), *Ind. Eng. Chem.*, 41, 2573.

Elimbi, A., H.K Tchakoute, D. Njopwouo (2011). “Effects of calcinations temperature of kaolinite clays on the properties of geopolymer cement”. *Construction and building materials*, volume 25, issue 6, 2805-2812.

Emofuriefa W.O. (1992), “Mineralogy, Geochemistry and Economic evaluation of the Kaolin deposits near Ubulu-Uku, Awo–Omena and Buan in Sorthern Nigeria”. *Mining and Geology* Vol 28 No. 2, p 211-220

Eva Mako, R.L.F., Janos Kristof and Erzsebet Horvath, (2001) “The effect of quartz content on the mechanochemical activation of kaolinite” *Journal of Colloid and Interface Science*. 244:

Ezekiel, A. A. (2014), p. 359-3642) “Petroleum Processing Technology”, *Joyce publishers, Nigeria*, p 205 – 229

Farhount, N., (1989). “Beneficiation of kaolins of islands of Milos”. *Ph.D thesis*, National Technical University, Athens.

Fernandez-Jimenez, A., Vallepu, R., Terai, T., Palomo, A. and Ikeda, K., (2006), “Synthesis and thermal Behavior of different aluminosilicate Gels”. *Chemical information*, volume 37, Issue 42, doi:10.1002/chin.200642211.

Flanigen, E. M. Breck D.W, (1960). “Crystalline zeolites V-Growth of zeolite crystals from Gels”, *137th Meet, ACS, division of inorganic chemistry. Cleveland, OH, Abstracts*, p.33-m.

Flanigen, E. M., H. A. Szymanski and H. Khatami (1971). “Infrared structural studies of zeolite frameworks”, *advances in chemistry*, 101:201-229.

Francis, R. and R. Annick,(2000),“Chemical Analysis”: *modern instrument method and techniques*, Chichester Wiley.

Freund E. F., (1976)“ Mechanism of the crystallization of zeolite X”. *Journal of crystal growth*, 34; p.1-23

Garn, P. D and Anthony, G.D (1969). “The questionable kinetics of kaolin dehydroxylation”. *Journal of thermal analysis*, 1, N1, 29-33.

Ginter, D. M., Bell, A. T., Radke, C.J (1992). “The effect of gel ageing on the synthesis of NaY zeolite from colloidal silica”. *Journal of Zeolites*, 12 (6), 742-749

Grimshaw, R.W. (1971). “Physics and chemistry of clay”, *4th ed. Ernest Benn*, London, ISBN: 0510,47701-47707.

Granizo, M. L., Blanco-Varela, M.T. and Palomo. A. (2000) “Influence of the starting kaolin on alkali-activated materials based on metakaolin. Study of the reaction parameters by isothermal conduction calorimetry.” *Journal of materials science* 35 (24): 6309-6315.

Greensfelder, B.S., Voge, H.H., and Good, G.M.(1949), *Ind. Eng. Chem.*, 41, 2573.

Guggenheim, S., Koval PV, Muller G, Neiva AMR, Radoslovich EW, Robert J-L, sassi FP, takeda H, Weiss Z and Wones D. R (1998). “Nomenclature of micas. Clay and clay minerals”, 46:586-505.

Groudev, S.N. (1999). “Biobeneficiation of mineral raw materials”. *Mineral metallurgical process*, 16, 19-28.

Hanykyr, V. and Kutzendoerfer, J. (2000). *Technologie keremiky. Silis praha a Vega hradec kralove.*

Hartmann, M.,(2005)“Ordered mesoporus materials for bio adsorption and biocatalysis”. *Chemical materials*, (17) P 4577-4593

Haynes, H.W., and Sarma, P.N, (1973).Reaction process of zeolite formation in the system $\text{Na}_2\text{O}-\text{Al}_2\text{O}_3-\text{SiO}_2-\text{H}_2\text{O}$. *AIChE J.*, 19, 1043

Horvath, I. and Kranz, G (1980). “Thermo analytic study of the high temperature dehydration of kaolins with different degree of the order”. *Silikarty* 24, N2, 149-160.

Horvath, I. Sedlec (1976). “Kaolin dehydroxylation kinetics”. 7th *conference on clay mineral and petrol*. Karlovy vary, 121-127.

Hosseini, M.R., Pazouki, M., Ranjbar, M., Habibian, M (2007). “Bioleaching of iron from highly contaminated kaolin clay by aspergillus niger”. *Applied Clay Science* 37, 251-257.

Hulbert, S. F., Huff, D. H. (1970). Kinetics of alumina removal from a calcined kaolin with nitric, sulphuric acid and hydrochloric acids, *clay minerals*, 8(337).340-345

<http://www.ch.ic.ac.uk/vchemlib/course/zeolite/structure.html>, 2013 (cited 16/07/13)

<http://cobweb.ecn.purdue.edu/~thormsonk/project.html>, 2013, *Reactivity in zeolite system*,. last cited 12/04/2013.

<http://www.rmrhc.com> accessed on 17th May, 2013

<http://www.chemicaland21.com> (2007) accessed on 10th August, 2013.

[Http://www.mindat.org](http://www.mindat.org),(2005) sighted on August 16th, 2013

IEA. (2008) “IEA World Energy Outlook 2008”. *Paris: International Energy Agency*

International Zeolite Association (IZA), 2012, <http://izasc.ethz.ch/fmi/xsl/IZA-SC/ft.xsl>, *Zeolite framework types* Last cited 23/07/2013

Janovic, O. B. (1978). “Dehydroxylation of kaolinite template under atmospheric pressure”. *Hem. Ind.* 32, N8, 512-516.*Journal of porous materials*, 16(3).

Jen Twu and P.K. Dutta, “Spectroscopic studies of the synthesis of faujasite zeolite: comparison of two silica sources Zeolites”, 1991. 11: p. 672-679.

Jiri, C., V.B. Herman, C. Avelino, and S. Ferdi (2007), *Introduction to zeolite science and practice* 3rd revised edition ed. 2007, Amsterdam Elsevier 1058.

Klinowski, J. and R. Joao,(1990) *29Si and 27Al Magic-angle-spinning NMR studies of the thermal transformation of kaolinite* *Physics and chemistry of minerals*. 17: p. 179-186.

Kovo, (2010) “Development of zeolites and zeolite membranes from Ahoko Nigerian Kaolin”, *Ph.D Thesis*, University of .Manchester, UK

Kozik, T. and Yatsunova, S. (1992). The temperature dependence of the electric conductivity of unfired porcelaini mixture. *Ceramics-silikaty*, 36, N2, 69-72.

Kullprathpanja, S. *Zeolites in industrial separation and catalysts*, (2010), Weinheim Wiley, VCH. 619.

Lee, S.R., Han, Y.S. and Choy, J.H., (2002). “2D_Y3D transformation of layered aluminosilicate upon base treatment solid state ionics” 151, 343-346.

Lee W. k. and Deventer, J. S. j.(2003). “The use of infrared spectroscopy to study geopolymerization of heterogeneous amorphous aluminosilicates Langmuir “19 (21): 8726-87734.

Lei, S., J. i. Miyamoto, T. Ohba, H. Kanoh, and K. Kaneko (2007), “Novel nanostructures of porous carbon synthesized with zeolite LTA-template and methanol”, *The Journal of physical chemistry C*,. 111(6): p. 2459-2464

Lee, H. and P. K. Dutta, (2002), “Charge Transport through a Novel Zeolite Y Membrane by a self-Exchange Process”. *The Journal of Physical Chemistry B*, 106(46): p. 11898- 11904

Levenspiel, O. (1972), *Chemical Reaction Engineering*, 257, John Wiley & Sons,

Ling, C. P.; Dutta, J. A. (2009), *Catalysis and zeolites; fundamentals and applications*, Weinheim, Wiley, Vut, 564.

Levenspiel, O. (1999). *Chemical Reaction Engineering*, Third Edition. John Wiley and Sons. New York. pp. 472-478

Liu, Y., T. J., and Pinnavaia, (2004) “Metakaolin as a reagent for the assembly of mesoporous aluminosilicates with hexagonal, cubic and wormhole framework structures from proto-faujasite nanoclusters”. *Journal of Material chemistry*, 2004. 14: p. 3416-3420.

Ling, H., Q. Wang, and B. Shen, (2009)., “Hydroisomerization and hydrocracking of hydrocracker bottom for producing lube base oil”. *Fuel producing technology*.. 90(4): p. 530-534

Lori, J.A., A.O. Lawal, and E.J. Ekanem, (2007) “Characterization and optimization of deferration of Kankara clay” *ARPJ Journal of Engineering and Applied Science*. 2(5): p. 60-73

Madani, A., Aznar, A.. Sanz, J and. Serratos J.M ,(1990),” 29Si and 27Al NMR study of zeolite formation from alkali-leached kaolinites. Influence of thermal preactivation ”. *Journal of physical chemistry*.,. 94: p. 760-765.

Mackenzie, R.C ed. IV (1978). “The smectite group, a dioctahedral smectites. In: differential thermal analysis”., academic press, London ,442-452 and 504-527.

Marcel D., (1979).

Mintova, S., Olson, N.H., Senker, J., Bein, T. (2002). “Mechanism of the transformation of silica precursor solutions into Si-MFL zeolite”. *Angewerson chemical international edition*, 41 (14), 2558-2561.

Mumpton, F.A., Sand L.B., 1978. “Natural zeolite: A new industrial mineral commodity Natural zeolites, occurrence, properties and use”, . *Oxford Pergamon*, ed 27.

Murat, M., A. Amokrane, J.P. Bastide, and L. Montanaro,(1992). “Synthesis of zeolites from thermally activated kaolinite. Some observations on nucleation and growth”. *Clay Minerals*, 27(1): p. 119.

Murray, H. H. (1951). “The structure of kaolinite and its relation to acid treatment” *Ph. D thesis*, University of Illinois, Urbana IIIonois.

Nigeria National Petroleum Corporation NNPC/KRPC, 2013, Chief Officers Course, Abuja.

Olson, D.H. and Hang, W.O. (1984). Transformation of Hydrocarbon on Zeolite Catalysts. *Am Chem Soc Symp Ser.* **248**, 275

Omoleye J.A., Susu A.A. (1986) “Mortality of mono and bi-metalic reforming catalysts and the existence of stability states’’, *Ph.D thesis*.University of Lagos

Omisanya N.O, Folayan C.O, Aku, S.Y. and Adefila s.s. (2012).“Synthesis and characterization of zeolite A for adsorption refrigeration application” *Advancies in Applied Science Research.* 3 (6):3746-3754

Okamoto, K.-i., H. Kita, K. Horii, K. Tanaka, and M. Kondo,(2001) “Zeolite NaA membrane preparation, single-gas permeation, and pervaporation and vapour permeation of water/organic liquid mixtures”. *Industrial and Engineering Chemistry Research*, 40(1): p. 163-175.

Parnham, E.R. and R.E. Morris (2007), “Ionothermal synthesis of zeolites, metal-organic framework and inorganic-organic hydrid”’s *Acc.Chem.Res*, (40): p. 1005-1013.

Patrylak, L., R. Likhnyovskyi, V. Vypyraylenko, R. Leboda, J. Skubiszewska-Zieba, and K. Patrylak, (2001), *Adsorption properties of zeolite-containing microspheres and FCC catalysts based on Ukrainian Kaolin.* *Adsorption Science and Technology*, 19(7): p. 525-540

Pickett, J, (2010) “Sustainable biofuels: Prospects and challenges, in policy document” 01/10. *The Royal Society*, pp. 3-91

Plank, C.J., and Rosinki, E.J (1964)., *US. Patent* 3, 140,253

Pradhan, N., Das, B., Gahan, C.S., Kar, R.N., Sukla, L.B (2006). “Beneficiation of iron ore slime using *Aspergillus niger* and *Bacillus circulans*”. *Bioresources Technology* 97, 1876-1879.

Ramírez, O.H.,(2007) *Second Year Ph.D Report.* The University of Manchester, Manchester, UK.

Ramirez, O.H.,(2009) *Hierarchical Bio-structures incorporating zeolite Y for wastewater treatment application,* PhD thesis, The University of Manchester,; Manchester, . p.229.

Renzo, F.D. and F. Fajula,(2005) “Introduction to molecular sieves: Trend of evolution of the zeolite community Zeolite and ordered mesoporous materials” *Progress and prospects*, ed. J. Cejka and H.V. Bekkum. 2005, Amsterdam Elsevier 1-12.

RMRDC (2004), “Raw material and consumer industries in Nigeria”.www.rmrdc.com

Ruthven, D.M., (1984), *Principles of Adsorption and Adsorption Processes*, p.154-167, John Wiley & Sons,

Sepoulveda, M.J.; Vallyathan v.; Attfield M.D.; Piacitelli L.; Tucker J .H. (1983) “Pneumoconiosis and lung function in a group of kaolin workers”. *Am Rev Respir Dis*, 127:231-235

Schweiker, G.C., (1978) “Sodium silicates and sodium aluminosilicates” *J. Am. Oil Chemist Soc.* 55: p. 36-40

Shan, W., Yu, T., Wang, B., Hu, J., Zhang, Y., Wang, X and Tang, Y. (2006) “Magnetically separable nanozeolites: Promising candidates for bio-Applications”. *Chemistry of materials*, 18(14): p. 3169-3172

Shannon, K.H. Gardner, R.H. Staley, G. Bergeret, P. Gallezot, A.Auroux, J., (1985) “Ion exchange Ultrastable Y zeolite :3Gas oil cracking over rare earth. Exchanged Ultrastable“. *Phys. Chem.* 89, 4778-4788.

Shell International Petroleum Company Limited, 1998.*The Petroleum Handbook*, 5th ed.

Shoumkov, S., Dimitrov, Z., Brakalov, L.,(1987). “High gradient magnetic treatment of kaolin”. *Interceram* 6, 26-28.*practice* 3rd revised edition ed. Amsterdam Elsevier 1058.

Suitch, P. R (1986).Mechanism for the dehydroxylation of kaolinite, dickite,and nacrite from room temperature to 455°C. *Journal of American Ceramic Society* 69, 61-65

Szostak, R., *Handbook of Molecular Sieves*. 1992, New York Van Nostrand Reinhold 584

Takhtamysheva, A.V. and L.D. Konoval'chikov (1990), “Synthesis of NaY of high phase purity from kaolin” *All Union Scientific-Research for Petroleum Processing* (8): p. 10-11.

Teo, B. K., Li, C. P. Sun, H.X. Wong, N.B. and Lee, S. T.(2003) “Silicon- Silica nanowires, nanotubes, and biaxial nanowires: Inside, Outside and side- by-side growth of silicon versus silica on zeolite”. *Inorganic chemistry*, 2003. 42(21): P.6723-6728.

Thomas, C.L. (1949), *Ind. Eng. Chem.*, 47, 2564

Toussaint F., Fripiat J.J. & Gastuche M.C. (1963). “Dehydroxylation of kaolinite Kinetics”. *Journal of Physical Chemistry* ,67, 26-30.

Tracy, M.M.J. and J.B. Higgins,(2001) “Collection of simulated XRD powder patterns of Zeolites” Fourth revised edition ed. 2001, Amsterdam Elsevier 379

Varga, G (2007). “The structure of kaolinite and metakaolinite”, *Epitoanyag* 59. *evf. I, szam.*

Accessed on http://www.szte.mtesz.hu/06_journal/2007_-1/pdf/epa-1-2.pdf.

Van der Puil, N., Dautzenberg, F.M., van Bekkum, H and Jansen, J.C. (1958) “Preparation and catalytic testing of zeolite coatings on preshaped alumina supports” *The Royal Society*, p 23-36

Veglio, F and Toro, L. (1994). Process development of kaolin bleaching using carbohydrates in acid media. *International Journal on Mineral Process* 41, 239-255.

Venuto P.B., and Habib, E.T., Jr. (2007). “Fluid Catalytic Cracking with Zeolite Catalysts”, *Journal of zeolite conference*, 30-31.

Weitkamp, J. and Puppe, L. (1999), “Catalysis and zeolites: fundamentals and applications”, *Berlin Springer* 564.

Wojciechowski, B.W; Best, D.A (1977,). *Catal*, 47, 11

Worrall, W.E. (1986). “Clays and ceramic raw materials”, *Elsevier Applied Science Publishers*, 2nd Edition. New York.

www.port.ac.uk.../reseach/zeolitemodlling/, (2008) *Molecular modelling of zeolites*, last cited on 15/06/13

Xu, R., W. Pang, J. Yu, and Q. Huo., Chen, (2007) “Chemistry of Zeolites and Related Porous Materials: Synthesis and Structure”, *Clementi loop Singapore John Wiley* 679.

Xu, R.,W.Pang, J.Yu, Q.Huo,and J. Chen (1971),”Some perspective on zeolite catalysis”’: *Advances in Chemistry series* 102 pp 260-281

Yaping, Y. Z. X, Weilan, Quian, Mingwen, Wang (2008), “synthesis of pure zeolite from Supersaturated silicon and aluminium alkali extract from fuel coal fly ash”

Young Chang Kim, J.Y. Jeong, J.Y. Hwang, S.D. Kim, and W.J. Kim (2008), “Influencing factors on rapid crystallization of high silica nano-sized zeolite Y without organic” *Zivanovic*,

Zhang, X.F, Wang, J.Q. Liu, H.O. and Liu, C. H. (2001)“Synthesis and factors affecting the synthesis of ZSM-5 zeolite membrane”. *Shiyou Xuebao, Shiyou Jiagong/Acta petroei Sinica (Petroleum Processing Section)*,.17 (3): P.9-15

APPENDIX A

A₁ Dealumination Calculation

asis 50g : Metakaolin

For Alumina

36.9wt% Al₂O₃ in 50g Metakaolin

$$\frac{36.9 \times 50}{100} = 18.45\text{g}$$

Molecular mass of Al₂O₃ = 102g

Therefore no of moles of Al₂O₃ in 50g Elefun Metakaolin is :

$$\frac{18.45\text{g}}{102\text{g/mol}} = 0.1809 \text{ mol}$$

For Silica

51.5wt% of SiO₂ in 50g Elefun metakaolin

$$\frac{51.5 \times 50}{100} = 25.75\text{g of silica in 50g metakaolin}$$

Molecular mass of SiO₂ = 60g/mole

Number of moles of silica in 50g metakaolin is :

$$\frac{25.75\text{g}}{60\text{g/mole}} = 0.4292\text{moles}$$

Since the silica/alumina ratio requirement for Zeolite Y is between 3 to 10, then

We assumed it be '5'

$$\text{As thus: } \frac{\text{SiO}_2}{\text{Al}_2\text{O}_3} = 5 \quad (\text{A1})$$

$$5 \text{ Al}_2\text{O}_3 = \text{SiO}_2 \text{ i.e}$$

$$\text{Al}_2\text{O}_3 = \text{SiO}_2 / 5$$

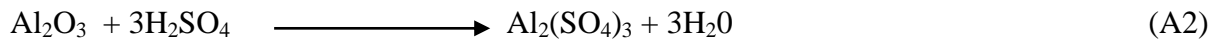
$$= 0.4292 / 5 = 0.0858\text{moles}$$

Weight of Al₂O₃ left after dealumination is expected to be :

$$0.0858 \text{ moles} \times 102 \text{ g/mole} = 8.751 \text{ g}$$

$$\text{Thus leaching out } 18.45 \text{ g} - 8.716 = 9.6984 \text{ g}$$

Equation of reaction for dealumination is



To determine the quantity of H₂SO₄ require for this leaching:

with 96% purity thus:

From the equation of reaction (stoichiometry), 102g aluminum oxide will require

102g of Al₂O₃ = requires 294g of H₂SO₄ with 100% purity while with 96% purity yields

$$\left(\frac{3 \times 98 \times 100}{96}\right) \text{ of } 96\% \text{ H}_2\text{SO}_4 = 306.25 \text{ g}$$

Therefore to leach out 9.698g Al₂O₃ from 50 g of Elefun metakaolin will require

$$\frac{306.25 \times 9.6984}{102} = 29.189 \text{ g } 96\% \text{ H}_2\text{SO}_4$$

To avoid complete dealumination of the metakaolin the required acid strength is 60% ,

therefore the need to convert to 60% H₂SO₄

$$\text{i.e. } \frac{29.189 \times 96}{60} = 46.702 \text{ g}$$

To convert the mass of acid to volume, Theoretical values of density for H₂SO₄ :

$$\text{Density of } 60\% \text{ H}_2\text{SO}_4 \text{ at } 25^\circ\text{C} = 1.494/\text{cm}^3$$

$$\text{Density of } 96\% \text{ H}_2\text{SO}_4 \text{ at } 25^\circ\text{C} = 1.8305/\text{cm}^3$$

But, density = mass/volume

Volume = mass/density

$$\text{Therefore, volume of } 96\% \text{ H}_2\text{SO}_4 = 46.702/1.8305$$

$$= 25.513 \text{ cm}^3 \text{ of } 96\% \text{ H}_2\text{SO}_4$$

Conversion from 96% to 60% to the component balance:

$$V_{60} \times \rho_{60} \times 60 = V_{96} \times \rho_{96} \times 96 \quad (A3)$$

$$\text{Therefore, } V_{60} = 25.513 \times 1.8305 \times 96 / 1.494 \times 60 = 49.895 \text{ cm}^3$$

To avoid slurry formation which may reduce efficient heat and mass transfer during dealumination, the volume of acid calculated above is multiplied by factor of 3.

$$V_{60} = 3 \times 49.895 \text{ cm}^3 \text{ of } 60\% \text{ H}_2\text{SO}_4 = 149.6864 \text{ cm}^3$$

$$\text{The volume of } 96\% \text{ H}_2\text{SO}_4 \text{ required is } V_{60} = 149.6864 \times 1.494 \times 60 / 1.8305 \times 96 = 76.3560 \text{ cm}^3$$

A₂ Dilution Calculation

From dilution formular

$$V_{60} \times \rho_{60} = V_{96} \times \rho_{96} + V_w \times \rho_w$$

Where

V_w = volume of water

ρ_w = density of water = 1 g/cm^3

$$V_w = \frac{V_{60} \times \rho_{60} - V_{96} \times \rho_{96}}{\rho_w}$$

$$V_w = \frac{(149.6864 \times 1.494) - (76.3560 \times 1.8305)}{1} = 83.86 \text{ cm}^3$$

Summary

To dealuminate 50g of Elefun Metakaolin , we used the followings:

149.6864 cm³ of 60% H₂SO₄

83.86 cm³ of deionized water

A₃ Gelation Calculation for DMK

Basis : 50g

Molar mass of SiO₂ - 60g/mol

Molar mass of Al₂O₃ - 102g/mol

Molar mass of Na₂O - 62g/mol

Molar mass of SO₃ - 80g/mol

Molar mass of K₂O = 94g/mol

Number of moles of SiO ₂	=	51.1/60	=	0.8517
Number of moles of Al ₂ O ₂	=	18.5/102	=	0.1814
Number of moles of SO ₃	=	5.1/80	=	0.0638
Number of moles of Na ₂ O	=	0/62	=	0
Number of moles of K ₂ O	=	0.522/94	=	0.0056
Silica Alumina ratio	=	0.8517	=	4.695
		0.1814		

Mass of dealuminated metakaolin

$$(60 \times 4.695) + 102 + 80 + 94 = 557.7\text{g/mol}$$

Moles of dealuminated Kaolin in 50g of sample

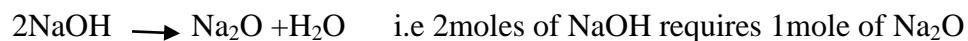
$$50/557.7 = 0.08965\text{moles}$$

$$\text{Mole of Silica in 50g of Sample} = 0.08966 \times 4.695 = 0.4210 \text{ moles}$$

$$\text{For Na}_2\text{O/SiO}_2 = 0.6$$

$$\text{Na}_2\text{O} = 0.6 \times \text{SiO}_2 = 0.6 \times 0.4210 = 0.2526$$

Considering the reaction



Therefore 0.2526 moles of Na₂O gives 2 x (0.2526) moles of NaOH which is equal to 0.5052 moles of NaOH

Also molar mass of NaOH = 40g/mol

$$\text{Therefore mass of NaOH needed} = 40 \times 0.5052 = 20.2080\text{g}$$

Na

$$\text{NaK}_2\text{O} = 0.9$$

$$\text{K}_2\text{O} = 0.522$$

$$= 0.522/94 = 0.0056$$

$$\frac{\text{Na}}{\text{Na} + \text{K}} = 0.9$$

$$\frac{\text{Na}}{\text{Na} + 0.0056} = 0.9$$

$$0.9 (\text{Na} + 0.0056) = \text{Na}$$

$$0.9 \text{Na} + 0.0050 = \text{Na}$$

$$0.0050 = \text{Na} - 0.9\text{Na}$$

$$0.0050 = 0.1\text{Na}$$

$$\text{Na} = 0.0050/0.1 = 0.05$$

$$\frac{\text{Na}}{\text{SO}} = 1$$

$$\text{SO}_3 = \frac{5.1}{80} = 0.0638$$

$$\frac{\text{Na}}{0.0638} = 1$$

$$\text{Na} = 0.0638 \times 1 = 0.0638$$

Total NaOH needed

$$= 20.2080 + 0.0500 + 0.0638$$

$$= \underline{20.3218\text{g}}$$

$$\text{For H}_2\text{O/Na}_2\text{O} = 30$$

$$\text{Moles of water needed} = 30 \times \text{Na}_2\text{O}$$

$$= 30 \times 0.2526 = 7.578$$

Molar mass of water = 18g/mol

Mass of water required = $18 \times 7.578 = 136.404\text{g}$

(Since density = 1g/cm^3)

Volume of H₂O required = 136.404cm^3

For Na₂O/SiO₂ = 0.65

Na₂O = $0.65 \times \text{SiO}_2 = 0.65 \times 0.4210 = 0.2737$

Considering the reaction

$2\text{NaOH} \rightarrow \text{Na}_2\text{O} + \text{H}_2\text{O}$ i.e 2moles of NaOH requires 1mole of Na₂O

Therefore 0.2737 moles of Na₂O gives $2 \times (0.2737)$ moles of NaOH which is equal to 0.5473 moles of NaOH

Also molar mass of NaOH = 40g/mol

Therefore mass of NaOH needed = $40 \times 0.5473 = \underline{21.8982\text{g}}$

For H₂O/Na₂O = 30

Moles of water needed = $30 \times \text{Na}_2\text{O}$
= $30 \times 0.2737 = 8.211$

Molar mass of water = 18g/mol

Mass of water required = $18 \times 8.211 = 147.798\text{g}$

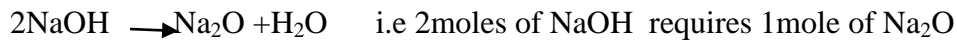
(Since density = 1g/cm^3)

Volume of H₂O required = 147.798cm^3

For Na₂O/SiO₂ = 0.70

Na₂O = $0.70 \times \text{SiO}_2 = 0.70 \times 0.4210 = 0.2947$

Considering the reaction



Therefore 0.2947 moles of Na_2O gives $2 \times (0.2947)$ moles of NaOH which is equal to 0.5894 moles of NaOH

Also molar mass of $\text{NaOH} = 40\text{g/mol}$

$$\text{Therefore mass of NaOH needed} = 40 \times 0.5894 = \underline{23.576\text{g}}$$

$$\text{For H}_2\text{O/Na}_2\text{O} = 30$$

$$\begin{aligned} \text{Moles of water needed} &= 30 \times \text{Na}_2\text{O} \\ &= 30 \times 0.2947 = 8.841 \end{aligned}$$

$$\text{Molar mass of water} = 18\text{g/mol}$$

$$\text{Mass of water required} = 18 \times 8.841 = 159.138\text{g}$$

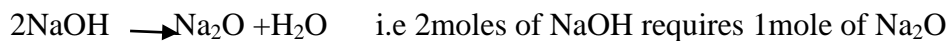
(since density = 1g/cm^3)

$$\begin{aligned} \text{Volume of H}_2\text{O required} &= \\ &\underline{159.138\text{cm}^3} \end{aligned}$$

$$\text{For Na}_2\text{O/SiO}_2 = 0.75$$

$$\text{Na}_2\text{O} = 0.65 \times \text{SiO}_2 = 0.75 \times 0.4210 = 0.3158$$

Considering the reaction



Therefore 0.3158moles of Na_2O gives $2 \times (0.3158)$ moles of NaOH which is equal to 0.6315 moles of NaOH

Also molar mass of $\text{NaOH} = 40\text{g/mol}$

$$\text{Therefore mass of NaOH needed} = 40 \times 0.6315 = \underline{25.26\text{g}}$$

$$\text{For H}_2\text{O/Na}_2\text{O} = 30$$

$$\text{Moles of water needed} = 30 \times \text{Na}_2\text{O}$$

$$= 30 \times 0.3158 = 9.474$$

$$\text{Molar mass of water} = 18\text{g/mol}$$

$$\text{Mass of water required} = 18 \times 8.211 = 170.532\text{g}$$

(since density = 1g/cm^3)

$$\text{Volume of H}_2\text{O required} = \underline{170.532\text{cm}^3}$$

$$\text{For Na}_2\text{O/SiO}_2 = 0.80$$

$$\text{Na}_2\text{O} = 0.65 \times \text{SiO}_2 = 0.80 \times 0.4210 = 0.3368$$

Considering the reaction



Therefore 0.3368 moles of Na_2O gives $2 \times (0.3368)$ moles of NaOH which is equal to 0.6756 moles of NaOH

Also molar mass of $\text{NaOH} = 40\text{g/mol}$

$$\text{Therefore mass of NaOH needed} = 40 \times 0.6756 = \underline{26.944\text{g}}$$

$$\text{For H}_2\text{O/Na}_2\text{O} = 30$$

$$\text{Moles of water needed} = 30 \times \text{Na}_2\text{O}$$

$$= 30 \times 0.3368 = 10.104$$

$$\text{Molar mass of water} = 18\text{g/mol}$$

$$\text{Mass of water required} = 18 \times 10.104 = 181.872\text{g}$$

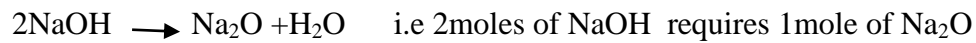
(Since density = 1g/cm^3)

$$\text{Volume of H}_2\text{O required} = \underline{181.872\text{cm}^3}$$

$$\text{For Na}_2\text{O/SiO}_2 = 0.90$$

$$\text{Na}_2\text{O} = 0.65 \times \text{SiO}_2 = 0.90 \times 0.4210 = 0.3789$$

Considering the reaction



Therefore 0.3789 moles of Na_2O gives $2 \times (0.3789)$ moles of NaOH which is equal to 0.7578 moles of NaOH

Also molar mass of $\text{NaOH} = 40\text{g/mol}$

$$\text{Therefore mass of NaOH needed} = 40 \times 0.7578 = \underline{30.312\text{g}}$$

$$\text{For H}_2\text{O/Na}_2\text{O} = 30$$

$$\begin{aligned} \text{Moles of water needed} &= 30 \times \text{Na}_2\text{O} \\ &= 30 \times 0.3789 = 11.367 \end{aligned}$$

$$\text{Molar mass of water} = 18\text{g/mol}$$

$$\text{Mass of water required} = 18 \times 11.367 = 204.606\text{g}$$

(Since density = 1g/cm^3)

$$\text{Volume of H}_2\text{O required} = \underline{204.606\text{cm}^3}$$

APPENDIX B

B₁ Results of Cyclohexane Cracking over Developed Zeolite γ and Commercial Zeolite Y Catalyst under Helium Atmosphere

Table B1: Effect of Flow Rate F (mL/min) on Cyclohexane cracking in Helium Carrier gas on synthesized Zeolite Y Catalyst at 520°C (P = 4.0KPa)

520°C				
F, mL/min	40	60	80	100
C ₃	86.246	83.903	81.370	79.140
C ₃ ⁻	-	-	-	-
iC ₄	4.837	4.284	9.218	11.763
nC ₄	0.273	0.292	0.367	0.340
C ₄	0.339	-	-	0.314
TRANS	-	-	0.354	0.164
CIS	0.208	0.118	0.186	0.120
iC ₅	0.223	0.184	0.219	0.156
nC ₅	7.589	0.043	0.235	0.000
C ⁺⁶	-	10.983	-	-

Table B2: Effect of Flow Rate F (mL/min) on Cyclohexane cracking in Helium Carrier gas on synthesized Zeolite Y Catalyst at 480°C (P = 4.0kg/cm²)

480°C				
C ₃	95.637	95.618	86.397	83.824
C ₃ ⁻	-	-	-	-
iC ₄	3.061	2.967	7.959	11.561
nC ₄	0.299	0.967	0.276	0.264
C ₄	0.243	0.287	0.129	0.123
TRANS	-	-	-	-
CIS	0.122	-	-	-
iC ₅	0.129	-	0.131	0.123
nC ₅	-	0.222	-	0.335

Table B3: Conversion using Zeolite Y matrix (25% HY: 75%Metakaolin) at 520°C

F(mL/min)	40	60	80	100
C ₃	99.645	98.500	98.011	97.268
C ₃ ⁻	-	-	-	-
iC ₄	-	-	-	-
nC ₄	-	-	-	-
C ₄ ⁻	-	-	-	-
TRANS	-	-	-	-
CIS	-	-	-	-
iC ₅	-	-	-	-
nC ₅	0.000	0.000	0.000	0.000
C ₆ ⁺	0.355	1.500	1.989	2.732

Table B4: Conversion using Zeolite Y matrix (25% HY: 75%Metakaolin) at 480°C

C ₃	98.571	97.351	95.803	96.813
C ₃ ⁻	-	-	-	-
iC ₄	-	-	-	-
nC ₄	0.094	1.204	2.889	0.889
C ₄ ⁻	-	0.629	1.226	1.781
TRANS	-	-	-	-
CIS	-	-	-	-
iC ₅	-	-	-	-
nC ₅	0.000	0.000	0.000	0.000

B₂ Cracking of Cyclohexane

Weight of catalyst $w = \text{constant} = 0.15\text{g}$

Length of packing = 0.05m

Vol of cyclohexane injected = $2\text{mL} = 2 \times 10^{-6}\text{m}^3$

Molecular formula of cyclohexane = C_6H_{12}

Molecular mass of Cyclohexane = 84g

Carrier gas flowrate = $Q = 40, 60, 80, 100\text{mL/s}$

Specific gravity of Cyclohexane = $0.778\text{g/mL} = 778\text{kg/m}^3$

$$\begin{aligned}\text{Mole of Cyclohexane injected} &= 2 \times 10^{-6}\text{m}^3 \\ &= 778 / 84 \text{ kg/m}^3 \\ &= 1.852 \times 10^{-5} \text{mole}\end{aligned}$$

$$\begin{aligned}\text{Volume of pipe} = V = \pi r^2 L &= 3.142 \times 0.006^2 / 4 \times 0.05 / 4 \\ &= 1.413 \times 10^{-6} \text{m}^3\end{aligned}$$

$$\begin{aligned}C_{A0} &= 1.852 \times 10^{-5} \text{kgmole} / 1.413 \times 10^{-6} \text{m}^3 \\ &= 14.286 \text{kgmole} / \text{m}^3\end{aligned}$$

Table: B5 Cracking of cyclohexane on developed zeoliteY at 520°C

F_{AO} (mol/sec)	57.144	85.716	114.288	142.86
X_A	0.9965	0.9850	0.9801	0.9727
$\frac{W}{F_{AO}} \times 10^{-3}$ (mole/sec)	2.625	1.750	1.312	1.050
$\ln \frac{1}{1 - X_A}$	5.675	4.264	3.997	3.709

Table: B6 Cracking of cyclohexane on developed zeoliteY at 480°C

F_{AO} (mol/sec)	57.144	85.716	114.288	142.86
X_A	0.9857	0.9735	0.9580	0.9681
$\frac{W}{F_{AO}} \times 10^{-3}$ (mole/sec)	2.625	1.750	1.312	1.050
$\ln \frac{1}{1 - X_A}$	4.309	3.729	3.309	3.559

Table: B7 Cracking of cyclohexane on developed zeoliteY at 460°C

F_{AO} (mol/sec)	57.144	85.716	114.288	142.86
X_A	0.9931	0.9870	0.9799	0.9790
$\frac{W}{F_{AO}} \times 10^{-3}$ (mole/sec)	2.625	1.750	1.312	1.050
$\ln \frac{1}{1 - X_A}$	5.0108	4.4000	3.9872	3.9461

TableB8: Cracking of cyclohexane on developed zeoliteY at 440°C

$F_{AO}(\text{mol/sec})$	57.144	85.716	114.288	142.86
X_A	0.9985	0.9888	0.9819	0.6362
$\frac{W}{F_{AO}} \times 10^{-3} (\text{mole/sec})$	2.625	1.750	1.312	1.050
$\ln \frac{1}{1 - X_A}$	6.502	4.492	4.012	1.011

Table B9: Cracking of cyclohexane on commercial zeolite Y at 520 °C

$F_{AO}(\text{mol/sec})$	57.144	85.716	114.288	142.86
X_A	0.9996	0.9978	0.9942	0.6363
$\frac{W}{F_{AO}} \times 10^{-3} (\text{mole/sec})$	2.625	1.750	1.312	1.050
$\ln \frac{1}{1 - X_A}$	7.824	6.119	5.150	1.011

Table B10: Cracking of cyclohexane on commercial zeolite Y at 480 °C

$F_{AO}(\text{mol/sec})$	57.144	85.716	114.288	142.86
X_A	0.9721	0.9658	0.9486	0.929
$\frac{W}{F_{AO}} \times 10^{-3} (\text{mole/sec})$	3.170	1.208	0.876	0.701
$\ln \frac{1}{1 - X_A}$	3.579	3.376	2.968	2.645

Table B11: Cracking of cyclohexane on comercial zeolite Y at 460 °C

$F_{AO}(\text{mol/sec})$	57.144	85.716	114.288	142.86
X_A	0.9612	0.9420	0.9244	0.7410
$\frac{W}{F_{AO}} \times 10^{-3} (\text{mole/sec})$	2.625	1.750	1.312	1.050
$\ln \frac{1}{1 - X_A}$	3.249	2.847	2.582	1.351

Table B12 : Cracking of cyclohexane on comercial zeolite Y at 440 °C

$F_{AO}(\text{mol/sec})$	57.144	85.716	114.288	142.86
X_A	0.9834	0.8614	0.7710	0.6320
$\frac{W}{F_{AO}} \times 10^{-3} (\text{mole/sec})$	2.625	1.750	1.312	1.050
$\ln \frac{1}{1 - X_A}$	4.098	1.976	1.474	0.999

Table B13: Data for Arrhenius plot of cracking cyclohexane over developed zeolite Y

K	2.024	1.413	1.174	1.977
T °C	520	480	460	440
lnK	0.705	0.346	0.160	0.682
1/T °C	1.923	2.083	2.174	2.273

B₃ Cracking of Gas Oil

Weight of catalyst $w = \text{constant} = 0.15\text{g}$

Length of packing = 0.05m

Volume Gas Oil injected = 2mL = $2 \times 10^{-6}\text{m}^3$

Molecular mass of Gas Oil = 285g

Carrier gas flowrate = $Q = 40, 60, 80, 100\text{mL/s}$

i.e $Q_1 = 40 \times 10^{-6} = 4 \times 10^{-5} = \text{m}^3/\text{s}$

$$Q_2 = 60 \times 10^{-6} = 6 \times 10^{-5} = \text{m}^3/\text{s}$$

$$Q_3 = 80 \times 10^{-6} = 8 \times 10^{-5} = \text{m}^3/\text{s}$$

$$Q_4 = 100 \times 10^{-6} = 10 \times 10^{-5} = \text{m}^3/\text{s}$$

Specific gravity of gas Oil = $0.869\text{kg}/\text{m}^3$

Density of gas oil = $869\text{kg}/\text{m}^3$

$$\begin{aligned} \text{Moles of vacuum gas oil} &= 2 \times 10^{-6}\text{m}^3 \times 869 / 285 \text{ kg/kgmole} \\ &= 6.0982 \times 10^{-6} \text{mole} \end{aligned}$$

$$\begin{aligned} \text{Volume of reactor} = V = \pi r^2 L &= 3.142 \times 0.006^2 / 4 \times 0.05 \\ &= 1.413 \times 10^{-6} \text{m}^3 \end{aligned}$$

$$C_{AO} = 6.0982 \times 10^{-6} \text{kgmole} / 1.413 \times 10^{-6} \text{m}^3$$

$$= 4.316 \text{ kgmole} / \text{m}^3$$

Table B14: Results of Cracking vacuum gas oil on developed zeolite HY at 520°C

$F_{AO} \times 10^{-4}(\text{mol/sec})$	1.726	2.530	3.453	4.316
X_A	0.996	0.984	0.605	0.851
$\frac{W}{F_{AO}} \times 10^{-23}(\text{mole/sec})$	8.691	5.929	4.344	3.475
$\ln \frac{1}{1 - X_A}$	5.521	4.135	0.929	1.903

Table B15: Results of cracking vacuum gas oil on developed zeolite HY at 480°C

$F_{AO}(\text{mol/sec})$	1.726	2.530	3.453	4.316
X_A	0.997	0.985	0.980	0.973
$\frac{W}{F_{AO}} \times 10^{-23}(\text{mole/sec})$	8.691	5.929	4.344	3.475
$\ln \frac{1}{1 - X_A}$	5.509	4.200	3.912	3.612

Table B16: Results of cracking vacuum gas oil on developed Zeolite HY at 460°C

$F_{AO}(\text{mol/sec})$	1.726	2.530	3.453	4.316
X_A	0.986	0.974	0.9580	0.968
$\frac{W}{F_{AO}} \times 10^{-23}(\text{mole/sec})$	8.691	5.929	4.344	3.475
$\ln \frac{1}{1 - X_A}$	4.269	3.650	3.170	3.440

Table B17: Results of cracking vacuum gas oil on developed zeolite HY at 440°C

$F_{AO}(\text{mol/sec})$	1.726	2.530	3.453	4.316
X_A	0.993	0.987	0.979	0.978
$\frac{W}{F_{AO X_A}} \times 10^{-23}(\text{mole/sec})$	8.691	5.929	4.344	3.475
$\ln \frac{1}{1 - X_A}$	4.962	4.343	3.863	3.817

Table B18: Arrhenius plot for cracking gas oil over developed zeolite Y

k	0.689	0.364	0.160	0.219
T	520	480	460	440
lnK	-0.373	-1.011	-1.833	-1.519
1/T	1.923	2.083	2.174	2.273

$$\text{Slope} = \frac{-E}{R} = -0.171$$

$$E = R \times 0.171$$

$$E = 8.314 \times 0.171 = 1.422 \text{ kcal/mole}$$

Table B19: Results of cracking vacuum gas oil over commercial zeolite Y at 520 °C

$F_{AO}(\text{mol/sec})$	1.726	2.530	3.453	4.316
X_A	0.998	0.989	0.982	0.639
$\frac{W}{F_{AO}} \times 10^{-33}(\text{mole/sec})$	8.691	5.929	4.344	3.475
$\ln \frac{1}{1 - X_A}$	6.215	4.510	4.017	1.019

Table B20: Results of cracking vacuum gas oil over commercial zeolite Y at 480 °C

$F_{AO}(\text{mol/sec})$	1.726	2.530	3.453	4.316
X_A	0.863	0.839	0.814	0.791
$\frac{W}{F_{AO}} \times 10^{-33} (\text{mole/sec})$	8.691	5.929	4.344	3.475
$\ln \frac{1}{1 - X_A}$	1.988	1.826	1.682	1.565

TableB21: Results of Cracking gas oil over commercial zeolite Y at 460 °C

$F_{AO}(\text{mol/sec})$	1.726	2.530	3.453	4.316
X_A	0.956	0.956	0.864	0.838
$\frac{W}{F_{AO}} \times 10^{-33} (\text{mole/sec})$	8.691	5.929	4.344	3.475
$\ln \frac{1}{1 - X_A}$	3.124	3.124	1.995	1.820

TableB22: Results of cracking vacuum gas oil over commercial zeolite Y at 440 °C

$F_{AO}(\text{mol/sec})$	1.726	2.530	3.453	4.316
X_A	0.936	0.921	0.842	0.643
$\frac{W}{F_{AO}} \times 10^{-33} (\text{mole/sec})$	8.691	5.929	4.344	3.475
$\ln \frac{1}{1 - X_A}$	2.749	2.538	1.845	1.030

TableB23: Arrhenius plot for cracking gas oil over commercial zeolite Y

k	0.518	0.078	0.253	0.592
T °C	520	480	460	440
lnK	-0.658	-2.551	-1.374	-0.524
1/T °C	1.923	2.083	2.174	2.273

TableB24: Results of adsorption coefficients for developed zeolite Y on cyclohexane

K_A	2.978	5.115	2.185	-7.610
T °C	520	480	460	440
ln K_A	1.091	1.632	0.782	
1/T °C	1.923	2.083	2.174	2.273

TableB25: Results of adsorption coefficients for commercial zeolite Y on cyclohexane

K_A	5.115	2.378	0.420	-2.169
T °C	520	480	460	440
ln K_A	1.632	0.866	-0.868	
1/T °C	1.923	2.083	2.174	2.273

TableB26: Results of adsorption coefficients for developed zeolite Y on gas oil

K_A	-0.211	0.850	0.451	0.668
T °C	520	480	460	440
$\ln K_A$		-0.163	-0.796	-0.403
1/T °C	1.923	2.083	2.174	2.273

TableB27: Results of adsorption coefficients for commercial zeolite Y on gas oil


K_A	0.848	0.103	0.233	-0.540
T °C	520	480	460	440
$\ln K_A$	-0.165	-2.273	-1.457	
1/T °C	1.923	2.083	2.174	2.273

Table B28: Effect of zeolite HY% in zeolite Y matrix on cyclohexane cracking at various temperatures (P=4.0 atm)

520 ⁰ C					
Zeolite HY (Wt%)	0%	25%	50%	75%	100%
Propane	0.24	0.32	0.48	0.94	1.00
480 ⁰ C					
Propane	0.24	0.20	0.34	0.89	0.95
460 ⁰ C					
Propane	0.21	0.17	0.31	0.73	0.93
440 ⁰ C					
Propane	0.18	0.13	0.17	0.65	0.78

APPENDIX C

Table C1: BET Isotherm data for zeolite NaY

Quantachrome NovaWin - Data Acquisition and Reduction for NOVA instruments ©1994-2013, Quantachrome Instruments version 11.03					
Analysis		Report			
Operator:	quantachrome	Date:	2014/03/29	Operator:	quantachrome
Sample ID:	1	Filename:	Zeolite NaY.qps	Date:	2014/03/30
Sample Desc:		Comment:			
Sample weight:	0.28 g	Sample Volume:	1 cc		
Outgas Time:	0.0 hrs	OutgasTemp:	0.0 C		
Analysis gas:	Nitrogen	Bath Temp:	273.0 K		
Press. Tolerance:	0.100/0.100 (ads/des)	Equil time:	60/60 sec (ads/des)	Equil timeout:	240/240 sec (ads/des)
Analysis Time:	36.9 min	End of run:	2014/03/29 7:27:12	Instrument:	Nova Station A
Cell ID:	1				

Isotherm : Linear

Data Reduction Parameters					
Adsorbate	Po override:	760.00 Torr			
	Nitrogen	Temperature	77.350K		
	Molec. Wt.:	28.013	Cross Section:	16.200 Å ²	Liquid Density:

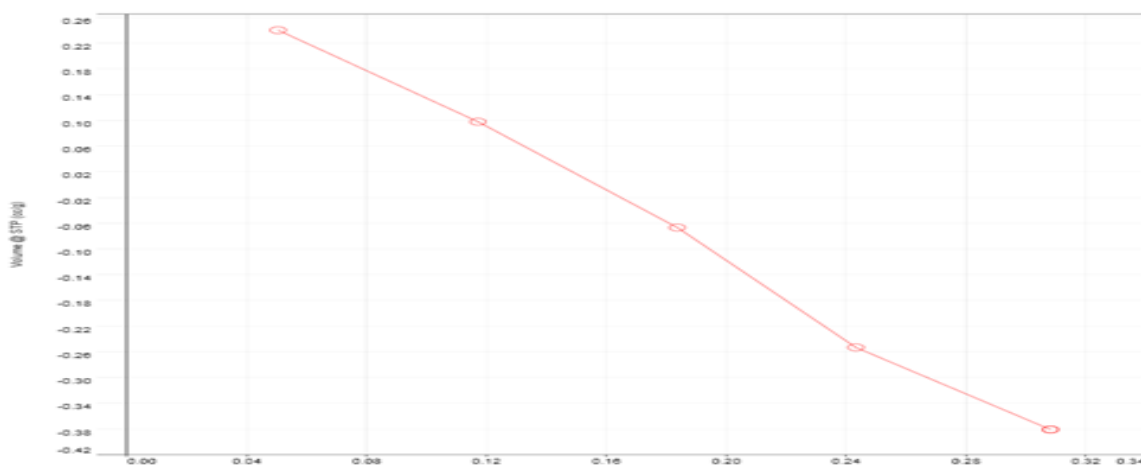



Figure C1: BET Isotherm data plot for zeolite NaY

Table C2: BET multi-point data for zeolite NaY

Quantachrome NovaWin - Data Acquisition and Reduction for NOVA Instruments ©1994-2013, Quantachrome Instruments version 11.03				
				
Analysis		Date: 2014/03/29	Report	Date: 2014/03/30
Operator:	quantachrome	Filename:	Operator:	quantachrome
Sample ID:	1	Comment:	Sample:	Zeolite NaY.qps
Sample Desc:		Sample Volume:	1 cc	
Sample weight:	0.28 g	Outgas Temp:	0.0 C	
Outgas Time:	0.0 hrs	Bath Temp:	273.0 K	
Analysis gas:	Nitrogen	Equil time:	60/60 sec (ads/des)	Equil timeout:
Press. Tolerance:	0.100/0.100 (ads/des)	End of run:	2014/03/29 7:27:12	Instrument:
Analysis Time:	36.9 min			Nova Station A
Cell ID:	1			

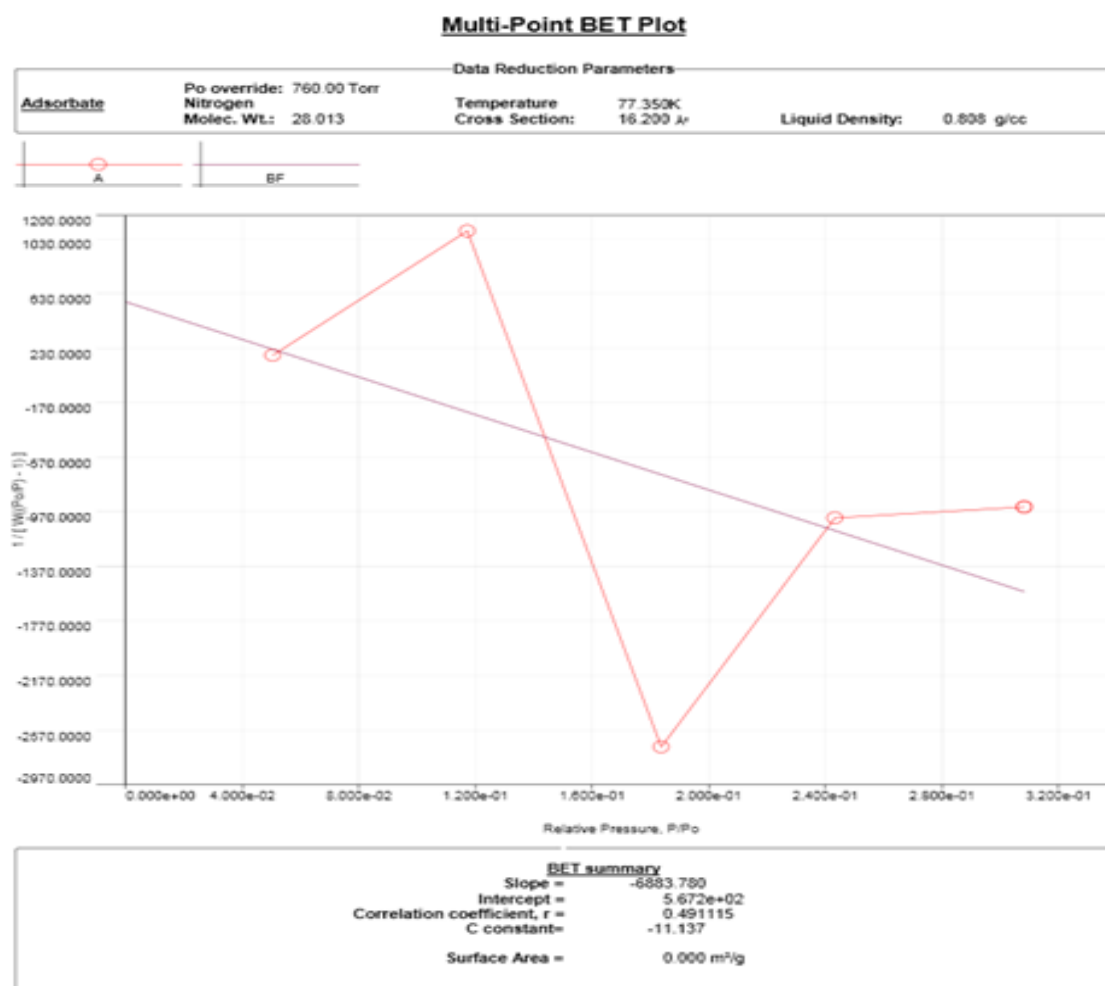


Figure C2: BET multi-point plot for zeolite NaY

Table C3: BET singlepoint surface area data for zeolite NaY

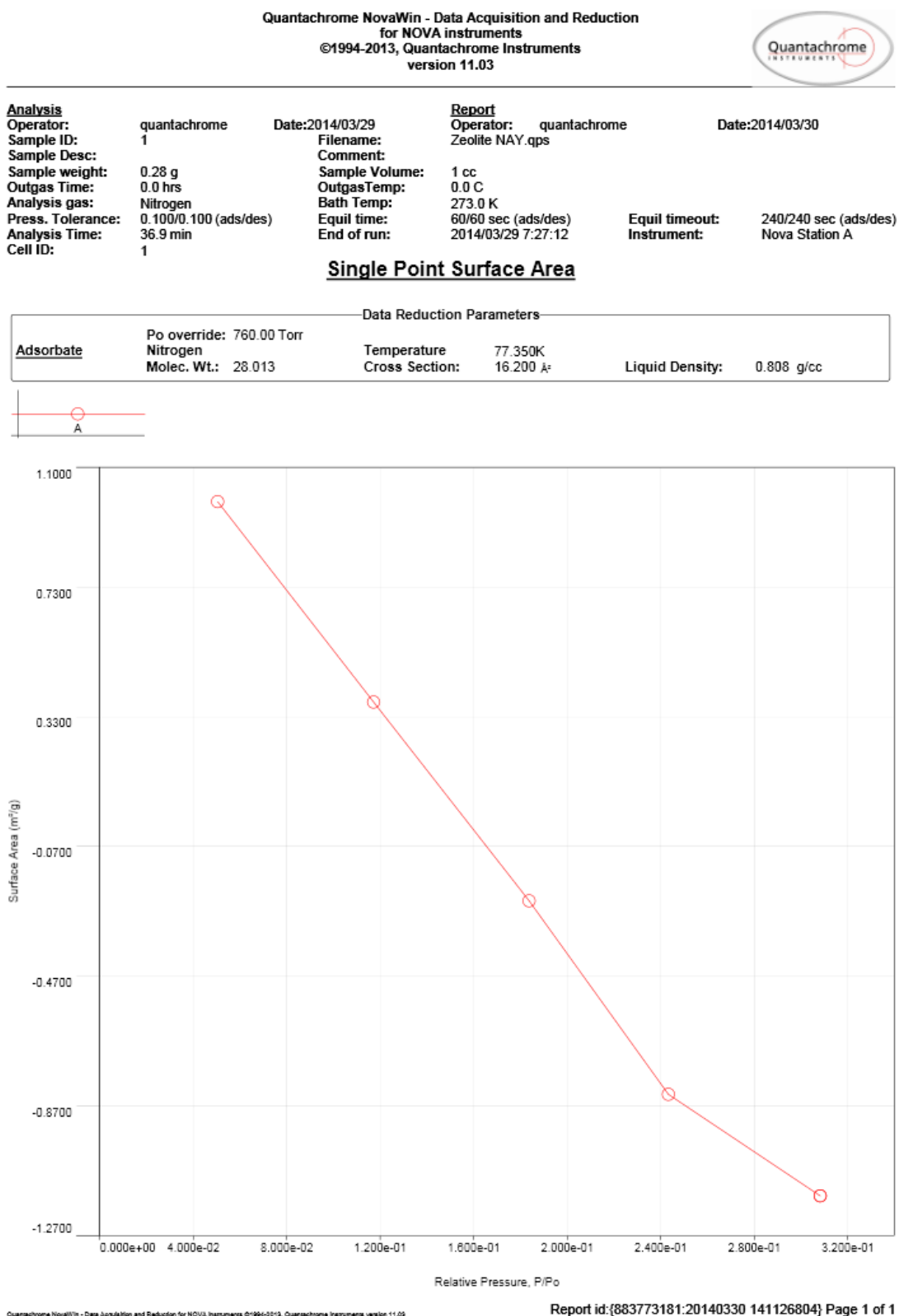


Figure C3: BET Singlepoint Surface area plot for zeolite NaY

Table C4: BET Langmuir data for zeolite NaY

Quantachrome NovaWin - Data Acquisition and Reduction
for NOVA instruments
©1994-2013, Quantachrome Instruments
version 11.03



<u>Analysis</u>		<u>Report</u>	
Operator:	quantachrome	Date:	2014/03/29
Sample ID:	1	Operator:	quantachrome
Sample Desc:		Filename:	Zeolite NAY.qps
Sample weight:	0.28 g	Comment:	
Outgas Time:	0.0 hrs	Sample Volume:	1 cc
Analysis gas:	Nitrogen	OutgasTemp:	0.0 C
Pres. Tolerance:	0.100/0.100 (ads/des)	Bath Temp:	273.0 K
Analysis Time:	36.9 min	Equil time:	60/60 sec (ads/des)
Cell ID:	1	End of run:	2014/03/29 7:27:12
		Equil timeout:	240/240 sec (ads/des)
		Instrument:	Nova Station A

Langmuir

Data Reduction Parameters Data

<u>Adsorbate</u>	Po override: 760.00 Torr	Temperature	77.350K	Liquid Density:	0.808 g/cc
	Nitrogen	Cross Section:	16.200 Å		
	Molec. Wt.: 28.013				

Langmuir Data

P/Po	P/Po/W [(g/g)]	P/Po	P/Po/W [(g/g)]
5.04850e-02	1.6810e-02	2.43283e-01	-7.6840e+02
1.17198e-01	9.6016e-02	3.08251e-01	-6.4704e+02
1.83719e-01	-2.1987e+03		

Langmuir summary

Slope = -5351.79924
Intercept = 469.27407
Correlation coefficient, r = 0.461
Surface Area = 0.000 m²/g

Table C5: BET Isotherm data for zeolite HY

Quantachrome NovaWin - Data Acquisition and Reduction
for NOVA instruments
©1994-2013, Quantachrome Instruments
version 11.03



Analysis		Report	
Operator:	quantachrome	Date:	2014/03/30
Sample ID:	1	Filename:	Zeolite HY.qps
Sample Desc:		Comment:	
Sample weight:	0.17 g	Sample Volume:	1 cc
Outgas Time:	0.0 hrs	OutgasTemp:	0.0 C
Analysis gas:	Nitrogen	Bath Temp:	273.0 K
Press. Tolerance:	0.100/0.100 (ads/des)	Equil time:	60/60 sec (ads/des)
Analysis Time:	33.0 min	End of run:	2014/03/30 19:11:18
Cell ID:	1	Equil timeout:	240/240 sec (ads/des)
		Instrument:	Nova Station A

Isotherm : Linear

Data Reduction Parameters			
Adsorbate	Po override: 760.00 Torr	Temperature	77.350K
	Nitrogen	Cross Section:	16.200 Å ²
	Molec. Wt.: 28.013	Liquid Density:	0.808 g/cc

○
Ads

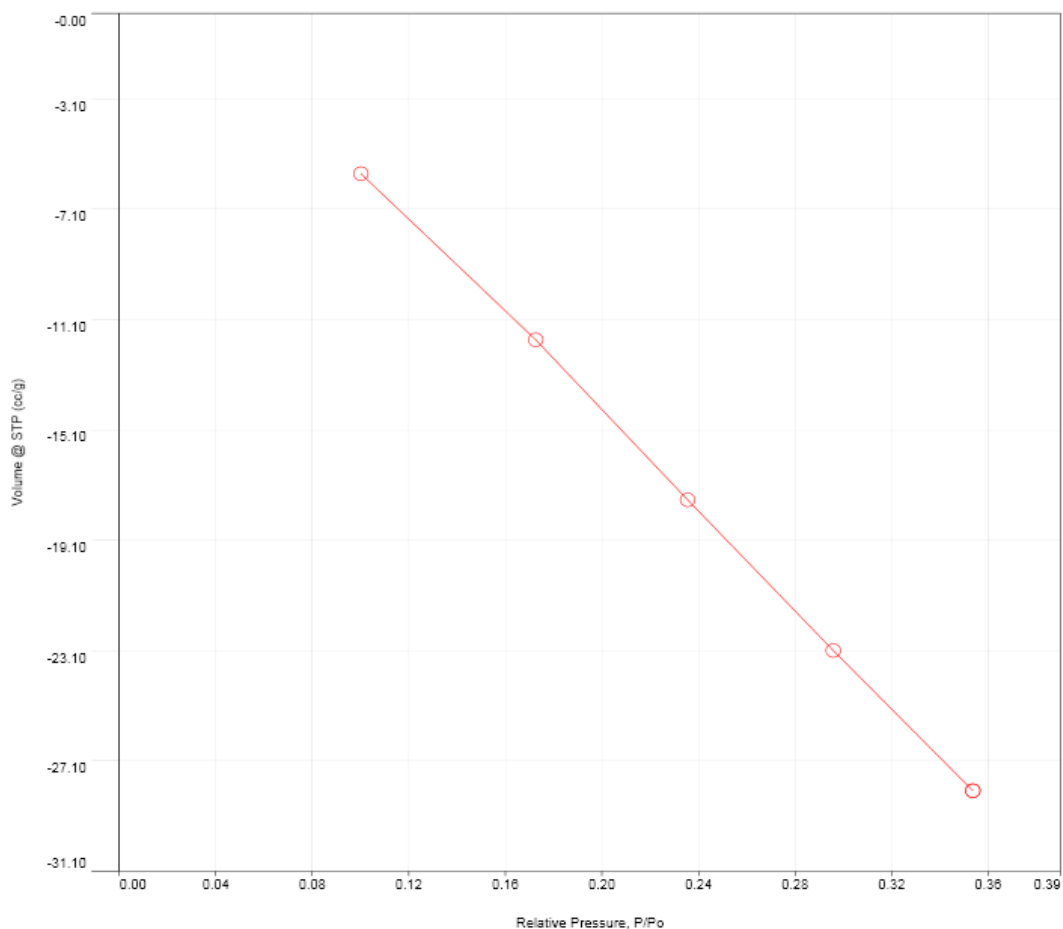


Table C6-a: BET Multi-point data for zeolite HY

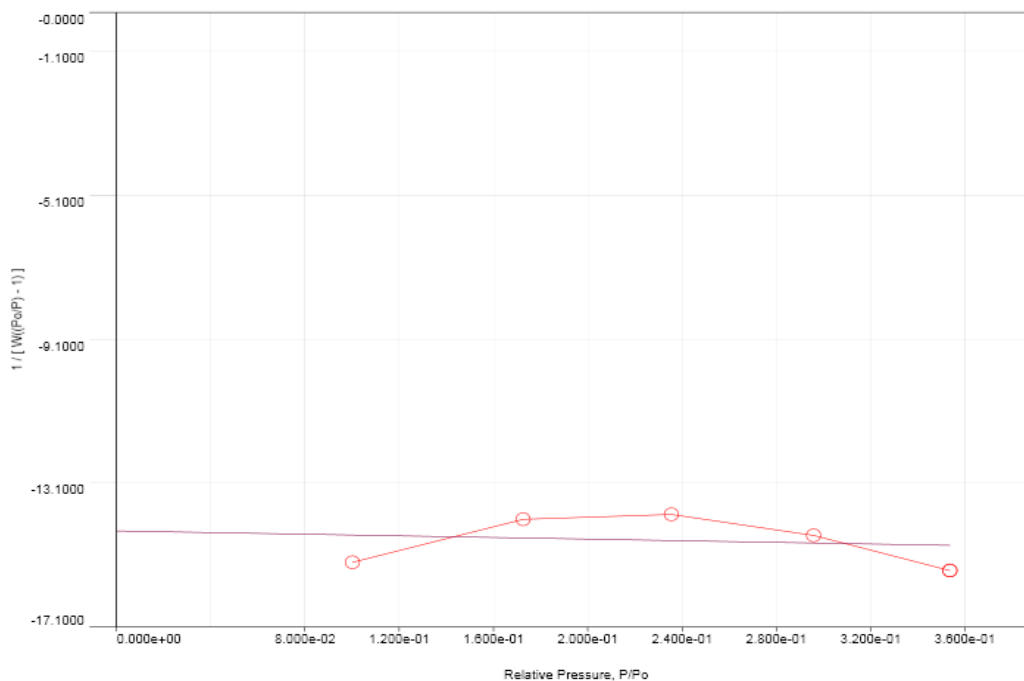
Quantachrome NovaWin - Data Acquisition and Reduction
for NOVA instruments
©1994-2013, Quantachrome Instruments
version 11.03



Analysis	quantachrome	Date:2014/03/30	Report	quantachrome	Date:2014/03/30
Operator:	1	Filename:	Operator:	Zeolite HY.qps	
Sample ID:		Comment:			
Sample Desc:		Sample Volume:	1 cc		
Sample weight:	0.17 g	OutgasTemp:	0.0 C		
Outgas Time:	0.0 hrs	Bath Temp:	273.0 K		
Analysis gas:	Nitrogen	Equil time:	60/60 sec (ads/des)	Equil timeout:	240/240 sec (ads/des)
Press. Tolerance:	0.100/0.100 (ads/des)	End of run:	2014/03/30 19:11:18	Instrument:	Nova Station A
Analysis Time:	33.0 min				
Cell ID:	1				

Multi-Point BET Plot

Data Reduction Parameters			
Adsorbate	Po override: 760.00 Torr	Temperature	77.350K
	Nitrogen	Cross Section:	16.200 Å²
	Molec. Wt.: 28.013	Liquid Density:	0.808 g/cc



BET summary	
Slope =	-1.129
Intercept =	-1.443e+01
Correlation coefficient, r =	0.160656
C constant =	1.078
Surface Area =	0.000 m²/g

Table C6-b: BET singlepoint surface area data for zeolite HY

Quantachrome NovaWin - Data Acquisition and Reduction
for NOVA instruments
©1994-2013, Quantachrome Instruments
version 11.03



Analysis		Report	
Operator:	quantachrome	Date:	2014/03/30
Sample ID:	1	Operator:	quantachrome
Sample Desc:		Filename:	Zeolite HY.qps
Sample weight:	0.17 g	Comment:	
Outgas Time:	0.0 hrs	Sample Volume:	1 cc
Analysis gas:	Nitrogen	Outgas Temp:	0.0 C
Press. Tolerance:	0.100/0.100 (ads/des)	Bath Temp:	273.0 K
Analysis Time:	33.0 min	Equil time:	60/60 sec (ads/des)
Cell ID:	1	End of run:	2014/03/30 19:11:18
		Equil timeout:	240/240 sec (ads/des)
		Instrument:	Nova Station A

Single Point Surface Area

Data Reduction Parameters			
<u>Adsorbate</u>	Po override: 760.00 Torr	Temperature	77.350K
	Nitrogen	Cross Section:	16.200 Å²
	Molec. Wt.: 28.013	Liquid Density:	0.808 g/cc

A

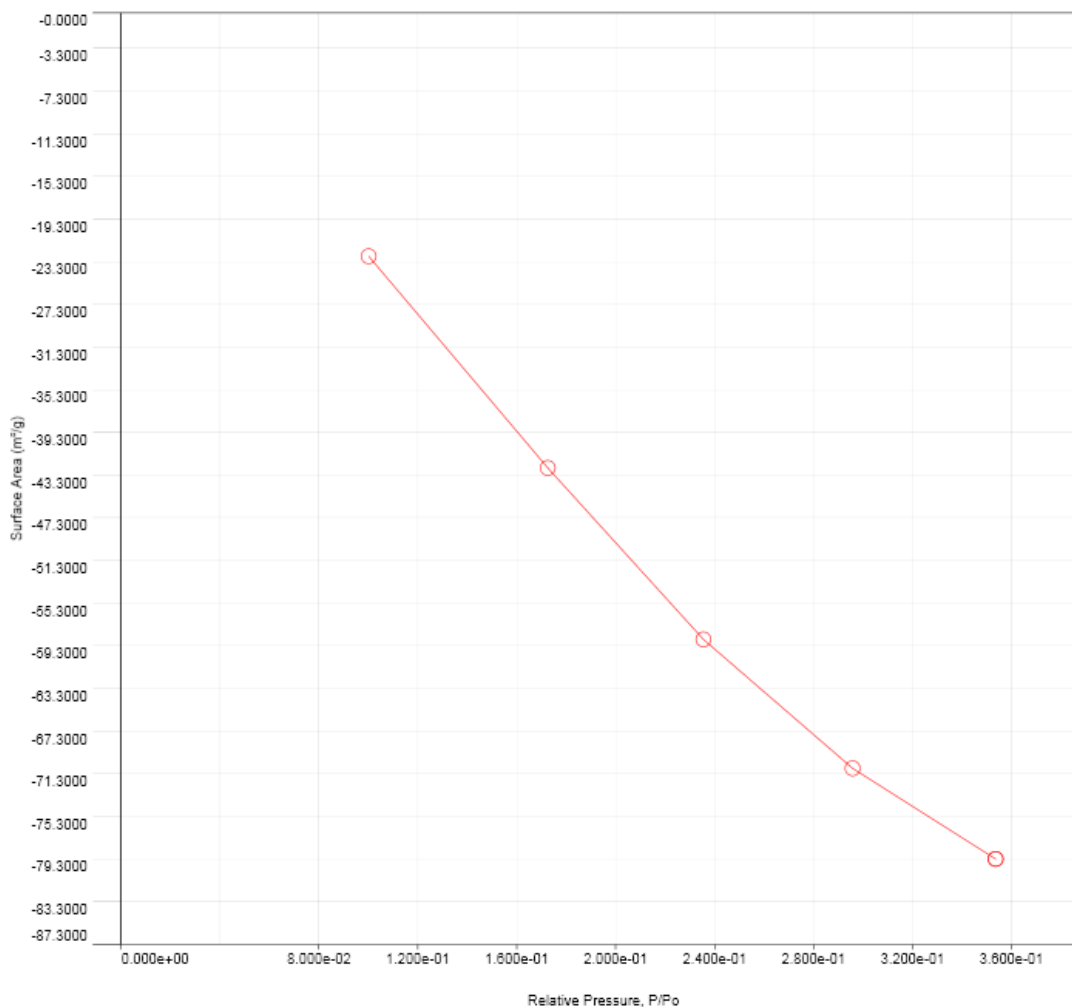


Table C7: BET Langmuir data for zeolite HY

Quantachrome NovaWin - Data Acquisition and Reduction
for NOVA instruments
©1994-2013, Quantachrome Instruments
version 11.03



Analysis		Report	
Operator:	quantachrome	Date:	2014/03/30
Sample ID:	1	Operator:	quantachrome
Sample Desc:		Filename:	Zeolite HY.qps
Sample weight:	0.17 g	Comment:	
Outgas Time:	0.0 hrs	Sample Volume:	1 cc
Analysis gas:	Nitrogen	OutgasTemp:	0.0 C
Press. Tolerance:	0.100/0.100 (ads/des)	Bath Temp:	273.0 K
Analysis Time:	33.0 min	Equil time:	60/60 sec (ads/des)
Cell ID:	1	End of run:	2014/03/30 19:11:18
		Equil timeout:	240/240 sec (ads/des)
		Instrument:	Nova Station A

Langmuir

Data Reduction Parameters Data

Adsorbate	Po override: 760.00 Torr	Temperature	77.350K	Liquid Density:	0.808 g/cc
	Nitrogen	Cross Section:	16.200 Å²		
	Molec. Wt.: 28.013				

Langmuir Data

P/Po	P/Po/W [[g/g]]	P/Po	P/Po/W [[g/g]]
1.00166e-01	-1.3769e+01	2.95883e-01	-1.0245e+01
1.72646e-01	-1.1666e+01	3.53660e-01	-1.0038e+01
2.35550e-01	-1.0679e+01		

Langmuir summary

Slope = 14.33618
Intercept = -14.59940
Correlation coefficient, r = 0.937
Surface Area = 242.918 m²/g

Table C8: BET AreaVolume data for zeolite HY

Quantachrome NovaWin - Data Acquisition and Reduction
for NOVA instruments
©1994-2013, Quantachrome Instruments
version 11.03



Analysis		Report	
Operator:	quantachrome	Date:2014/03/30	Operator: quantachrome
Sample ID:	1	Filename:	Zeolite HY.qps
Sample Desc:		Comment:	
Sample weight:	0.17 g	Sample Volume:	1 cc
Outgas Time:	0.0 hrs	OutgasTemp:	0.0 C
Analysis gas:	Nitrogen	Bath Temp:	273.0 K
Press. Tolerance:	0.100/0.100 (ads/des)	Equil time:	60/60 sec (ads/des)
Analysis Time:	33.0 min	End of run:	2014/03/30 19:11:18
Cell ID:	1	Equil timeout:	240/240 sec (ads/des)
		Instrument:	Nova Station A

Area-Volume Summary

Data Reduction Parameters Data

t-Method DR method HK method SF method Adsorbate Adsorbent	Thermal Transpiration: on	Eff. mol. diameter (D): 3.54 Å	Eff. cell stem diam. (d): 4.0000 mm
	Po override: 760.00 Torr		
	Calc. method: de Boer		
	Affinity coefficient (B): 0.3300		
	Tabulated data interval: 1		
	Temperature	77.350K	
	Molec. Wt.: 28.013	Cross Section: 16.200 Å²	Liquid Density: 0.808 g/cc
	Critical Temp.: 126.200 K	Critical Press.: 33.500 atm	SuperCritic. K.: 1.000
	Carbon		
	DR. Exp (n): 2.000		

Surface Area Data

SinglePoint BET.....	-7.931e+01 m²/g
Langmuir surface area.....	2.429e+02 m²/g
t-method external surface area.....	-2.072e+02 m²/g
t-method micropore surface area.....	2.072e+02 m²/g
DR method micropore area.....	2.049e-06 m²/g

Pore Volume Data

t-method micropore volume.....	6.778e-02 cc/g
DR method micropore volume.....	7.280e-10 cc/g
SF method micropore volume.....	1.808e+00 cc/g

Pore Size Data

DR method micropore Half pore width.....	2.065e-06 Å
HK method pore Radius (Mode).....	1.562e+00 Å
SF method pore Radius (Mode).....	2.261e+00 Å

Table C9: BET Isotherm data for spent zeolite HY

Quantachrome NovaWin - Data Acquisition and Reduction
for NOVA instruments
©1994-2013, Quantachrome Instruments
version 11.03



Analysis			Report	
Operator:	quantachrome	Date:2014/03/30	Operator:	quantachrome
Sample ID:	1	Filename:	Spent Zeolite HY.qps	Date:2014/03/30
Sample Desc:		Comment:		
Sample weight:	0.27 g	Sample Volume:	1 cc	
Outgas Time:	0.0 hrs	OutgasTemp:	0.0 C	
Analysis gas:	Nitrogen	Bath Temp:	273.0 K	
Press. Tolerance:	0.100/0.100 (ads/des)	Equil time:	60/60 sec (ads/des)	Equil timeout:
Analysis Time:	34.1 min	End of run:	2014/03/30 20:01:44	Instrument:
Cell ID:	1			Nova Station A

Isotherm : Linear

Data Reduction Parameters

Adsorbate	Po override: 760.00 Torr	Temperature	77.350K	Liquid Density:	0.808 g/cc
	Nitrogen	Cross Section:	16.200 Å²		
	Molec. Wt.: 28.013				

○
Ads

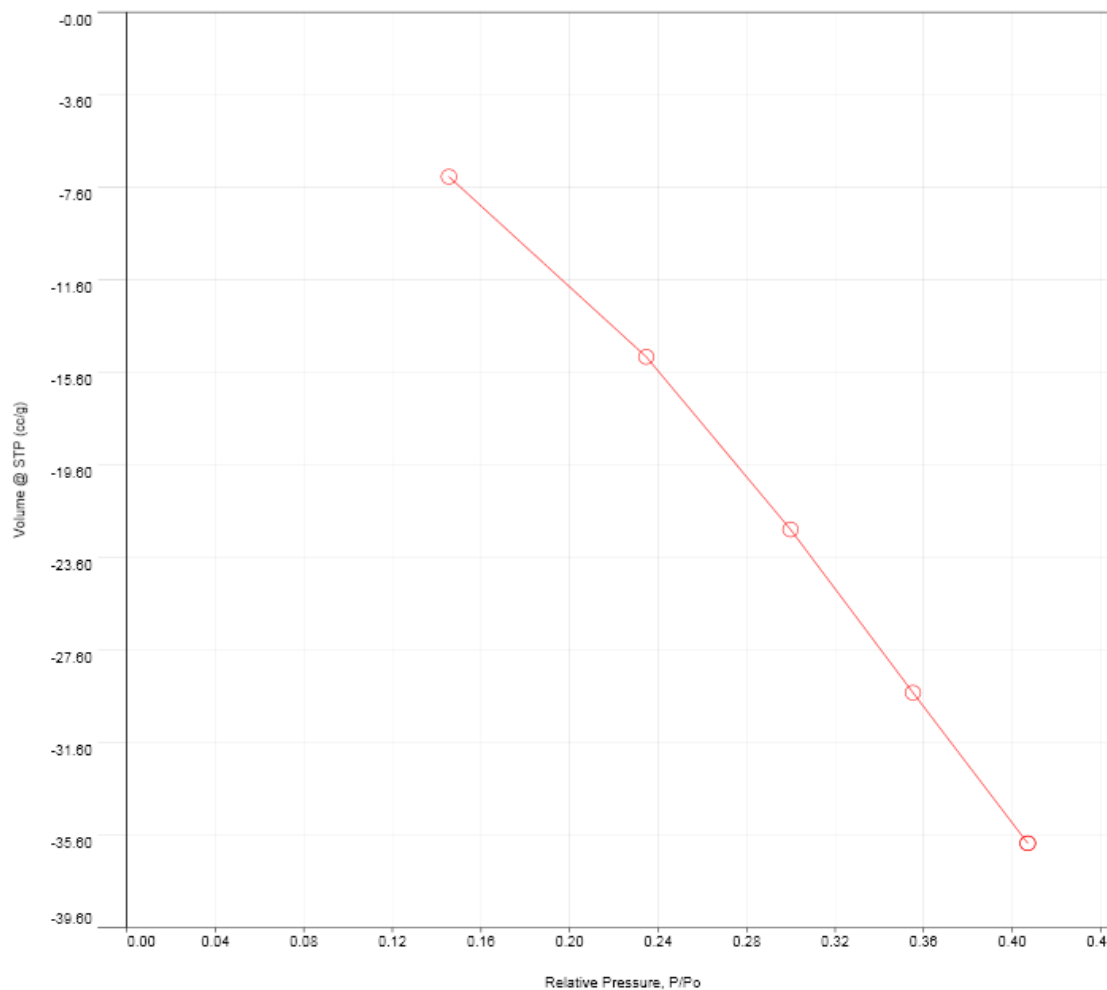


Table C10: BET Multi-point data for spent zeolite HY

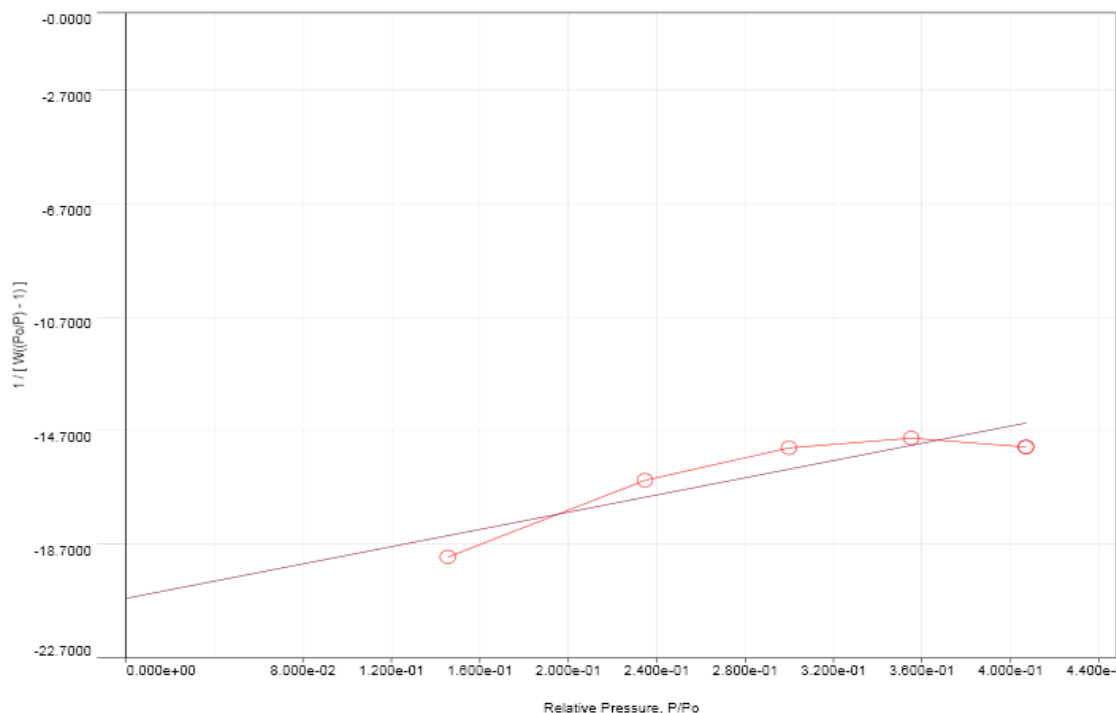
Quantachrome NovaWin - Data Acquisition and Reduction
for NOVA instruments
©1994-2013, Quantachrome Instruments
version 11.03



Analysis	quantachrome	Date: 2014/03/30	Report	quantachrome	Date: 2014/03/30
Operator:	1	Filename:	Spent Zeolite HY.qps		
Sample Desc:		Comment:			
Sample weight:	0.27 g	Sample Volume:	1 cc		
Outgas Time:	0.0 hrs	Outgas Temp:	0.0 C		
Analysis gas:	Nitrogen	Bath Temp:	273.0 K		
Press. Tolerance:	0.100/0.100 (ads/des)	Equil time:	60/60 sec (ads/des)	Equil timeout:	240/240 sec (ads/des)
Analysis Time:	34.1 min	End of run:	2014/03/30 20:01:44	Instrument:	Nova Station A
Cell ID:	1				

Multi-Point BET Plot

Data Reduction Parameters			
Adsorbate	Po override: 760.00 Torr	Temperature	77.350K
	Nitrogen	Cross Section:	16.200 Å²
	Molec. Wt.: 28.013	Liquid Density:	0.808 g/cc



BET summary	
Slope =	15.156
Intercept =	-2.060e+01
Correlation coefficient, r =	0.900496
C constant =	0.264
Surface Area =	0.000 m²/g

Table C11: BET singlepoint surface area data for zeolite HY

Quantachrome NovaWin - Data Acquisition and Reduction
for NOVA instruments
©1994-2013, Quantachrome Instruments
version 11.03



Analysis	quantachrome	Date:2014/03/30	Report	quantachrome	Date:2014/03/30
Operator:	1	Filename:	Spent Zeolite HY.qps		
Sample ID:		Comment:			
Sample Desc:		Sample Volume:	1 cc		
Sample weight:	0.27 g	Outgas Temp:	0.0 C		
Outgas Time:	0.0 hrs	Bath Temp:	273.0 K		
Analysis gas:	Nitrogen	Equil time:	60/60 sec (ads/des)	Equil timeout:	240/240 sec (ads/des)
Press. Tolerance:	0.100/0.100 (ads/des)	End of run:	2014/03/30 20:01:44	Instrument:	Nova Station A
Analysis Time:	34.1 min				
Cell ID:	1				

Single Point Surface Area

Data Reduction Parameters					
Adsorbate	Po override: 760.00 Torr		Temperature	77.350K	
	Nitrogen		Cross Section:	16.200 Å²	Liquid Density: 0.808 g/cc
	Molec. Wt.: 28.013				

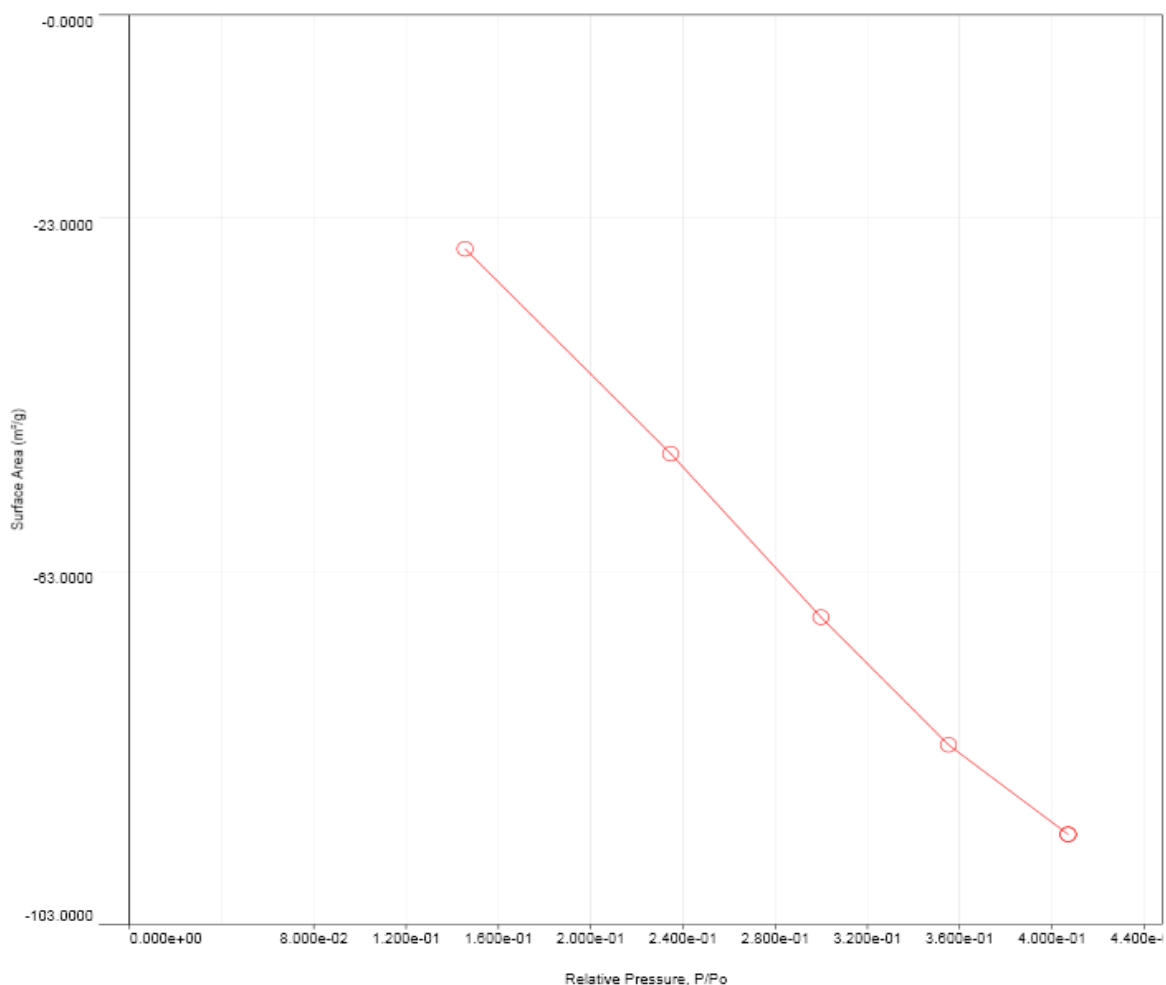


Table C12: BET Area-Volume data for spent zeolite HY



Analysis		Report	
Operator:	quantachrome	Date:	2014/03/30
Sample ID:	1	Operator:	quantachrome
Sample Desc:		Filename:	Spent Zeolite HY.qps
Sample weight:	0.27 g	Comment:	
Outgas Time:	0.0 hrs	Sample Volume:	1 cc
Analysis gas:	Nitrogen	Outgas Temp:	0.0 C
Press. Tolerance:	0.100/0.100 (ads/des)	Bath Temp:	273.0 K
Analysis Time:	34.1 min	Equil time:	60/60 sec (ads/des)
Cell ID:	1	End of run:	2014/03/30 20:01:44
		Equil timeout:	240/240 sec (ads/des)
		Instrument:	Nova Station A

Area-Volume Summary

Data Reduction Parameters Data

Thermal Transpiration: on	Eff. mol. diameter (D): 3.54 Å	Eff. cell stem diam. (d): 4.0000 mm
Po override: 760.00 Torr		
Calc. method: de Boer		
Affinity coefficient (β): 0.3300		
Tabulated data interval: 1		
Tabulated data interval: 1		
Nitrogen	Temperature	77.350K
Molec. Wt.: 28.013	Cross Section:	16.200 Å²
Critical Temp.: 126.200 K	Critical Press.:	33.500 atm
Carbon	Liquid Density:	0.808 g/cc
DR. Exp (n): 2.000	SuperCritical. K.:	1.000

Surface Area Data

SinglePoint BET.....	-9.282e+01 m²/g
Langmuir surface area.....	1.244e+02 m²/g
t-method external surface area.....	-2.606e+02 m²/g
t-method micropore surface area.....	2.606e+02 m²/g
DR method micropore area.....	1.290e-06 m²/g

Pore Volume Data

t-method micropore volume.....	9.490e-02 cc/g
DR method micropore volume.....	4.584e-10 cc/g
HK method micropore volume.....	5.502e-03 cc/g
SF method micropore volume.....	8.771e-01 cc/g

Pore Size Data

DR method micropore Half pore width.....	4.733e-06 Å
HK method pore Radius (Mode).....	1.562e+00 Å
SF method pore Radius (Mode).....	1.744e+01 Å

Table C13: BET Langmuir data for spent zeolite HY

Quantachrome NovaWin - Data Acquisition and Reduction
for NOVA instruments
©1994-2013, Quantachrome Instruments
version 11.03



Analysis		Report	
Operator:	quantachrome	Date:	2014/03/30
Sample ID:	1	Operator:	quantachrome
Sample Desc:		Filename:	Spent Zeolite HY.qps
Sample weight:	0.27 g	Comment:	
Outgas Time:	0.0 hrs	Sample Volume:	1 cc
Analysis gas:	Nitrogen	Outgas Temp:	0.0 C
Press. Tolerance:	0.100/0.100 (ads/des)	Bath Temp:	273.0 K
Analysis Time:	34.1 min	Equil time:	60/60 sec (ads/des)
Cell ID:	1	End of run:	2014/03/30 20:01:44
		Equil timeout:	240/240 sec (ads/des)
		Instrument:	Nova Station A

Langmuir

Data Reduction Parameters Data

Adsorbate	Po override: 760.00 Torr	Temperature	77.350K	Liquid Density:	0.808 g/cc
	Nitrogen	Cross Section:	16.200 Å ²		
	Molec. Wt.: 28.013				

Langmuir Data

P/Po	P/Po/W [(g/g)]	P/Po	P/Po/W [(g/g)]
1.45631e-01	-1.6353e+01	3.55240e-01	-9.6489e+00
2.34767e-01	-1.2587e+01	4.07135e-01	-9.0557e+00
2.99913e-01	-1.0716e+01		

Langmuir summary

Slope = 27.98725
Intercept = -19.74758
Correlation coefficient, r = 0.975
Surface Area = 124.432 m²/g

APPENDIX D

TableD: Results of conversion of Cyclohexane and gas oil in a cracking experiment using Developed zeolite Y and commercial Zeolite respectively.

TableD1: Result of cracking experiment using developed zeolite Y (HY) at 420°C

S/No	Hydrocarbon	Retention Time	Specific Area	Height	Moles%	Area Factor	Specific Gravity Factor	Specific Weight
1	C ₁	1.803	1805.500	446.878	74.853	2.360	0.300	22.456
2	C ₂	1.920	434.200	70.514	18.001	1.670	0.374	6.732
3	C ₃	2.280	72.05	9.349	2.987	1.310	0.508	1.517
4	iC ₄	3.196	94.64	7.813	3.924	1.040	0.563	2.209
5	nC ₄	3.663	1.496	0.234	0.062	1.000	0.584	0.036
6	C ₄	-			-	1.050	0.609	-
7	Trans	5.020	0.112	0.014	.005	1.000	0.610	0.003
8	Cis	5.320	0.121	0.015	.005	0.980	0.627	0.003
9	iC ₅	6.010	0.256	0.019	.011	0.840	0.625	0.007
10	nC ₅	6.890	0.675	0.039	0.028	0.810	0.631	0.018
11	C ₆₊	7.360	3.026	0.116	0.125	0.690	0.664	0.083
TOTAL			2412.076		100.000			

TableD2: Result of cracking experiment using developed zeolite HY at 440°C

S/No	Hydrocarbon	Retention Time	Specific Area	Height	Moles%	Area Factor	Specific Gravity Factor	Specific Weight
1	C ₁	1.806	859.559	202.372	63.255	2.360	0.300	18.98
2	C ₂	1.926	325.480	53.365	23.952	1.670	0.374	8.958
3	C ₃	2.293	38.970	5.059	2.868	1.310	0.508	1.457
4	iC ₄	2.556	0.381	0.082	0.028	1.040	0.563	0.016
5	nC ₄	2.833	7.430	1.085	0.547	1.000	0.584	0.319
6	C ₄	3.243	44.461	4.566	3.272	1.050	0.609	1.993
7	C ₄ ⁻	3.710	49.898	1.369	3.672	1.050	0.609	2.236
7	Trans	-	-			1.000	0.610	
8	Cis	4.806	24.284	2.097	1.787	0.980	0.627	1.120
9	iC ₅	5.653	7.984	7.984	0.587	0.840	0.625	0.367
10	nC ₅	-				0.810	0.631	
11	C ₆ ⁺	7.473	0.422	0.422	0.031	0.690	0.664	0.021
TOTAL			1358.869		100.000			

TableD3: Result of cracking experiment using developed zeolite HY at 480°C

S/No	Hydrocarbon	Retention Time	Specific Area	Height	Moles%	Area Factor	Specific Gravity Factor	Specific Weight
1	C1	1.796	1942.514	459.711	74.731	2.360	0.300	22.419
2	C2	1.916	463.824	72.002	17.844	1.670	0.374	6.674
3	C3	2.276	82.348	9.326	3.168	1.310	0.508	1.609
4	iC4	-	-	-	-	1.040	0.563	-
5	nC4	3.196	81.960	6.099	3.153	1.000	0.584	1.841
6	C4	-	-	-	-	1.050	0.609	-
7	C4 ⁻	-	-	-	-			-
7	Trans	3.660	1.092	0.179	0.042	1.000	0.610	0.026
8	Cis	-	-	-	-	0.980	0.627	-
9	iC5	5.956	23.486	0.464	0.903	0.840	0.625	0.564
10	nC5	-	-	-	-	0.810	0.631	
11	C6 ⁺	7.393	4.124	0.100	0.159	0.690	0.664	0.106
TOTAL			2599.348		100.000			

TableD4: Result of cracking experiment using developed zeolite HY at 520°C

S/No	Hydrocarbon	Retention Time	Specific Area	Height	Moles%	Area Factor	Specific Gravity Factor	Specific Weight
1	C1	1.796	1942.514	459.711	74.731	2.360	0.300	22.419
2	C2	1.916	463.824	72.002	17.844	1.670	0.374	6.674
3	C3	2.276	82.348	9.326	3.168	1.310	0.508	1.609
4	iC4	-	-	-	-	1.040	0.563	-
5	nC4	3.196	81.960	6.099	3.153	1.000	0.584	1.841
6	C4	-	-	-	-	1.050	0.609	-
7	C4 ⁻	-	-	-	-			-
7	Trans	3.660	1.092	0.179	0.042	1.000	0.610	0.026
8	Cis	-	-	-	-	0.980	0.627	-
9	iC5	5.956	23.486	0.464	0.903	0.840	0.625	0.564
10	nC5	-	-	-	-	0.810	0.631	
11	C6 ⁺	7.393	4.124	0.100	0.159	0.690	0.664	0.106
TOTAL			2599.348		100.000			

TableD5: Result of cracking experiment using commercial zeolite at 440°C

S/No	Hydrocarbon	Retention Time	Specific Area	Height	Moles%	Area Factor	Specific Gravity Factor	Specific Weight
1	C1	1.780	4186.092	943.981	99.394	2.360	0.300	29.818
2	C2	-	-	-	-	1.670	0.374	-
3	C3	2.253	9.780	2.379	0.232	1.310	0.508	0.118
4	iC4	-	-	-	-	1.040	0.563	-
5	nC4	3.190	11.019	1.196	0.262	1.000	0.584	0.153
6	C4	3.373	2.823	0.359	0.067	1.050	0.609	0.041
7	C4 ⁻	-	-	-	-			-
7	Trans	3.620	1.919	0.189	0.046	1.000	0.610	0.028
8	Cis	-	-	-	-	0.980	0.627	-
9	iC5	-	-	-	-	0.840	0.625	-
10	nC5	-	-	-	-	0.810	0.631	-
11	C6 ⁺	-	-	-	-	0.690	0.664	-
TOTAL			4211.633		100.000			

TableD6: Result of cracking experiment using commercial zeolite at 480°C

S/No	Hydrocarbon	Retention Time	Specific Area	Height	Moles%	Area Factor	Specific Gravity Factor	Specific Weight
1	C1	1.800	2854.873	887.917	97.442	2.360	0.300	29.233
2	C2	-	-	-	-	1.670	0.374	-
3	C3	2.633	0.872	0.229	0.232	1.310	0.508	0.118
4	iC4	2.736	4.643	0.506	-	1.040	0.563	0.285
5	nC4	3.163	0.333	0.052	0.262	1.000	0.584	0.153
6	C4	-	-	-	-	1.050	0.609	
7	C4 ⁻	-	-	-	-			-
7	Trans	-	-	-	-	1.000	0.610	-
8	Cis	5.800	68.942	1.463	2.353	0.980	0.627	1.475
9	iC5	-	-	-	-	0.840	0.625	-
10	nC5	-	-	-	-	0.810	0.631	-
11	C6 ⁺	10.663	0.148	.007	0.005	0.690	0.664	0.003
TOTAL			2929.811		100.000			

TableD7: Result of cracking experiment using developed zeolite Y (NaY) at 440°C

S/No	Hydrocarbon	Retention Time	Specific Area	Height	Moles%	Area Factor	Specific Gravity Factor	Specific Weight
1	C1	1.756	38.218	7.200	47.300	2.360	0.300	14.19
2	C2	-	-	-	-	1.670	0.374	-
3	C3	2.256	2.765	0.434	3.414	1.310	0.508	1.734
4	iC4	2.756	3.951	0.659	4.879	1.040	0.563	2.747
5	nC4	3.175	7.480	0.976	9.237	1.000	0.584	5.394
6	C4		-	-		1.050	0.609	
7	C4 ⁻	-	-	-	-			-
7	Trans	4.666	11.286	1.154	13.937	1.000	0.610	8.502
8	Cis	5.476	9.030	0.690	11.151	0.980	0.627	6.992
9	iC5	6.983	0.775	0.057	0.957	0.840	0.625	0.598
10	nC5	8.850	5.566	0.213	6.873	0.810	0.631	4.337
11	C6 ⁺	9.856	1.910	0.087	2.359	0.690	0.664	1.566
TOTAL			80.980		100.000			

TableD8: Result of cracking experiment using developed zeolite Y (NaY) at 480°C

S/No	Hydrocarbon	Retention Time	Specific Area	Height	Moles%	Area Factor	Specific Gravity Factor	Specific Weight
1	C1	1.743	17.400	1.949	23.145	2.360	0.300	6.943
2	C2	2.040	3.996	0.489	5.314	1.670	0.374	1.987
3	C3	2.236	3.382	0.334	4.499	1.310	0.508	2.285
4	iC4	2.540	2.891	0.433	3.846	1.040	0.563	2.165
5	nC4	2.960	4.092	0.582	5.443	1.000	0.584	3.179
6	C4	3.150	7.963	0.631	10.592	1.050	0.609	6.451
7	C4 ⁻	4.446	6.795	0.04	9.039	1.050	0.609	5.505
7	Trans	4.633	9.260	0.829	12.317	1.000	0.610	7.513
8	Cis	5.256	4.873	0.485	6.482	0.980	0.627	4.064
9	iC5	6.910	2.130	0.060	2.833	0.840	0.625	1.771
10	nC5	8.676	8.998	0.249	11.969	0.810	0.631	7.552
11	C6 ⁺	9.730	3.398	3.398	4.520	0.690	0.664	3.001
TOTAL			75.178		100.000			

TableD9: Result of cracking experiment using developed zeolite-NH₄Y at 420°C

S/No	Hydrocarbon	Retention Time	Specific Area	Height	Moles%	Area Factor	Specific Gravity Factor	Specific Weight
1	C1	-	-			2.360	0.300	-
2	C2	-	-			1.670	0.374	-
3	C3	2.346	60.408	10.357	16.065	1.310	0.508	8.161
4	iC4	2.483	250.370	27.430	66.583	1.040	0.563	37.486
5	nC4	2.943	9.548	1.643	2.539	1.000	0.584	1.483
6	C4	3.290	2.697	0.356	0.717	1.050	0.609	0.437
7	C4 ⁻	4.140	51.578	3.976	13.717	1.050	0.609	8.354
7	Trans	-				1.000	0.610	
8	Cis	-				0.980	0.627	
9	iC5	-				0.840	0.625	
10	nC5					0.810	0.631	
11	C6 ⁺	9.453	1.426	0.049	0.379	0.690	0.664	0.252
TOTAL			376.027		100.000			

TableD10: Result of cracking experiment using developed zeolite-NH₄Y at 440°C

S/No	Hydrocarbon	Retention Time	Specific Area	Height	Moles%	Area Factor	Specific Gravity Factor	Specific Weight
1	C1	-	-			2.360	0.300	-
2	C2	-	-			1.670	0.374	-
3	C3	2.320	63.772	11.013	14.894	1.310	0.508	7.566
4	iC4	2.453	250.190	27.989	58.433	1.040	0.563	32.898
5	nC4	2.906	9.865	1.665	2.304	1.000	0.584	1.346
6	C4	3.246	2.615	0.353	0.611	1.050	0.609	0.372
7	C4 ⁻	4.080	49.467	3.894	11.553	1.050	0.609	7.036
7	Trans	-				1.000	0.610	
8	Cis	-				0.980	0.627	
9	iC5	6.560	51.186	0.996	11.955	0.840	0.625	7.472
10	nC5					0.810	0.631	
11	C6 ⁺	9.276	1.073	0.041	0.251	0.690	0.664	0.167
TOTAL			428.168		100.000			

TableD11: Result of cracking experiment using developed zeolite- NH₄Y at 480°C

S/No	Hydrocarbon	Retention Time	Specific Area	Height	Moles%	Area Factor	Specific Gravity Factor	Specific Weight
1	C1	-	-			2.360	0.300	-
2	C2	-	-			1.670	0.374	-
3	C3	2.290	65.448	11.452	15.863	1.310	0.508	8.058
4	iC4	2.423	245.119	27.980	59.411	1.040	0.563	33.448
5	nC4	2.866	9.261	1.652	2.245	1.000	0.584	1.311
6	C4	3.200	2.497	0.344	0.605	1.050	0.609	0.368
7	C4 ⁻	4.020	46.752	3.678	11.332	1.050	0.609	6.901
7	Trans	-				1.000	0.610	
8	Cis	-				0.980	0.627	
9	iC5	6.346	42.627	0.870	10.349	0.840	0.625	
10	nC5					0.810	0.631	
11	C6 ⁺	9.146	0.877	0.037	0.213	0.690	0.664	0.141
TOTAL			412.581		100.000			

TableD12: Result of cracking experiment using developed zeolite-NH₄Y at 520°C

S/No	Hydrocarbon	Retention Time	Specific Area	Height	Moles%	Area Factor	Specific Gravity Factor	Specific Weight
1	C1	-	-			2.360	0.300	-
2	C2	-	-			1.670	0.374	-
3	C3	2.276	68.973	12.047	16.444	1.310	0.508	8.354
4	iC4	2.410	247.588	28.347	59.028	1.040	0.563	33.233
5	nC4	2.850	9.248	1.661	2.205	1.000	0.584	1.288
6	C4	3.180	2.421	0.339	0.577	1.050	0.609	0.351
7	C4 ⁻	3.993	50.747	3.734	12.099	1.050	0.609	7.368
7	Trans	-				1.000	0.610	
8	Cis	-				0.980	0.627	
9	iC5	6.880	39.672	0.806	9.458	0.840	0.625	
10	nC5					0.810	0.631	
11	C6 ⁺	9.023	0.792	0.036	0.189	0.690	0.664	0.125
TOTAL			419.441		100.000			

Table D13 Cyclohexane cracking without any catalyst (reference experiment)

S/No	Hydrocarbon	Retention Time	Specific Area	Height	Moles%	Area Factor	Specific Gravity Factor	Specific Weight
1	C1	1.783	7.885	1.319	10.023	2.360	0.300	-
2	C2	-	-			1.670	0.374	-
3	C3	-				1.310	0.508	
4	iC4	-				1.040	0.563	
5	nC4	-				1.000	0.584	
6	C4	-				1.050	0.609	
7	C4 ⁻	-				1.050	0.609	
7	Trans	-				1.000	0.610	
8	Cis	-				0.980	0.627	
9	iC5	-	-			0.840	0.625	
10	nC5	-	-	-	-	0.810	0.631	
11	C6 ⁺	8.333	70.761	1.695	89.974	0.690	0.664	
TOTAL			78.646					

Table D14 2nd experiment feed: 40mL/s of gas oil using HY catalyst at 480°C

S/No	Hydrocarbon	Retention Time	Specific Area	Height	Moles%	Area Factor	Specific Gravity Factor	Specific Weight
1	C1	-	-			2.360	0.300	-
2	C2	-	-			1.670	0.374	-
3	C3	2.210	160.635	22.629	99.560	1.310	0.508	
4	iC4					1.040	0.563	
5	nC4	2.820	0.055	0.03	0.019	1.000	0.584	
6	C4	3.480				1.050	0.609	
7	C4 ⁻					1.050	0.609	
7	Trans		0.069	0.012	0.043	1.000	0.610	
8	Cis					0.980	0.627	
9	iC5	6.360	0.312	0.015	0.193	0.840	0.625	
10	nC5					0.810	0.631	
11	C6 ⁺					0.690	0.664	
TOTAL			161.344					

Table D15 feed: 60mL/s of gas oil using HY catalyst at 480°c

S/No	Hydrocarbon	Retention Time	Specific Area	Height	Moles%	Area Factor	Specific Gravity Factor	Specific Weight
1	C1	1.590	125.507	18.160	43.133	2.360	0.300	-
2	C2	-	-			1.670	0.374	-
3	C3	2.210	160.635	25.274	55.205	1.310	0.508	
4	iC4					1.040	0.563	
5	nC4	2.820	0.052	0.013	0.018	1.000	0.584	
6	C4					1.050	0.609	
7	C4 ⁻					1.050	0.609	
7	Trans	3.480	0.372	0.018	0.128	1.000	0.610	
8	Cis					0.980	0.627	
9	iC5	6.360	4.413	0.099	1.517	0.840	0.625	
10	nC5					0.810	0.631	
11	C6 ⁺	-	-	-		0.690	0.664	
TOTAL			290.979					

Table D16 feed: 80mL/s of gas oil using HY catalyst at 480°c

S/No	Hydrocarbon	Retention Time	Specific Area	Height	Moles%	Area Factor	Specific Gravity Factor	Specific Weight
1	C1	-	-			2.360	0.300	-
2	C2	-	-			1.670	0.374	-
3	C3	2.320	173.013	22.629	96.577	1.310	0.508	
4	iC4					1.040	0.563	
5	nC4	2.960	0.075	0.016	0.042	1.000	0.584	
6	C4					1.050	0.609	
7	C4 ⁻					1.050	0.609	
7	Trans	3.640	0.054	0.014	0.030	1.000	0.610	
8	Cis					0.980	0.627	
9	iC5	6.620	6.003	0.118	3.351	0.840	0.625	
10	nC5					0.810	0.631	
11	C6 ⁺	-	-	-	-	0.690	0.664	
TOTAL			179.145					

Table D17 feed: 100mL/s of gas oil using HY catalyst at 480°C

S/No	Hydrocarbon	Retention Time	Specific Area	Height	Moles%	Area Factor	Specific Gravity Factor	Specific Weight
1	C1	-	-			2.360	0.300	-
2	C2	-	-			1.670	0.374	-
3	C3	2.460	1,636.354	225.682	99.862	1.310	0.508	
4	iC4					1.040	0.563	
5	nC4	3.100	1.490	0.273	0.091	1.000	0.584	
6	C4					1.050	0.609	
7	C4 ⁻	4.380	0.764	0.049	0.047	1.050	0.609	
7	Trans					1.000	0.610	
8	Cis					0.980	0.627	
9	iC5					0.840	0.625	
10	nC5					0.810	0.631	
11	C6 ⁺					0.690	0.664	
TOTAL			1638.608					

Table D18: Cracking gas oil on HY at 420°C

S/No	Hydrocarbon	Retention Time	Specific Area	Height	Moles%	Area Factor	Specific Gravity Factor	Specific Weight
1	C1	-	-			2.360	0.300	-
2	C2	-	-			1.670	0.374	-
3	C3	2.350	140.374	20.381	100	1.310	0.508	
4	iC4					1.040	0.563	
5	nC4	-				1.000	0.584	
6	C4					1.050	0.609	
7	C4 ⁻	-				1.050	0.609	
7	Trans					1.000	0.610	
8	Cis					0.980	0.627	
9	iC5					0.840	0.625	
10	nC5					0.810	0.631	
11	C6 ⁺					0.690	0.664	
TOTAL			140.374					

TableD19: Result of cracking experiment using developed zeolite Y (HY) at 440°C

S/No	Hydrocarbon	Retention Time	Specific Area	Height	Moles%	Area Factor	Specific Gravity Factor	Specific Weight
1	C1	-	-			2.360	0.300	-
2	C2	-	-			1.670	0.374	-
3	C3	2.430	1179.789	161.554	98,408	1.310	0.508	
4	iC4					1.040	0.563	
5	nC4	3.070	3.244	0.546	0.271	1.000	0.584	
6	C4					1.050	0.609	
7	C4 ⁻	4.350	15.840	1.112	1.32	1.050	0.609	
7	Trans					1.000	0.610	
8	Cis					0.980	0.627	
9	iC5					0.840	0.625	
10	nC5					0.810	0.631	
11	C6 ⁺					0.690	0.664	
TOTAL			1198.873					

TableD20: Result of cracking experiment using developed zeolite Y (HY) at 480°C

(3)

S/No	Hydrocarbon	Retention Time	Specific Area	Height	Moles%	Area Factor	Specific Gravity Factor	Specific Weight
1	C1	1.580	9.088	1.008	6.160	2.360	0.300	-
2	C2	-	-			1.670	0.374	-
3	C3	2.360	89.248	12.852	60.495	1.310	0.508	
4	iC4					1.040	0.563	
5	nC4	3.000	0.086	0.017	0.091	1.000	0.584	
6	C4					1.050	0.609	
7	C4 ⁻	4.270	0.096	0.011	0.065	1.050	0.609	
7	Trans					1.000	0.610	
8	Cis					0.980	0.627	
9	iC5					0.840	0.625	
10	nC5					0.810	0.631	
11	C6 ⁺	8.510	49.011	0.927	33.221	0.690	0.664	
TOTAL			147.529					

TableD21: Result of cracking experiment using developed zeolite-HY at 520°C

S/No	Hydrocarbon	Retention Time	Specific Area	Height	Moles%	Area Factor	Specific Gravity Factor	Specific Weight
1	C1	1.430	14.559	0.142	7.343	2.360	0.300	-
2	C2		-			1.670	0.374	-
3	C3	2.420	168.761	21.872	85.118	1.310	0.508	
4	iC4					1.040	0.563	
5	nC4	3.070	0.571	0.088	0.288	1.000	0.584	
6	C4	3.790	0.097	0.017	0.049	1.050	0.609	
7	C4 ⁻	4.360	3.740	0.208	1.886	1.050	0.609	
7	Trans					1.000	0.610	
8	Cis					0.980	0.627	
9	iC5					0.840	0.625	
10	nC5					0.810	0.631	
11	C6 ⁺	10.320	10.540	0.196	5.316	0.690	0.664	
TOTAL			198.268					

Table D22:Matrices of produced zeolite HY : Metakaolin (25% :75%) feed: gas oil at 420°C

S/No	Hydrocarbon	Retention Time	Specific Area	Height	Moles%	Area Factor	Specific Gravity Factor	Specific Weight
1	C1	-	-			2.360	0.300	-
2	C2	-	-			1.670	0.374	-
3	C3	2.310	1918.029	298.240	100	1.310	0.508	
4	iC4					1.040	0.563	
5	nC4					1.000	0.584	
6	C4					1.050	0.609	
7	C4 ⁻					1.050	0.609	
7	Trans					1.000	0.610	
8	Cis					0.980	0.627	
9	iC5					0.840	0.625	
10	nC5					0.810	0.631	
11	C6 ⁺					0.690	0.664	
TOTAL			1918.029					

Table D23: Matrices of produced zeolite HY: Metakaolin (25%:75%) feed: gas oil at 440°C

S/No	Hydrocarbon	Retention Time	Specific Area	Height	Moles%	Area Factor	Specific Gravity Factor	Specific Weight
1	C1	-	-			2.360	0.300	-
2	C2	-	-			1.670	0.374	-
3	C3	2.290	1869.933	294.496	100	1.310	0.508	
4	iC4					1.040	0.563	
5	nC4					1.000	0.584	
6	C4					1.050	0.609	
7	C4 ⁻					1.050	0.609	
7	Trans					1.000	0.610	
8	Cis					0.980	0.627	
9	iC5					0.840	0.625	
10	nC5					0.810	0.631	
11	C6 ⁺					0.690	0.664	
TOTAL			1869.370					

Table D24: Matrices of produced zeolite HY: Metakaolin (25%:75%) feed: gas oil at 480°C

S/No	Hydrocarbon	Retention Time	Specific Area	Height	Moles%	Area Factor	Specific Gravity Factor	Specific Weight
1	C1	-	-			2.360	0.300	-
2	C2	-	-			1.670	0.374	-
3	C3	2.320	1905.466	294.631	100	1.310	0.508	
4	iC4					1.040	0.563	
5	nC4					1.000	0.584	
6	C4					1.050	0.609	
7	C4 ⁻					1.050	0.609	
7	Trans					1.000	0.610	
8	Cis					0.980	0.627	
9	iC5					0.840	0.625	
10	nC5					0.810	0.631	
11	C6 ⁺					0.690	0.664	
TOTAL			1906					

Table D25: Matrices of produced zeolite HY : Metakaolin (25% :75%) feed: gas oil at 520°C

S/No	Hydrocarbon	Retention Time	Specific Area	Height	Moles%	Area Factor	Specific Gravity Factor	Specific Weight
1	C1	-	-			2.360	0.300	-
2	C2	-	-			1.670	0.374	-
3	C3	2.290	1889.920	298.308	100	1.310	0.508	
4	iC4	-	-	-		1.040	0.563	
5	nC4	-	-	-		1.000	0.584	
6	C4	-	-	-		1.050	0.609	
7	C4 ⁻	-	-	-		1.050	0.609	
7	Trans	-				1.000	0.610	
8	Cis	-				0.980	0.627	
9	iC5	-	-			0.840	0.625	
10	nC5			-		0.810	0.631	
11	C6 ⁺			-		0.690	0.664	
TOTAL			1889.920					

TableD26: Matrices of produced zeolite HY: Metakaolin (50%:50%) at 420°C

S/No	Hydrocarbon	Retention Time	Specific Area	Height	Moles%	Area Factor	Specific Gravity Factor	Specific Weight
1	C1	1.550	2.096	0.092	0.199	2.360	0.300	-
2	C2	2.040	0.291	0.043	0.028	1.670	0.374	-
3	C3	2.250	1038.044	154.964	98.571	1.310	0.508	
4	iC4					1.040	0.563	
5	nC4	2.860	9.760	1.570	0.927	1.000	0.584	
6	C4					1.050	0.609	
7	C4 ⁻	4.310	0.988	0.087	0.094	1.050	0.609	
7	Trans	4.600	0.947	0.057	0.009	1.000	0.610	
8	Cis	5.620	0.104	0.010	0.010	0.980	0.627	
9	iC5	6.620	0.238	0.019	0.023	0.840	0.625	
10	nC5	8.16	0.345	0.022	0.033	0.810	0.631	
11	C6 ⁺	9.350	0.284	0.015	0.027	0.690	0.664	
TOTAL			1,053.097					

TableD27: Matrices of produced zeolite HY: Metakaolin (50%:50%) at 440°C

S/No	Hydrocarbon	Retention Time	Specific Area	Height	Moles%	Area Factor	Specific Gravity Factor	Specific Weight
1	C1	1.650	1.071	0.097	0.103	2.360	0.300	-
2	C2	1.900	0.661	0.067	0.026	1.670	0.374	-
3	C3	2.290	1019.580	147.644	98.351	1.310	0.508	
4	iC4	-	-	-	-	1.040	0.563	
5	nC4	2.900	9.748	1.532	0.940	1.000	0.584	
6	C4	-	-	-	-	1.050	0.609	
7	C4 ⁻	4.120	3.411	0.228	0.329	1.050	0.609	
7	Trans	4.660	1.001	0.550	0.096	1.000	0.610	
8	Cis	5.470	0.539	0.027	0.052	0.980	0.627	
9	iC5	6.650	0.260	0.025	0.025	0.840	0.625	
10	nC5	8.12	0.238	0.021	0.023	0.810	0.631	
11	C6 ⁺	9.460	0.170	0.018	0.016	0.690	0.664	
TOTAL			1,036.679					

TableD28: Matrices of produced zeolite HY: Metakaolin (50%:50%) at 480°C

S/No	Hydrocarbon	Retention Time	Specific Area	Height	Moles%	Area Factor	Specific Gravity Factor	Specific Weight
1	C1					2.360	0.300	-
2	C2					1.670	0.374	-
3	C3	2.450	1032.864	137.550	98.803	1.310	0.508	
4	iC4	-	-	-	-	1.040	0.563	
5	nC4	3.100	9.296	1.769	0.889	1.000	0.584	
6	C4	-	-	-	-	1.050	0.609	
7	C4 ⁻	4.240	2.360	2.360	0.226	1.050	0.609	
7	Trans	4.990	0.532	0.040	0.051	1.000	0.610	
8	Cis	-	-	-	-	0.980	0.627	
9	iC5	-	-	-	-	0.840	0.625	
10	nC5	7.130	0.132	0.010	0.013	0.810	0.631	
11	C6 ⁺	8.070	0.195	0.012	0.019	0.690	0.664	
TOTAL			1,045.379					

TableD29: Matrices of produced zeolite HY: Metakaolin (50%:50%) at 520°C

S/No	Hydrocarbon	Retention Time	Specific Area	Height	Moles%	Area Factor	Specific Gravity Factor	Specific Weight
1	C1	-	-	-	-	2.360	0.300	-
2	C2	-	-	-	-	1.670	0.374	-
3	C3	2.250	1032.864	23.116	98.803	1.310	0.508	
4	iC4	-	-	-	-	1.040	0.563	
5	nC4	2.850	9.296	0.239	0.889	1.000	0.584	
6	C4	-	-	-	-	1.050	0.609	
7	C4 ⁻	3.890	2.360	0,046	0.226	1.050	0.609	
7	Trans	-	-	-	-	1.000	0.610	
8	Cis	-	-	-	-	0.980	0.627	
9	iC5	-	-	-	-	0.840	0.625	
10	nC5	-	-	-	-	0.810	0.631	
11	C6 ⁺	-	-	-	-	0.690	0.664	
TOTAL			1,045.052					

TableD30: Matrices of produced zeolite HY: Metakaolin (75%:25%) at 420°C

S/No	Hydrocarbon	Retention Time	Specific Area	Height	Moles%	Area Factor	Specific Gravity Factor	Specific Weight
1	C1	-	-	-		2.360	0.300	-
2	C2	-	-	-		1.670	0.374	-
3	C3	2.400	1,305.216	190.627	99.311	1.310	0.508	
4	iC4		-	-		1.040	0.563	
5	nC4	3.030	0.579	0.109	0.044	1.000	0.584	
6	C4		-	-		1.050	0.609	
7	C4 ⁻	4.340	0.686	0.049	0.052	1.050	0.609	
7	TransS	-	-	-	-	1.000	0.610	
8	Cis	5.900	6.800	0.117	0.517	0.980	0.627	
9	iC5	-	-	-	-	0.840	0.625	
10	nC5	8.200	0.995	0.012	0.076	0.810	0.631	
11	C6 ⁺	-	-	-	-	0.690	0.664	
TOTAL			1,314.276					

TableD31: Matrices of produced zeolite HY: Metakaolin (75%:25%) at 440°C

S/No	Hydrocarbon	Retention Time	Specific Area	Height	Moles%	Area Factor	Specific Gravity Factor	Specific Weight
1	C1	-	-	-		2.360	0.300	-
2	C2	-	-	-		1.670	0.374	-
3	C3	2.410	1,311.831	191.529	98.696	1.310	0.508	
4	iC4		-	-		1.040	0.563	
5	nC4	3.040	0.575	0.111	0.043	1.000	0.584	
6	C4		-	-		1.050	0.609	
7	C4 ⁻	4.160	16.753	0.079	1.260	1.050	0.609	
7	Trans	-	-	-	-	1.000	0.610	
8	Cis	-	-	-	-	0.980	0.627	
9	iC5	-	-	-	-	0.840	0.625	
10	nC5	-	-	-	-	0.810	0.631	
11	C6 ⁺	-	-	-	-	0.690	0.664	
TOTAL			1,329.159					

Table: Result of cracking experiment using developed zeolite- γ (HY) at 410°C

TableD32: Matrices of produced zeolite HY: Metakaolin (75%:25%) at 480°C

S/No	Hydrocarbon	Retention Time	Specific Area	Height	Moles%	Area Factor	Specific Gravity Factor	Specific Weight
1	C1	-	-	-		2.360	0.300	-
2	C2	-	-	-		1.670	0.374	-
3	C3	2.400	1,327.000	195.671	98.696	1.310	0.508	
4	iC4		-	-		1.040	0.563	
5	nC4	3.020	0.566	0.113	0.043	1.000	0.584	
6	C4		-	-		1.050	0.609	
7	C4 ⁻	4.130	0.567	0.042	1.260	1.050	0.609	
7	Trans	-	-	-	-	1.000	0.610	
8	Cis	-	-	-	-	0.980	0.627	
9	iC5	-	-	-	-	0.840	0.625	
10	nC5	-	-	-	-	0.810	0.631	
11	C6 ⁺	10.590	0.308	0.039	-	0.690	0.664	
TOTAL			1,329.159					

TableD33: Matrices of produced zeolite HY: Metakaolin (75%:25%) at 520°C

S/No	Hydrocarbon	Retention Time	Specific Area	Height	Moles%	Area Factor	Specific Gravity Factor	Specific Weight
1	C1	-	-	-		2.360	0.300	-
2	C2	-	-	-		1.670	0.374	-
3	C3	2.430	1,300.351	187.126	99.893	1.310	0.508	
4	iC4		-	-		1.040	0.563	
5	nC4	3.060	0.557	0.109	0.043	1.000	0.584	
6	C4		-	-		1.050	0.609	
7	C4 ⁻	4.170	0.835	0.045	0.064	1.050	0.609	
7	Trans	-	-	-	-	1.000	0.610	
8	Cis	-	-	-	-	0.980	0.627	
9	iC5	-	-	-	-	0.840	0.625	
10	nC5	-	-	-	-	0.810	0.631	
11	C6 ⁺	-	-	-	-	0.690	0.664	
TOTAL			1,301.743					

Table D34: Matrices of produced zeolite HY: Metakaolin (90%:10%) at 420°C

S/No	Hydrocarbon	Retention Time	Specific Area	Height	Moles%	Area Factor	Specific Gravity Factor	Specific Weight
1	C1	-	-	-		2.360	0.300	-
2	C2	-	-	-		1.670	0.374	-
3	C3	2.280	1,695.141	262.179	99.858	1.310	0.508	
4	iC4		-	-		1.040	0.563	
5	nC4	2.860	1.606	0.322	0.095	1.000	0.584	
6	C4		-	-		1.050	0.609	
7	C4 ⁻	3.880	0.189	0.029	0.011	1.050	0.609	
7	Trans	4.030	0.663	0.054	-	1.000	0.610	
8	Cis	-	-	-	-	0.980	0.627	
9	iC5	-	-	-	-	0.840	0.625	
10	nC5	-	-	-	-	0.810	0.631	
11	C6 ⁺	-	-	-	-	0.690	0.664	
TOTAL			1,697.599					

Table D35: Matrices of produced zeolite HY: Metakaolin (90%:10%) at 440°C

S/No	Hydrocarbon	Retention Time	Specific Area	Height	Moles%	Area Factor	Specific Gravity Factor	Specific Weight
1	C1	-	-	-		2.360	0.300	-
2	C2	-	-	-		1.670	0.374	-
3	C3	2.450	1,642.652	227.246	99.887	1.310	0.508	
4	iC4		-	-		1.040	0.563	
5	nC4	3.080	1.384	0.259	0.084	1.000	0.584	
6	C4		-	-		1.050	0.609	
7	C4 ⁻	4.340	0.477	0.043	0.003	1.050	0.609	
7	Trans	-	-	-	-	1.000	0.610	
8	Cis	-	-	-	-	0.980	0.627	
9	iC5	-	-	-	-	0.840	0.625	
10	nC5	-	-	-	-	0.810	0.631	
11	C6 ⁺	-	-	-	-	0.690	0.664	
TOTAL			1,644.513					

Table D36: Matrices of produced zeolite HY : Metakaolin (90% :10%) at 480°C

S/No	Hydrocarbon	Retention Time	Specific Area	Height	Moles%	Area Factor	Specific Gravity Factor	Specific Weight
1	C1	-	-	-		2.360	0.300	-
2	C2	-	-	-		1.670	0.374	-
3	C3	2.450	1,689.464	236.130	99.881	1.310	0.508	
4	iC4		-	-		1.040	0.563	
5	nC4	3.070	1.436	0.269	0.085	1.000	0.584	
6	C4		-	-		1.050	0.609	
7	C4 ⁻	4.330	0.573	0.043	0.034	1.050	0.609	
7	Trans	-	-	-	-	1.000	0.610	
8	Cis	-	-	-	-	0.980	0.627	
9	iC5	-	-	-	-	0.840	0.625	
10	nC5	-	-	-	-	0.810	0.631	
11	C6 ⁺	-	-	-	-	0.690	0.664	
TOTAL			1,691.473					

Table D37: Matrices of produced zeolite HY: Metakaolin (90%:10%) at 520°C

S/No	Hydrocarbon	Retention Time	Specific Area	Height	Moles%	Area Factor	Specific Gravity Factor	Specific Weight
1	C1	-	-	-		2.360	0.300	-
2	C2	-	-	-		1.670	0.374	-
3	C3	2.420	1,678.817	238.263	99.888	1.310	0.508	
4	iC4		-	-		1.040	0.563	
5	nC4	3.030	1.398	0.259	0.083	1.000	0.584	
6	C4		-	-		1.050	0.609	
7	C4 ⁻	4.270	0.484	0.043	0.029	1.050	0.609	
7	Trans	-	-	-	-	1.000	0.610	
8	Cis	-	-	-	-	0.980	0.627	
9	iC5	-	-	-	-	0.840	0.625	
10	nC5	-	-	-	-	0.810	0.631	
11	C6 ⁺	-	-	-	-	0.690	0.664	
TOTAL			1,680.699					

TableD38: Cracking of gas oil using commercial Zeolite at 420°C.

S/No	Hydrocarbon	Retention Time	Specific Area	Height	Moles%	Area Factor	Specific Gravity Factor	Specific Weight
1	C1	1.520	0.109	0.021	0.022	2.360	0.300	-
2	C2	1.943	0.194	0.015	0.039	1.670	0.374	-
3	C3	2.196	434.252	66.621	86.246	1.310	0.508	
4	iC4	2.816	24.357	3.246	4.837	1.040	0.563	
5	nC4	-	1.384	0.259	0.275	1.000	0.584	
6	C4	3.900	1.707	0.230	0.339	1.050	0.609	
7	C4 ⁻	4.300	1.164	0.100	0.231	1.050	0.609	
7	Trans	-	-	-	-	1.000	0.610	
8	Cis	4.600	1.048	0.069	0.208	0.980	0.627	
9	iC5	6.046	1.125	0.085	0.223	0.840	0.625	
10	nC5	7.300	38.214	0.699	7.589	0.810	0.631	
11	C6 ⁺	-	-	-	-	0.690	0.664	
TOTAL			503.506					

TableD39: Cracking of gas oil using commercial Zeolite at 440°C.

S/No	Hydrocarbon	Retention Time	Specific Area	Height	Moles%	Area Factor	Specific Gravity Factor	Specific Weight
1	C1	-	-	-	-	2.360	0.300	-
2	C2	-	-	-	-	1.670	0.374	-
3	C3	2.190	512.904	79.400	83.903	1.310	0.508	
4	iC4	2.806	26.187	3.528	4.284	1.040	0.563	
5	nC4	-			-	1.000	0.584	
6	C4	3.890	1.787	0.248	0.292	1.050	0.609	
7	C4 ⁻	4.296	1.057	0.098	0.173	1.050	0.609	
7	Trans	-	-	-	-	1.000	0.610	
8	Cis	4.600	0.720	0.637	0.118	0.980	0.627	
9	iC5	6.026	1.252	0.094	0.184	0.840	0.625	
10	nC5	7.103	0.261	0.015	0.043	0.810	0.631	
11	C6 ⁺	8.223	67.141	1.247	10.983	0.690	0.664	
TOTAL			611.309					

TableD40: Cracking of gas oil using commercial Zeolite at 480°C.

S/No	Hydrocarbon	Retention Time	Specific Area	Height	Moles%	Area Factor	Specific Gravity Factor	Specific Weight
1	C1	-	-	-	-	2.360	0.300	-
2	C2	-	-	-	-	1.670	0.374	-
3	C3	2.196	447.772	69.464	93.370	1.310	0.508	
4	iC4	2.810	25.013	3.383	5.218	1.040	0.563	
5	nC4	3.486	1.761	0.258	0.367	1.000	0.584	
6	C4	3.890	1.698	0.230	0.354	1.050	0.609	
7	C4 ⁻	4.296	0.890	0.088	0.186	1.050	0.609	
7	Trans	-	-	-	-	1.000	0.610	
8	Cis	4.586	1.048	0.056	0.219	0.980	0.627	
9	iC5	6.026	1.125	0.097	0.235	0.840	0.625	
10	nC5	7.943	0.004	0.010	0.001	0.810	0.631	
11	C6 ⁺	8.223	0.253	0.010	0.053	0.690	0.664	
TOTAL			479.568					

TableD41: Cracking of gas oil using commercial Zeolite at 520°C.

S/No	Hydrocarbon	Retention Time	Specific Area	Height	Moles%	Area Factor	Specific Gravity Factor	Specific Weight
1	C1	-	-			2.360	0.300	-
2	C2	-	-			1.670	0.374	-
3	C3	2.226	520.523	79.674	94.140	1.310	0.508	
4	iC4	2.856	26.337	3.509	4.763	1.040	0.563	
5	nC4	3.546	1.882	0.272	0.340	1.000	0.584	
6	C4	3.953	1.735	0.233	0.314	1.050	0.609	
7	C4 ⁻	4.363	0.908	0.088	0.164	1.050	0.609	
7	Trans	-	-	-	-	1.000	0.610	
8	Cis	4.656	0.661	0.058	0.120	0.980	0.627	
9	iC5	6.126	0.861	0.085	0.156	0.840	0.625	
10	nC5	7.326	0.023	0.007	0.004	0.810	0.631	
11	C6 ⁺	-	-	-	-	0.690	0.664	
TOTAL			552.930					

APPENDIX E

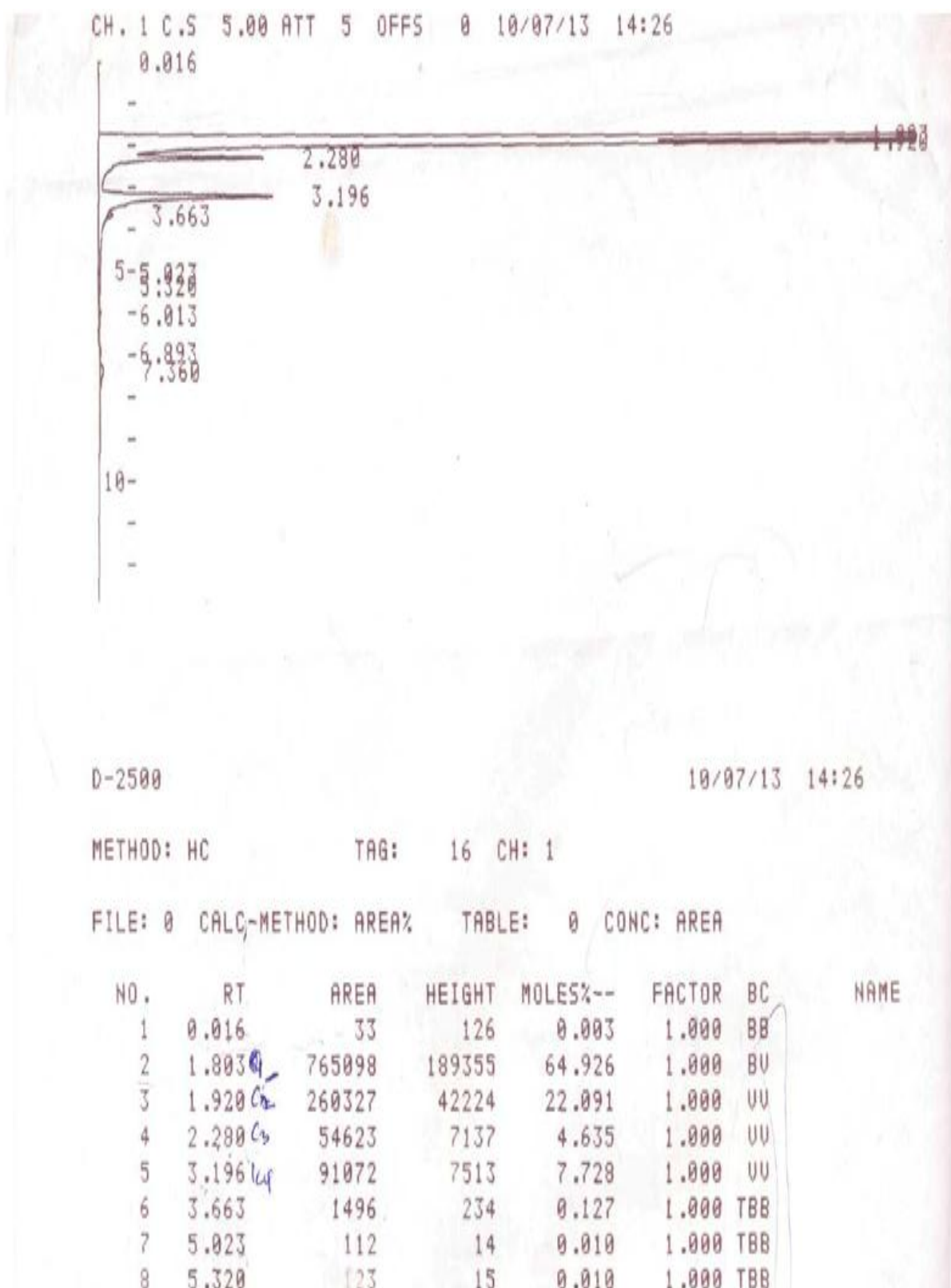


Figure E₁: Chromatograph of Cyclohexane cracking over developed zeolite HY at 420°C

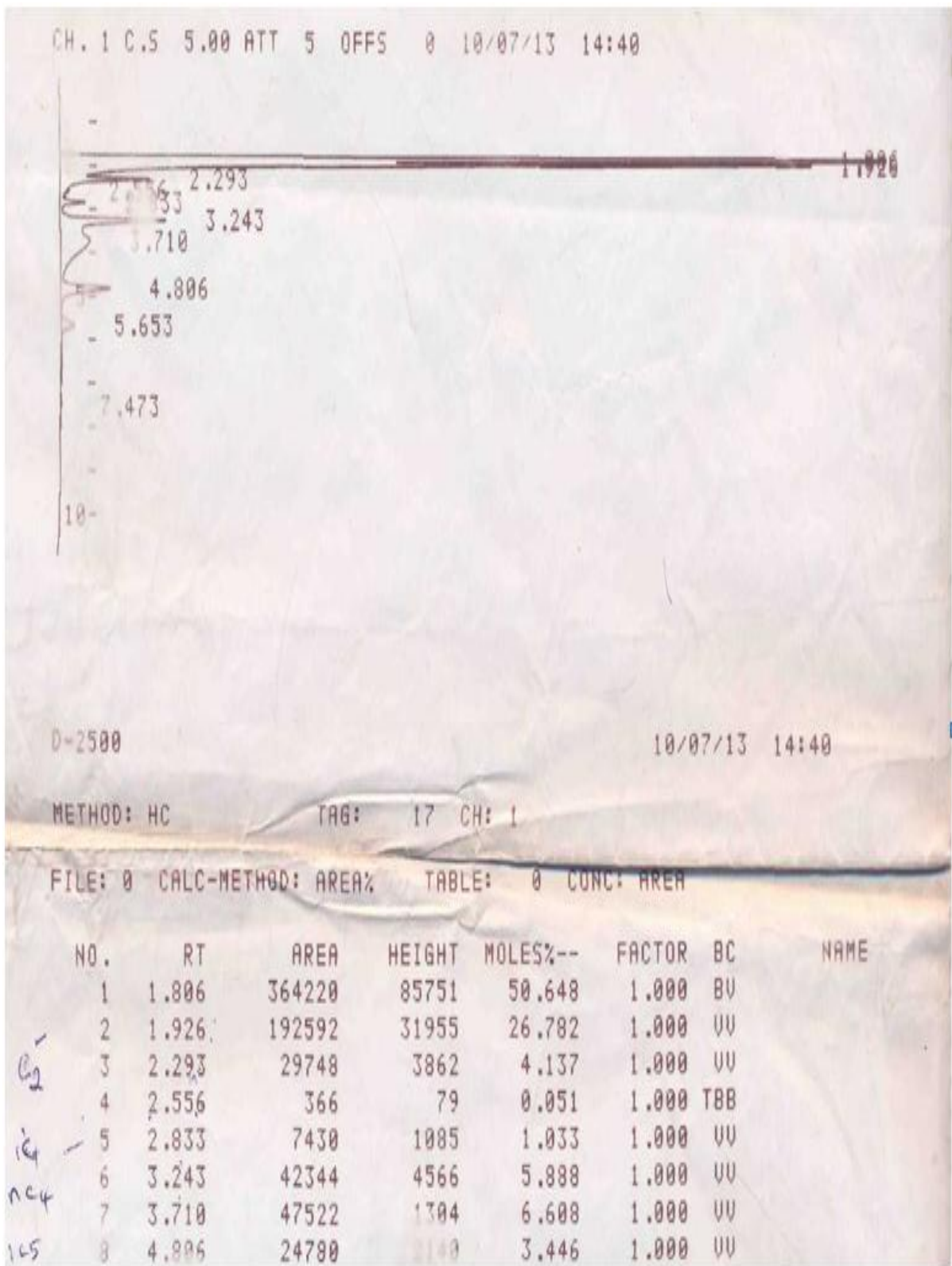


Figure E2: Chromatograph of Cyclohexane cracking over developed zeolite HY at 440°C

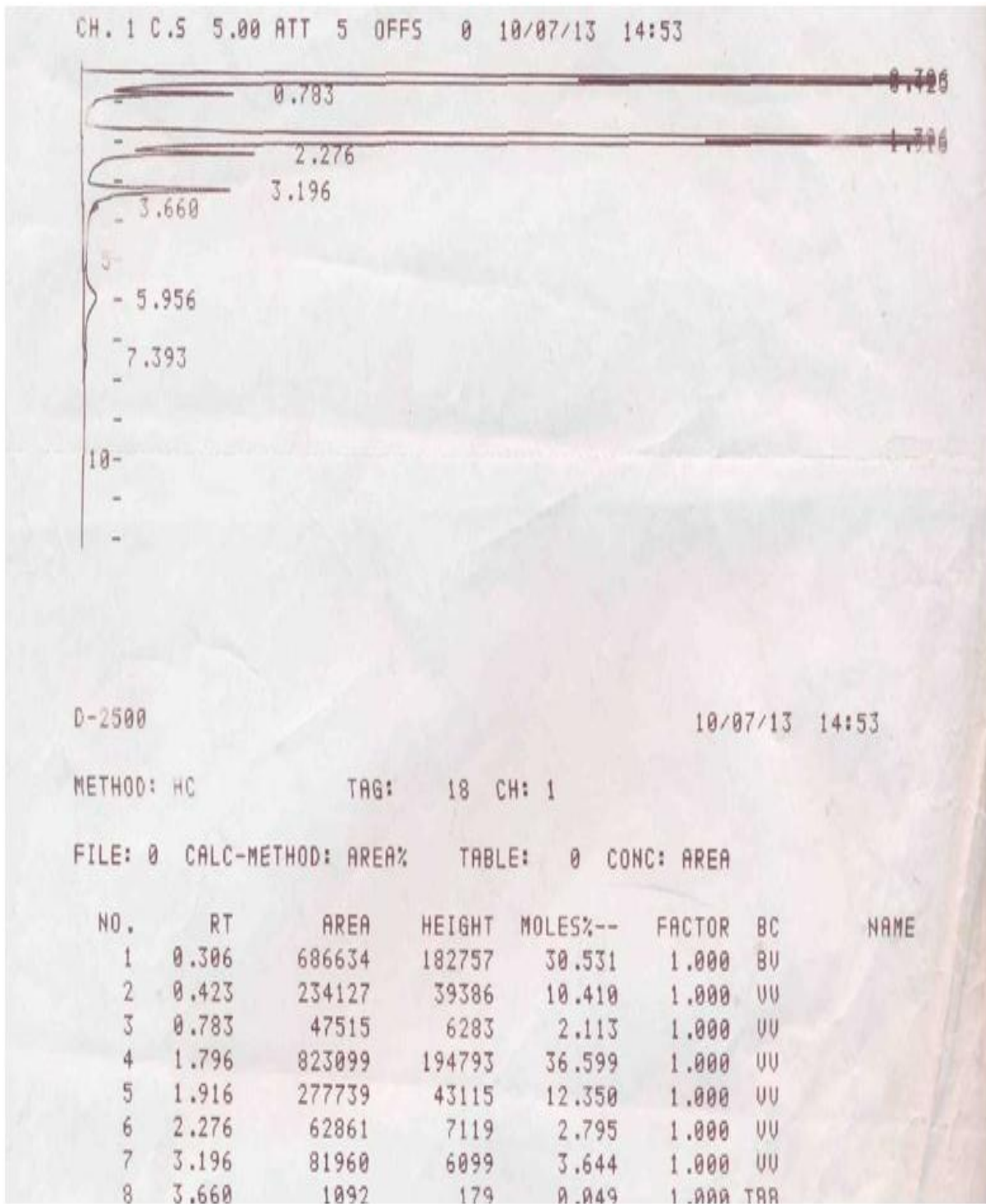


Figure E3: Chromatograph of Cyclohexane cracking over developed zeolite HY at 480°C

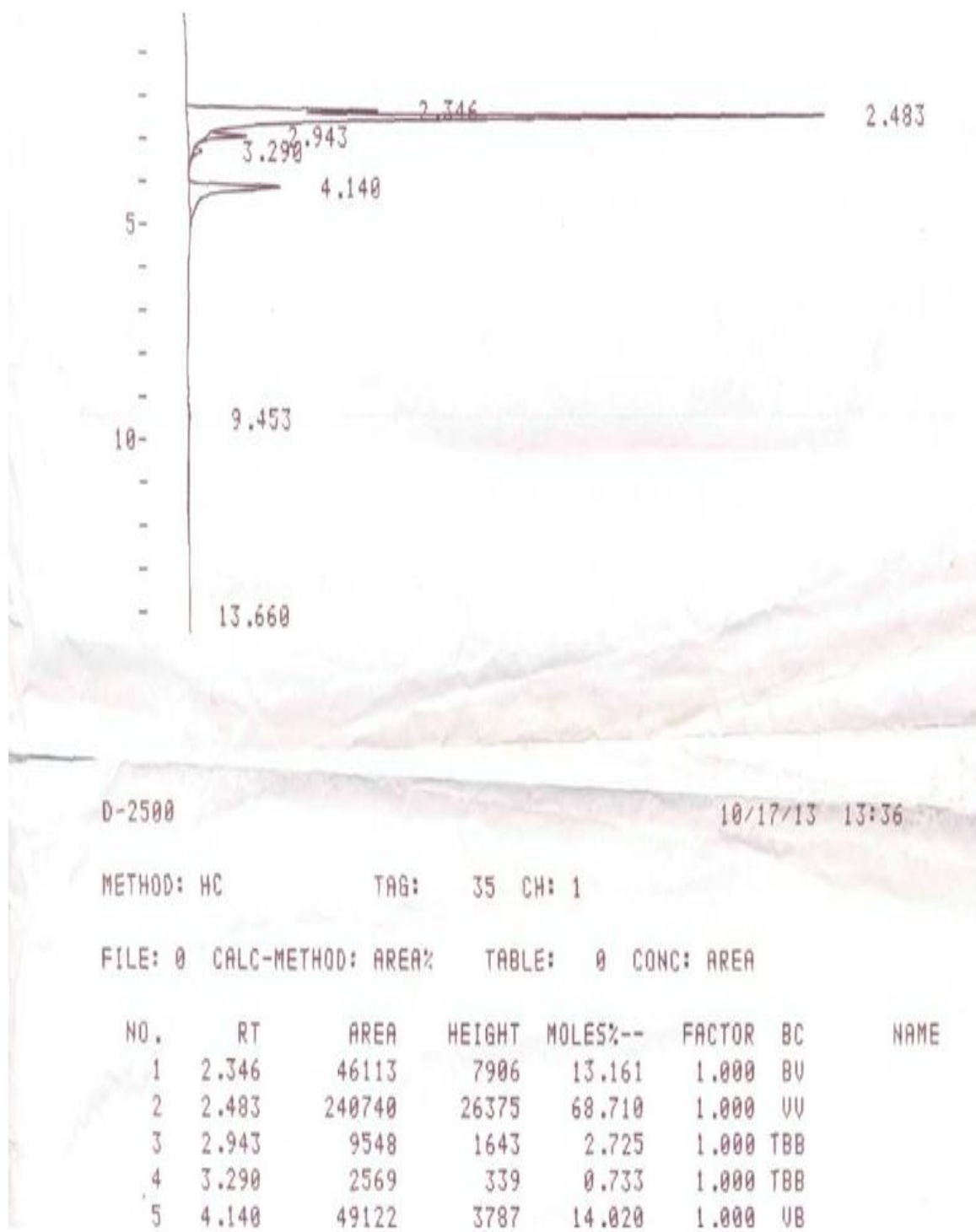
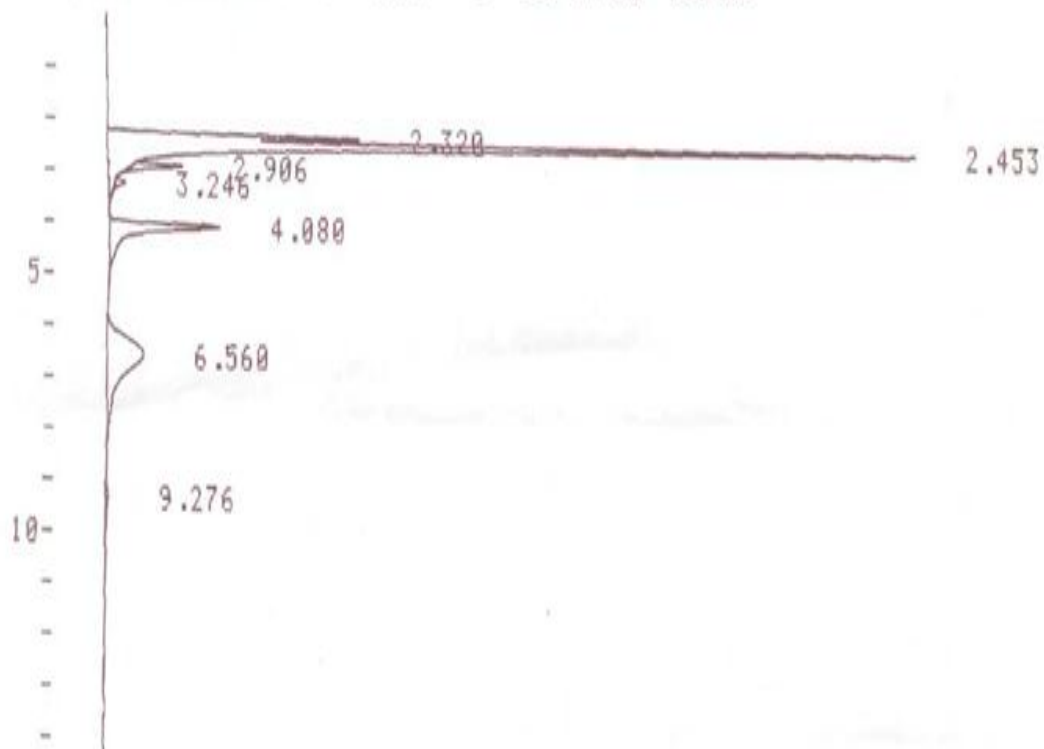


Figure E4: Chromatograph of Cyclohexane cracking over developed zeolite HY at 520°C

CH. 1 C.S 5.00 ATT 5 OFFS 0 10/17/13 13:52



D-2500

10/17/13 13:52

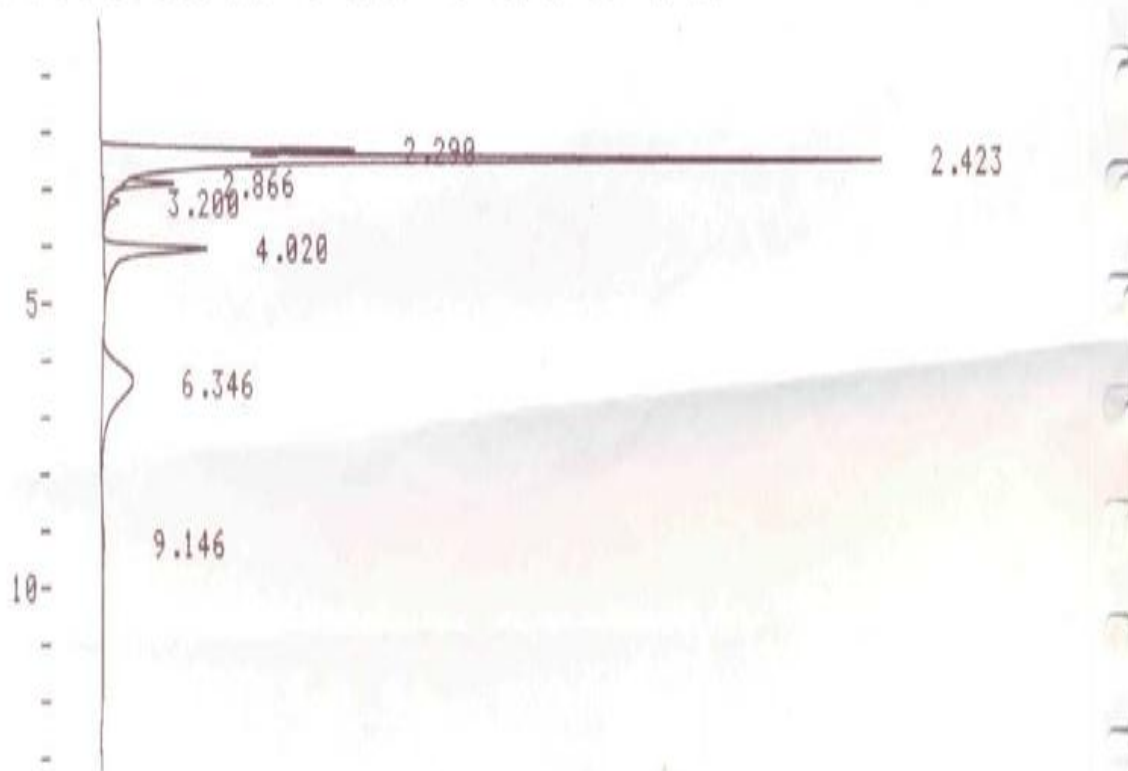
METHOD: HC TAG: 36 CH: 1

FILE: 0 CALC-METHOD: AREA% TABLE: 0 CONC: AREA

NO.	RT	AREA	HEIGHT	MOLES%--	FACTOR	BC	NAME
1	2.320	48681	8407	11.850	1.000	BV	
2	2.453	240568	26913	58.557	1.000	VV	
3	2.906	9486	1665	2.309	1.000	TBB	
4	3.246	2490	336	0.606	1.000	TBB	
5	4.080	47111	3789	11.467	1.000	BB	

Figure E5: Chromatograph of Cyclohexane over commercial zolite Y at 420°C

CH. 1 C.S 5.00 ATT 5 OFFS 0 10/17/13 14:09



D-2500

10/17/13 14:09

METHOD: HC TAG: 37 CH: 1

FILE: 0 CALC-METHOD: AREA% TABLE: 0 CONC: AREA

NO.	RT	AREA	HEIGHT	MOLES%--	FACTOR	BC	NAME
1	2.290	49960	8742	12.686	1.000	BV	
2	2.423	235691	26904	59.845	1.000	VV	
3	2.866	9261	1652	2.351	1.000	TBB	
4	3.200	2378	328	0.604	1.000	TBB	
5	4.020	44526	3583	11.306	1.000	VB	
6	6.346	50747	1036	12.885	1.000	BB	

Figure E6: Chromatograph of Cyclohexane over commercial zeolite Y at 440°C

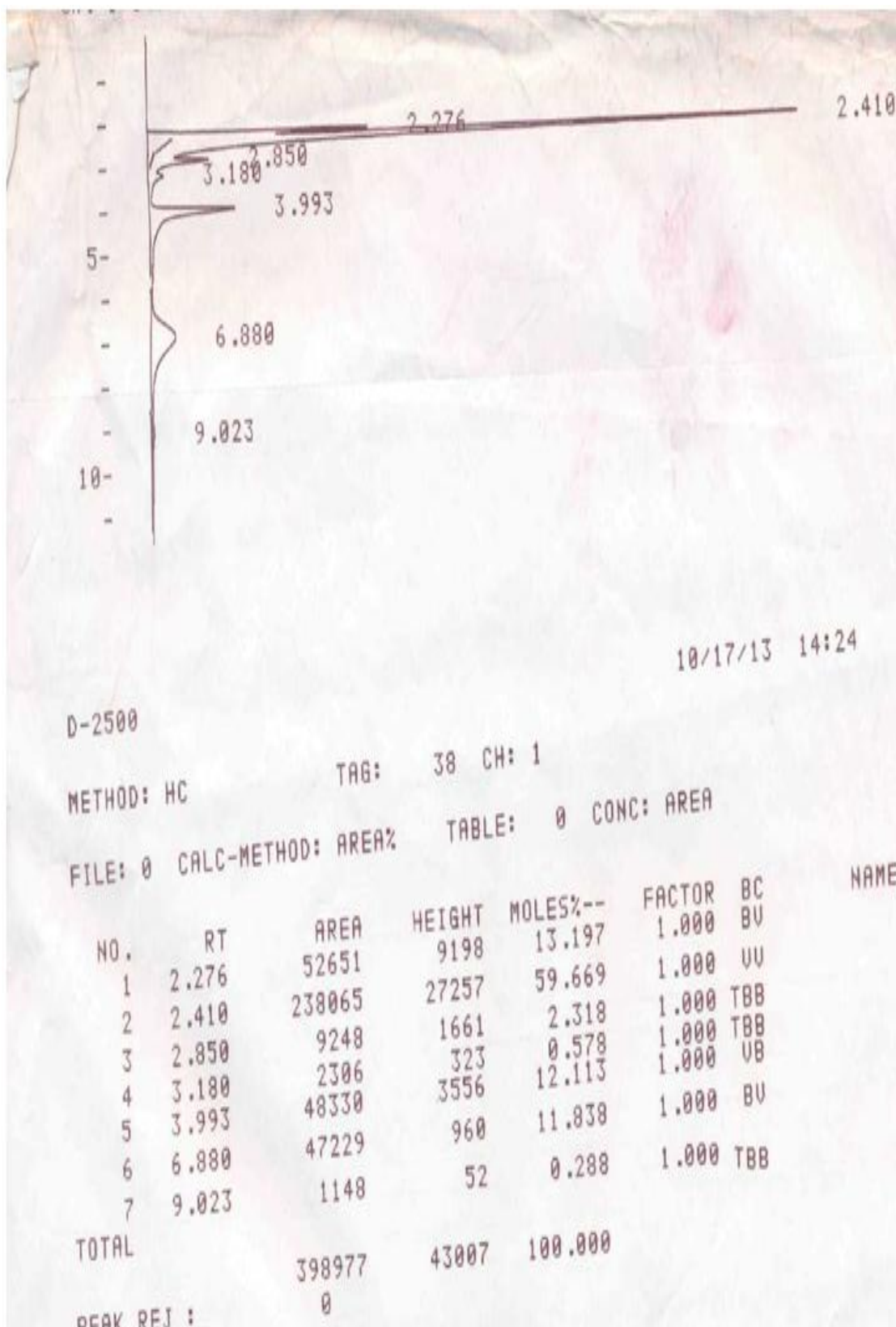


Figure E7: Chromatogram of Cyclohexane over commercial zeolite Y at 480°C

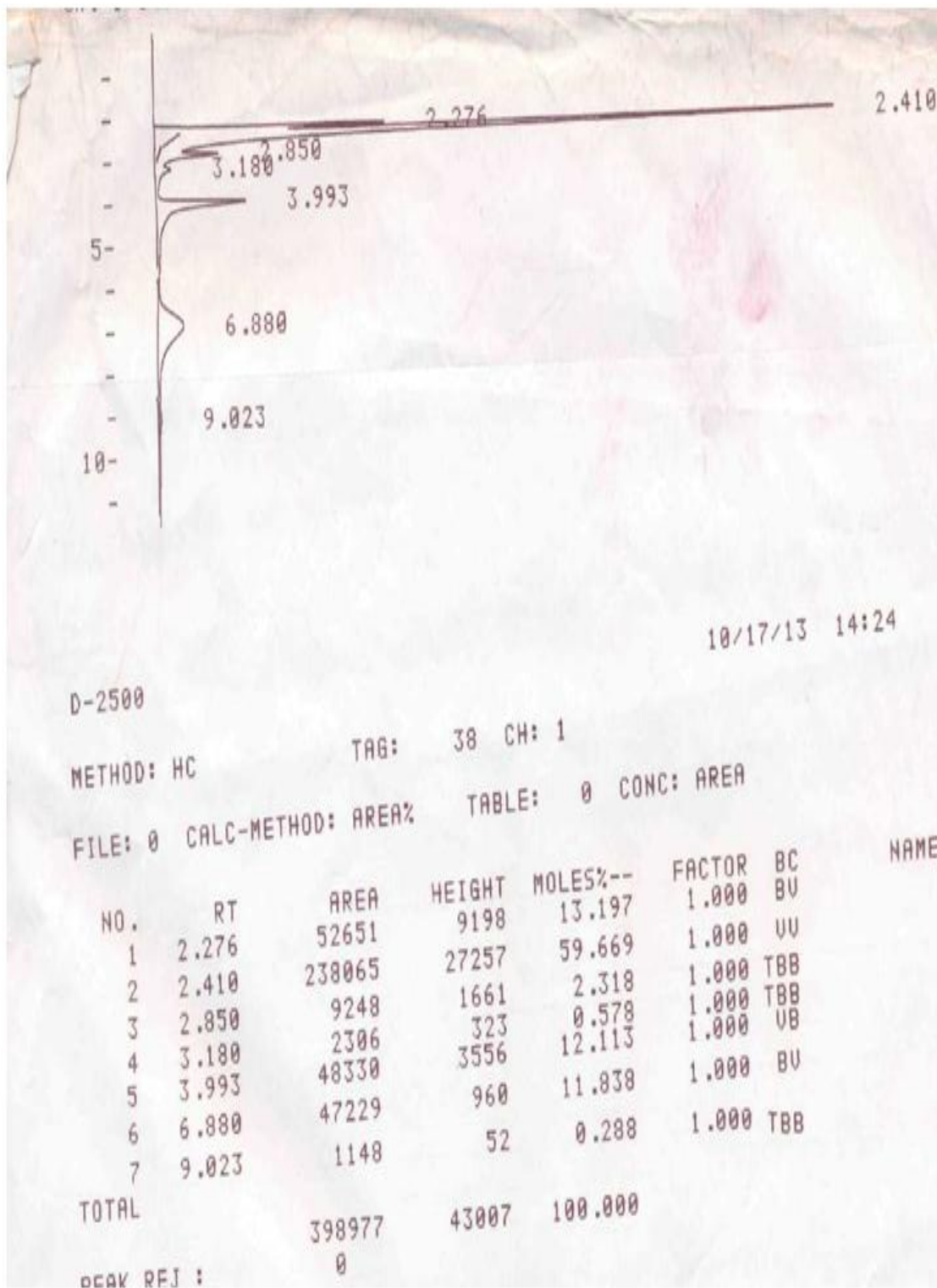


Figure E8: Chromatograph of Cyclohexane over commercial zeolite Y at 520°C

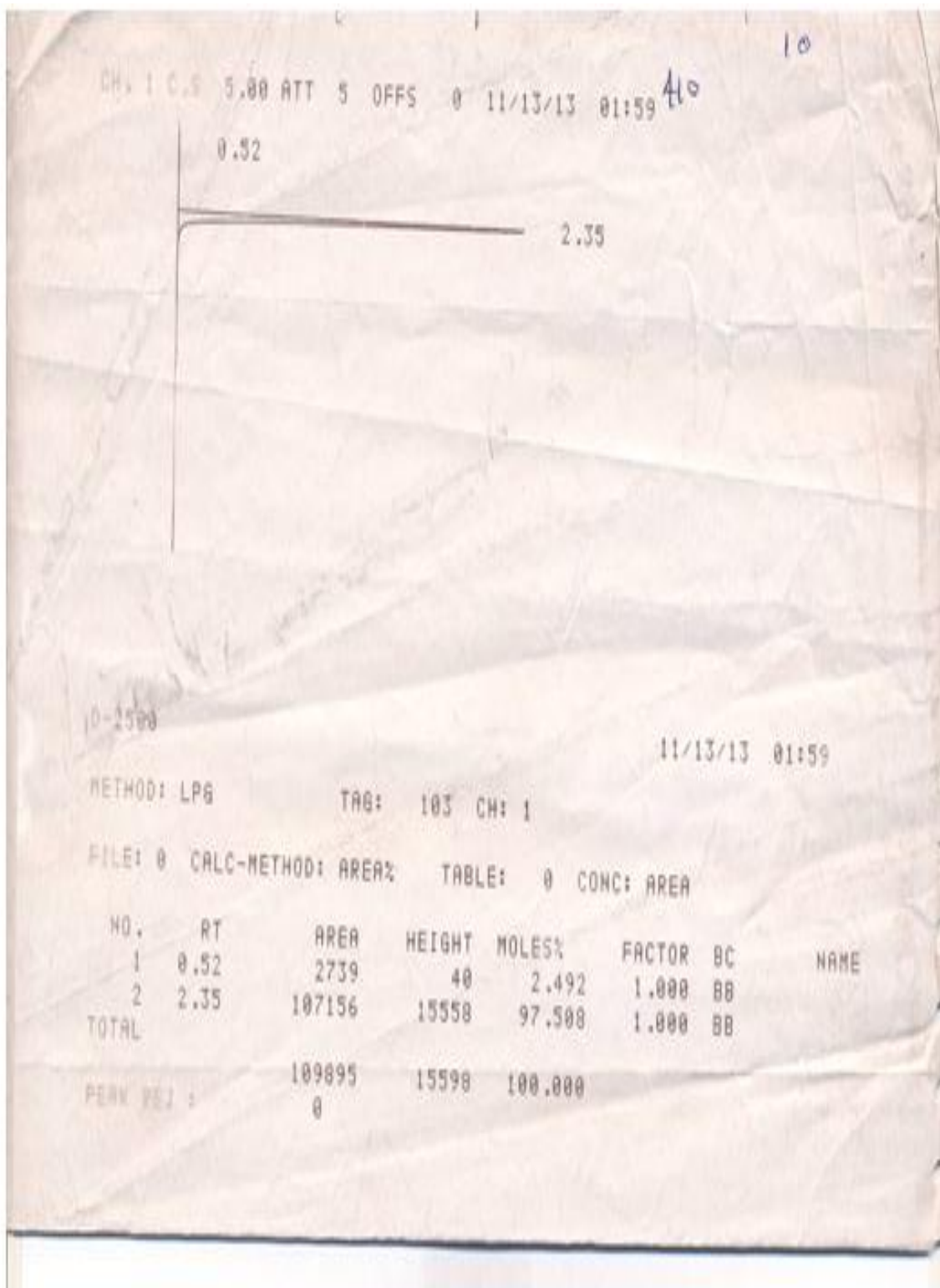


Figure E9: Chromatograph of gas oil cracking over zeolite HY at 420°C

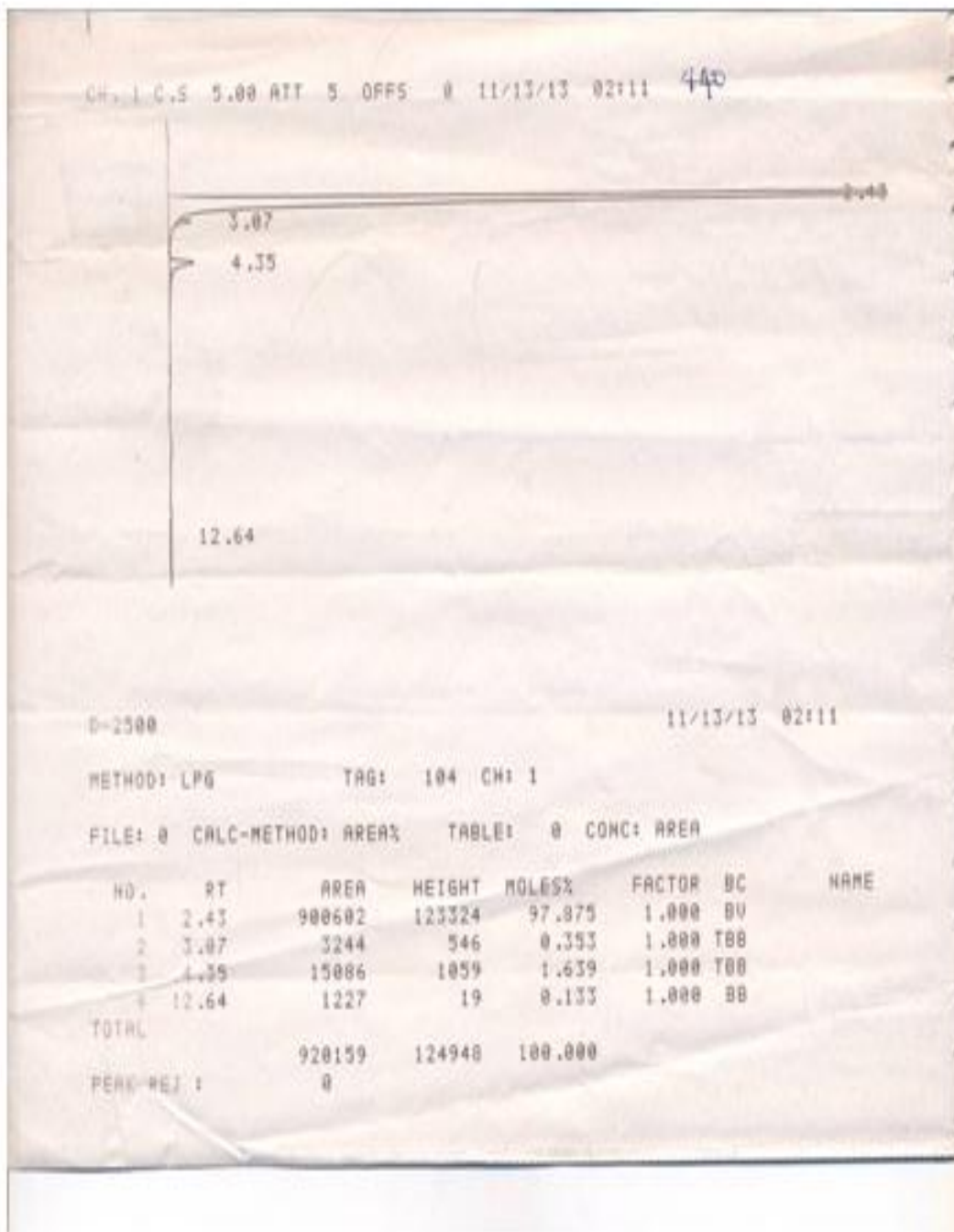


Figure E10: Chromatograph of gas oil cracking over zeolite HY at 440°C

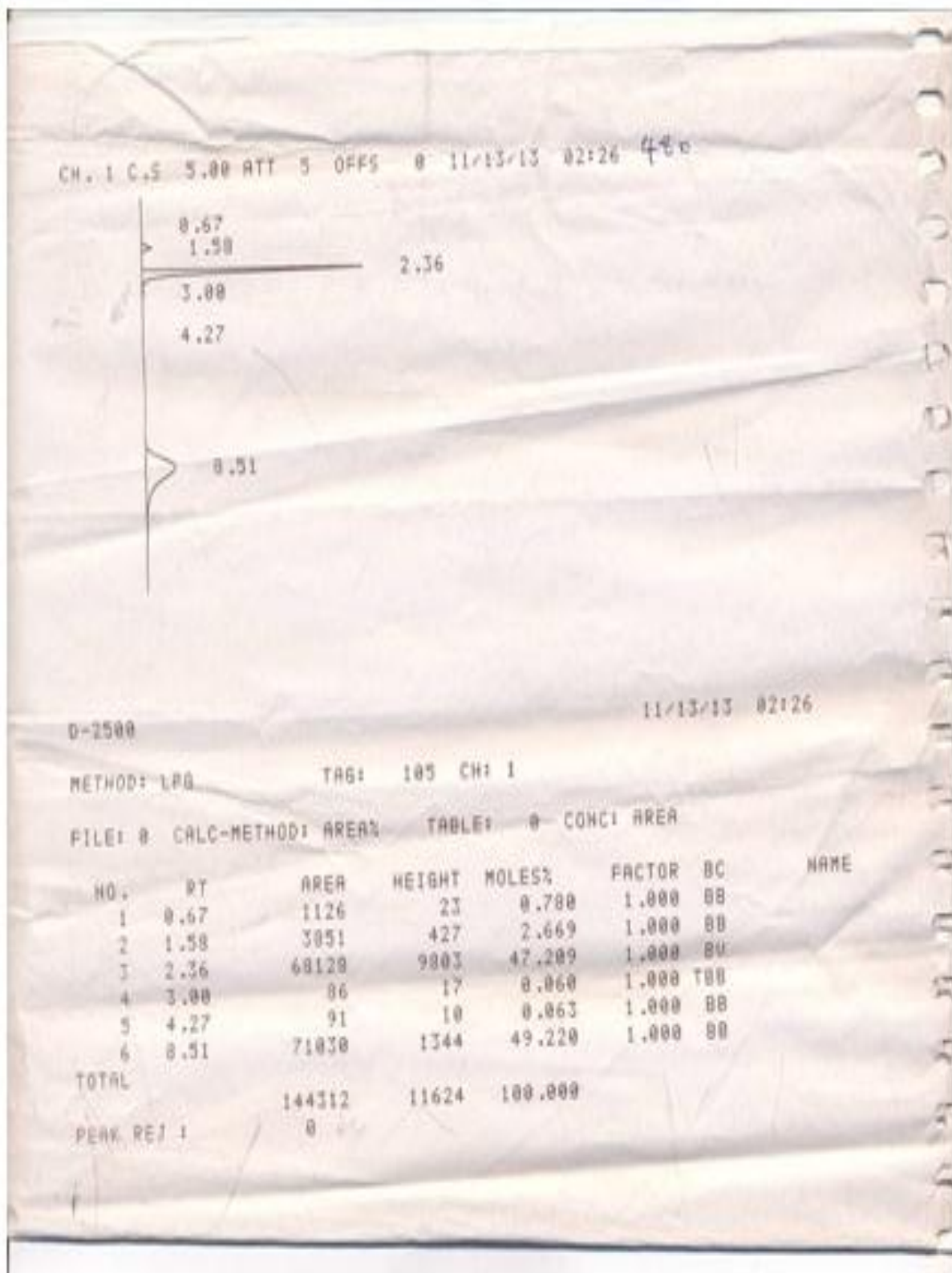


Figure E11: Chromatogram of gas oil cracking over zeolite HY at 480°C

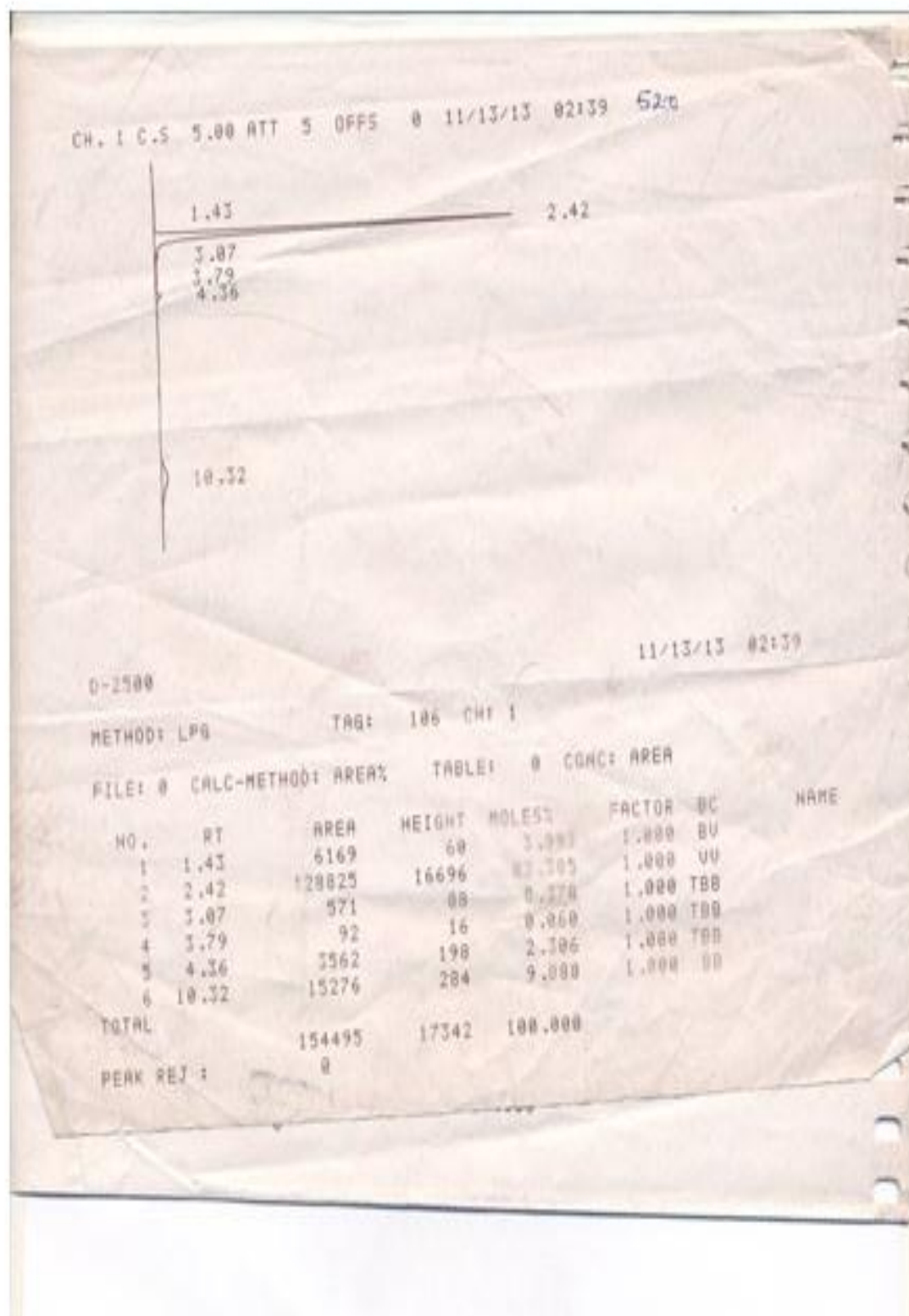


Figure E12: Chromatograph of gas oil cracking over zeolite HY at 520°C

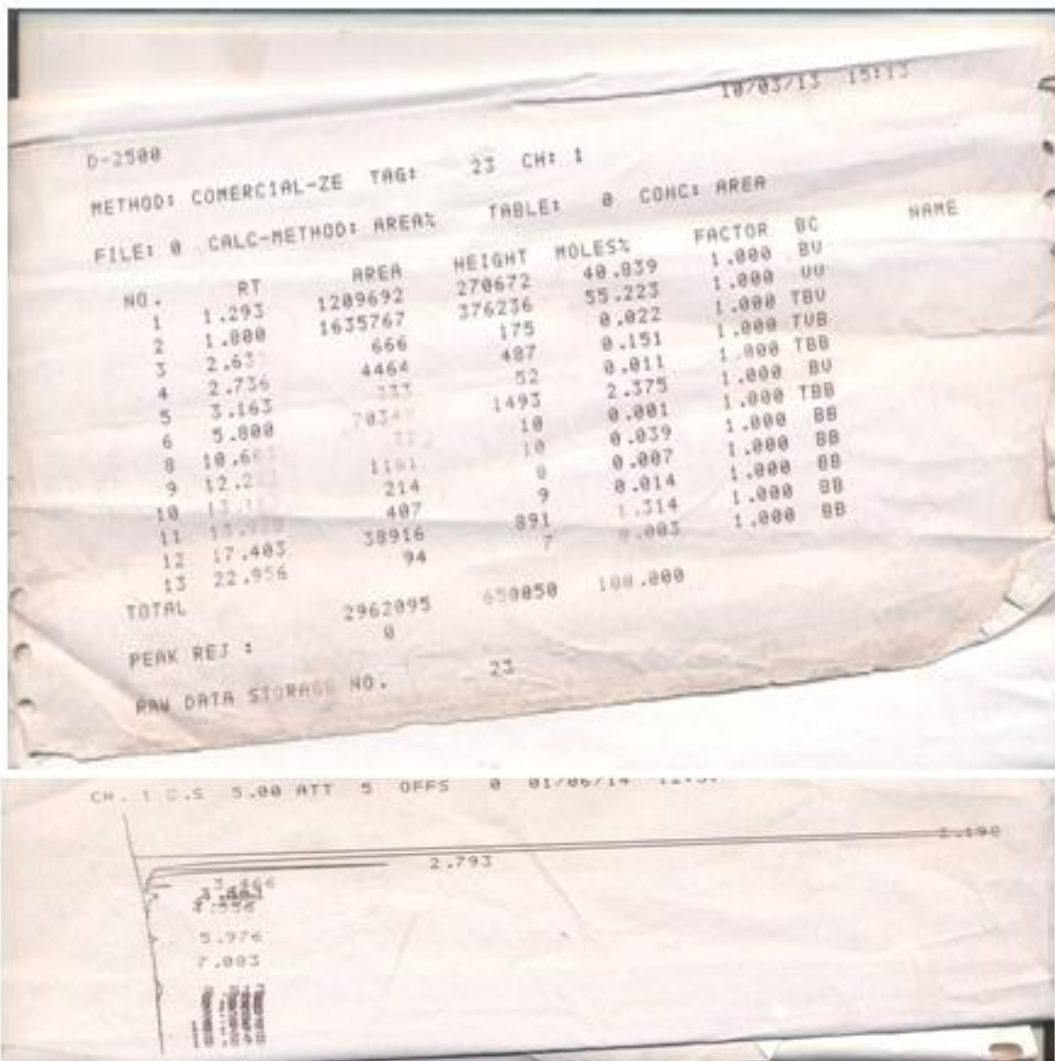
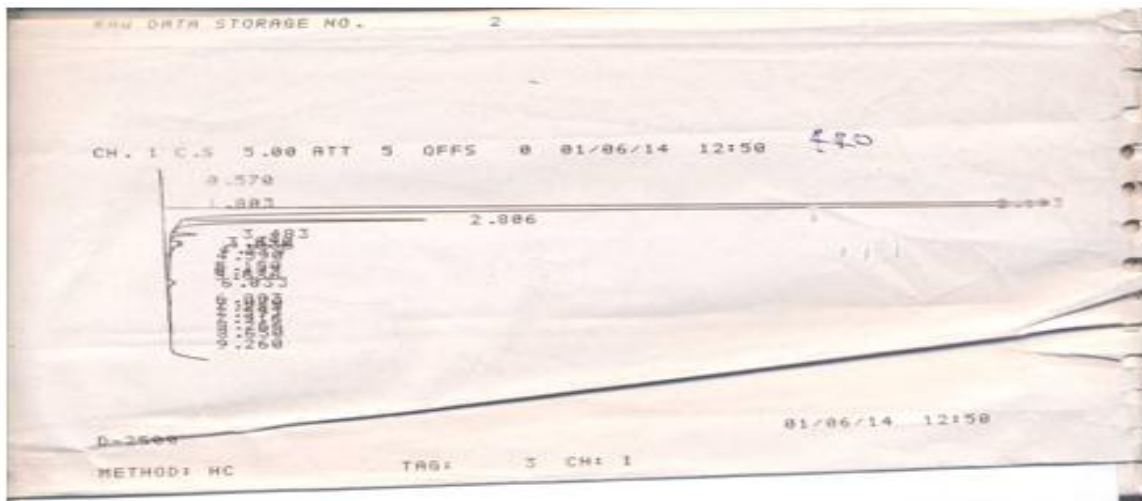


Figure E13: Chromatograph of cyclohexane over Commercial zeolite at 420°C



01/06/14 12:37

D-2500

METHOD: HC TAG: 3 CH: 1

FILE: 0 CALC-METHOD: AREA% TABLE: 0 CONC: AREA

NO.	RT	AREA	HEIGHT	MOLES%	FACTOR	BC	NAME
1	2.190	1618049	263395	93.812	1.000	PH	
2	2.793	65230	9273	3.782	1.000	TE	
3	3.466	6619	985	0.384	1.000	TBB	
4	3.863	5131	619	0.297	1.000	UU	
5	4.803	6500	634	0.377	1.000	UU	
6	4.253	3455	286	0.200	1.000	UB	
7	4.556	2767	184	0.160	1.000	UB	
8	5.976	3484	283	0.197	1.000	BB	
9	7.003	1834	49	0.860	1.000	BU	
10	8.513	9868	208	0.572	1.000	UU	
11	8.790	985	89	0.852	1.000	UU	
12	8.926	293	53	0.017	1.000	UU	
13	9.020	147	42	0.009	1.000	UU	
14	9.096	225	38	0.013	1.000	JL	
15	9.246	156	26	0.009	1.000	UB	
16	9.500	181	25	0.010	1.000	BB	
17	9.803	367	27	0.021	1.000	BB	
18	10.063	121	14	0.007	1.000	BB	
19	10.166	31	9	0.002	1.000	BB	
20	10.293	64	10	0.004	1.000	BB	
21	10.710	187	16	0.011	1.000	BB	
22	10.890	43	10	0.002	1.000	BB	
TOTAL		1724785	276265	100.000			

PEAK REJ: 0

Figure E14: Chromatograph of cyclohexane over Commercial zeolite at 440°C



NO.	RT	AREA	HEIGHT	MOLES%	FACTOR	BC	NAME
1	0.316	1479	23	0.000	1.000	03	
2	2.193	1591732	258851	95.065	1.000	00	
3	2.806	61663	8580	3.603	1.000	T00	
4	3.406	6040	890	0.361	1.000	T00	
5	3.806	2663	381	0.159	1.000	T00	
6	4.036	3739	407	0.223	1.000	T00	
7	4.203	1294	130	0.077	1.000	T00	
8	4.590	860	86	0.051	1.000	T00	
9	6.036	3376	224	0.202	1.000	T00	
10	7.066	502	29	0.030	1.000	T00	
11	7.546	67	11	0.004	1.000	T00	
12	8.270	504	22	0.030	1.000	T00	
13	9.091	236	14	0.014	1.000	T00	
14	10.543	214	8	0.013	1.000	00	
TOTAL							
		1674369	269661	100.000			
PEAK REJ :		0					
RAW DATA STORAGE NO							

Figure E16: Chromatogram of cyclohexane over Commercial zeolite at 520°C